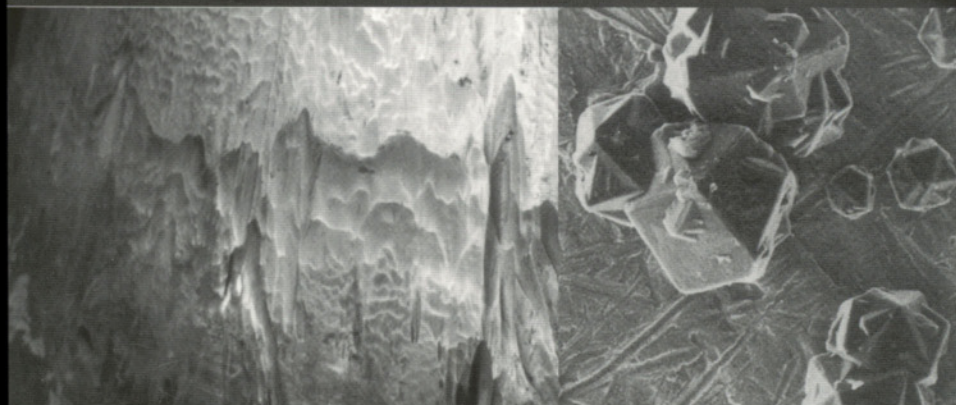


ADVANCED THERMALLY ASSISTED SURFACE ENGINEERING PROCESSES



BY
RAMNARAYAN CHATTOPADHYAY



Kluwer Academic Publishers

**ADVANCED THERMALLY
ASSISTED SURFACE
ENGINEERING PROCESSES**

This page intentionally left blank

ADVANCED THERMALLY ASSISTED SURFACE ENGINEERING PROCESSES

by

Ramnarayan Chattopadhyay
Mumbai , India

KLUWER ACADEMIC PUBLISHERS
NEW YORK, BOSTON, DORDRECHT, LONDON, MOSCOW

eBook ISBN: 1-4020-7764-5
Print ISBN: 1-4020-7696-7

©2004 Kluwer Academic Publishers
New York, Boston, Dordrecht, London, Moscow

Print ©2004 Kluwer Academic Publishers
Dordrecht

All rights reserved

No part of this eBook may be reproduced or transmitted in any form or by any means, electronic, mechanical, recording, or otherwise, without written consent from the Publisher

Created in the United States of America

Visit Kluwer Online at: <http://kluweronline.com>
and Kluwer's eBookstore at: <http://ebooks.kluweronline.com>

DEDICATION

To my father

Jatindra Mohan Chatterjee

Guiding spirit in the pursuit of intellectual excellence

This page intentionally left blank

Contents

Preface	xi
Acknowledgements	xv
CHAPTER 1	
WEAR, SURFACE, HEAT AND SURFACE ENGINEERING	1
1.1 Wear	2
1.2 Corrosion	6
1.3 Surface Properties and Wear	16
1.4 Heat Energy & Thermal Processes	23
1.4.1 Phase Rule & Phase Transformations	27
1.4.2 Surface Property Modification & Thermal Processes	33
1.4.3 Heat Sources	34
References	46
CHAPTER 2	
PLASMA ASSISTED THERMAL PROCESSES	49
2.1 Formation & Properties of Plasma	49
2.2 Non-Transferred Arc Plasma Spraying	52
2.2.1 DC Arc Plasma Spray System	52
2.2.2 Non-Transferred Arc Plasma Scan Hardening	77
2.2.3 Post Spraying Processes	78
2.3 Plasma Transferred Arc Processes	78
2.3.1 Transferred Arc-Plasma Surface Treatment by Scanning	90
2.4 Plasma Nitriding	90
2.5 Plasma Carburizing	95
2.6 Plasma Paste Boronizing	96
2.7 Plasma Assisted Vapor Phase Deposition	97
2.7.1 Plasma Assisted PVD	97
2.7.2 Plasma Assisted CVD (PCVD)	101
2.7.3 Vapor Phase Deposition Techniques of Diamond	103
2.8 Vapor Phase Deposition of Amorphous Materials	105
2.9 Plasma Assisted Polymer Surface Modification	106
References	112

CHAPTER 3

ION BEAM PROCESSES	117
3.1 Ion Source	117
3.2 Ion Beam Assisted Vapor Deposition Processes	118
3.2.1 Types of Coating	120
3.2.2 Dual IBAD	124
3.3 Ion Implantation	125
3.3.1 Plasma Source Ion Implantation	130
3.3.2 Reactive Ion Sputtered Coating	130
3.4 Ion Beam Assisted EBPVD	132
References	132

CHAPTER 4

ELECTRON BEAM PROCESSES	135
4.1 Electron Beam	135
4.2 Electron Beam Assisted Physical Vapor Deposition	136
4.3 Electron Beam Welding	145
References	146

CHAPTER 5

MICROWAVE ASSISTED SURFACE MODIFICATION PROCESSES	149
5.1 Formation & Properties of Microwave	149
5.2 Microwave Assisted Plasma CVD Process	152
5.3 Microwave Assisted Surface Diffusion	154
5.4 Microwave Sintering	155
5.5 Fused Ceramic Surfacing by Microwave	155
References	155

CHAPTER 6

LASER ASSISTED SURFACE ENGINEERING PROCESSES	157
6.1 Formation & Properties of Laser	157
6.1.1 Lasing Elements	158
6.1.2 Pumping Systems	158
6.1.3 Techniques for Laser Formation	159
6.1.4 Laser Focusing	164
6.1.5 Variables Affecting the Laser Assisted Processes	165
6.2 Laser Assisted Surface Modification Processes	167
Lasershot Peening	168
Transformation Hardening	169
Laser Melting	170
Laser Surface Alloying	175
Laser Ablation	176
Laser Fusion of Thermal Sprayed Deposit	177
Laser Assisted Vapor Deposition	178

Laser Welding	179
Laser Spraying	186
Direct Metal Deposition (DMD) by Laser	188
References	189
CHAPTER 7	
SOLAR ENERGY FOR SURFACE MODIFICATIONS	193
7.1 Solar Heating	193
7.1.1 Solar Furnace	193
7.2 Solar Hardening	197
7.3 Sunbeam Fusing	197
References	199
CHAPTER 8	
COMBUSTION PROCESSES FOR SURFACE MODIFICATION	201
8.1 Heat & Flame Generated by Oxy-Fuel Combustion Processes	201
8.1.1 Surface Modification Processes by Furnace Atmosphere Control	203
8.2 Normal to Moderate Capacity Flame Spray/Fusion Systems	204
8.2.1 High Velocity Flame Spraying	207
8.2.2 Hyper Velocity Impact Fusion (HVIF)	212
8.3 Hot Chemical Gas Flame for Diamond Film Deposition	213
8.4 Flame Assisted Vapor Deposition (FAVD) Process	215
References	216
CHAPTER 9	
FRiction WELD SURFACING	219
9.1 Principles of Friction & Frictional Heat	219
9.2 Friction Surfacing	222
References	226
CHAPTER 10	
INDUCTION SURFACE MODIFICATION PROCESSES	229
10.1 Induction Heating of the Surface	229
10.2 Induction Hardening	230
10.2.1 Induction Hardening of Cast Iron Surface	233
10.3 Induction Fusing	233
10.4 Induction Coupled RF Plasma	236
References	237
CHAPTER 11	
SURFACING BY SPARK DEPOSITION PROCESSES	239
11.1 Capacitance Discharge or Spark Deposition Process	239

11.2 Applications	242
References	242
CHAPTER 12	
ARC ASSISTED ADVANCED SURFACE ENGINEERING PROCESSES	243
12.1 Arc Phenomena in Welding & Developments	243
12.1.1 Gas Tungsten Arc Welding	246
12.1.2 Gas Metal Arc Welding	247
12.1.3 Plasma Arc Welding with Rod/Wire	251
12.1.4 Submerged Arc Welding (SAW) Process	254
12.1.5 Electroslag Welding	258
12.2 Arc Light Assisted Processes	259
12.3 Advanced Arc Spraying Process	261
12.4 Electroconsolidation Cladding	263
References	264
CHAPTER 13	
HOT ISOSTATIC PRESS	267
13.1 HIP Process	267
13.2 Diffusion Bonding by HIP	268
13.3 Hip Quenching of Diffused Layer	270
References	270
CHAPTER 14	
FLUID BED PROCESSES	271
14.1 Fluid Bed Processes for Thermal Treatments	271
14.2 Fluidised Gas Bed	272
14.2.1 Fluidised Gas Bed Carburizing	272
14.3 Thermal Processing in Molten Salt Bath	273
References	274
CHAPTER 15	
POLYMERIC SURFACES	275
15.1 Thermally Assisted Surface Modification of Polymeric Materials	275
15.2 Polymer Coatings on Metallic Substrate	276
15.3 Parylene Coatings	277
References	278
CHAPTER 16	
CERAMIC SURFACES	279
16.1 Ceramic Surface Modifications	279
16.2 Ceramic Coatings Materials/Processes	281
16.2.1 Ceramic Oxides	282

16.2.2	Ceramic Carbides, Nitrides and Composites	282
References		283
CHAPTER 17		
DIFFUSED AND CVD COATINGS OF SINGLE AND MULTIPLE ELEMENTS		285
17.1	Diffusion Process	285
17.2	Diffusion Coatings of Interstitials	288
17.3	Diffusion Coating of Substitutional Elements	292
17.3.1	Pack Alunising	293
17.3.2	Pack Chromising	296
17.3.3	Siliconizing or Ihregizing	297
17.3.4	Chemical Vapor Deposition of Multilayer Coating	299
17.4	Diffusion Sinter Cladding	302
References		303
CHAPTER 18		
MISCELLANEOUS PROCESSES		307
18.1	Fused Paste Coating	307
18.2	Wear Plates	308
18.3	Hard Top Casting	309
18.4	High Density Infrared Processing of Surface Layer	310
References		310
CHAPTER 19		
QUALITY OF THE ENGINEERED SURFACES		311
19.1	Quality Checks of Engineered Surface	311
19.1.1	Microstructure	312
19.1.2	Composition	314
19.1.3	Hardness	315
19.1.4	Surface Roughness	317
19.1.5	Performance Tests	318
19.2	Surface Modification Processes and Surface Qualities	319
19.2.1	Diffusion Control Processes	319
19.2.2	Vapor Phase Deposition	320
19.2.3	Ion Implanted Surfaces	323
19.2.4	Thermal Spraying	324
19.2.5	Welding	326
References		328
CHAPTER 20		
PROGNOSTIC AND LIFE CYCLE EXTENSION		331
20.1	Prognostic	331
	Fracture Toughness & Life Cycle	334

Fatigue Life	339
Creep Life	342
Wear Life in Different Wear Processes	344
Adhesive Wear Life	345
Abrasive Wear Life	346
Erosive Wear Life	347
Thermal Wear	350
Zero Wear or (IBM) Equation	351
Corrosion Wear Life	352
Corrosion Life using Fracture Mechanics	352
Wear Life from Long Time Wear Simulation Tests	354
On-line Wear Health Monitoring	355
Thin Layer Activation	356
Acoustic Emission	356
References	356
Subject Index	359
About Author	375

PREFACE

Surfaces are the bounding faces of solids. The interaction of component surface with the working environment results in wear & corrosion. Estimated loss due to wear & corrosion in USA is around \$500 billion. Engineered surfaces are the key to the reduction of losses due to wear and corrosion. In the USA, around 9524 establishments (including automotive, aircraft, power and construction industries) depend on engineered surfaces with support from 23,466 industries. Around 65 top academic institutions world-wide are engaged in surface engineering research and teaching.

There has been a paradigm shift in surface engineering from age-old electroplating to processes such as vapor phase deposition, diffusion, thermal spray & welding using advanced heat sources like plasma, laser, ion, electron, microwave, solar beams, pulsed arc, pulsed combustion, spark, friction and induction. Metal, ceramic, polymer and composite surfaces are modified by application of heat or thermally assisted coatings with dissimilar materials. In addition to conventional materials it is possible to develop newer coating materials by processes such as RSP (metallic glasses), plasma polymerization (polymers and copolymers) and thermal spray (graded deposits). The application range includes critical components from almost all major industries, such as automotive, power, steel ,aerospace, nuclear, cement, petrochemical, chemical, construction, tools & dies and biomedical equipments. Quality control of the engineered surface assures improved and consistent performance. A wear prognostic approach has been found useful to assess, monitor and improve the life of components in aging equipments and machineries. An attempt has been made to cover all these and few more topics in this book.

There are surface engineering books on specific processes such as thermal spraying and vapor phase deposition or about specific heat sources such as plasma or laser. However, there are few, if any, covering the whole range of advanced surface engineering processes. The manufacturing (OEM) and maintenance (M&R) of modern equipments and machineries, such as jet engines, require a number of advanced surface engineering processes for reliable, consistent and improved performance in the most hostile environment. It is imperative that those who are engaged in these and other related areas should be conversant with the newer competitive surface engineering processes. The present book has been structured to provide assistance & guidance to the engineers, researchers and students in choosing the right process from the galaxy of newer surface engineering techniques using advanced heat sources.

This page intentionally left blank

Acknowledgement

I am grateful to my ex-colleague & friend Prof. Joaquin Lira-Olivares, Professor of Material Science, Centro de Ingenieria de Superficies, Universidad Simon Bolivar, Caracas, Venezuela, for making an excellent pre-publication review. I appreciate the constructive pre-publication review made by Louis G. Hector, Jr., Ph.D, Research Scientist, R&D and Planning, General Motors MC, USA. I am thankful to Dr. James B. Adams, Professor, Chemical and Materials Engineering, Arizona State University Tempe, AZ, for helping me in the review process.

I would like to thank the following accomplished technologists for their help & support in this project:- Dr. C.K. Gupta, ex-Director, Materials Group, Dr. M.K. Totlani, ex-Head, Surface Engineering, and G.L. Goswami, Laser Processing & Advance Welding, of Bhabha Atomic Research Center, Mumbai, India.

Dr. A.K. Nath, Head, Laser Programme, Center for Advance Technology, Indore, India; Dr. P.I. John, Institute of Plasma Research, Gandhinagar, India. Dr. K. Shridhar, Naval Materials Research Laboratories, Mumbai.

Thanks to Gregory T. Franklin, Carol Day and all other staff members of Kluwer Academic Publishers who have done commendable work in publishing the book in the shortest possible time frame. Thanks to Ms. Poonam for her help in making the camera ready copy of the book.

My elder son Romik (University of Texas at Austin) & his wife Robin and younger son Raunak (Motorola, Texas) have given me unfailing support all through the project. Thanks to all of them. Thanks to Chiraranjan for providing assistance especially in designing the cover page.

My wife Mandira (Vice Principal & Reader), despite her extremely busy schedule has devoted considerable time in correcting and sequencing the manuscript in its final form. I shall be failing in my duties if I do not acknowledge her generous support and help in this mission.

This page intentionally left blank

Chapter 1

WEAR, SURFACE, HEAT AND SURFACE ENGINEERING

1.0 Introduction

Surfaces of a solid are the bounding faces forming interfaces with the surrounding environment. Bulk of the material constitutes ‘bulk phase’ and the free bounding faces are known as ‘surface phase’. The surface of the solid retains sufficient free energy in order to remain in equilibrium with the surrounding. The environmental degradation of materials occurs due to interaction of the surface phase with the surroundings, a process called wear. Based on the types of interaction involving different environments with the solid material surface, the different wear processes are termed as abrasion, adhesion, erosion, corrosion and thermal. Wear is not an intrinsic property of the material and occurs due to interaction of the bounding faces with the working environment. It is therefore possible to control wear of materials by altering surface properties. The main surface properties, which are controlled for minimizing wear include surface energy, morphology, composition and hardness. The term wear surface engineering includes the processes for development of wear resistant surfaces. The surface engineering processes involving phase transformations and diffusion require heat energy. The quantum of heat required for the processes depends on the specific heat and latent heat of the material. The phase diagrams provide complete data on the concentrations and temperatures at which different phases are at equilibrium. These data can be gainfully employed in designing the processes and consumables.

The advance heat sources such as rocket combustion, laser, plasma, electron etc are capable of producing higher heat intensities and energies. The advanced heat sources provided the impetus to the development of newer techniques and processes. The chapter covers brief discussions, including basic principles of wear and corrosion, surface properties controlling wear, use of heat energy in transformation processes, equilibrium diagrams and their use, heat sources and use in thermal processes for wear surface engineering.

1.1 Wear

The interaction of exposed solid surface with the surrounding environment results in loss of material from the surface by a process known as wear. Wear of material occurs from those surfaces of the component, which are exposed to working environment. The definition does not include loss in dimension due to plastic deformation, although for all practical purposes wear has occurred despite no material removal. Wear is not an intrinsic property of the material but a system property. The wear environment or system envelope causing wear has been defined in DIN 50320. In accordance with DIN 50320, the performance of the material shall depend on the concerned **wear system or system envelope (6)** (Fig. 1.1.1). In a given system envelope (6) which is determined by the boundary conditions of the system, the wear shall occur only when the following conditions are satisfied:- i) There is a wear-causing counter-body or **counter-material (1)** in contact with the **base material (3)** or with the interposition of an **intermediate material (2)** of similar or dissimilar nature. The combination can be referred to as the **wear mating**. ii) There is a **relative movement (5)** between the wear mating components under **load (4)**. The movement and the load factors are together referred to as the primary actions.

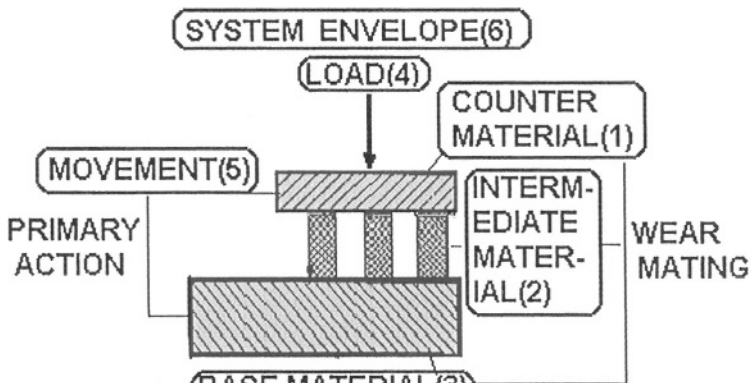


**Fig1.1.1.WEAR SYSTEM
(DIN 50320)**

According to DIN 50320, the different wear processes are classified in four types based on wear mechanisms (Table 1.1.1). The interaction of solid surface with various kinds of counterbodies and wear envelopes can cause different types of wear. For example, counterbody may be another solid surface (resulting in adhesive wear), or abrasive particle (causing abrasive wear), or suspended particle in fluid media (resulting in erosive wear), or reactive fluid (causing corrosive wear) or heat (resulting in thermal wear) etc.

A more comprehensive classification (1) than that listed in Table 1.1.1, includes additional types like erosion, corrosion, thermal etc (Table 1.1.2).

Table 1.1.1 Classification based on Wear Mechanism(DIN50320)

Wear Type	Mechanism
Adhesion	Formation of interfacial adhesions("weld") junction the action of molecular forces.
Abrasion	Grooving by scratching and micro-cutting
Surface Fatigue	Cracking at the surface due to stresses or strains varying in magnitude or direction.
Tribological Reaction	Formation of reaction products by a combined effect of tribological action between base material and counter-material and chemical reaction with the surrounding medium.

Table 1.1.2 Wear classification based on environmental interactions(1)

Type / mode	Interacting Environment	Control
1. ADHESIVE	Similar or dissimilar material	*Alter surface properties *Lubrication
2. ABRASIVE	Solid particles	*Alter surface properties
3. EROSION	Suspended particles in fluid media / liquid jets (e.g. rain drops)	*Alter surface properties *Change particle or jet impingement angle by changing design or use buffer plate
4. CORROSION	Reactive fluids/solids	*Alter surface properties *Electrochemical means
5. CAVITATION	Collapsing bubbles	*Alter surface properties
6. THERMAL	Heat	*Alter surface properties
7. FATIGUE	Alternative/cyclic stress	*Alter surface properties *Develop compressive stresses at surface

Apart from system envelope and counterbodies, the wear process is also dependent on the surface properties, such as, surface energy, morphology, composition and hardness. The alterations in these properties provide the key for the development of wear resistant surface.

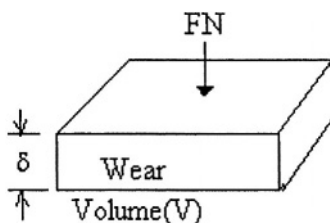
In most of the surface engineering processes, the modified surface properties result in higher hardness. Amongst the mechanical properties, hardness at the surface has a major role to play in controlling various types of wear.

General Wear Equation :-The general form of wear equation is based on the relationship developed by Holm (2) for electrical contacts and later work of Archard (3).The wear volume (V) is directly proportional to sliding distance (d) and applied normal force (FN) and inversely proportional to hardness or yield stress (H) of the softer surface as follows :

$$V = K \cdot \frac{FN}{H} \cdot d$$

and the depth of wear can be expressed as:-

$$\delta = K \cdot \frac{FN}{H} \cdot \frac{d}{A}$$



where A = Area of Contact, $V = \delta A$ and K = Wear Coefficient.

The wear constant 'K' is a proportionality number and is equal to wear volume for unit sliding distance with the applied normal force producing stress equals to hardness or yield stress of the softer material. Only material property included in the wear equation is the yield strength or hardness of the material. Surface modification processes for minimizing wear are therefore oriented towards the development of higher hardness or strength at the surface.

The relation amongst different types of wear with the hardness of the materials are as follows:-

- a. Abrasive Wear:- Hardness of abrasive (Ha) with respect to that of metal surface (Hm) is an important parameter for abrasive wear. The empirical relationship between the hardness of abrasive particles (Ha) and the hardness of abraded surface (Hm) can be expressed as follows (4):

$H_m/H_a \geq 0.7$ for low wear

$H_m/H_a \leq 0.7$ for high wear.

The transition from low to high wear takes place at a ratio of H_m/H_a is in the range of 0.7 to 1.1.

- b. Repetitive Impact Wear:- According to Zero Impact wear equation (5), hardness is directly proportional to both to N , the number of cycles for causing detectable wear, since shear yield stress is directly proportional to hardness:-

$$H \propto \tau_y \propto N,$$

where H = hardness, τ_y = shear yield strength, N = number of cycles to wear.

- c. Hot Hardness and Thermal Wear (6):- The wear volume (V) is an inverse function of hardness (H) or $VH = K$. Based on the room temperature K values and high temperature hardness (H) data, the wear volumes (V) at different temperatures can be calculated. The inverse of wear volume is the wear factor (WF).
- d. Erosion:- Erosive wear (7) depends on hardness of the material and the angle of impingement, as follows: $V_{max} \propto f(\alpha \cdot H)$, where α is the angle of impingement and H is the hardness of the material.

For ductile or low hardness materials, wear rate increases with the increase in angle of impingement and reaches maximum (V_{max}) at angle $\alpha \approx 18.5^\circ$ and then decreases with the increasing striking angle. For brittle or high hardness materials, wear rate increases with the increasing angle of impingement and reaches the maximum value (V_{max}) at a striking angle of 90° .

- e. Wear of Ceramics:- According to Evans & Marshall equation (8), wear volume (V) is inversely proportional to roughly $H^{3/2}$ or more precisely as follows:-

$$H^{1.425} \propto 1/V$$

Increase in hardness has a large effect in decreasing the wear rate.

- f. Wear of Plastics:- With low hardness combined with narrow hardness range, there is very little effect of hardness on wear of polymeric materials. Compositional change by use of fillers can improve wear resistance of polymeric materials. Also morphological changes by plasma polymerization and co-polymerization can cause improvement in wear resistance.

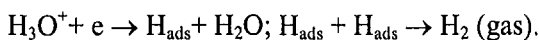
Higher hardness materials are produced by modifying surface morphology and/or composition by processes, such as, carburising, coating by CVD & PVD, weld overlay and thermal spray.

1.2 Corrosion

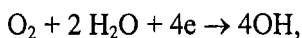
Another major process leading to environmental degradation of material is known as corrosion, which is also referred to as corrosive wear. In corrosion, the loss of material occurs through electrochemical reaction at the surface. Like wear corrosion is also environment specific, i.e., corrosion rates need to be stated along with the specific environmental conditions.

Principles of corrosion :-

The dissolution of metallic elements by formation of ions due to loss of electrons is known as anodic reaction; e.g., $\text{Fe} \rightarrow \text{Fe}^{++} + 2 \text{ electrons}$. $\text{Zn} \rightarrow \text{Zn}^{++} + 2 \text{ electrons}$ which takes place in anodic areas. The reaction with water or oxygen with electrons from the surface is known as cathodic reaction, which occurs in cathodic areas. For example the hydrogen evolution reaction occurring at cathodic area can be expressed as follows :



Similarly the oxygen reduction reaction occurs as follows :-



ii: Corrosion Current and Corrosion Rate:-The rate controlling equation for corrosion can be expressed as follows:-

$$C_T = C_0 (\Delta G^* / RT) \quad (1.2.1)$$

where C_T is the rate at $T^\circ\text{K}$; C_0 is the rate at 0°K ; R is the gas constant; ΔG^* is the activation energy of corrosion reaction. By putting equation 1.2.1 in logarithmic form, and using energy terms as potentials and rates as currents, the relationship between corrosion current (I_c) and measured potential (E) of the specimen can be expressed as follows:-

$$E - E_c = \beta \cdot \log I / \log I_c, \quad (1.2.2)$$

where, E = measured potential of the specimen (current flowing), E_c = corrosion potential (no current flowing), I = impressed current, I_c = corrosion current (no external current), and β = constant. Putting $\eta = E - E_c =$

overvoltage in equation 1.2.2, the relation between η and I_c is expressed by Tafel's equation as follows:-

$$\eta = \beta (\log I - \log I_c) \quad (1.2.3)$$

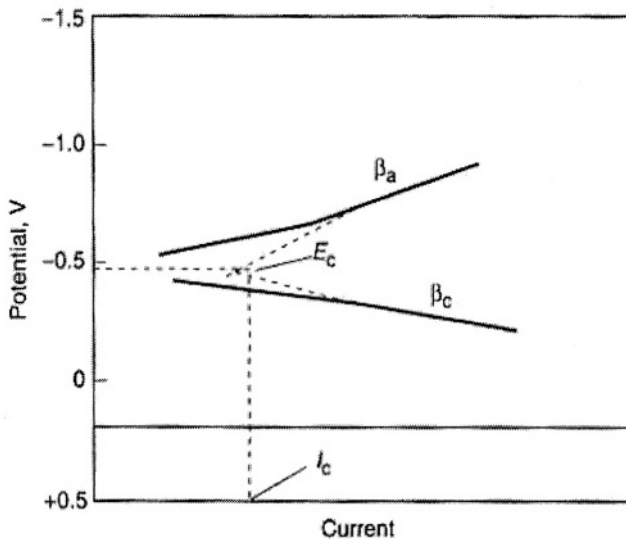


Fig. 1.2.1 : Schematic Polarisation Curve

The plot of η against $(\log I - \log I_{corr})$ shall produce a straight line with slope β . β is known as Tafel's constant. From the plots of anodic and cathodic reactions, the respective Tafel's constants, β_A & β_B , can be obtained. The anodic & cathodic polarisation curves approach each other until the difference in potential between anodic and cathodic areas is sufficient to pass the resultant corrosion current across the resistance in the corrosion cell (Fig. 1.2.1). The current and voltage at the intersection are known as corrosion current (I_c) and corrosion voltage (E_c) respectively. The rate of metal loss is related to corrosion current (I_c) by Faraday's Law.

$$\text{Corrosion Rate (mpy)} = \frac{0.131 \times I_c \times E_w}{\rho} \quad (1.2.4)$$

where E_w = Equivalent weight of the alloy and ρ = density of the alloy. Corrosive wear like other wear process is expressed in terms of loss in dimensions, such as mpy (mil per year), $\mu\text{m/year}$, inch/year etc.

Variables affecting corrosion :- Important variables affecting corrosion are as follows:-

- Current and Voltage*:- Schematic diagram for polarisation (anodic) of stainless steel in an acidic solution (Fig. 1.2.2) shows three regions, viz; active, passive and transpassive depending on the current and potential. The current density and corrosion rate are lowest in passive zone. The change from active to passive zone depends on the maximum current density, I_{max} , at E_{ph} . Any increase in potential beyond E_{ph} results in rapid fall in current density to a low value. Therefore I_{max} is a measure of the ease with which an alloy can be passivated.

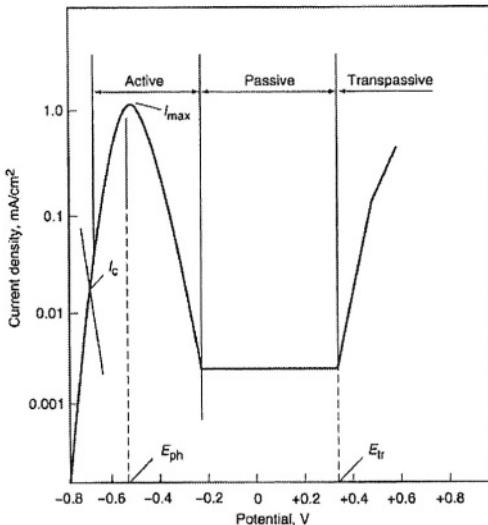


Fig.1.2.2. Schematic polarization curve(stainless steel in acid)

- Composition*:- Effect of different alloying elements on I_{max} and E_{pp} are shown in Fig. 1.2.3. Elements causing decrease in E_{pp} and I_{max} are also responsible in reducing corrosion rates. In stainless steel, chromium addition is advantageous with respect to both E_{pp} and I_{max} . Sulfur and to a certain extent manganese can cause an increase in I_{max} . Molybdenum and copper addition results in a substantial drop in I_{max} . The value of I_{max} decreases with nickel addition. An increase in E_{pp} occurs due to the addition of Ni, Cu and Mo.
- Stress*:- Applied or residual stress, particularly, the static stress in the material accelerates the corrosion process and may cause stress corrosion cracking.
- Microstructure*:- Microstructural features need to be controlled for minimizing corrosion, e.g., the presence of brittle martensite in microstructure may result in early failure due to hydrogen embrittlement.

Also chromium depletion at grain boundaries may result in weld decay of stainless steel weld overlay.

- v. **Moisture:** - Moisture normally enhances the corrosion rate, e.g., mild steel does not rust in air until the relative humidity of the atmosphere exceeds 30%.
- vi. **Salts, acid and alkali:** - Salts although neutral, can get ionised in the presence of moisture and cause enhanced corrosion.

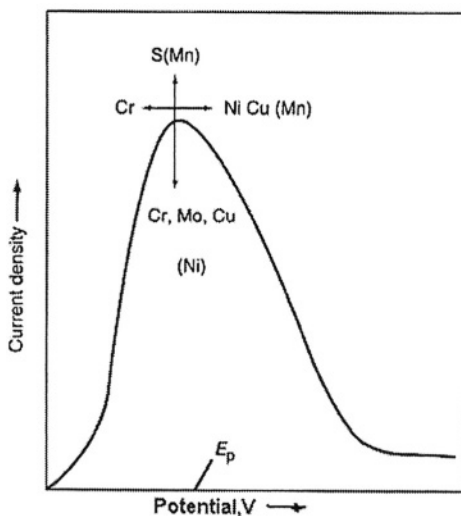


Fig.1.2.3. Effect of alloying elements on polarization of stainless steel in acid

The non-oxidising acids, like HCl, may cause reduction in hydrogen overvoltage through profuse evolution of hydrogen. The oxidising acids may cause corrosion or may form a passive film depending on the stability of the protective film.

Alkaline corrosion rate at room temperature is normally very low.

Types of Corrosive Attack

- a. **General Corrosion:** - The average rate of corrosion on the surface is uniform in general corrosion. Uniformly corroded surface of an alloy is shown in Fig. 1.2.4.
- b. **Galvanic:** - When two dissimilar metals are in contact with each other in a conductive solution(electrolyte), the more anodic metal shall get corroded while the cathodic metal remains unaffected. For a metal pair in a given solution, the metal with anodic solution potential shall undergo accelerated galvanic corrosion. The direction of current is from anode to

cathode thus leading to corrosion of anodic material in a galvanic pair. The magnitude of current determines the rate of corrosion.

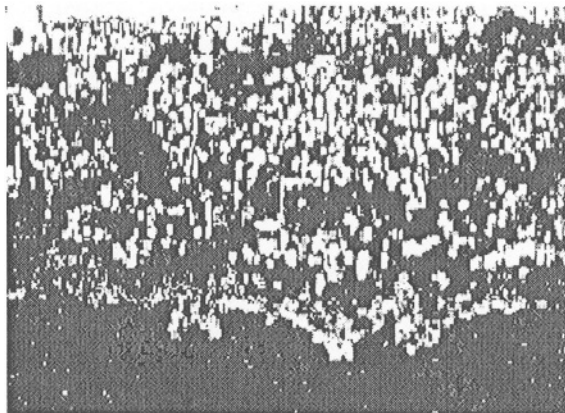


Fig.1.2.4 Uniform corrosion on the surface of a Ni-base alloy, X100

For galvanic corrosion, the solution potentials of the galvanic pairs in a given solution provide a more dependable guideline in comparison to that of e.m.f values. For example, in a Zn-Al galvanic pair in aqueous solution, Zn with anodic solution potential dissolves in preference to Al, despite the fact that Al is anodic with respect to Zn in e.m.f. series.

The surface area of contact between anodic and cathodic material is an important factor determining galvanic corrosion. In general, the smaller the surface of anodic metal compared to cathodic metal, the more severe is the corrosion of the anodic metal.

- c. Intergranular Corrosion : A common example of intergranular corrosion is weld decay. During welding or heat treatment of stainless steels, holding or slow cooling in the temperature zone of 500°C to 850°C, results in the formation of chromium carbides at grain boundaries. The chromium depleted grain boundary regions are susceptible to intergranular corrosion in a corrosive environment. Intergranular corrosion can occur in various copper alloys, such as aluminium brasses, silicon bronze, Muntz metal & admiralty metal, in applications involving high pressure steam.
- d. Parting Corrosion : The preferential removal of an element from an alloy by corrosion process is known as parting corrosion or selective leaching. Examples of parting corrosion includes, dezincification of brass (<85% Cu compositions) in water containing dissolved oxygen, denickelification in Cu-Ni alloy in fresh water and graphitic corrosion of grey cast iron. In

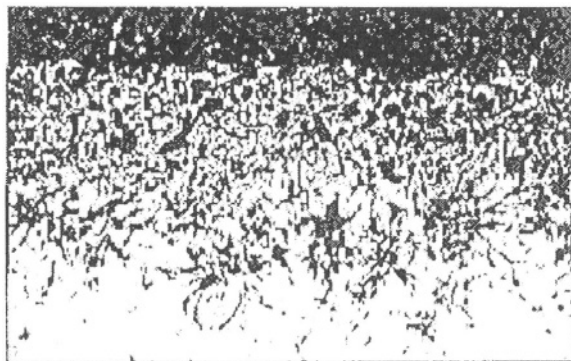


Fig.1.2.5 Parting Corrosion in CI,X150

mild aqueous solution or in buried pipes and fittings, the iron is selectively leached away from grey cast iron leaving behind graphite network (Fig. 1.2.5).

- e. Crevice Corrosion : This type of corrosion usually occurs in recesses, crevices or enclosed areas produced by mating parts such as gaskets, sleeves or screw threaded fittings, where the access to oxygen for the entrapped liquid is restricted. The lower oxygen content of liquid entrapped in the crevices compared to freshly circulated liquid leads to formation of an oxygen concentration cell in which the metal surface in contact with low oxygen liquid shall get corroded at a fast rate.
- f. Pitting : This is a localised corrosion causing depression or pit formation on the surface. For example, stainless steels are susceptible to pitting corrosion in chloride containing solution. The addition of molybdenum ($>2\%$) to stainless steels dramatically increases resistance to pitting. The pits or cavities formed at the surface act as stress raiser and may ultimately cause failure of the component.
- g. Stress Corrosion : When a component is subjected to high static tensile stress in presence of corrosive environment, stress corrosion cracking may occur. Stress corrosion cracking is mostly intergranular, but transgranular cracking may also occur. In addition to applied & residual stresses and the presence of certain chemicals, the alloy composition and microstructure are important variables affecting stress corrosion cracking. For example, brasses containing 20 to 40% Zn are highly susceptible to stress-corrosion cracking, while brasses with Zn content less than 15% are highly resistant to stress-corrosion cracking. Intergranular cracks in a stainless steel formed due to stress corrosion are illustrated in Fig. 1.2.6.

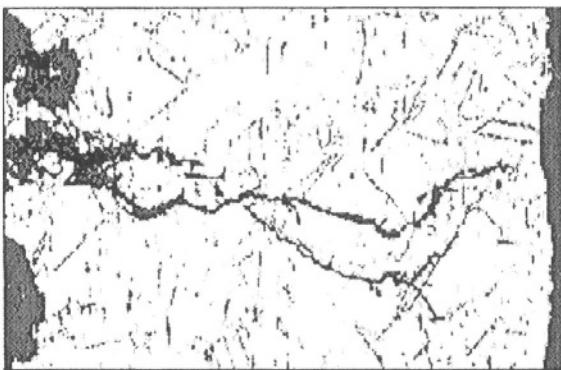


Fig.1.2.6.Stress Corrosion Cracking,X200

Corrosion Prevention:-

Similar to wear corrosion damage can be minimized by surface engineering processes. By suitably altering the surface properties, such as composition and microstructure it is possible to minimize corrosive attacks. Thermally assisted surface engineering processes used to minimize corrosion include the followings:-

- i. Thermally Spraying:- In thermal spraying, various types of coating materials are used to prevent the corrosive media from directly attacking the component's surface. The coating materials may be inert materials, such as polymers and ceramics, or metallic materials which are anodic to the substrate. Inert material forms a physical barrier between the metal and corrosive fluid. However, in the event of corrosive chemicals finding entry through the cracks or porosities in the coating, extensive corrosion of substrate material can result. The polymer and ceramic coatings are extensively used for protection of metallic surface against corrosion. Thermally sprayed dense ceramic coatings are used as seals in pumps carrying corrosive fluids. The surface pores of sprayed ceramic or metallic deposits are to be sealed to prevent ingress of corrosive media. The sealing is carried out by using a suitable sealant such as epoxy or wax or by fusing the surface by suitable a heat source, such as laser. Metallic coating of zinc on steel substrate continues to be effective even when the coating becomes discontinuous exposing the substrate to corrosive environment. Since zinc is anodic to steel and the area of exposed cathodic steel is small, zinc corrodes at a slow rate and the steel remains protected for a long period.

Bridges and structures are protected by thermal sprayed zinc and zinc-aluminium alloy. Some of the Ni-Cr-B-Si-C self fluxing alloys are used for protection of splash zone in offshore well rig. WC-Co deposits improve life of sink rolls in galvanising plant. The Ni-Cr powder alloy provides effective coating on boiler tubes using high sulphur (1.5-5% S)

coal. Reinforcing steel bars for concrete structures last longer with epoxy coating.

- ii. Thermal diffusion of corrosion-resistant elements:- Surface layer can be enriched with corrosion resistant elements like Cr, Al, Si by thermal diffusion processes such as, chromising, aluminising & siliconising. Chromium enriched low carbon steel surface with more than 11% Cr offers corrosion resistance similar to that of 11% Cr-ferritic stainless steel. High chromium surface layer resists high temperature oxidation up to a temperature of around 1000°C. Al-enriched layer can resist high temperature oxidation up to 1200°C.
- iii. Weld overlay:-Working surfaces or the surfaces coming in contact with the corrosive fluids are coated with corrosion-resistant alloy to prevent the structure from corroding. Some recent applications of weld overlays for protection against corrosion include Hastelloy C276 on evaporator plate using sea water, AISI 410 with additional nitrogen for continuous casting rolls (prevents fire-cracking associated with stress corrosion cracking and corrosion fatigue) etc.
- iv. Cathodic protection:-The metallic component is made cathodic by using an impressed voltage by a sacrificial anode. For steel, commonly used sacrificial anode materials are Zn and Mg. The impressed voltage across the metal to be protected and an auxiliary anode (e.g., scrap iron) are provided a direct current source, such as battery. The sacrificial or auxiliary anode materials get corroded and are to be replaced periodically. Cathodic protection is used to prevent corrosion in offshore oil rigs, ships, buried pipelines etc.
- v. Anodic protection or passivation:- The active anodic materials can be made passive by using a overvoltage (Fig. 1.2.2) to form a passive film on the surface of the metal to be protected. The impressed voltage can be found from anodic polarisation curve for the metal in the given corrosive solution. For example, anodic protection of aluminium can be provided by forming a passive film of aluminium oxide with applied overvoltage. The process is known as anodising and the passive film remains even after the withdrawal of applied voltage.
- vi. In joining metals and alloys the best practice is to use same material as welding consumable. In joining two dissimilar metals a more noble metal than either of the two is to be selected as welding.

High Temperature Corrosion & Control (9,10,11):-

Thermally assisted deposit coatings are used to minimize high temperature corrosion in otherwise good creep resistance base material forming the bulk of the components. The corrosion reactions occurring at high temperature are as follows –

- i) Oxidation:- The oxidation behavior of the material depends on the affinity for oxygen of the elements forming the alloy. A variety of oxides can form on the surface, but the resistance to further oxidation shall depend on the oxide forming a stable continuous film. The creep resistant low alloy Cr-Mo steels and low carbon steels (boiler quantity) are capable of withstanding temperatures up to 430°C, without appreciable oxidation. The high chromium (16-28% Cr) containing alloys, such as Fe-Cr (stainless steels), Ni-Cr (Inconels) and Co-Cr (Stellites) alloys, show excellent resistance to oxidation up to a temperature of 980°C, because of stable Cr_2O_3 film. Due to volatile nature of Cr_2O_3 at a temperature of 1000°C, the high chromium containing alloys are susceptible to oxidation at and above 1000°C. The addition of aluminum (up to 5%) to the Fe-Cr, Ni-Cr, Co-Cr superalloys leads to the formation of Al_2O_3 film, which is more adherent than Cr_2O_3 and non-volatile at 1000°C. In a chromium containing alloy less aluminum is required to form aluminum oxide film. The aluminum and chromium containing alloys can withstand temperatures above 1000°C without being subjected to excessive oxidation.
- ii) Carburizing:-The hydrocarbon and carbon monoxide containing atmosphere present in processing equipments, such as, ethylene pyrolysis furnace operating at high temperature may lead to formation of carbides and consequent embrittlement of the alloys. High Ni and Cr containing alloys such as HK 40 (cast Fe-25 Cr-20 Ni), HP alloys (high Ni & Cr plus Nb, W, Mo & Si addition) or more recent one containing aluminum (Alloy 214) resist carburising.
- iii) Nitridation:- Nitrogen containing atmosphere e.g, ammonia in reducing environment can lead to the formation of nitrides in nitriding steels, such as, chromium containing steels at a temperature of around 500°C. The formation of brittle nitrides can cause early failure of the component. Many austenitic stainless steels and nickel based alloys exhibit adequate resistance to nitriding in ammonia.
- iv) Halogen Erosion:- The attack from chlorine (without O_2) at elevated temperatures is resisted best by austenitic stainless steels followed by ferritic stainless steels, cast iron, carbon steel in the order of decreasing resistance. For atmospheres with chlorine plus oxygen, Alloy 214 has shown good resistance at high temperature i.e.; 1000°C. In gaseous hydrochloric acid atmosphere, the use of Inconel 625 (Ni-20 Cr-Cb) and HastelloyC-4 (Ni-Cr-Mo) are recommended.
- v) Sulphidation:- The sulphidation reaction occurs due to presence of either H_2S or SO_2 and salt causing sulphur deposition in oxidising atmosphere. The alloys which are used for resisting sulphidation are SS304, Hast-X, HA-188 and CoCrAlY.

vi) Molten-Salt Corrosion:-The molten salt corrosion or “hot corrosion” is a process of enhanced oxidation and fluxing that destroys protective oxide layers, results mainly from sodium and sulfur from the fuel and the gas stream. The molten deposits of sulphates (Na_2SO_4), chlorides (NaCl) and oxides (V_2O_5) attack the base material after removal of protective oxide film.

The hot corrosion process consists of two stages, viz., initiation and propagation. Since none of the known alloys is immune to attack from hot corrosion, hence the selection is restricted to alloy with a long initiation period .The recommended alloy should contain 10-12% Al, e.g., Co-20 Cr-12 Al-0.5 Y. Deposit-modified corrosion or hot corrosion is observed in boilers, incinerators, diesel engines, mufflers of internal combustion engines, and gas turbines.

Tab.1.2.1 High Temperature Corrosion Service & Alloys(ref 11,12,13)

Corrosion Type	Service Temperature/Application	Coating Alloys
1) Oxidation	980 deg C.	Inconel 600 / 625. Hastelloys, Haynes Alloys. 230 / 188 / 25
2) Carburising	Ethylene Pyrolysis	HK 40 HP Type Alloys Alloy 214
3) Nitridation	Ammonia, Nitric Acid, Melamine and Nylon 66, Production Process	Austenitic SS with high Ni and Co content
4).Halogen i) Chlorine	Metal production industries, viz, Ti, Zr, Nb, W & Ni Manufacture of TiO_2 , SiO_2 Manufacture of Ethylene Dichloride.	C. Steel \rightarrow Cl. \rightarrow Ferric SS \rightarrow Austenitic SS (higher resistance \rightarrow)
	ii) $\text{Cl}_2 + \text{O}_2$	Alloy 214
	iii) Gaseous Hydrochloric	Inconel 625 / Hastelloy C-4
5). Sulphidation	i) $\text{H}_2 \text{ H}_2\text{S}$ Mixture or S-vapour with Low O_2 content/ Gas mixture in catalytic Reforming units in Petroleum Refining.	Fe-Cr, Ni-Cr & Co-Cr alloys with higher chromium content.
	ii) Reducing gas environments containing H_2 - H_2O , CO , CO_2 , H_2S , with O_2 activities high enough to form Cr_2O_3	High Cr alloys, 446, HK-40, HL-40, Inconel 657/ 671 & Haynes 6B, HR-160.
	iii) SO_2 bearing environment.	Ni-Cr alloys with high Cr
6). Basic Fluxing	i) Na_2SO_4 .	Fe-Cr-Al
	ii) V_2O_5	Ni-Cr-Al Co-Cr-Al with 10-12%Al

The purity & type of fuel and air affect the hot corrosion process significantly. For example, the hot corrosion is observed more in industrial and marine turbine than aircraft gas turbine. For aircraft, a special low sulfur fuel, known as ATS grade is used. The various high temperature corrosion applications and the recommended alloys are listed in Table 1.2.1. Coating processes are discussed in the subsequent chapters.

1.3 Surface Properties & Wear

The surface engineering processes are designed to produce wear resistant surfaces by modifying one or more of the following surface properties:-

- Surface Energy
- Surface Morphology, includes macro- & micro-structures, and roughness
- Surface Composition
- Hardness

It is important to know how these surface properties are related to wear and to design surface modification processes accordingly.

Surface Energy:-The surface of the solid or the 'surface phase' retains sufficient free energy in order to remain in equilibrium with the surrounding. Surface free energy is comprised of energy at free surface, which includes energy due to grain boundaries, twin boundaries etc. Residual or internal stress retained in the grains due to deformation, thermal cycling or transformation add to the surface energy of the material.

The effects of surface energy on wear and fracture of the materials are listed in Table 1.3.1. Surface energy is directly related to wear volume and friction coefficient. Alison et.al, (12) have calculated the amount of stored energy per unit volume, E, in the surface region of fully abraded material based on following equation:- $E = f g \mu (M/W\rho)$, where, ρ = density, W = Load, g = acceleration due to gravity, f = the fraction (incremental) work done in causing the specimen to slide on the abrasive surface (0.1% to 0.5% for the fully abraded, work - hardened surface), μ = frictional co-efficient, M = mean wear per cm. The calculated E value is approximately 10^8 ergs / cm² equivalent to $\sim 10^{12}$ dislocations/cm². Assuming f as constant for different metals, Alison et.al, (13) found a linear relation between E, (surface energy in the abraded metal) and H (microhardness) in hexagonal metals. The relation between E and H for cubic metal was found to be parabolic.

Low solid-vapor surface energy (γ_{sv}), large dihedral angle (Ω_s), less grain boundary precipitation and segregation causing promote toughness. According to Smith (14) after prolonged annealing i.e., at equilibrium, the dihedral angle (Ω_s) is a function of the surfaces and grain boundaries

involved. At the equilibrium configuration the dihedral angle is related to surface (γ_{sv}) and grain boundary (γ_{gb}) energies by the following equation:-

$$\gamma_{gb} = 2 \cdot \gamma_{sv} \cdot \cos(\Omega_s / 2) \quad 1a.2$$

With smaller grain diameters (d), larger number of grains results in higher total grain boundary energy at the surface. Grain boundaries offer resistance to dislocation movement. Hence more number of smaller grains compared to less number of large grains in the same surface area shall offer more resistant to dislocation movement. Small grains lead to improved yield strength and fracture toughness.

Table 1.3.1 Effect of surface energy on wear and fracture

Relations	Properties	References
$\gamma \propto \frac{M \mu}{P}$	M=mass, P = density μ = friction coeff.	Alison's equation
$\gamma_{SV} \propto \cos \Omega$	Ω = dihedral angle	Smith's equation
$\gamma_{SS} \propto \frac{\sigma^2}{c}$	σ = applied stress, c= crack length	Griffith's equation
$\frac{\gamma_{SV}}{H} \propto \text{Wear}$	H=hardness	Robinowitz
$\gamma_{SF} \propto 1/WH$	WH= work hardening γ_{SF} = stacking fault energy	Meyer's index
$\gamma_{SF}/H \propto \text{Wear}$	Except for Cu-Zn & Cu-Al alloys	Blau
$\gamma_{SF} \propto \text{creep strain}$	Creep resistant alloys have low γ_{SF}	
$\sigma_R \propto 1/\text{fatigue strength}$	σ_R = compressive residual stress	

The solid-solid surface energy (γ_{ss}) has been calculated from the measurement of fracture stress σ at various temperatures using Griffith equation of fracture.

Griffith's equation on stress required (σ) to form a crack of a length (2a) is as follows:-

$$\sigma = \frac{(2 \cdot \gamma_{ss} \cdot E)^{1/2}}{\pi a}$$

where, γ_{ss} is surface tension and E is Young's modulus.

Hall & Petch equation (15) relates yield stress (σ_y) with grain size (d) as follows:-

$$\sigma_y \propto d^{-1/2}$$

Finer grains improve yield stress and the toughness of the materials. Wear rate is inversely proportional to square root of grain size (1):-

$$\text{Wear rate} \propto d^{-1/2}$$

Robinowicz's (16) equation relates surface energy (γ_{sv}), hardness (H) and wear as follows:-

$$\gamma_{sv}/H \propto \text{Wear rate}$$

Lower surface energy (γ_{sv}) and higher hardness reduces wear rate. Blau (17) found following relation between stacking fault energy (γ_{SF}), hardness (H) and wear:

$$\gamma_{SF}/H \propto \text{Wear rate}$$

Lower stacking fault energy (γ_{SF}) leads to more faulted areas (twins) causing less wear.

The effects of different types of surface energy and wear including fracture are listed in Table 1.3.1.

Surface Morphology: The morphological features of the surface in both macro-and-micro levels are important factors governing the wear and corrosion behavior of the material. On the macro-scale, the surface roughness or general topography of the surface can be considered as the index for surface morphology. The use of a microscope enhances the possibilities of studying the finer details, such as, grain and grain boundaries, different phases, defects, porosities etc, the amount and distribution of which affect the surface properties.

Surface Roughness (18) : The shape of a solid surface in terms of roughness is the deviation of the solid's actual topography from its nominal surface. The surface roughness is expressed normally as the statistical average of undulations in wavelength or height distributions with reference to a line parallel to the nominal surface (19). The roughness of solid surface or surface topography or texture or shape influences the interactive processes of the

surface with the environment. Dawson's (19) work on pitting was probably the first quantitative relationship between surface roughness and wear. Smooth surfaces are less prone to pitting. Dawson in his disc type wear tests, found that for a small slide/roll ratio, the increasing oil film thickness reduces the pitting tendency and the more important factor controlling pitting is the ratio of surface roughness to oil film thickness, i.e., the 'D' ratio. The correlation between the number of revolutions before pitting occurs and the D ratio is almost linear over a 500-fold variations in D-ratio. Onions and Archaid (20) repeated the experiment using actual gears and discs, and found that the life was dependent on 'D'-ratio for both disc and gear. However using the same material, the life of a gear was found to be one-hundredth of the discs. Fatigue failure of clean steel, i.e.; inclusion-free steel, is strongly dependent on the ratio of film thickness to surface roughness, i.e., D ratio. In view of improvements in steelmaking practice resulting in the production of inclusion free steels, the bearing industries are now have to concentrate on surface roughness of the bearings. The surface roughness also plays an important role in the failure of gears by scuffing. The fatigue strength of shafts possessing different UTS are evaluated over a range of surface roughness for 10^7 reversals (Fig. 1.3.1). The fatigue strength of shaft with same UTS has been found to decrease with increasing surface roughness values (1). For example, for a 80 t.s.i (1100 MPa) shaft, the polished surface with Ra of 0.25 to 0.5 micron (A) resulted in a fatigue strength of 40 t.s.i (550 MPa), ground surface of Ra as 1.0 to 1.5 micron (B) indicated fatigue strength of 35 t.s.i (480 MPa) the HVOF sprayed surface of R_A is 1.5 to 2.2 micron (C) had the strength of 30 t.s.i (410 MPa) and the milled surface of 2 to 2.5 micron (D) resulted in fatigue strength of 27 t.s.i. (370 MPa). The HVOF process of deposition of material on the surface generally has no effect on fatigue strength excepting slight increase in certain cases due to surface preparation by grit blasting before spraying. The relation, between surface roughness and wear properties are summarized in Table 1.3.2.

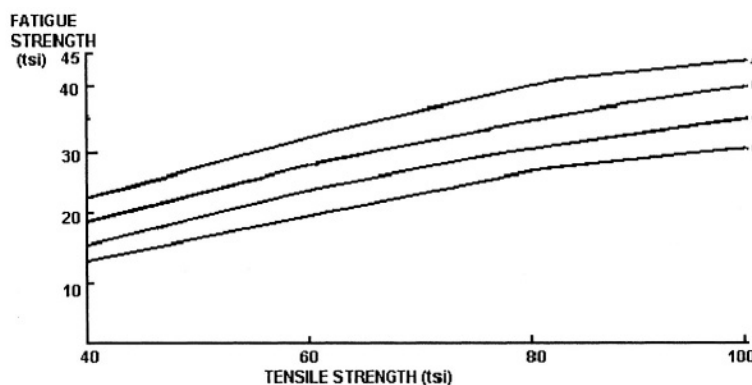


FIG.1.3.1. FATIGUE STRENGTH Vs. SURFACE FINISH

Table 1.3.2. Surface Roughness and Wear Properties

Surface Roughness(SR)	Properties	Application
1.Very low SR(less lubrication)	directly related to wear	Galling or Seizure
2.S.R/oil film thickness(D ratio)	directly related Pitting	Gears
3.SR	inversely related to fatigue life	Clean bearing steel
3i.Hardened shaft(SR)	ditto	
3ii.Nitrided shaft(SR)	ditto	

Surface Microstructure : The wear of materials depend on the type, amount and distribution of different phases present in the surface. Micro-constituents of crystalline materials consist of grains (of single or multiple phases), precipitates, inclusions and defects. The type of matrix (e.g., hard martensitic or soft austenitic) along with the amount and distribution of other micro-constituents, such as, precipitates (carbide/boride/aluminides/silicides), inclusions (MnS , SiO_2 , Al_2O_3), twins etc. are important factors affecting the wear & other properties of the material.

- *Grain size*: Finer grains of the modified surface shall result in improved wear and crack resistance properties. Grain refining process is thus a recommended step for refining coarse grained structure produced by surface hardening treatment such as carburising.
- *Matrix structure*: Hardness and the wear resistance of a medium carbon steel increases as the matrix changes from pearlite (+ferrite) through bainite to martensite. While martensitic matrix has been found to cause least wear in case hardened surfaces of gears, shafts, pinions, axles etc, fully pearlitic fine structure has shown low wear in railroad rails. The rapid workhardening of the tough austenitic 14% Mn steel (Hadfield steel) under repetitive impact load results in highly wear resistant surface. The material is extensively used as weld overlays for railway crossings, crushing hammers, crusher mantle etc.
- *Other phases*: Fine, uniformly distributed hard precipitate phases, such as carbides, borides, aluminides, silicides lead to improvement in the wear resistance properties of the material. For example in a Ni-Cr-Fe-Si-C alloy used for hard facing engine valves the amount and distribution of carbides and silicides play an important role in determining the high temperature wear properties.
- *Inclusion*: The presence of elongated type-II, MnS inclusion can lead to lamellar tearing (21), whereas uniformly distributed fine sulphide inclusions improve mach inability. The subsurface inclusion is partly responsible for flaking of surface layer from the weld overlay of railway crossing (22).

- *Point, line and plane defects* :- The presence of point defects leads to distortion of the lattice and therefore higher applied stress is required to cause deformation. The yield point phenomenon in carbon steel has been explained as due to the stress required to separate carbon atoms associated with the lattice defects. The movement of line defects or dislocations leads to deformation of materials by the process known as slip. The deformation process leads to the formation of work-hardened surface areas with high dislocation density. The work hardened surface of the pre-stressed or stressed in-situ during use shows low wear rates.

Plane defects are the boundary regions separating materials of same crystal structure but of different orientation. Some examples of plane defects are grain boundaries, stacking faults and twins. In low stacking fault energy materials, such as FCC metals (Fe, Cu), fault occurs in the stacking sequence resulting in the formation of HCP structure in the faulted region. The stacking fault in the lattice also interferes with the slip process. Some of the effects of micro-constituents on wear are listed in Table 1.3.3.

Table 1.3.3 Effect of Microconstituents on Wear Behavior(1)

Microconstituents	Size/Shape/Distribution	Wear /ref
1. Grains	Small/equiaxed/uniform	High YS/low wear High toughness/low wear
2. Martensitic matrix	Twinned Acicular* lath martensite**	High hardness/low wear Ultra high strength/low wear!
3. Precipitates	Fine/discrete/uniform	High hardness/low wear
4. Hard carbides/nitrides borides/silicides in coatings	Fine/layered deposit in Thermal spray process in Spray fused deposit*** in Vapour phase deposit in Weld overlay**	High hardness/low wear
5. Aluminides e.g., Ni ₃ Al	Fine/discrete/uniform	Improves creep rupture properties Improves Oxidation resistance(>1000)
6. TCP phases e.g., Ni ₃ Si	Fine/discrete/uniform	Improves high temp.wear resistance
7. Glassy structure (cooling rate>10 ⁴ K/s)	Amorphous	Improves wear & corrosion properties

*(0.5-1.0% C-steel) ** (maraging steel matrix) ***(metal matrix)

Surface Composition:- Surface composition plays a leading role in resisting wear. Large numbers of thermally assisted processes have been used to alter surface composition in order to minimize wear. The capacity of a given surface to resist wear is improved by either altering the surface composition or by coating the surface with a chemistry conforming to that of a wear resistant material.

The role of composition in minimizing wear can be summarised as follows:-

i. *In the processes for modification of original surface:-*

- *thermal cycling process*:- Composition of steel in induction or flame heated surface should be such as to form martensite during quenching in specified quenching medium. The cooling rate should exceed the critical cooling rate, and material should be cooled through Ms-Mf range. Critical cooling rate, Ms, Mf & Ms-Mf range depend on the composition of the steel. The addition of carbon & other alloying elements in general reduces the quenching severity required for martensite formation. By thermal cycling there is no change in surface composition excepting the formation of a thin decarburized layer.
- *diffusional processes* :Diffusion of interstitial and or substitutional elements leads to increase in alloying elements in the surface layer. The addition of Interstitial in the surface layer allows martensite to form in this region on quenching. The additions of substitutionals like Cr, Mo, improve corrosion & wear resistance of the enriched diffused layer at the surface.

ii. *Coating Processes*: Fresh wear resistant surface layer is added in the coating processes. However the base material surface compositions may or may not change depending on the process employed.

- *thermal spraying & PVD* :- Base material composition is not affected.
- *spray fusion & CVD*:- Diffusion of coating material occurs in the high temperature CVD and spray fusion processes.
- *welding*:-The mixed weld pool containing molten consumable and the surface layer of the base metal has different composition than that of the consumable electrode or base metal. Thus the dilution of the weld overlay by elements from base metal occurs in welding processes. The high dilution can drastically change the wear resistance properties of the weld overlays.

Surface Hardness:- High hardness in the surface layer is normally developed by controlling the surface composition and microstructure. Hardness of a surface is inversely proportional to the wear rate. Thermally assisted surface engineering processes are designed mostly to increase the surface hardness to a level where the particular type of wear can be reduced to a low value. Some

of the widely used wear surfacing processes, like welding & thermal spraying are called **hardfacing**. The wear resistant consumables are known **hardfacing alloys**. The surface hardness is the commonly accepted index for wear in hardfacing industry.

1.4 Heat Energy & Thermal Processes in Surface Engineering :-

The heat energy is used to modify the surface properties, such as, morphology and composition in the thermally assisted surface engineering. The heat energy is primarily used to carry out the unit processes in surface engineering such as solid state transformation, diffusion, melting and evaporation. Materials are heated to high temperatures for structural transformation or for faster diffusion of elements or to melt a thin layer in the surface. Alternatively, the wear resistant coating materials are deposited onto the substrate as molten or semi-molten or vapor phase. Materials differ in their heat requirements to attain the same temperature level, due to differences in their specific heat values. For phase transformation to occur at the equilibrium temperature, additional heat equivalent to the latent heat of the transformation is to be supplied or abstracted. Following phase rules, the boundaries amongst the thermodynamically stable phases in equilibrium at different temperatures and concentrations are shown in the phase diagram. Phase diagram has been used to design various surface engineering practices. The thermal processes, like, diffusion, vapor phase deposition, welding and thermal spraying can be carried out by using different heat sources, such as, combustion, plasma, laser, electron, ion etc.

Heat Energy:-

The heat unit is defined as the heat energy required to raise the temperature by 1 degree for a unit mass of water. The correlation amongst the different energy units are as follows:-

1 Kcal = 1000 cal = 3.968 Btu = 4186 Joules; 1 Btu = 2520 cal = 777.9 ft.lb; 1 eV = 3.827×10^{-20} cal = 1.519×10^{-22} Btu = 1.602×10^{-19} Joules. (1 joule = 1 watt-sec 1 watt = 1.341×10^3 HP = 0.7376 ft-lb/sec = Btu/h = 0.2389 cal/sec).

Specific heat & heat capacity

The ratio of heat ΔQ supplied to a body to its corresponding temperature rise ΔT is the heat capacity, C_h of the material. The heat capacity, C_h , is thus the heat input required per unit temperature rise. The heat capacity per unit mass of a body is called specific heat 'C', where

$$C = C_h / \text{mass} = \Delta Q / \Delta T$$

or temperature rise in the material, $\Delta T = \Delta Q/mC$, where m is the mass of the material.

Higher heat input, ΔQ , is required to raise the temperature to the same extent (i.e., same ΔT) for larger mass of materials or materials of higher specific heats.

Tab. 1.4.1 Specific heat and molar heat capacity of some solids

Materials	Sp.heat, C_p cal/gm °C	Atomic weight gm/mole	Molar heat capacity cal/mole °C
C	0.121	12.0	1.46
Mg	0.2436	24.3	5.92
Al	0.215	27.0	5.82
Cu	0.0923	63.5	5.85
Ag	0.0564	108	6.09
Ni	0.1047	58.7	6.14
W	0.0321	184	5.92
Fe	0.1047	56	5.86

Specific heat varies with temperature, pressure and volume. To obtain a unique value of C , the conditions need to be specified, such as, constant pressure C_p , or constant volume C_v . The molar heat capacity (specific heat x molecular weight) increases rapidly with temperature and reaches a limiting value of $3R = 6$ cal/mole at Debye characteristic temperature, θ , or higher. Few exceptions to this rule includes carbon. (Table 1.4.1).

Free energy and latent heat for phase changes:-

The polymorphic or phase changes occur by a decrease in free energy, with lower energy phase becoming stable. The change in free energy (ΔF) is related to change in internal energy (ΔE) and the entropy change (ΔS) as follows:-

$$\Delta F = \Delta E - T\Delta S,$$

where S can be expressed in terms of C_p , as follows:-

$$S = \int_0^T (C_p/T) dT$$

The free energy decreases as the temperature increases. The free energy decreases rapidly with increasing specific heat., The phase with lower free energy is the stable phase. According to free energy considerations, the WC phase is least stable compared to TiC, TiN, & Al_2O_3 over the whole range of temperatures for applications of tungsten carbide cutting tools. For example, over a temperature range of 600-1800K, free energy of formation of WC is approximately (-) 5 Kcal g-atom⁻¹, compared to that of TiC as approximately (-) 20 Kcal g-atom⁻¹ (23). The free energy values for TiN & Al_2O_3 are much less. This is the main reason for coating tungsten carbide with more stable compounds such as TiN, TiC or Al_2O_3 . The vapor phase deposition of the coating materials on WC lead to vast improvement in the wear resistance of carbide cutting tools. During the phase transition occurring on heating or cooling, practically all the energy is absorbed or liberated in terms of heat, and in such cases the change is sensibly equal to the latent heat, ΔQ , which can be measured calorimetrically. Since the free energies of the old and new phases are equal at the change point, $\Delta F = 0$, and thus $0 = \Delta E - T\Delta S$, or

$$\Delta S = \Delta E/T = \Delta Q/T,$$

The entropy change is thus the latent heat divided by the transition temperature. Due to differences in cohesion, the latent heats of melting are spread widely over the range of 500 to 5000 cal./mol. Since the melting point also increases with increasing cohesive strength, the entropy of melting (latent heat divided by melting point, $\Delta Q/T$) is insensitive to differences in cohesion. In fact, the entropies of melting most metals fall in the range of 2 to 5 cal/deg/mol. The latent heat of fusion data for some materials are given in Table 1.4.2.

Table 1.4.2 · Enthalpy of Phase

Transitions ($\Delta H/\text{kJmol}^{-1}$)

Material	Enthalpy of Fusion	Enthalpy of Vaporisation
NH ₃	5.633	23.4
Hg	2.33	58.1
Ag	11.3	254
Na	2.601	98.01

The phase transitions include evaporation ($\Delta H_{\text{vap}} = \text{enthalpy of vaporization or latent heat of vaporization}$), melting or fusion, (ΔH_{melt}) and changes in

crystal form or transition (ΔH trans). The total heat required for phase transformation = Heat required to rise the material to transition temperature by ΔT + Latent heat for the transformation = $\Delta Q + \Delta H = \Delta T \cdot m \cdot C + \Delta H$.

The melting of pure metals and compounds and also the polymorphic changes are called *first order changes* where entire transition occurs at a single temperature, since the heat (latent heat) is absorbed without a rise in temperature.

Melting

The heat required for melting a material at the melting point is the latent heat of fusion plus the heat required to raise the temperature to the melting point. Heat required for melting = $\Delta Q (\Delta T \cdot m \cdot C) + \Delta H_{melt}$. The latent heat of melting increases with the melting point of the material, thus requiring more heat for melting high temperature materials. Surface melting in a short span requires a high intensity heat source like laser. For fast melting of consumables in welding or thermal spraying arc, laser, plasma and electron guns are used.

Vaporization & Condensation

A solid like liquid has a definite but low vapor pressure. The vapor pressure of solid increases with temperature. The change from solid to vapor is accompanied by analogous change from liquid to vapor, by absorption of heat, i.e., the latent heat of sublimation, represented by L_s cal. per mole.

Using Clapeyron-Clausius equation for solid-vapor equilibrium:

$$\frac{dp}{dt} = \frac{L_s}{T(V_v - V_s)}$$

By neglecting the volume of solid V_s with respect to V_v , and assuming latter behavior corresponds to that of an ideal gas (i.e. $pV_v = RT$), the following equation can be derived:-

$$\frac{d \ln p}{dt} = \frac{L_s}{RT^2} = \frac{\Delta H}{RT^2}$$

where $\Delta H = L_s$ and represents the heat absorbed at constant pressure per mole of solid vaporized. Some data on the enthalpies of phase transition during melting and vaporization are given in Table 1.4.2.

The heat required for vaporization of a material at the melting point is the enthalpy of evaporation plus the heat required to raise the material to the vaporization temperature.

$$\text{Heat required for vapourisation} = \Delta Q (\Delta T \cdot m \cdot C) + \Delta H_{vap}$$

The enthalpy for vaporization is several fold higher than enthalpy for melting. Thus the heat required for evaporation is much more than that of melting. The rate of evaporation of atoms from the surface is expressed by derivatives of Langmuir equation as follows (24):-

$$J = 5.83 \times 10^{-2} (M/T)^{1/2} \pi$$

where J = flux in $\text{g/cm}^2\text{s}$; T = degree Kelvin; M = atomic weight of evaporating species; π = vapor pressure of the evaporating species in torr. The evaporation equation is valid only for evaporation in perfect vacuum. The vapor pressure is an exponential function of the temperature and therefore, the rate of evaporation increases dramatically where the surface temperature is high. The heat sources for evaporation normally consist of rays and beams (plasma, electron and ion etc) which can be focused to small areas to develop high heats required for higher vaporization. In a multi-component system the vapor pressure of any component varies from its pure state vapor pressure by the relationship:-

$$P_i = a_i P_i^0$$

where P_i = actual vapor pressure of the component, a_i = activity (approximately concentration) of the component in the system, P_i^0 = vapor pressure of the component in its own liquid (or solid) at the same temperature. The evaporation rates of different components in a multiphase alloy can vary widely depending on the concentrations, vapor pressures and the melting points of individual species.

Unlike other evaporation processes, sputtering permits transformation of the original material to the vapor phase as a direct result of impulse ablation of the target without any intermediate liquid phase. Also there is less danger of decomposition in a multi-component alloy than in the case of electron beam induced vaporization (25).

When the substrate is held at very low temperature, vacuum evaporation and subsequent condensation of the vapor on the substrate may lead to the formation of amorphous phase. Other alternative is to form volatile compounds like halides of the metal to be deposited, where a wider choice of heat source is available. In chemical vapor deposition process, the vapor phase can be a reactive gas or volatile compound, such as CO or metal halide (e.g. AlCl_3) which decomposes on substrate surface resulting in deposition of metallic or nonmetal elements. In CVD, the substrate is also heated.

1.4.1 Phase Rule & Phase Transformations

In a condensed system (where effect of pressure is not included), containing C numbers of components, and P number of phases in equilibrium,

thermodynamic considerations lead to allowed degrees of freedom, F, as follows:-

$$F = C - P + 1$$

The phase or equilibrium diagrams defining the phase boundaries of alloy systems with the variation in temperature and concentration are drawn in accordance to the phase rules. Phase diagram is the blue print of the alloy system. The diagrams can provide information on the complete range of possible alloys & phases at different temperatures and compositions at equilibrium in multicomponent systems. The available data include the followings:-

- i. *Eutectic, eutectoid, peritectic transformation* take place at a fixed temperature & composition. For example, at eutectic or peritectic point, the degrees of freedom (F) for a binary system (C = 2) with three phases (P = 3) involved is zero, and therefore no change in temperature or concentration can occur until the transformation is complete. For ternary system, four phases at equilibrium leads to eutectic transformation.
 - *Eutectoid reaction* (Fig. 1.4.1), at $727^{\circ}\text{C}/0.77\% \text{ C}$, $\gamma \rightarrow \alpha + \text{Fe}_3\text{C}$, leads to pearlite formation. In eutectoid, hard & soft phases are uniformly distributed (Fig. 1.4.2) resulting in strong, tough and wear resistant material. Pearlitic steel (0.8% C) is used for as 90 kg rails to resist wear in high GMT (gross million tons carried over the rails per year) tracks.
 - *Peritectic reaction*, at $1495^{\circ}\text{C}/\text{C } 0.17$, Liquid + $\delta \rightarrow \gamma$ leads to decrease in delta ferrite content. To reduce the hot cracking austenitic stainless steel weld overlay, minimum of 4% delta ferrite is required. Fast cooling of the weld ensure presence of delta ferrite ($\geq 4\%$).
 - *Eutectic reaction* (Fig. 1.4.2), at $1148^{\circ}\text{C}/4.3\% \text{ C}$, Liquid $\rightarrow \gamma + \text{Fe}_3\text{C}$, leads to the formation ledeburite eutectic (Fig. 1.4.3), which has a herring-bone type structure. Ledebuile containing alloyed white CI is used for weld overlay to resist abrasive (mining) or erosive wear (ID fan).
- ii. *Melting points & solidification* temperatures of alloys conforming to any composition of the system can be obtained from the equilibrium diagram. Eutectic composition is the lowest melting point alloy in the system. The near eutectic compositions in hypo- and hyper- ranges are the low melting alloys in an alloy system. Low melting point alloys are used in designing low heat input hardfacing consumables for welding and thermal spraying.

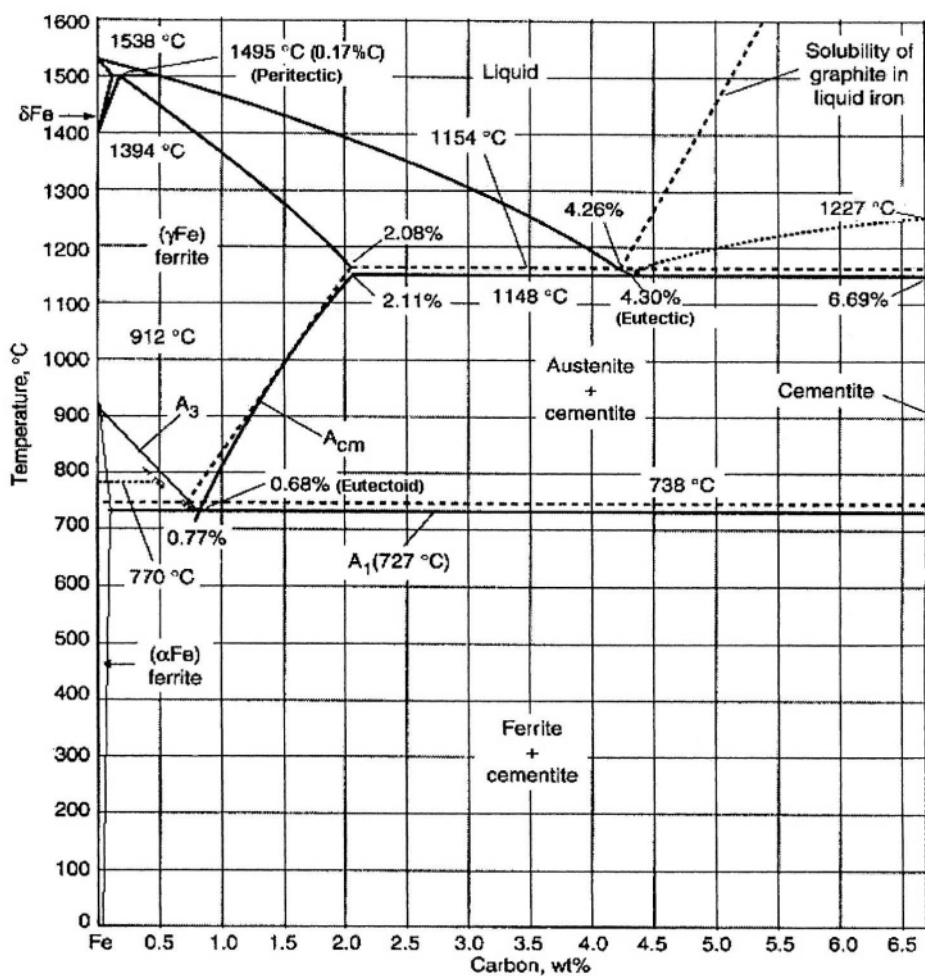


Fig. 1.4.1. Fe-Fe₃C Equilibrium Diagram (---lines represent Fe-C diagram)

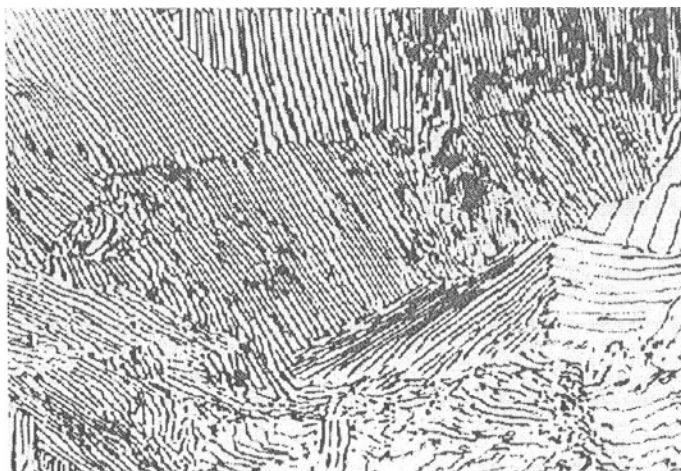


Fig.1.4.2. Eutectoid Pearlite in Fe-0.8%C steel; Alternate lamellae of ferrite(white) & cementite(dark)

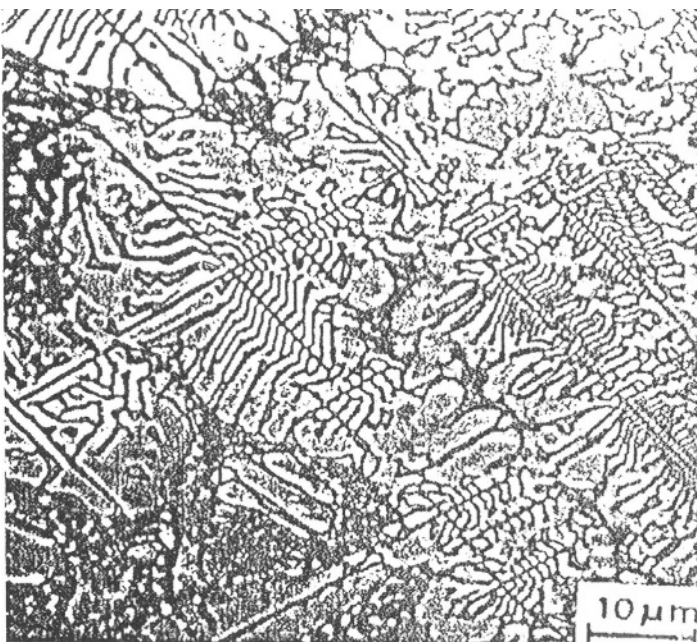


Fig. 1.4.3. Ledeburite Eutectic in Alloyed Cast Iron

A series Ni-Cr-B-Si alloys fusing in the range of 900-1050°C has been used in a large number of industrial applications involving steel or cast iron substrate. The quaternary diagrams comprising of Ni-Cr-B-Si has been used

to find the equilibrium phases and their amounts & fusion temperature ranges. In these alloys, the formation of hard borides and silicides are responsible for making the deposits wear resistant (1).

iii. *Information on transformation temperatures* and thus the heat treatment & hot working temperatures of the composition conforming to that of the work piece can be obtained from phase diagram. In Fe-C system, the austenising temperature varies from 910°C ($\text{C} \approx .01\%$) to 723°C ($0.8\% \text{ C}$). For the heat treatment operations, such as carburizing, annealing etc., involve heating up to γ -region. The optimum temperature close to phase boundaries is normally selected since higher temperatures lead to grain coarsening & embrittlement by grain boundary melting.

iv. *Diffusion of elements* in an equilibrium system follows the phase rule. In a binary system, diffusion can occur in single phase region ($F = 2 - 1 + 1 = 2$), concentration can vary even if temperature remains fixed. For example, in Ni-Cu system, Ni and Cu are soluble in each other over the entire range of temperature and composition without any intermediate phase formation, and therefore Ni-Cu diffusion couple at 700°C shall result in a gradual concentration gradient of Cu in nickel substrate (Fig. 1.4.4a). However, if there is an intermediate phase formation, then $F = 2 - 2 + 1 = 1$, and at a fixed temperature there is no change in concentration. For example in Cu-Ag diffusion couple at 700°C , the diffusion of Cu in Ag shows a sudden discontinuity at the two phase interface due to a stable phase formation (Fig. 1.4.4b).

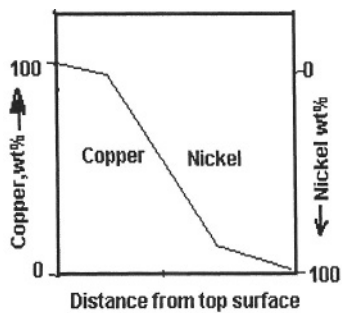


Fig.1.4.4a Concentration gradient in Cu-Ni diffusion couple (Schematic)

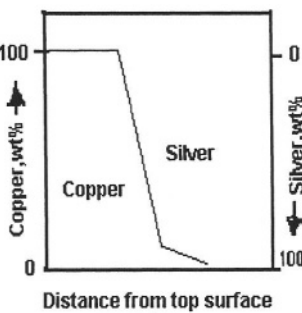


Fig.1.4.4b. Concentration gradient in Cu-Ag diffusion couple (Schematic)

Therefore the formation of a second stable phase, such as stoichiometric compound with no measurable solid solubility shall restrict the diffused layer at a very thin coating thickness of up to the interface with the compound. Also the compound should act as a diffusion barrier to further

diffusion of coating elements inside the substrate at the elevated service temperatures, and thereby reducing the chances of embrittlement at greater depth and alteration in coating composition.

Beyond binary nitrides and carbides, further development of wear resistant coatings by vapor phase deposition include innovative hard compounds belonging to ternary and quarternary systems such as Ti-Al-N, Ti-Zr-N and Ti-Al-V-N (26). For example, in a ternary Ti-Al-N system, the formation of a stable thin oxide layer on the (Ti, Al)N coating when used at high temperature shall serve to diminish diffusion from or into the coating. The diffusion wear is one of the main wear mechanisms affecting cutting tools, the drastic reduction of which shall result in vast increase in tool life (25).

- v. *Phase stability at different temperatures*:- It is possible to stabilize a high temperature phase to room temperature by altering compositions as required by the equilibrium diagram of the components.

For example, high temperature austenitic phase is made stable at room temperature with the addition of 18% Cr and 8% Ni to low carbon steel. Surface alloying by laser fusion or by diffusion processes are used to alter the surface compositions, so as to form wear and corrosion resistant phases at the surface. The addition of 10% MgO to ZrO_2 results in the stabilization of cubic phase. Without stabilization, zirconia rapidly transforms from a monoclinic to a tetragonal form and back again upon heating and cooling. Thermal expansion and contraction associated with transformations occurring during thermal cycling lead to cracking in unstabilised ZrO_2 coatings. The stabilized ZrO_2 is used extensively as thermal barrier coating material in gas turbine and diesel engine components.

Equilibrium & Reaction Kinetics: The diagrams based on phase rules or phase diagrams of different systems provide information on the possible equilibrium phases in a system, which can exist over the range of compositions and temperatures. However the kinetics would ultimately decide the course of the reaction. For example, the thermodynamically stable phase in Fe-C system (Fig. 1.4.1) is graphite, but the slow reaction kinetics of graphite do not favor its formation. The carbide is formed on normal cooling from equilibrium temperatures. The first stage graphitization requires heat treatment for around 10 hours at 925°C to decompose carbides into equilibrium phases, namely, gamma and graphite. For second stage decomposition of gamma into alpha and graphite it requires holding at eutectoid temperature range (760-700°C) for around 25 hours. The decomposition reactions are faster at higher temperatures and thus possible to reach equilibrium faster at higher temperatures.

Rapid solidification process (RSP) of the thin molten layer leads to the formation of fine crystalline to amorphous material depending on the cooling rate. Rapid solidification from liquid state can result in following three types of metastable metals and alloy, viz., supersaturated solid solutions (solute atoms retained in the parent lattice in excess of equilibrium concentration), non-equilibrium crystalline phases, (rapid quenching from liquid, can lead to the formation of a crystalline phase which does not exist under equilibrium conditions), and amorphous phases (if crystallization process can be suppressed by rapid quenching from melt, vapor or solution, amorphous state can be obtained). Rapid cooling from austenitising temperature results in the formation of non-equilibrium phases such as bainite and martensite depending on the cooling rates and compositions.

1.4.2 Surface Property Modification & Thermal Processes

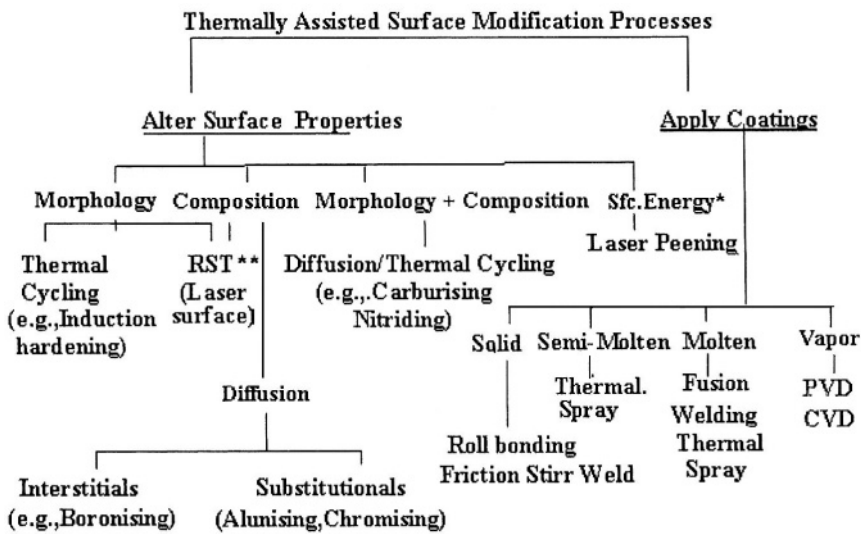
In thermally assisted surfacing processes the heat energy is used for making changes in surface properties, such as morphology, composition and energy in order to develop the required wear resistant properties. The thermal energy is used for either altering the existing surface properties or depositing suitable wear resistant coating (Table 1.4.3).

Thermal cycling is used to change the ferrite-pearlite structure to hard martensite in alloy or medium carbon steels. On rapid cooling from austenitising temperature, the transformation of austenite to martensite results in the formation of a hard wear resistant surface layer. Surface melting in a short span requires a high intensity heat source like laser. Rapid solidification of laser melted thin surface layer can result in the formation of glassy or amorphous structure. The surface with amorphous structure has excellent corrosion resistance properties.

Diffusion of substitutional alloys like chromium or aluminium produces high chromium or aluminium containing wear and hot corrosion resistant surface. Diffusion of interstitial elements, like carbon or nitrogen to low carbon steel surface produces interstitial enriched surface, which on rapid cooling results in the formation of hard wear resistant martensite.

The coating of wear and corrosion resistant materials leads to the formation of a new surface with altered composition and morphology. In fusion welding the base metal also melts forming a molten pool along with wear resistant alloys. In thermal spraying the composition of base material remains unaltered. High temperature CVD process is accompanied by diffusion of coating material. PVD is similar to thermal spraying and the base material composition does not alter. Vapor phase deposition processes are used to deposit thin layer of refractory materials, such as, hard carbides, nitrides and diamond coatings. Weld overlay mainly confined to metallic deposits. However heat sources like plasma and laser has been used to deposit

number of metal matrix composites containing refractory materials. In welding it is possible to deposit thick overlays. Thermal spraying can be used to coat metal ceramic and plastic on any one of these as substrate materials. The coating thickness of thermal spray deposit is normally confined to 3 mm.



Tab.1.4.3. Surface properties & modification processes using thermal energy
(Sfc. Energy* = Surface Energy; RST = Rapid solidification of melt or vapor)

1.4.3 Heat Sources

A large number of thermally assisted processes used for surface modification is based on the application of heat energy. Newer sources of thermal energy, such as plasma, laser & solar beams are increasingly being used to modify the surface properties. The innovations in conventional heat sources, such as arc, spark, induction & combustion processes have resulted in the development of newer & more efficient systems for surface modifications. Different sources for heat energy, power densities and maximum power generation capabilities are listed in Table 1.4.4 (1). Power density is expressed as KW/m^2 . The power density of beams, such as, laser, electron, ion and light can be enhanced by focusing onto a small spot area. Therefore the power densities of beams and rays are more than that of conventional combustion system.

Tab.1.4.4 : POWER DENSITY OF DIFFERENT HEAT SOURCES

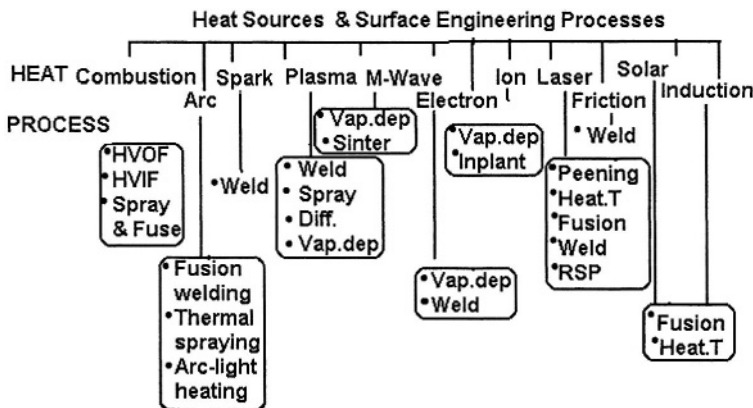
Sources	Power Density $\times 10^3 \text{ W/m}^2$	Maximum Power $\times 10^5 \text{ W}$
Sunlight (focussed)	0.01	--
Combustion (Furnace)	0.01 - 0.05	--
Arc Light (Focussed)	0.05	0.01
Rocket Combustion	0.1	-
Arc (Welding)	0.2 - 7.0	0.05
Ion Beam	1 - 5	0.1
Plasma Beam	1 - 100	1-5
Electron Beam	10 - 1000	1-1.2
Laser Beam	10 - 1000	0.1

Power density of welding arc is only $0.2-7 \times 10^3 \text{ W}$, compared to $10-100 \times 10^3 \text{ W}$ for plasma and more than $100 \times 10^3 \text{ W}$ for laser. Laser and electron beams can be accurately focused to very small areas thus increasing power density several times compared to other sources. Combustion processes can produce power densities of $0.01-0.05 \times 10^3 \text{ W}$ (in furnace) to $0.1 \times 10^3 \text{ W}$ (in rocket). Solar energy, which is normally received on earth at 14 KW/m^2 can be focused to yield few MW/m^2 . The heat generated by frictional processes in welding is in the range of $3.25 \times 10^3 \text{ W}$.

Microwaves (radar waves) or MM-waves (1), are defined as the electromagnetic radiation spectrum at frequency range between 3×10^9 to $3 \times 10^{11} \text{ c/s}$, wavelength of 10^{-1} to 10^{-3} m and photon energy of 10^{-5} to 10^{-3} eV . Microwaves are part of electromagnetic spectra in the frequency range between 300MHz to 300GHz, which on striking a non reflecting surface result in heating .The electromagnetic energy of the absorbed microwaves are converted into thermal energy. Microwave has been successfully used in CVD process to produce diamond film on suitable substrate.

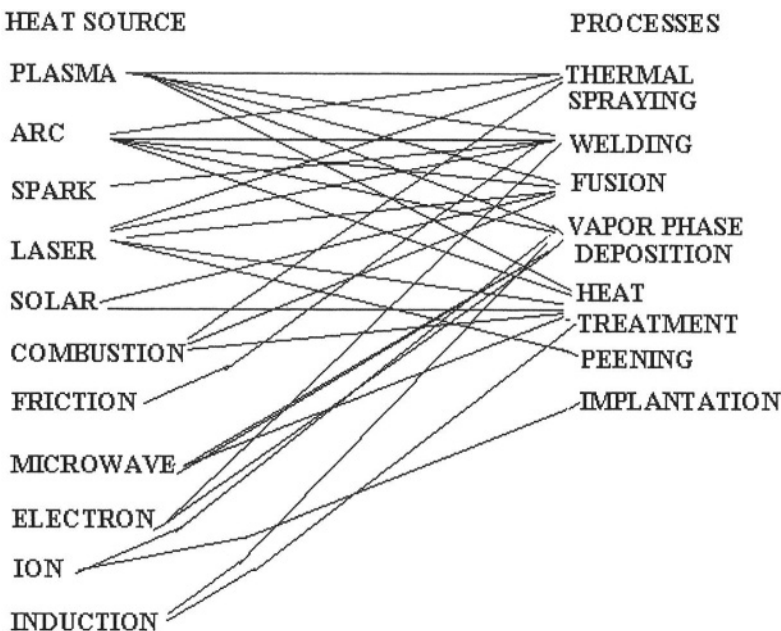
The various surface engineering processes based on different heat sources are tabulated in Table 1.4.5. The correlation between heat source and the processes are listed in Fig. 1.4.5.

During recent years, the heat energy of plasma has been used for a large number of surface modification processes, such as, carburising, nitriding, vapor phase deposition of hard carbides & nitrides, thermal spraying and welding.



Tab.1.4.5.Advanced processes based on eleven different heat sources
(Vap.dep. = vapor phase deposition,Heat.T= transformation hardening)

Fig.1.4.5.Relation Amongst Processes & Heat Sources



In most of the thermal spray processes, higher heat energy sources are used to melt or partially melt the particles to be deposited during the short dwell time of high velocity processes. Advanced heat sources such as plasma or efficient internal combustion processes are used to produce high velocity flames for thermal spraying. Molten or semi molten particles with high

velocity produce dense coating with good bonding to substrate. Hotter flames also need less dwell time for the particles to get molten and hence less chance of oxidation or decomposition. In fusion welding high intensity heat sources are used to melt narrow width of the adjoining base material along with faster melting of the consumables. The use of high intensity heat source results in welds with low dilution, narrow HAZ and less distortion.

High energy laser beams are being used for surface modification by peening, heating, fusing and welding. Besides welding, arc light beams have been used successfully for surface modification by heating. Pulsed arc welding results in vast improvement in the properties of weld overlays. Induction fusing of thermally sprayed deposit has obviated the need to heat the whole component while using conventional flame fusing system. Spark deposition process has been used to deposit thin layers of hard carbides on cutting tools. The concentrated solar beams have been used both for heat treating and fusing the surface. In friction stir welding, frictional heat has been used to make weld overlay of wear resistance alloys on solid surface. Combustion process has been used in the advanced thermal spraying system, known as, high velocity oxy fuel (HVOF).

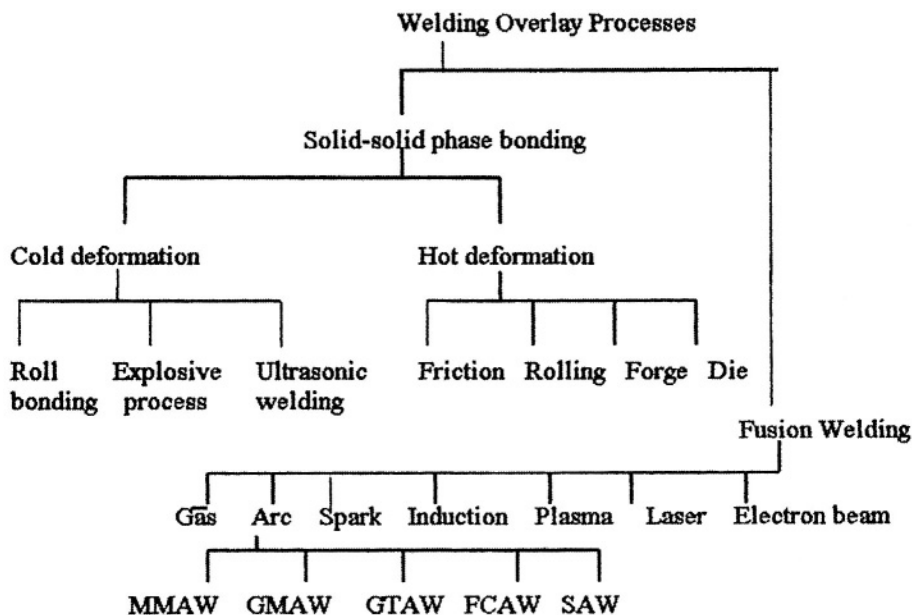
The thermal processes like welding can only be used for deposition of metallic materials on metallic substrate. On the other hand plasma, laser etc are been used to modify the surfaces of metal, polymer, ceramic and composites.

Advanced Heat Sources in Welding:- Welding is the most widely used technique for heavy deposition of wear resistant metallic materials on metallic surface. The weld surfacing with wear resistant material can be carried out by solid state bonding or through fusion processes (Table 1.4.6).

Solid phase bonding between metallic surfaces is obtained by cold or hot deformation processes. Hot deformation processes include friction, forge and roll bonding. The cold processes, such as, roll, explosive and ultrasonic bonding involve cold deformation.

The fusion welding processes derive their names from the heat source, such as, oxy-acetylene, arc, spark, resistance, induction, plasma, laser and electron beam. In hot deformation processes, no external source of heat is required. Heat generated by friction at the abutting surfaces by the applied load is sufficient to weld the materials involved.

Tab.1.4..6: WELD OVERLAY PROCESSES



In fusion welding the abutting surfaces are joined by fusing the interfacial areas with or without additional consumable materials. Excepting gas and manual metal arc techniques, all other fusion welding processes can be automated. The commonly used processes include gas metal arc (GMA), gas tungsten arc (GTA), flux-cored arc (FCA), electro-slag (ES) and submerged arc (SA) welding. Advanced processes with more intense heat sources include plasma transferred arc, laser and electron beam welding

Due to low dilution of the deposited coatings, the plasma transferred arc welding (PTAW) using powder alloys is gaining popularity as the key process for deposition of wear and corrosion resistant coating materials. In PTAW, the dilution level can be restricted within 5% resulting in a single layer thin deposit with composition conforming to that specified for the wear & corrosion resistant alloys. With laser welding it is possible to have deposits with lower dilution than PTAW. However the high capital cost of the laser welding system has restricted the use to fewer applications.

The practical range of heat intensities employed in welding varies from 10^3 W/m^2 for processes such as gas, electroslag to 10^6 W/m^2 for techniques using electron beam and laser beam (Fig. 1.4.6) (ref. 26). Such a large increase in heat intensities using advanced heat sources result in higher productivity with improved weld properties. The comparative process efficiency improves from mere 1% for gas welding to 99% in electron and

laser beam processes. The weld quality is mainly dependent on the intensity of heat source in welding. The correlations amongst main variables controlling the weld quality and the intensities of the heat sources are discussed in chapter 19 on quality.

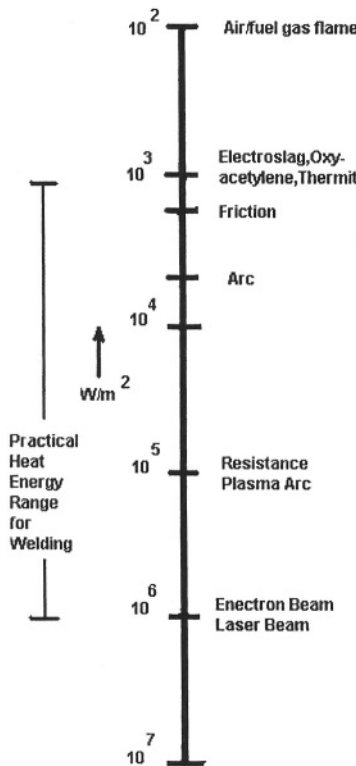
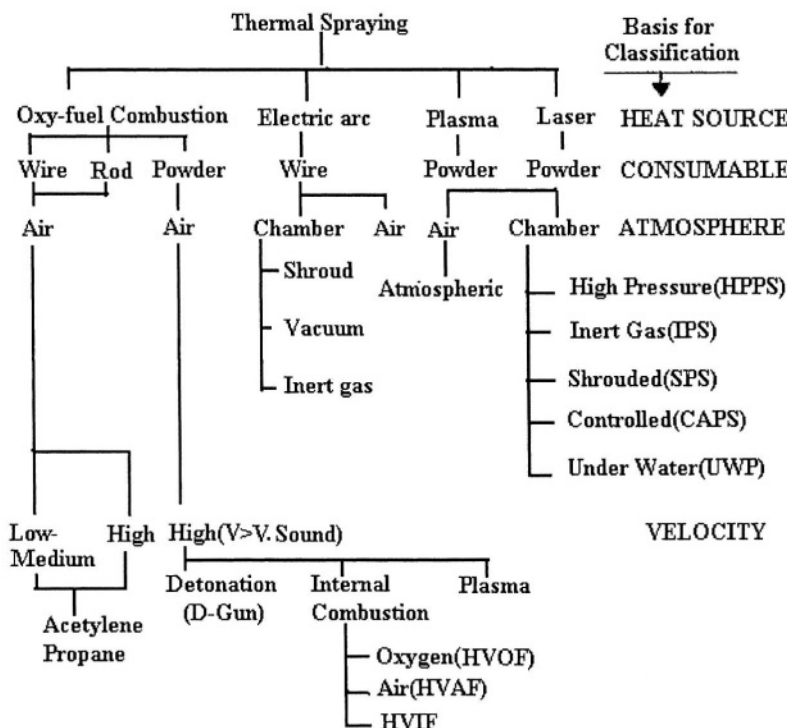


Fig. 1.4.6 Heat Sources, Intensities and Welding Processes

Advanced Heat Sources in Thermal Spraying:- Thermal spraying processes are classified based on flame temperature and velocities (Table 1.4.7) (ref 1). The operating parameters and the resulting properties are listed in Table 1.4.8.



Tab.1.4.7 Classification of Thermal Spray Processes

(HVOF=high velocity oxy-fuel ; HVAF=high velocity air fuel;

HVIF =high velocity impact forging)

Tab.1.4.8..Heat Sources,Flame & Particle Temperatures in Thermal Spray Processes

Parameters	Thermal Spray Processes						
	LVOF	HVOF	D-Gun	HVIF	Arc	Plasma Arc	Vacuum Plasma
Flame Temp. ($\times 10^3$ °K)	3.5	5.5	5.5	4.0	15	15	12
Power Input (kW)	20	150-300	---	---	2-5	40-200	40-200
Particle Temp. ($\times 10^3$ ° C)	2.5	3.3	----	---	3.8min.	3.8min.	3.8min

Flame Temperature: High flame temperature results in formation of molten or semi-molten powders of refractory materials at the shortest possible time. The refractory carbides, borides and composites containing them can be sprayed at higher speed to form dense coatings with superior bond strength. High temperature flames are produced from high intensity heat source like plasma or through improved combustion systems such as detonation and more recently by employing the principle of combustion similar to that of rocket engine. The power inputs from advanced heat sources for thermal spraying are several times higher than that produced by low velocity oxyacetylene torches. For example power input of LVOF is 20 KW compared to that of plasma torch at 200 KW and that of HVOF at 300 KW. Flame temperatures of the high intensity arc and plasma are in the range of 15000°K. The flame temperature of HVOF is 5000°K and that of LVOF is 3500°K.

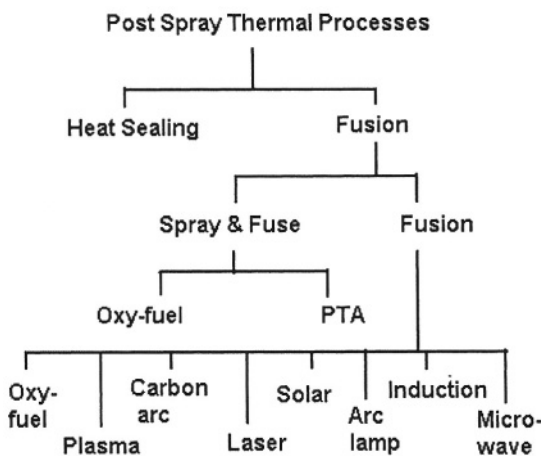
Velocity:- High temperature produced inside a plasma torch chamber or in a rocket engine leads to the expansion of plasma gas (for plasma spray) or combustion product (in oxy-fuel combustion), which emerges through the torch orifice at velocities exceeding that of sound. The high kinetic energy ($1/2mv^2$, where m & v are mass & velocity respectively) of the fast moving micron sized particles of small mass in the emerging jet is directly related to $(velocity)^2$. Therefore the particle velocity in the 400-800 m/s range increases vastly the kinetic energy of the impacting particles in HVOF and plasma processes. Dense coating with improved bonding forms by particles with high kinetic energy.

Impact Forging:- A variation in thermal spray process is the high velocity impact forging (HVIF). The process is similar to HVOF but with higher jet velocities produced by combustion under pressure results in forging of the impacted particles.

Flame temperature increases from LVOF to HVOF by more than 11/2 times whereas the flame temperature in arc and plasma is almost three times compared to that of HVOF. However the increase in particle temperature for HVOF and plasma in comparison to LVOF is not high due to high flame velocity and the corresponding shorter dwell time of particles in the flame. Power requirements for producing high temperature flames are low in direct arc heating, compared to plasma heating. HVOF system requires more power than plasma to produce flame temperatures $1/3^{rd}$ than that of plasma.

A number of applications require post spray fusion operation for closing the pores and also to obtain better bonding to substrate. Post spray processes for further consolidation of the deposits include fusing the deposit by oxyacetylene flame, induction, plasma, laser beam and solar beam (Table 1.4.9). The selection of the heat source depends on the type of materials, coating thickness and shape & size of the job. For example, removal of

surface pores or fusion of ceramic coating is normally carried out by laser beam but can also be done by solar beam or arc lamp. Induction fusion is applicable for ferromagnetic coatings, like self-fluxing nickel base alloy deposits. Oxy-acetylene flame is used for low fusion temperature ($<1050^{\circ}\text{C}$) self-fluxing alloys. Plasma transferred arc is used for fusing coating deposited either through thermal spraying or applied in the form of paste.



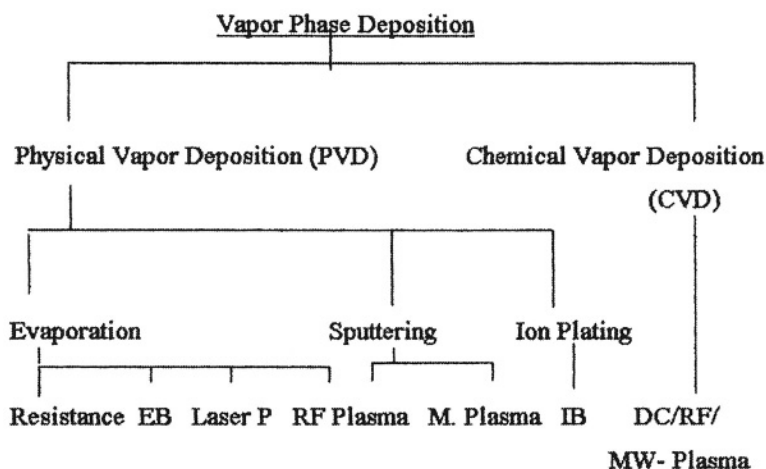
Tab.1.4.9.Post Spray Processes

Sealing of the open pores is carried out by spray deposition of wax or epoxy while the substrate is maintained above the fusion temperature of the sealant. Simultaneous deposition and fusion processes of powder materials are carried out with plasma transferred arc (PTA) process or with specially designed oxy-fuel torch. Both metallic and metal matrix composites can be sprayed and fused simultaneously. Alternatively, sprayed deposit with metallic matrix can be fused by using any one of the heat sources, such as, combustion, plasma, carbon arc, laser, solar, arc-lamp, or induction. Induction melting is possible for ferromagnetic materials only.

Thermally sprayed ceramic deposits are normally fused by using high intensity beams, such as laser, solar & microwave. Microwave can be used to heat ceramic material without heating directly the metallic substrate. Microwave can be used for consolidation of the ceramic deposits, such as WC-Co through sintering.

Advanced Heat Sources for Vapor Phase Deposition Processes: The process consists of vaporizing in vacuum and subsequent deposition of coating material from the vapor phase onto the substrate. When the evaporation of the

coating material is carried out with high intensity beam or ions, or electrical heating the process is known as Physical Vapor Deposition (PVD) process. The deposition rate, atmospheric composition, and pressure, and substrate temperature would determine the character of the coating. Due to differing vapor pressures of the elements constituting the alloy the control of alloy composition in the deposit is difficult when only one molten alloy is used. An independently controlled source for each of the alloy components provides the best compositional control of the deposit. With a very low substrate temperature, it is possible to produce amorphous phase coating on the surface. Alternatively, volatile compound of the coating material in vapor phase at high temperature is allowed to decompose on the substrate so as to deposit the required elements or alloys on the surface. The alternative technique is known as Chemical Vapor Deposition (CVD) process, In this process the substrate is heated to the required temperature for decomposition of volatile compound and thus to deposit the required element. The high temperature of the substrate allows the diffusion of the elements to form a surface enriched with deposited element. The CVD process also occurs during carburising and nitriding, viz, high temperature deposition on the surface and diffusion of elements towards interior to form a hard case of required depth. (Table 1.4.10).

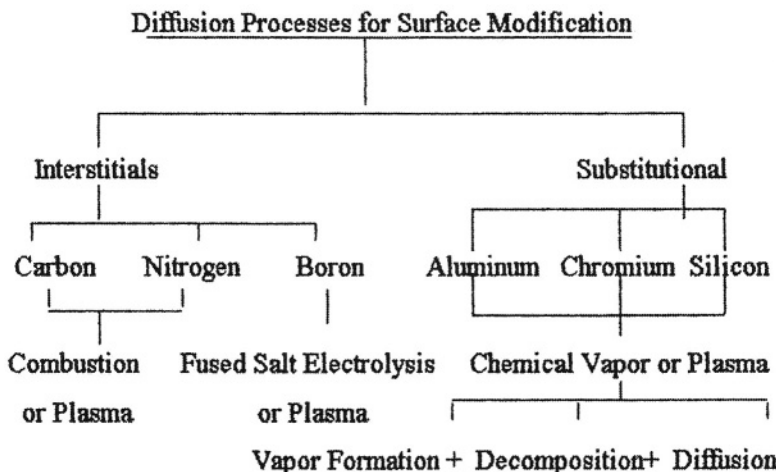


Tab 1.4.10. Advanced Heat Sources For Vapor Phase Deposition

(Legend; EB= Electron Beam, P = Pulsed, RF=Radio Frequency,
M= Magnetron, MW= Microwave)

Advanced Heat Sources & Diffusion Processes: Diffusion of interstitial (C, N, B) and substitutional elements (Al, Cr, Si) to the surface layer is a common

process of forming wear and/or corrosion resistant surface (Table 1.4.11). The diffusion of interstitial elements like carbon, nitrogen and boron leads to the formation of hard martensite matrix, which on quenching and on tempering forms carbides, nitrides and borides depending on the element added.



Tab 1.4.11. Surface Modification Processes by Diffusion & the Heat Sources

The process of surface enrichment consists of two steps. In the first step element enriched vapor phase is formed and in the second phase the vapor phase is allowed to diffuse in the surface layer to the required depth. For interstitial elements like carbon the vapor phase is formed by combustion of charcoal, oil, alcohol etc, while for nitrogen ammonia is burnt. Both the generation of atmosphere and diffusion operations are carried out in a furnace which is generally heated electrically. Boronising is carried out by electrolysis in a molten salt bath containing boron. The comparatively recent development of plasma nitriding, carburising and boriding processes utilise plasma to generate the ions of respective species and to diffuse the same into the substrate surface. For substitutional elements chemical vapor deposition process (CVD) is used to deposit the elements on the surface. Subsequent diffusion of element to the interior occurs by maintaining the substrate at elevated temperature.

Summary:

In brief, *wear* occurring on the *surface* of material can be controlled by *heat* (thermally) assisted *surface engineering processes*.

Wear occurs due to interaction of the surface with the environment. Types of wear processes include abrasion (by solid particles), adhesion (mating with similar or dissimilar materials), erosion (by solid particles or liquid droplets), thermal (by heated counterbody) and corrosion (electrochemical process). Wear equations (excepting for corrosion) relate volume loss inversely with hardness. Corrosion, like other wear processes is environment specific. Both corrosion and wear loss are expressed in terms of dimensional loss in specific environment. Types of corrosion include galvanic, pitting, intergranular, parting, crevice etc. Hot corrosion reactions include oxidation, nitridation, sulphidation etc.

Surfaces are bounding faces of solid interfacing with hostile working environment. Wear of solids occurs at these interfaces. Wear control exercise involves control of surface properties such as, morphology (surface roughness and microstructure), composition, energy and hardness by surface engineering processes. Surface composition and morphology changes can cause effective barrier to corrosion.

Heat energy is required for phase transformation, such as, from solid to liquid or vapor or other solid phase. The quantum of heat required for different processes, such as, melting (fusion welding), evaporation (vapor deposition), diffusion (carburizing) and solid state transformation (transformation hardening) depends on the specific heat of the material, process temperature and the latent heat of transformation. Phase diagram provides useful data on the various phases in equilibrium at different temperatures and concentrations. The list of advanced heat sources used in surface engineering include plasma, laser, electron, ion, microwave, arc, spark, induction and newer combustion systems. Rays and beams can be focused to a small spot size producing concentrated high intensity heat for fast melting and evaporation.

Surface engineering processes, such as thermal spray, weld overlay, vapor deposition and diffusion are used to produce wear resistant surfaces. Advanced surface engineering processes are based on newer heat sources.

References

1. R. Chattopadhyay, Surface Wear Analysis, Treatment & Prevention, book published by ASM International, July, 2001
2. R. Holm, Electrical Contacts, Almquist & Wiksells, Stockholm, 1946, sec 49.
3. J.F Archard, Contact & Rubbing of Flat Surfaces, *J. Appl. Physics*, 24, 1953, 24.
4. M.M. Kruchov & M.A. Babichev, Friction & Wear in Machinery, ASME Translation, 17, 1962, 1.
5. R.G. Bayer, A.T. Schacky & A.R. Wayson, *Machine Design*, 1969, 41(1), 142-151
6. R. Chattopadhyay, Microstructural Science, vol 19, ASM International, 1992, 447-504.
7. I. Finnie, Source Book of Wear Control Technology, ASM Int., 1978, 220-236
8. A.G. Evans and D.B. Marshall, Fundamentals of friction and wear of materials;
9. G.Y. Lai, *JOM*, November, 1994, p54
10. F.S. Petit and C.S. Giggins, Chapter on Hot Corrosion, in book Superalloy II, Ed. C.T. Sims & others, John Wiley & Sons, Inc., 1987, p327-384
11. L.L. Shrier, Corrosion Handbook, vol 1 & 2, Newnes-Butterworths, London, 1976.
12. J. Alison, M.F. Strand & M. Wilman, 3rd Annual Conv. of Lubrication & Wear Gp, paper 10, May 1960, Inst of Mechanical Engineers, UK.
13. J. Alison & H Wilman, *Brit. J. Appl. Physics*, 1964, 15, 281-289.
14. C.S. Smith, *Trans. AIME*, 1948, vol 175, 15-52.
15. W.J. Petch, Proc. Fracture Conf., Swampscott, Mass; April, 1959, 54.
16. E. Robinowicz, Friction & Wear of Metals, Wiley, NY, 1965.
17. P.J. Blau, Ph.D. Thesis, Ohio State University, 1979
18. T.R. Thomas (Ed.), Rough Surfaces; Longman Group, UK, 1982.
19. P.H. Dowson, *J. Mech. Eng. Science*, 1982, 4, 16-21.
20. R. Onion and J.F. Archaid, Proc. Int. Conf. Mechanical Engineers, vol 188, 1974, p673-682.
21. R. Chattopadhyay, Microstructural Science, vol 12, p487-494, 1985, ASM-International,
22. R. Chattopadhyay, Int. Symp. on Tribology, 18-23 Feb, 1993, Beijing, China,
23. Bernard North, Substitution of Ceramics for Conventional Cutting Tools, *Engineering Applications of Ceramic Materials, Source Book*, ASM, p 154-166, 1985

24. S. Dushman and J.M. Lafferty, *Scientific Foundations of Vacuum Sciences*, John Wiley, New York, 1962, pp 15-21
25. O. Knoteck, T. Leyenderker, M. Bohmer, & W.D. Munz, *On the Wear Behavior of PVD Ti, Al, Zr, V, N Coatings*, WOM, 1987, Proc. Int. Conf. on Wear of Materials, Houston Texas, 5-9 April, 1987, Ed. K.C. Ludema, vol 2, p551-555, ASME
26. Patricio F. Mendz & Thomas W. Eager, *AM&P*, May, 2001, p39-43

This page intentionally left blank

Chapter 2

PLASMA ASSISTED THERMAL PROCESSES

2.0 Introduction

Plasma, the fourth stage of matter, has been used extensively for a large number of thermally assisted surface engineering processes. The list of surface engineering processes based on plasma includes thermal spraying, welding and vapor phase deposition. In this chapter the formation and properties of plasma, surface engineering processes using plasma and major applications are discussed.

2.1 Formation & Properties of Plasma (1, 2, 3, 4):-

Solid material when heated transforms into various stages as follows:-

Solid \rightarrow Liquid \rightarrow Gas \rightarrow Plasma

With the increasing temperature, solid transforms to liquid and liquid to gas. Further increase in temperature results in the transformation of the third stage of matter i.e., gas atoms to charged particles, and the material enters the plasma stage. Plasma, the fourth stage of matter is a conducting gas consisting of appreciable proportion of charged particles. The ionization of atoms can be achieved by heat, radiation or electric discharge. The production of plasma by electric discharge across an inert gas stream is shown schematically in Fig. 2.

The degree of ionization is described by the famous Saha equation for ionization:-

$$Ni/Nn = 24 \times 10^{15} \times T^{3/2} e^{-U_i/kT} / Ni$$

Where, Ni = density of ionised atoms, Nn = density of neutral atoms, T = Kelvin gas temperature, k = Boltzmann constant & U_i = ionization energy of the gas. To sustain plasma a small degree of ionization is required. Usually 3-5% of the gas must be ionized, i.e., $Ni/Nn \geq 0.3$. At one atmospheric pressure, the ionization energy (U_i) required to generate plasma is generally between 50 – 24 eV. Plasma must have appreciable ionization to become conductive and heated electrically. The temperature at which a significant amount of gaseous atoms will be ionized and the plasma state achieved falls in the range of 4,000 to 25,000°C.

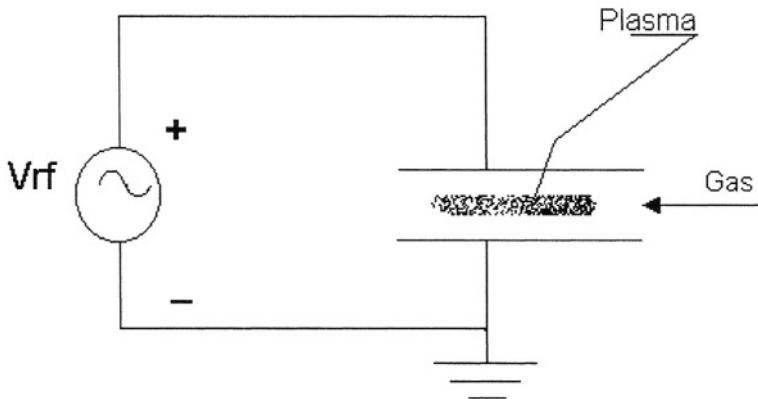
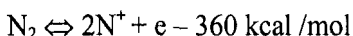


Fig 2. Plasma Formation(Schematic)

The basic requirements for the formation of a plasma are :-

- Strong electric field capable of producing high temperature which would lead to ionization of plasmagenic gases.
- Plasmagenic gases should ionize,at least partly,by the application of heat from electrical energy, as follows:-



The production of charged particles requires enormous amount of energy (360 kcal/mol) and hence ionization can be observed at temperatures of the order of the tens of thousands of °C. In order to enable the plasma particles to travel in a straight line with constant velocity, the energy of interaction between particles at the mean distance amongst them must be considerably less than the mean kinetic energy of the particle. In other words, PE (potential energy) <<< KE (kinetic energy).

In Fig. 2.1, a plot of n (plasma densities) vs Te (the units of energy measure as electron temperature, & express in electron volts) indicates the various types of plasma formation zones(1).

Plasma assisted surface modification processes

Low-temperature plasma is used in thermal spraying and other surface modification processes, in which density of charged particles (electrons & ions) is lower than that of neutral particles. In this low temperature plasma the mean energy of electrons or ions is much lower than the ionization potential of the gas. The other kind of plasma known as hot plasma has much higher mean energy of ions and electrons than the ionization potential of the gas. Such plasma contains ions and electrons and practically retains very few, if

any neutral particles. An example of hot plasma is that formed during thermo nuclear reaction involving deuterium nuclei or deuterium and tritium.

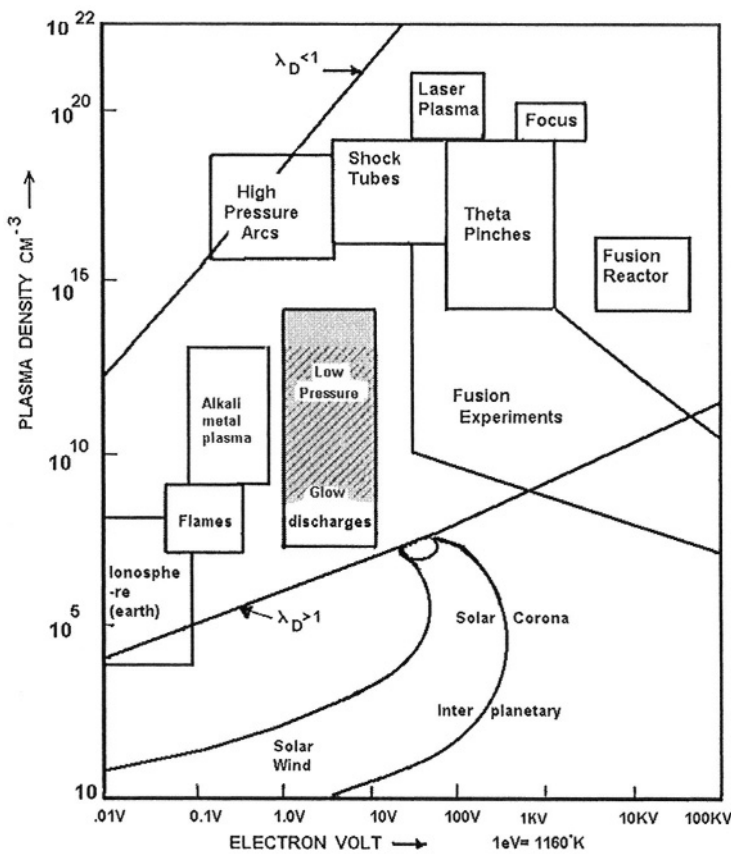


Fig.2.1 PLASMA DENSITY VS. ELECTRON VOLT

(Ref.1.Michael A.Libermann & Alan J.Lichtenberg,book on 'Principles of Plasma Discharge & Materials Processing',1994,p9. The material is used by permission of John Wiley & Sons,Inc)

The current list of surface modification processes involving plasma includes welding, thermal spraying, vapour phase deposition, carburising, nitriding and polymerisation. Electric field used for plasma formation includes gas discharge, induction (R.F) and DC arc.

Plasma flame with an average plasma density of around 10^8 cm^{-3} with energy in the range of 0.07 to 0.7 eV (Fig. 2.1) is used in thermal spraying. The high energy flame travels at velocities more than that of the sound carrying with it the powder particles, which become molten or semimolten before depositing on the prepared substrate. The high energy flame is capable of melting even high melting point ceramics during the in-flight short

dwelling time. In a plasma flame, the core temperature is very high compared to cool peripheries, where the neutral gas formed in field free condition tends to attend room temperature.

In comparison to plasma flame, glow discharge plasma (Fig. 2.0.1) has higher energy band in the range of 1 to 10 eV, and also higher plasma density covering a wide range from 10^7 to 10^{14} cm⁻³. Glow discharge plasma is used for vapor phase deposition of wear resistant material on clean substrate. Plasma heat is used for evaporation of coating material in physical vapour deposition. Abnormal glow discharge is used for plasma nitriding & carburising. Plasma heat is used for diffusion of boron in the near surface region so as to form a hard boride coat on the surface. Reactive plasma is used for chemical vapour deposition process. Arc plasmas with high plasma densities in the range of 10^{16} to 10^{18} cm⁻³ and with energies in the range of 0.1 to 5 eV are used for producing weld overlay of wear resistant materials. The arc forming the plasma is transferred to the base for plasma transferred arc welding. Corona discharge plasma is used for plasma polymerisation. These and other related plasma assisted surface modification processes are to be discussed in the subsequent sections.

2.2 Non-transferred Arc Plasma Process Spraying (4, 5, 6, 7, 8)

The non-transferred arc plasma techniques for thermal spraying are classified in terms of electric field (arc or induction), stabilizer fluid (gas or liquid), power (high or low), and anode design (twin anode, grator guard, gas tunnel), as indicated in Table 2.1.0.

2.2.1 DC Arc Plasma Spray System

In dc arc plasma spraying, plasma flame formed by striking a dc arc across an inert gas(es) stream, is used for spraying powder material onto a prepared surface of base material. The base material is not electrically connected or in otherwords, the plasma arc is not transferred to the base. The base material can therefore be nonconductive, such as ceramics or plastics. Coating material in powder form is introduced in the plasma jet for deposition onto substrate.

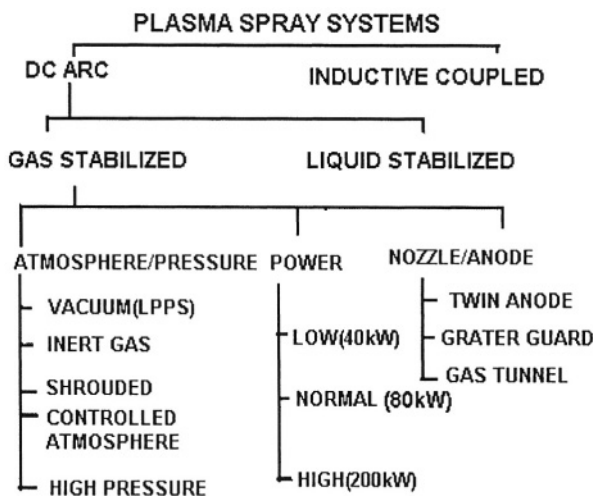


Table 2.1.0. Classification of Plasma Spray Systems

Plasma flame is used to heat the powder particles to molten or semimolten state. The high velocity of plasma jet increases the striking velocity of molten or semi-molten particles beyond that of the velocity of the sound. The heat and the speed of the plasma flame are used to produce dense adherent deposit. Both conductive metals and nonconductive ceramics or plastic can be sprayed by plasma system.

Base material temperature normally remains at room temperature. The process is used to coat metal, ceramic, plastic and composites on similar or dissimilar materials. The process has also been used to develop composite and graded coating.

Schematic diagram of the dc arc plasma spray system is shown in Fig. 2.1.1. The system consists of a spray gun, plasmagenic and carrier gas supply manifold, torch cooling water circulation unit, power pack and controls. Controlled quantity of plasmagenic gas is fed in the torch to form the plasma flame with applied voltage across the gas stream between the tungsten cathode and copper anode. An inert gas stream carries the powder particles from the feeder onto the plasma jet. The torch is cooled by circulating water. Based on power supply, plasma spray units can be portable 40 KW or standard 80 KW or high power 200 KW system.

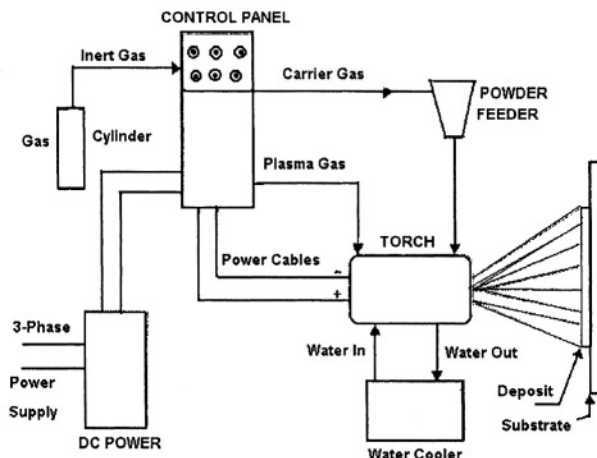


Fig.2.1.1 Schematic Diagram of Plasma Spray System

i. Spray Gun or Torch:- The heart of the system is the torch. Torch (Fig. 2.1.1.1) consists of an thoriated tungsten cathode enclosed by a water cooled copper anode, with a constant flow of plasmagenic gas in the intervening space. The arc is struck between cathode and anode. The cathode tip ignites the gas to form plasma. The plasma thus formed flows through the extended anode nozzle and emerges out at a high velocity through the torch orifice. The constricted nozzle can be convergent, convergent-divergent or straight depending on the application. Different nozzle designs are used, such as, twin anode, grater guard and gas tunnel nozzles.

Twin Anodes:- In this system, two anode torches are placed symmetrically opposite to each other and perpendicular to cathode torch in the extended anode area. The cathode and anodes are protected by flow of inert gas in the intervening space. With this arrangement arc stability is far better than conventional system. In this system it is possible to adjust plasma gas speed and enthalpy over a wide range with a power level of 10 to 100 KW, enabling formation of hypersonic plasma in which shock waves in the form of diamond can be observed. High temperature plasma at hypersonic speed results in superior WC-Co coatings with low decomposition, high adhesion and high wear resistance properties. The spraying condition can be maintained stable over 200 hours.

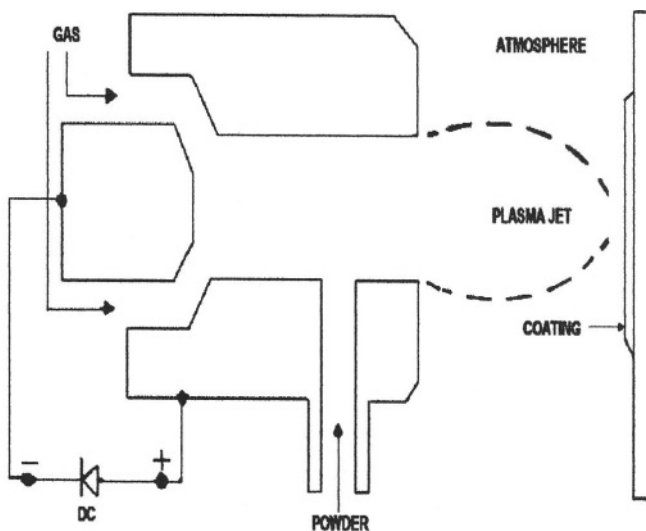


Fig. 2.1.1.1 : Plasma Spray Torch

Grator Guard:- The most significant difference with respect to normal plasma spray system is the use of a patented accelerator placed where particles are introduced in the plasma stream. The particles are accelerated until a velocity of 1220 to 1520 m/s (4000 to 5000 ft/s) is reached. High velocity particles travelling through the plasma flame improves bond strength, decreases porosity and oxide content of the deposit. The process was originally developed by United Technologies (Pratt and Whitney Aircraft) to produce high quality coatings on aircraft gas turbine fan blades.

Plasma jet travelling outside nozzle is field free and therefore there is rapid fall in temperature and velocity with increasing distance from the nozzle orifice. For example the core temperature of the plasma plume decreases to 500°K or below from a exit temperature of 20,000°K. Similiarly, plasma jet emerging out of the nozzle at a velocity exceeding that of the sound can get reduced to 10 m/s in an atmosphere plasma. High energy torches such as, 80 KW torch needs chilled water for cooling wheras lower energy ones, like 40 KW torch requires circulating water at room temperature for cooling.

ii. Gas:- *Plasmagenic gas:*

For producing plasma, the gases, such as, argon, helium, nitrogen & hydrogen are normally used. Diatomic gases (N₂H) have higher specific enthalpy and thermal conductivity than monatomic gases (Ar,He), hence produce smaller arc with higher temperature of plasma. Although the peak temperature of diatomic gas is higher, the deposition efficiency tends to be lower than monatomic gas. Nitrogen plasma is highly reactive with metals,

titanium & aluminium and forms nitride. Helium is costly but has been used as replacement for hydrogen for avoiding hydrogen embrittlement. Argon is the best all-purpose gas and addition of 10% diatomic hydrogen results in a hotter and more concentrated plasma for thermal spraying.

Carrier gas & Feeder

The coating material in the form of powder is carried from the feeder by carrier inert gas for injection onto plasma flame. Argon is used as carrier gas for transporting powder in argon plasma. The commercially available powder feeding devices include both mechanical and fluidised bed systems. The use of powder feeder based on fluidised bed system ensures uniform delivery of all the constituents in powder mix of different densities at any point of time. Twin feeders are often used to feed two different materials simultaneously at the same or different rates to produce composite coatings of varied compositions.

iii Power Supply and Cooling System:-

Plasma spraying system normally operates on D.C power. Welding rectifiers with a drooping characteristic to prevent instability in arc, are generally used. A high open circuit voltage is required to cover the range of gases used, e.g., typical voltages are 80 V for argon, 160 V for nitrogen and 300 V for hydrogen. Typical power rating of 40 or 80 kW is used in commercial units. Mobile unit is the 40 kW and does not require chilled water for cooling the torch. In 80 kW unit, the torch needs chilled water for cooling. It is normal to initiate the arc with a high frequency discharge.

iv. Plasma spray atmosphere

Plasma spray operation is carried out by either of the processes such as atmospheric plasma spray (APS), shrouding the plasma flame (SPS), inert gas cover to plasma flame (IPS), spraying inside a vacuum chamber (LPPS), and maintaining high inert gas pressure (HPPS).

Reduced or Low Pressure Plasma:-

The reduction in plasma chamber pressure shall lead to higher particle velocity but reduced heat exchange between particles and plasma. The reactive materials, such as titanium, aluminium and their alloys can be sprayed without any loss through oxidation in a low pressure plasma.

A step further in the low pressure plasma is the use of vacuum plasma system (VPS). The plasma spraying in vacuum can produce deposit purity level as that of original powder material, and comparable to that of PVD and CVD coatings. It is possible to produce good quality composite coatings through VPS. The advantages of VPS (also LPPS) include followings (9):-

- Speed and length of the flame become higher and longer in low pressure conditions
- Flame temperature is higher than atmospheric plasma
- High velocity argon plasma in vacuum leads to virtually no oxidation of highly oxidisable metals.
- Deposit is oxide free, dense and has high bond strength
- High deposition rate combined with high deposition efficiency(less spray loss)
- Reversed transfer arc cleaning prior to spraying reduces the preheat cycle time and removes surface oxides and contaminants, thus creating excellent bonding between coating and substrate
- Since the continuous deposition is accomplished at high temperatures, self annealing of coating leads to stress relief and recrystallisation.
- Spraying in vacuum plasma spray is normally carried out by programmed robotic system. The programme can be stored and recalled for repeat jobs thus ensuring consistent coating quality.
- Since VPS or LPPS is carried out in an enclosed vacuum chamber, hence neither the sprayed powder nor the supersonic noise of the jet can cause pollution of the atmosphere or become hazardous to the operator. In vacuum plasma spraying the size of job is restricted to vacuum chamber size. In argon shrouded plasma spraying (ASPS), the use of argon shield around the plasma gun and the workpiece protects molten particles and substrate against air ingress. The coatings obtained from such a system is clean, well-bonded and relatively free from oxides. A typical application of ASPS is the coating of M-Cr-Al-Y as thermal barrier layer in turbine hot suction components in gas turbine.

High Pressure Plasma Spraying in Controlled Atmosphere : The advantages of high pressure inert gas in the spray include followings:-

- Increase in heat transfer to the spray particles resulting in improved spray efficiency and less porosity.
- Effective cooling of the substrate.
- High pressure can suppress or induce chemical reaction. In the HPS chamber, pressure above 1000 m bar of inert gas is maintained by a close loop pump combined with gas cooling and filter unit. The pressure is kept constant by outletting the plasma gases fed through the torch during the spray process by means of a blowoff valve. In the reactive nitrogen atmosphere, the spray of titanium powder in high pressure plasma results in coating of hard and fine grained TiN.

Water Stabilised Plasma Guns:- In addition to normally available gas stabilised plasma arc system, liquid (mainly water) stabilised plasma is used for some special applications. Similar to gas stabilised arc, a water vortex can be used for the electric arc constriction and stabiliztion. The outer layer of water cools the specially shaped chamber walls while the inner layers are ionised, thus providing the plasma stream. The water stabilization enables higher energy dissipation for a given arc current and plasma flow with higher energy density. The system works with a rotating anode and graphite cathode, with power from 120 to 200 KW and tap water. The water stabilised plasma is not highly oxidising and thus can be used for metallic coatings.

Substrate Surface Preparation, Bond & Top Coat Materials for Thermal Spraying (10):

Thermal spray processes in general require the substrate surface to be specially prepared and a bond coat to be applied before the wear resistant top coat material is sprayed. The pre-spray processes and the consumables used in thermal spraying are discussed in this section.

Cleaning the surface : The component surface should be free from oil, grease or dirt. The surface is commonly cleaned by solvents like trichloroethylene. However, in more difficult cases, cleaning of the surface can be carried out by hot vapour degreasing, vapour blasting, pickling, ultrasonic cleaning or a combination of processes.

Surface Roughening : The clean substrate surface is made rough in order to increase the effective surface area and to improve adhesive bonding of the sprayed deposit. The surface roughness is increased by abrasive grit blasting, machining or rough grinding. The grit blasting is the most commonly used practice of surface roughening. In this process, the substrate surface is blasted with compressed air jets carrying the abrasive grits. The angular particles of chilled cast iron or ceramic are used as grits. The grits of 16-60 mesh size are used for metal substrate and 60-100 mesh for plastic. For ceramic substrate hard ceramic grits are used. For thin substrates, fine grits (25 to 120 mesh) and for thick coatings, coarse grits (18 to 25 mesh) are recommended. The compressive residual stress on the grit blasted surface improves fatigue resistance of the component. With rougher surface finishes, the coating adherence improves .The best adhesive bond is associated with roughness dimension comparable to 3/4th of the diameter of the particles sprayed.

Bond Coat (10) : A thin layer of special bond coat material on the substrate is normally required in order to obtain good bonding of the top coat. The function of bond coat is like an adhesive between the substrate and the layer

above it. The common bonding materials are molybdenum, nickel-aluminium and nickel-chromium alloys. A list of bond coat materials and their properties are given in Table 2.1.1. Some of the bonding materials are used as coatings for resisting high temperature oxidation. The bond coat of Ni+5%Al can withstand temperatures of up to 1010°C. The coating of MCrAlY (M = Co or Ni), another bond coat material, has been used on jet engine components to resist oxidation upto a temperature of 1300°C. Some specially formulated powder alloys do not require bond coat. These alloys are known as single step powders. However in applications, where surface preparation is difficult e.g., for very thin or hard substrate or difficult configuration for blasting, even for single step powder it is necessary to use bond coat. The thickness of bond coat should be sufficient to cover the rough surface and is normally 0.08 to 0.18 mm. There is no additional advantage of a thicker bond coat layer.

Table 2.1.1. Bond Coat Materials

Materials	Maximum Temperature in Service, (°C)	Bonding Interface
Molybdenum	315	Metal/metal
80 Ni-20 Al	620	Metal/metal/ceramic
89 Ni/6 Al/5 Mo	-	-ditto-
94 (Ni+Cr)+6Al	980	-ditto-
95 Ni + 5 Al	1010	-ditto-
80 Ni+20 Cr	1260	-ditto-
MCrAlY, e.g. NiCrAlY/CoCrAlY	1260-1316	For ceramic coat on metal
Zn/Al	-	For plastic substrate
Al-Si	-	Al- substrate for ceramic coat

Top Coat Materials (10): Metallic, ceramic, polymeric and composite materials can be sprayed on same or different materials forming substrate.

- Metalllic Materials** : Thermal spray coatings of zinc and aluminium are used extensively for protection of bridges and structures against atmospheric corrosion. Nickel, iron, cobalt and copper-base alloys form the bulk of thermal spray metallic materials (Table 2.1.2). Metal matrix composites, erosive wear.

Tab.2.1.2 Metallic Materials for Thermal Spraying

Type of Material	Form			Typical Applications
	Powder	Wire rod*	Tubular Wire**	
Grade 410 SS	✓	✓	✓	Yankee Dryer
Grade 316 L SS	✓	✓	✓	Corrosion Resist coat in chemical plant chimney
Zn/Al/Zn + Al	✓	✓	✓	Bridges & Structures
High Cr Iron	✓	✗	✓	Boiler tubes erosion
Fe-Cr-Mo-Al	✓	✓	✓	Boiler/Erosion
Fe-Cr-Ni-Al	✓	✓	✓	Superheater Tubes
Nickel Alloys				
a. Self Fluxing Ni-Alloys	✓	✗	✓	Shafts, Bearing etc.
b. Inconel (Uns: NO6600)	✓	✓	✓	Bond Coat
c. Ni/Cr, 50/50	✓	✓	✓	Boiler tubes
Co-Cr-M-C, M=W/Mo/Cb	✓	✗	✓	Turbine blades/ Impeller, I.D fan
Copper Alloys : Al-Bronze Cu+10% Al)	✓	✓	✓	Bearing / shaft

[Used for Oxy-fuel*(sec.8.2) & Arc Spray** (sec.12.3) respectively]

The thermal spray metallic coatings cover a vast range of applications which include Yankee dryer, boilers, evaporators, turbines, shafts, bearings etc. Thermal spraying produces lamellar microstructure with the flattened successive layers making up the coating thickness.

b. Ceramic Materials: Ceramic materials used include oxides, carbides, nitrides and ceramic based composites. The oxides, such as, alumina, titania, chromium oxide and zirconia are used extensively to produce wear resistant coating by thermal spraying.

Different combinations of oxides are also used. Ceramic oxide materials are available in the form of sintered rods or powders for thermal spray applications. Thermal spray coating of alumina is used in engine valve to minimise wear due to high temperature corrosion, oxidation and friction. Thermowells are coated with alumina to resist particle erosion at high temperature. Titanium dioxide produces hard and dense coating. The dense

coating is useful to resist corrosive attacks of acids and alkalis. $TiO_2 + Al_2O_3$ coatings resist wear due to erosion, fretting, cavitation and corrosion.

The dense deposit of Cr_2O_3 can resist particle erosion, corrosion and cavitation wear. The chromium oxide is used to coat thread guide and guide rolls in artificial fibre industry.

Pure ZrO_2 while cooling, transforms from high temperature cubic form to room temperature monoclinic form, accompanied by large volume change and cracks in the deposit. The transformation can be avoided by stabilising high temperature cubic form by the addition of CaO , MgO , Y_2O_3 , CeO_2 , either alone or in combination. Low thermal conductivity of zirconia makes it an ideal material for thermal barrier coating. It is also a conductor for oxygen ions, a property utilised for making oxygen sensor in boilers and car exhaust systems.

The high thermal expansion coefficient results in poor thermal shock resistance of the coating. However the problem can be overcome by using partially stabilized zirconia (PSZ), which is produced by using right amount of stabilizer and firing at a high temperature.

- c. Composites:- The thermal spray composites consisting of combinations of different ceramics, ceramic plus metal, ceramic plus plastic are used for a large number of wear resistant applications. The composites spraying techniques and typical applications are listed in Table 2.1.3.
- d. Polymers : Examples of thermosetting resins, which are extensively used for coating on metal surfaces include epoxy, polyester, epoxy-polyester, hybrids, acrylics and fluorocarbons. The powder coating from thermoplastic group includes polyethylene, polypropylene, nylons and polyvinyl chloride. The applications and spray properties are given in Table 2.1.4.

The primer/bond coats are normally selected according to the top coat materials to be used e.g.

- a. Primer HDPE + Top Coat LDPE
- b. Primer Polyethylene + Top Polyvinyl acetate
- c. Primer Epoxy + Chlorinated Polyethylene

Epoxy can be spray bonded without any binder. Epoxy coatings are used on reinforcing steel bars in concrete structure, gas and oil pipe line to resist corrosion. The thin, smooth and glossy polyester coat has excellent corrosion and electrical resistance. The coating is used for transformers and exteriors of equipment.

Table 2.1.3: Composites for Thermal Spraying

Materials	Process	Applications
Metal & Ceramic Composites		
MCrAlY (M = Ni/Co/Fe)	HVOF/ Plasma	Bond coat/high temperature oxidation
SiO ₂ + ZrO ₂ + CoCrAlY + Al ₂ O ₃	-do-	Hearth rolls of cont. annealing
CoCrAl -Y ₂ O ₃ + CrB ₂	-do-	-do-
75%Cr ₃ C ₂ + NiCr	-do-	Piston ring/boiler tube
Ni-Cr-B-Si-C + Cr ₃ C ₂	-do-	Con. Cast. Mould
5.5 BN + Ni ₁₄ Cr ₈ Fe + 3.5 Al	-do-	Self cleaning of rolls in SS annealing furnace
BN/Graphite + Ni	Plasma	Aeroengine-abradable coating
WC-Co + Stellite	HVOF/plasma	Fan blades
Plastic and composites		
Al-Si + MCrAlY + Polymer + Lubricant	Plasma	Abradable coating in gas turbine turbo-compressor
Al-bronze + polyester	Oxyfuel	Corrosion resist coating
SS + LDP	-do-	Prime coat for SS on plastic

Table 2.1.4: Properties of Some Polymers for Coating on Metal

Polymer	Primer/No primer	Processing temperature (°C)		Hardness (Rockwell)
		Softening	Curing	
Thermosetting				
Epoxy	No	180	200	—
Polyester	No	140	200	—
Thermoplastic				
Nylon 6/66	No	—	> 270	109-110 R
Polypropylene	No	167	> 176	105-106 R
Polyvinylchloride	Yes	—	> 212	52 M
Polyethylene	No			
LD		—	>115	23-25 R
HD		—	>137	59-62 R

Nylon 6/66 coating has low coefficient of friction and good lubricating properties. The coating is used for sliding or rotating bearing applications, e.g., automotive spindle, shaft, relay plunger, shift forks, etc.. However, polypropylene coating material adheres to metal surface only after heating to 360°C. The coatings resist abrasion and corrosion from a large number of solvents at room temperature. The typical applications include conveyor chute, chemical processing pipe, drum and tank.

A primer coat is required to bond polyvinyl chloride to metal surface. The coating resists impact and chemicals. The coating is used for dishwasher baskets, conduit, cable trays etc.. Polyethylene coating resists most acids, alkalis, salts and alcohols upto ~100°C and has zero water absorption property. Coated components are used for fume exhaust, ducts, pump & impellers.

- e. Polymer Composites: An important application of polymer composites is the abradable coating in gas turbines. The reduction in the clearance of blade tips and casing can improve the efficiency of gas turbines in aeroengines by 5%. Similar improvement in efficiency can be achieved in stationary gas turbines, turbo compressors, diesel compressors, turbo chargers, and pumps.

The thermally sprayed coatings on shrouds are so designed as to release fine wear debris when machined by high velocity blades without causing any blade wear. The coating materials are composed of metal or ceramic particles (Al-Si alloy or MCrAlY or YSZ), polymer and solid lubricant. During thermal spray deposition, the polymer phase lowers the coating stresses, thereby allowing thick deposits. Also polymer gets burnt out at the application temperatures of 400°C (Al-Si), 700°C. (MCrAlY) or still higher at 1200°C (Y₂O₃-stabilised ZrO₂), thus generating porosities and improving abrability. The functional properties of the polymer materials can be further improved by incorporating fillers, e.g. stabiliser (copper salts) addition in nylon to ensure long term performance at high temperature, or 2-3% carbon black addition to avoid degradation against UV light etc.

Properties of Thermal Spray Coatings:-

Bond Strength:- Bond strength of the coating is determined in accordance with the stipulation made in ASTM C633-74. The method covers the determination of the degree of adhesion (bonding strength) of a coating to the substrate, or the cohesive strength of the coating in a tension normal to the surface. The bond strength values of plasma spray deposits are normally in the range of 7000 psi to 9000 psi.

Porosity & Hardness:- Dense coatings produced by plasma and other high velocity spray system result in higher surface hardness. Some of the important properties of the single ceramic oxides (13) are indicated in Table 2.1.5. The indicated property values for most of the oxides fall within a range. For thermal spraying the four main oxides used include alumina, titania, chromium oxide and zirconia. Thermal conductivities at room temperature and at elevated temperature of most of these oxides are within the range of 1.7 to 17 W/m.K, excepting for Al_2O_3 (35 W/m.K). Similarly linear coefficient of expansion is within the range of 0.2 to 1.5% , excepting for Cr_2O_3 (0.1%). Microhardness values of the oxides are in the range of $600\text{-}1000 \text{ kg/mm}^2$ excepting for Al_2O_3 (3000 kg/mm^2). Young modulus values of oxides are within 205-415 GPa without any exception. The properties of plasma spray oxide deposits can differ from those indicated in Table 2.1.4 for pure oxides. The hardness and thermal conductivity of the sprayed deposits are lower than pure oxides due to porous nature of the coating.

Tab.2.1.5. Some Selected Properties of Single Oxides($\text{Al}_2\text{O}_3, \text{TiO}_2, \text{Cr}_2\text{O}_3, \text{ZrO}_2$)

Properties	Room Temp.	1095°C	Outside the Range
Thermal Conductivity (W/m K)	1.7-17	1.7-6.9	$\text{MgO}(52\text{W/m K})$ $\text{Al}_2\text{O}_3(35\text{W/m K})$
Linear Thermal Expansion(%)	0.2 – 0.3	0.8-1.5	$\text{Cr}_2\text{O}_3(0.1)$
Microhardness(kg/mm^2)	600 – 1000		$\text{Al}_2\text{O}_3(3000)$
Youngs Modulus,Gpa. (10^6 psi)	205-415, (30-60)	205-345 (30-50)	

Microstructure:-

Thermally sprayed deposits show a typical lamellar structure. Typical microstructures of plasma sprayed deposits of chromium oxide, zirconia, alumina, titania, and titania plus alumina are shown in Figs. 2.1.2, 2.1.3, 2.1.4a, 2.1.4b, 2.1.5, and 2.1.6 respectively.

The bulk of the coating cross section consists of the lamellae formed by the splat of molten powder particles on impacting the substrate or previous deposit surface (Fig. 2.1.4b). The unmolten particles retain their original crystalline compositions and shapes. There are several types of porosities identified in SEM and STEM studies, such as, less than 0.1 micron in diameter formed by coalescence of microvoids between the lamellae, 0.5-2 micron diameter formed mostly by unmolten particle and dark voids in the

lamellae with bright rounded nodules mostly formed by trapped volatile gases within the lamellae.

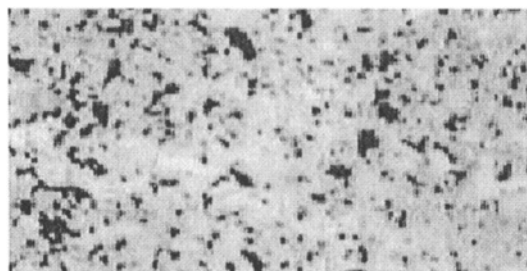


Fig.2.1.2. Plasma sprayed chromium oxide coating

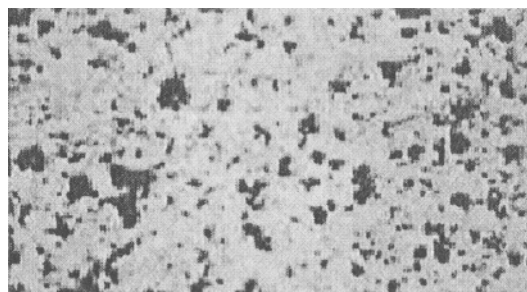


Fig 2.1.3. Plasma sprayed zirconia coating

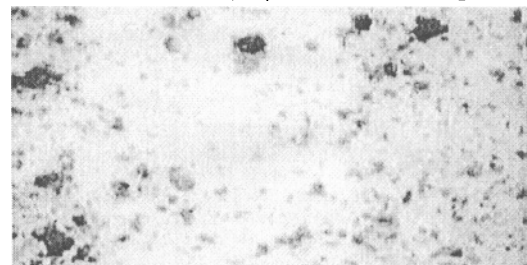


Fig.2.1.4. Microstructure of Plasma Sprayed Al₂O₃

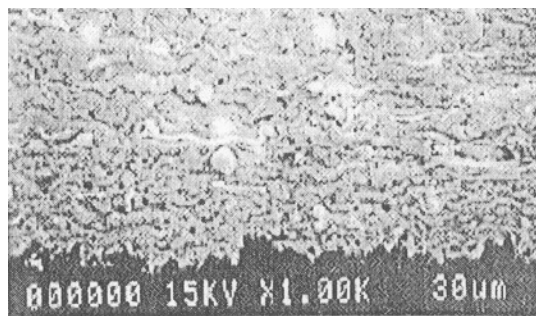


Fig.2.1.4b. Plasma sprayed Al₂O₃ deposit (SEM)

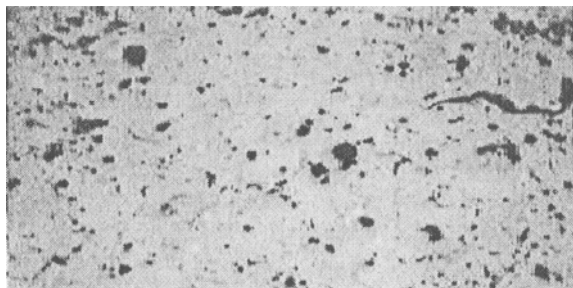


Fig.2.1.5. Microstructure of Plasma Sprayed TiO₂

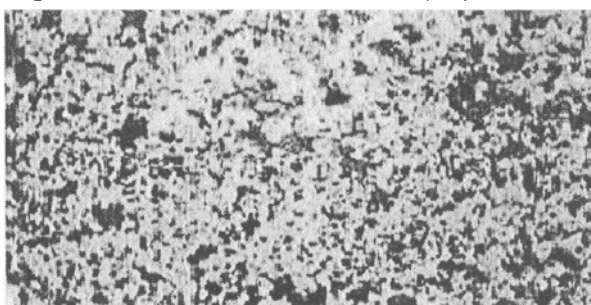


Fig.2.1.6 Microstructure of Al₂O₃ + TiO₂ (plasma)

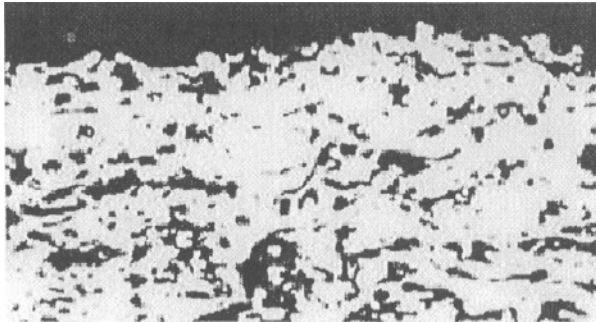


Fig.2.1.7. Plasma Sprayed Coating of MCrAlY

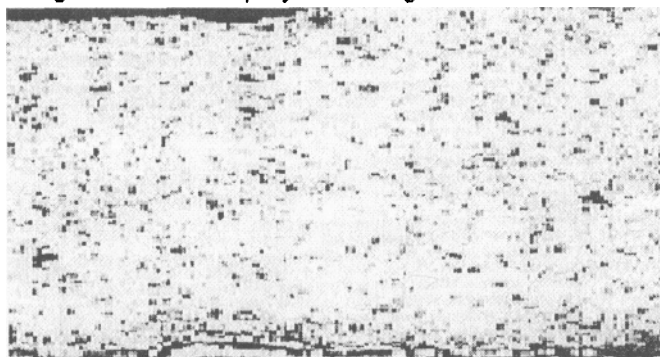


Fig.2.1.8 Vacuum plasma sprayed MCrAlY coating

The microstructures of an atmospheric and a vacuum plasma sprayed deposits are shown in Figs. 2.1.7 and 2.1.8 respectively. The coating material is MCrAlY. The atmospheric plasma spray coating exhibits lack of homogeneity and contains large number of oxides and voids. On the other hand, the vacuum plasma deposit of same material is comparatively more homogeneous and contains less of oxides and voids.

Applications

Thermal spraying has probably the largest range of applications covering almost all the industries with a vast range of coating and substrate materials. Most widely used in aircraft industries (compressor, combustor & turbine), followed by others including engineering (compressors, pumps, guide rolls, dies etc), chemicals & petrochemicals (pumps, valves, vessels, thread guide, rolls, Yankee drier), automotive (piston crown, ring & groove, tappet valves), medical (implants like hip joint) etc.

From the list of main applications industry-wise, some typical industrial applications are discussed as follows:-

Paper and Pulp Industry:- The wear in rolls (e.g. forming, breast, wire, suction, felt etc) and cylinders (for coating, drying, creping and cooling) used in paper and pulp industries is mainly due to heat, corrosion, adhesion and abrasion. In the pulp industry, wear in black liquor recovery boilers is due to corrosion and erosion.

MG Cylinder (11) :-

The most widely studied application in this area is the wear control of the drying cylinder, called MG Cylinder (or Yankee Dryer) through the development of suitable thermally sprayed coating.

These are large (10-20 ft diameter \times 22 ft maximum length) cast iron steam heated cylinders used for drying the wet paper, esp, tissue paper. The cylinder rotates at speeds up to 100 RPM and produces dried paper at rates of 6000 ft/min. maximum. In operation wet tissue is delivered to dryer on a felt web running over a pressure roll or rolls, and remains on dryer surface until it is removed by a scraping doctor blade at the other end. The cylinder surface is subjected to adhesive wear due to doctor blade, abrasive action (& paper) of paper and felt, and corrosive action of the liquid (3.5 to 8.5 pH).

Plasma Spray Method:- Grind the dryer to proper contour/Grit blast with chilled CI grits/Plasma Spray to 1mm thickness/Grind finish to 0.9mm with a belt grinder.

Performance:- Mo + NiCr coating showed the superior heat transfer rate, better sheet adhesion and release, longer doctor blade life, increased wear resistance. Coating materials used so far on the cast iron (grade 60) cylinder of 220-25 HRC are indicated in Table 2.1.6.

Tab2.1.6.Thermal Spray Coating Materials on MG Cylinder

Spray system	Material	Hardness (HRC)	Deposit thickness(mm)	Finish	Bond Strength (psi)
Arc	AISI 420	33-37	4.0	2.0 to 3.0	3,500
Flame	Ni-Cr-B-Si-C	38-42	2.0	1.5 to 1.0	3000
Plasma	Mo + NiCr	45	1.0	0.9	5000

Textile

The highly abrasive synthetic fibers can cause severe abrasive wear on parts like rolls, friction discs, hot plates, thread guides, heater tracks in textile industry. Plasma sprayed ceramic coatings of alumina, alumina plus titania and chromium oxide are normally used to minimize wear in these components. The coating density and hardness of ceramic oxide deposits are found to improve by using oxygen containing carrier gas instead of usual argon (12). The density and hardness of zirconia and titania show highest increase followed by chrome oxide and alumina-titania and pure alumina showing least improvement. By switching over from argon to oxygen containing carrier gas the average coating hardness (Knoop 100) shows an increase from 260 to 488 for zirconia, 409 to 703 for titania, 995 to 1135 for alumina-titania, 936 to 1231 for chrome oxide and 644 to 814 for alumina.

Automotive Industry

In developing high performance engine, it was found necessary to coat several engine components with plasma spray deposits at the OEM stage. Some of the components and the coating materials used are listed in the Table 2.1.7.

Thermal Barrier Coating on Piston Crown : The efficiency of most commercially available engines can be improved by coating the piston crown with an insulating material like stabilised zirconia. For a 180 KW (240 HP) diesel engine, thermal barrier coating of zirconia can increase the engine efficiency by 4% (14). The main requirements of the thermal barrier coating materials include a low thermal conductivity, resistance to corrosive and erosive environments, coefficient of thermal expansion high enough to be compatible with metal, and thermal shock resistance. The plasma sprayed

stabilized zirconia is used extensively in aeroengines as an ideal thermal barrier coating material. Yttria is the preferred stabilising agent for zirconia, although coatings with calcia, magnesia and ceria stabilized zirconia have also been used. The stabilised zirconia has been successfully tried as thermal barrier coating on piston crown, esp., with steel or cast iron pistons.

Tab.2.1.7. Plasma Spray Coatings on Automobile Components

Components	Wear	Coating Materials
1.Piston Crown	TBC	Mg- or Y_2O_3 or Ce-stabilised ZrO_2
2.Piston Ring	Adhesion	Mo+NiCrBSi,Mo+MoO,NiCr+CrC
3.Cam Follower	Adhesion	Mo,Mo+NiCrBSi
4.Piston Ring Grooves	Adhesion	Mo,Mo+ NiCrBSi,NiCr+CrC
5.Taper Valve Face	TBC	Alumina
6.Taper Valve Head	Adhesion	Mo+NiCrBSi
7.Synchronize Ring (Inner surface)	Adhesion	50Al-Si alloy +50Mo

Plasma sprayed magnesia stabilised zirconia coating with a bond coat of NiCrAlY has been successfully tried (14). The thermal properties of coating and base material are as in Table 2.1.8. The magnesia stabilized zirconia with a bond coat of NiCrAlY has been successfully tried as thermal barrier coating on CI piston crown (14). Multilayered graded coating with compositions varying from predominantly metallic at the interface to ceramic at the top has been used to minimize mismatch in thermal properties across the coating to base metal.

The differences in thermal properties between light weight aluminum silicon alloy as engine material and the stabilized zirconia as TBC top layers are listed in Table 2.1.8. In order to reduce the thermal property mismatch and to obtain good bonding, the recommended practices are as follows (15):-

- Change in bond coat material from NiAlCrY or NiAl to Al-Si alloy containing two times more silicon than base metal

- Use of compliant fibrous felt in between the base & coating to reduce thermal spalling
- Use of graded coating

Tab.2.1.8 Thermal Properties of Base & TBC Coating Materials

Material	Thermal Conductivity	Thermal Expansion Coeff
	(W/m.K)	(α) $^{\circ}\text{C}^{-1}$
Coating (25% MgO + ZrO_2 , & NiCrAlY)	0.78	9.0×10^{-6}
CI	46.86	11.6×10^{-6}
C-Steel	51.88	10.5×10^{-6}
Al-Si Alloy	146.44	21.5×10^{-6}

In order to obtain consistency in entire deposit quality, process automation may be necessary. Thinner coatings of less than one millimeter thick (including bond coat) is preferred. Apart from coating properties such as, microstructure and severity of thermal cycling, the failure of plasma sprayed zirconia and other thermal barrier coatings has been identified as due to amount of contaminants such as vanadium, sodium and sulphur in the fuel. Failure of the coatings normally occurs due to spalling through separation across the ceramic-bond coat interface. Next generation of zirconia based thermal barrier coatings (TBC) is expected to be those stabilised with ceria (approximately 25 wt%). Ceria stabilized zirconia coatings provide improved resistance to thermal shock resistance and high temperature corrosion. The coating of this type has been suggested as ideally suited in cases where fuel impurities are present such as, diesel engines and jet engines.

Wear Resistant Coating on Piston Ring : In the piston ring of high performance engines, thermal sprayed coatings of refractory materials are being introduced in place of earlier used hard chromium plating. The piston rings consist of top ring, second ring, and oil rings. The conventional surface treatments along with the current trends in hard surfacing the piston rings are indicated in the following Table 2.1.9. The requirements of piston rings of higher performance has led to a shift towards thermal sprayed coatings from the conventional hard chromium plating. The current trend is also to replace cast iron base material by stainless steel. Amongst the other processes tried, such as, gas nitriding, composite plating, PVD etc, physical vapor deposition (PVD) is found to be most promising. However, the process restriction of using vacuum chamber results in low productivity when using PVD process.

Thermal Spraying has been used advantageously as a high productive process (16).

Tab.2.1.9. Surface treatment processes for piston rings

Piston Ring	Base materials		Surface treatment	
	Conventional	Current Trend	Conventional	Current Trend
Top Ring	Alloyed SG iron	Austenitic	Cr-plating	Flame
	Low alloy steel		Cr-plating	or
	Austenitic stainless steel		Gas nitriding	HVOF
Second Ring	SG iron	stainless	Cr-plating	or
	Grey cast iron		Cr-plating	Plasma
3-Piece Oil Ring		steels	Cr-plating	
Side Rail	Carbon steel		Gas nitriding	Spray
Expander	Austenitic stainless steel			of Mo-MoO or Mo-NiCrBSiC or NiCr-Cr ₂ C ₃
2-Piece Oil Ring			Cr-plating	
Oil Ring	Carbon steel		Gas nitriding	
Expander	Austenitic stainless steel			

The ideal coating on piston ring should have following properties:-

- Less wear of coating in comparison to Cr-plating
- less wear of cylinder bore in comparison with Cr-plating
- More resistance to scuffing in comparison to molybdenum
- Superior resistance to break out in comparison to Cr-plating.

The most promising coating materials based on above considerations include Mo + MoO, Mo + NiCrBSiFeC, and NiCr + Cr₂C₃. The materials are deposited on piston ring by thermal spraying processes, such as, flame spraying, HVOF or plasma spraying.

High hardness coating is required to be high in order to resist scuffing and wear. Flame sprayed molybdenum coating contains 8 to 10% oxygen and the oxygen content of plasma sprayed coating is around 1%. Due to the large difference in oxide contents, the microhardness of flame spray molybdenum is 950 VPN compared to that of plasma sprayed molybdenum as 400 VPN (17). In order to improve the hardness of plasma sprayed deposit, preoxidised molybdenum containing 8 to 10% oxygen is used for spraying. Alternatively

microhardness of the deposit can be increased to 790 VPN by adding around 30% of high hardness self fluxing NiCrBSiCFe powder to molybdenum. Another high hardness composite powder used for plasma spraying on the piston ring is Chromium carbide (Cr_3C_2) plus 20 wt% NiCr. The disadvantages of high hardness plasma spray coating includes the difficulty of getting fine surface finish of the coating and high wear of cylinder bore.

Piston Ring Grooves : The plasma sprayed NiCr- Cr_3C_2 or molybdenum coatings in grooves show coating qualities as equal to or better than that of hard chromium plating (14). With the grooves of 9 to 18 mm gap, it is difficult to get a good adherence of the deposit at a spray angle between 35° to 55°.

Cylinder Bore : Cylinder bore (normally 70 to 110 mm diameter) surface interacts with the piston ring and the intermediate layer of lubrication in an internal combustion engine. An iron base plasma sprayed material has been reported (18) to produce coating with low coefficient of friction against piston ring under boundary lubrication condition, good thermal shock resistance, minimum scuffing tendency and well distributed porosities for retention of lubrication.

Power :

Boiler Tubes : The fossil fuelled boilers are either coal or oil fired. In a fossil fired boiler, the fireside corrosion occurs in the furnace wall, the superheater and reheater areas, causing tube wall thinning and premature failure. In the oil-fired boilers the vanadium and sulfur level in the oil (19) are important in fireside corrosion. In the coal-fired boilers, in addition to sulfur, chlorine content (19) of the coal is important in promoting corrosion. The rates can vary from less than 50 nm per hour to 300 nm per hour and more, thus giving tube lives ranging from more than ten years to two years and less (20). Erosion of boiler tubes is caused by the ash and also the dust contents of the gas stream and from soot blower operation. The erosion rate increases with the ash contents of the coal. The cost effective solution to reduce wear due to corrosion and or erosion in boiler tubes is to apply wear resistant coating by thermal spraying. Plasma spraying has been found to provide a dense, adherent coating of good quality. The best results for protection against erosion were obtained on surfaces coated with Cr_3C_2 (75%) in 80 Ni-20 Cr or with Al_2O_3 . The coating thickness for chrome carbide +NiCr was 0.75mm and that of alumina was 0.4 to 0.75 mm. A bond coat of Ni-Al was used in both the cases. However chrome carbide + NiCr coating with higher thermal conductivity than alumina is preferred for boiler tube application (20). For corrosion, 50 Cr : 50 Ni alloy out performed all other coating materials. The FeCrAl alloy possesses fairly good corrosion resistance properties but has a

tendency to spall (20). In order to obtain a dense adherent coating, it is necessary to develop a qualified procedure for spraying mainly based on the following factors:-

- Develop adequate surface finish by using specified grade of alumina and carrying out the blasting operation under optimum conditions.
- Clean & preheat the surface by dry & preheated air blasting.
- Spraying should start immediately after preheating allowing very little time for the surface to get oxidised.
- Maintain proper spray angle ($\approx 90^\circ$) by the use of manipulator consisting of a rectangular framework mounted on the boiler scaffolding with a carriage which can move along the length of each tube under power at a predetermined speed. The perpendicular motion allows the torch to be moved from tube to tube. Also the torch is mounted on a quadrant device allowing the angle of spray adjusted to $\approx 90^\circ$ according to the circumferential position of the tube.
- Avoid overlapping, since a local area of double thickness leads to excessive stresses and spalling.

Protective Coating on Cooling Water System: Thermal spray polymeric coating are used to resist corrosion in cooling water systems where sea or estuarine water is the cooling media. Coating material used include epoxy, polyester and polyurethanes. Such coatings on steel and cast iron components prolong the lifetime by two or three times (19) than that of non-coated surface.

Plasma Sprayed Coatings for Gas Turbine: In aeroengines, mean turbine blade temperature is 950°C but the peak temperature may exceed 1100°C . In marine and industrial services, a maximum temperature of 850°C is encountered but the environment is more erosive (21). The corrosion and oxidation are caused by high temperature combustion products while the erosion is due to particles resulting from incomplete combustion. The accepted service life of aircraft turbine is below 10,000 hours and for industrial turbine is 50,000 hours (21). The basic concept in selecting materials for critical components of the turbine is to specify high creep strength nickel base alloys, such as Nimonic (Ni-Cr-Mo-Al-Ti alloys) as substrate and use surface coating to guard against environmental degradation. The plasma spray coatings in gas turbine components are used to serve one or more of the following purposes:-

- Resist Oxidation & corrosion
- Resist Fretting & Erosion
- Become Abradable
- Act as Thermal Barrier.

In addition, coating properties should include the following:-

- Interface stability, i.e., there should be low rate of diffusion across interface and no embrittling phase formation at the high operating temperature
- The stress mismatch between coating and substrate during formation and use should not be high enough to cause poor coating adhesion & subsequent spalling. The coating should have enough strength to withstand operating stresses at the surface. The coating materials used for different purposes are listed in Table 2.1.10.

Tab.2.1.10.Turbine Coating Materials & Wear Applications

Coating Materials	Purpose	Applications
MCrAlX(M=Fe,Ni,Co) X=Y, Si, Ta, Hf	Corrosion & oxidation resistance coating	Turbine blades
WC-Co	Fretting & erosion resistance coating	Mid span damper
NiCrAl+Bentonite(700°C)** Nickel graphite (700°C)** AlSi+RA*(450°C)	Abradable coating	In engine casing, between rotor blade & casing; labyrinth seal.
MCrAlY+RA*+Polymer(700°C)** YSZ+RA*+Polymer(1200°C)**		Non-eroengine components like, radial compressor, turbo- -charger, turbo-compressor etc
Stabilised Zirconia + MCrAlY bond coat	Thermal barrier coating	Primary zone sections of combustors, nozzle, guide vanes

*RA=Release Agent; **Maximum Operating Temperature

Oxidation & Corrosion Resistance Coatings: The composition of M-Cr-Al system is so selected as to give a good balance between corrosion resistance and coating ductility, while active element additions can enhance oxide scale adhesion and decrease oxidation rates. A successful cobalt base coating composition is Co-25Cr-14Al-0.5Y. Recent coatings are based on more complex MCrAlX system, where M = Fe, Co, Ni or a combination of these plus the active elements X, such as Y, Si, Ta and Hf. A combination of active elements has been found to reduce coating degradation through their synergistic interaction. In gas turbine hot corrosion occurs mainly due to salt contaminants, such as $\text{Na}_2\text{SO}_4/\text{NaCl}$ mixtures, dissolving protective coatings through formation of low melting point alkali compounds. Based on the different proposed mechanisms, the hot corrosion processes are classified as

high temperature (type I, 800-950°C), low temperature (type II, 650-800°C), and hot salt corrosion. Overlay coatings generally perform better at high temperatures (>900°C) reflecting good adherence of alumina scales which is promoted by the presence of active elements such as yttrium. However the corrosion rate is high at lower temperatures, 650°C–850°C. The corrosion resistance can be further improved by use of platinum underlayer and overlayers (22) or by other additions such as Ti, Zr, Hf, Si and Ta. Plasma spray methods have found wide acceptance particularly argon shrouded and vacuum plasma spray processes. The high deposition rate of plasma spray system can be used to produce thick coatings with compositions similar to that of powder feedstock. The lamellar, equiaxed microstructures of plasma spray deposit are without any leader defects as found in EBPVD coating containing columnar structure. Argon shrouding or vacuum process reduces the possibilities of oxidation & loss of reactive elements such as aluminum. The porosity is further reduced by post coating thermomechanical processes. The plasma spraying is a line of sight process requiring complex robotic manipulations for complete coverage.

Thermal Barrier Coatings: Thermal barrier coating is used to protect flare heads and primary zone sections of combustors against the effects of hot spots, thereby improving considerably combustor life. In view of the success achieved in this area, the attention was diverted towards the use of thermal barrier coating on blades and vanes. However the present use is restricted to platforms of nozzle guide vanes. The duplex thermal barrier coating consists of a bond coat of M-Cr-Al-Y and a top coat of stabilised zirconia. The bond coat not only provides an adhesive bonding between ceramic top and metal substrate, but also provides corrosion protection to the base metal against any ingress of corrosive gas through the porous top layer. Bond coat also accommodates the difference in Young's modulus and thermal expansion coefficients between metal and ceramic. The bond coat of 125 μm is normally applied by using low pressure plasma spray system (LPPS). The rough surface produced by low pressure plasma spraying is utilised to achieve good adhesion between bond layer and the ceramic top. A bond layer exceeding 12.7 micrometers roughness average can be produced by using low pressure plasma spray. The advantage of using LPPS to deposit a bond coat is the ability to add Hf, or other elements, which enhance the adhesion of aluminium oxide scale thus improving the life of the deposited thermal barrier coating. The top ceramic coat of stabilised zirconia can be carried out by air plasma.

Antifretting Coating: The vibration of fan and compressor blades in jet engines is controlled by mid-span dampers. A mid-span damper provides contact point between the blades to constrain lateral and torsional motion which could result in flutter causing damage to the blade. Plasma sprayed

WC-Co coating is applied to the contact surfaces of mid-span dampers to reduce wear. The coating failure can cause damage and cracks in mid-span damper. The continued propagation of the cracks formed may result in engine failure. The damper performance is improved by inducing compressive residual stresses on the coated surface (23).

Diffusion Barrier Coating : In order to increase efficiency, the trend is to operate engines at higher temperatures and reduced cooling. At these higher operating temperatures, the coating life is severely impaired by interdiffusion of elements between coating and substrate. Therefore it is necessary to minimise diffusion of key elements from coatings to substrate by providing an intermediate diffusion barrier layer. For example, an ion plated diffusion barrier layer of Ni-13%Al between top layer of high chromium and superalloy substrate reduces considerably the diffusion rates of chromium at higher operating temperatures (24).

Graded Coating : In addition to diffusion layer, it is possible to develop a multilayered coating with increasing amounts of key elements like chromium and aluminium from interfacial to top layer. The mismatch of composition as well as other properties between the consecutive layers being gradual, the stability of graded coating is excellent. The lower concentration gradient reduces the diffusion rates and thus retaining the heat, corrosion and oxidation resistance of the top layers at the higher operating temperatures.

Abradable Coating : The gas turbine engines operate by compressing inlet air through a series of rotating blades enclosed within an outer casing and mounted to a center drive shaft. Engine efficiency depends, amongst other factors, on the clearance between the rotor blades and engine casing. The reduction of the clearance between blade tip to casing can cause blades rubbing against the shroud. By coating the shroud with abradables, it is possible to close the gap between interacting surfaces. Thermally sprayed abradable coating of composite materials (Table 2.1.10) applied to casing are sacrificial during clearance changes while providing a tight seal without damaging expensive rotor blade tips. The sacrificial coatings are also used in labyrinth seal locations to channel engine cooling air. The coatings are designed to be readily abradable but also should be able to resist particle erosion of abrasive dusts at high velocities coming out of the engine. In order to increase fuel efficiency, the operating temperatures of jet engines are increased to such an extent that the abradable shroud linings should be able to withstand a maximum temperature of 1200°C, instead of earlier requirement of 350°C. In addition to aeroengines, abradables are also used in most of the other rotating machineries such as stationary gas turbines, turbo compressors, radial compressors, turbo chargers and pumps.

The coating materials consist of fine powder particles as matrix, a polymer to generate porosity and solid lubricants or release agents to act as dislocators within the coating. During thermal spray deposition, the polymer phase lowers the coating stresses, thereby allowing thick deposits. Also polymer gets burnt out at the application temperatures of 400°C (Al-Si), 700°C. (MCrAlY) or still higher at 1200°C (Y_2O_3 -stabilised ZrO_2), thus generating porosities and improving abradability. Compressor blades made from fibre-reinforced polymers, titanium-alloys and steels, are used at comparatively low operating temperatures. The selection of coating materials is based on operating temperature and is normally restricted to polymers, AlSi + polymer, and metal matrix with solid lubricant etc. The superalloy compressor blades operating at higher temperatures (~700°C) need MCrAlY matrix, Ni-graphite or ceramic matrix. For operating temperature above 900°C in jet engine turbines, only ceramic-based abradables are recommended. In ceramic based abradables, there is no need to use releasing agent, since ceramics wear in a brittle manner. In order to protect the blade interfacing with hard ceramic abradables, it is necessary to harden the blade tip. Excellent performance has been reported for blade tips hardened by laser melting with simultaneous injection of hard particles (25). Atmospheric plasma spraying (APS) and HVOF are preferred processes due to their controllable spraying parameters, thus assuring reproducible quality. Due to the high coating density of APS and HVOF deposit it is essential to incorporate a sacrificial phase such as polymer that can be burnt out to generate porosity.

Plasma Spray Coating on Ti-alloys used in fighter Aircraft:- Fighter aircraft, such as F-22 uses large quantity of titanium alloys, approximately 42% of its weight for airframe and some critical systems (26). The Ti-alloys are used in aerospace industries because of their high strength to weight ratio. The alloys, such as, Ti-6Al-4V and Ti-6Al-2Sn-4Zn-2Mo, possess excellent resistance to fatigue, high temperature and environmental effects. However, these alloys are prone to sub-surface embrittlement caused by in-service oxidation at elevated temperatures. Vacuum –plasma sprayed coatings of MCr or MCrAlY are used as effective oxygen barrier.

2.2.2 Non-Transferred Arc Plasma Scan Hardening (5)

A highly concentrated non-transferred arc plasma jet with power density similar to electron & laser beams ($10^4 - 10^5 \text{ W/cm}^2$), has been successfully used for surface hardening of a submerged arc weld overlay. SAW Overlay material is a 5% Cr die steel (5Cr-0.5Mo-1.5%V-0.2C). A 30-KW non-transferred arc torch with a special interelectrode insert is used with following main variables:-

1. Torch nozzle orifice diameter (D) = 6.0 & 4.0 mm.

2. Current (I) = 300 & 400 A.
3. Torch travel speed (S) = 7.0 & 9.0 mm/s

Combinations of above parameters produced different surface temperatures and cooling rates, as follows:-

1. Highest surface temperature ($1282^{\circ}\text{C} > A_3$) & cooling rate (9.12×10^5 c/s) obtained by using large diameter nozzle ($D = 6.0$ mm), high current ($I = 400$ A), & low traverse speed ($S = 7$ mm/s).
2. Lowest surface temperature ($663^{\circ}\text{C} < A_1$) and cooling rate (3.16×10^5 c/s) obtained by using small nozzle orifice ($D = 4.0$ mm), low current ($I = 300$ A) & high traverse speed ($S = 9.0$ mm/s). All other combinations of parameters in between 1 & 2 led to surface temperatures between A_3 - A_1 and also above A_3 . By using optimum parameters, plasma scanning results in the development of around 3.5 mm thick case with uniform hardness of 520-540 from 5% Cr-weld overlay of 390-410 HV. Most of the carbides dissolves during heat treatment and thus on cooling the microstructure contains traces of Fe_3C , 2% Mn_{23}C_6 , 7.2% retained austenite and high hardness martensite. Ductile microstructure with discrete carbide particles in the finely dispersed martensitic matrix of high dislocation density leads to rise in impact strength and dynamic fracture toughness. High compressive residual stresses on the plasma hardened surface improve the fatigue properties of the component. Application areas include tools, dies and machine components used for hot deformation process. The components are made of either 5 %Cr steel or weld overlay of 5%Cr steel on cheaper substrate. Plasma treatment results in 65% improvement in wear life compared to untreated components.

2.2.3 Post Spraying Processes (ref 1-ch 1):

The spray coats usually require some surface finishing operation before putting in service. The spraying processes may include machining/grinding, fusing the deposited surface or sealing the surface pores with organic compounds, like wax or epoxy (Fig. 1.4.9, chapter 1). Advanced systems for fusion of spray deposits includes plasma, induction, laser and solar beams. The advanced post spray processes, excluding those using plasma are to be covered in the appropriate sections.

2.3 Plasma Transferred Arc Process (6, 7, 8, 27, 28):

In this process, the primary plasma arc column struck between anode and cathode is transferred to the base. In other words, by connecting the substrate to negative terminal, plasma arc column is formed between anode and the base material. The powder materials fed into plasma get molten along with the

surface layer forming weld overlay on the substrate. The schematic of the system is shown in Fig. 2.2.1.

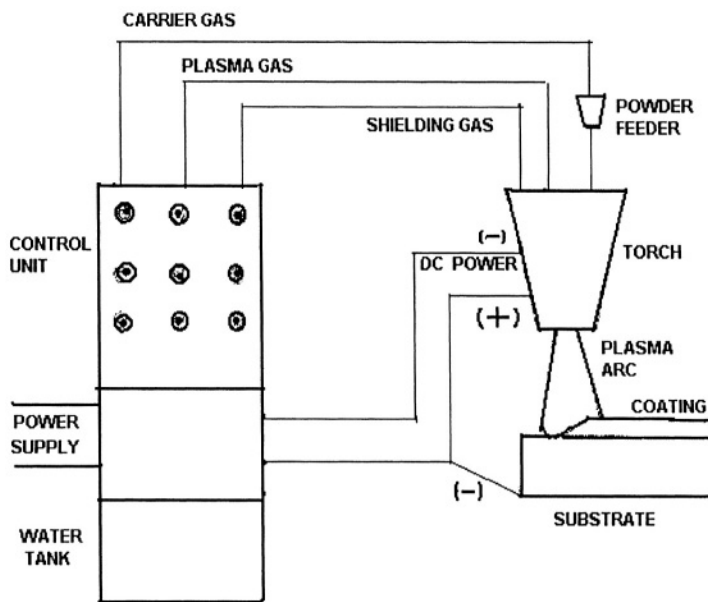


FIG.2.2.1 PLASMA TRANSFERRED ARC POWDER WELDING SYSTEM (SCHEMATIC)

Torch:- Similar to plasma spray, the torch consists of the central thoriated tungsten cathode and water cooled copper anode block. Plasma is generated in argon passing through an annular channel between anode and cathode. The anode block is provided with a channel to convey the metal powder using argon as carrier gas into the plasma arc. The molten droplets and deposit are protected from atmospheric contamination by a stream of shielding gas of argon or argon + hydrogen passing through the outer annular space in the torch (Fig. 2.2.2).

Gas:-

The commonly used plasma gas in PTA is argon. Argon or argon plus 10% hydrogen is used as shielding and carrier gas. Gas manifold is used to maintain the required supply pressure.

Power Supply:-

In PTA, primary arc is struck between the anode and cathode in the torch and the plasma column so formed is extended to the base by transferring the arc to the base metal.

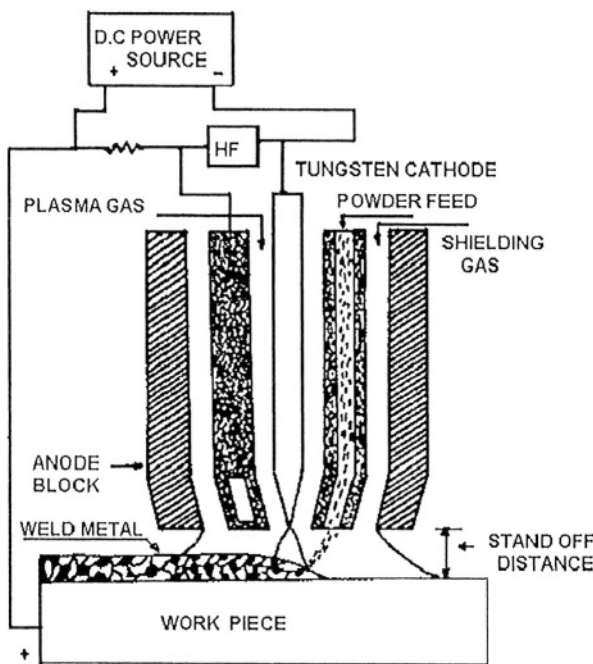


Fig.2.2.2. PLASMA TRANSFERRED ARC

Plasma weld surfacing using powder is normally done with direct current electrode negative (DCEN) polarity. Power sources available in the market include a wide range of currents, e.g., 0.1 to 500 amps. Low amperage range (upto 80 amps) is known as microplasma. Standard units cover 100-300 amps range, and above 300 amps units are known as high power PTA. The use of inverters, i.e., the primary pulsed power sources instead of conventional transformers has reduced the weight of power pack considerably. Portable inverter base power pack is now available from all the major manufacturers.

Advantages of using inverters include microprocessor controls & digital display (may provide memory functions), shuts HF starts immediately after the arc is established thus minimizing any potential interference with electronic equipment. Inverter based units can incorporate pulse welding capabilities. Inverters offer many possibilities; their applications are limited to lower output and thus cannot be used for high amps range of PTAW (27). Alternative to the inverter is secondary pulsed and conventional sources. Although inverters are in use since late 1980, improvements made in last few years have made possible some inverters to approach the reliability levels to that of conventional power source (28).

Pilot Arc:-

A small auxiliary power source is required for pilot arc. High frequency spark is required to start the primary plasma arc and to start the pilot arc.

Torch Oscillation:-

Arc oscillation can be achieved by mounting the torch on a open-slide that provides movement of the torch transverse to the line of travel. By controlling cross-feed speed, amplitude & dwell time of oscillation, it is possible to obtain required weld overlay bead size and shape.

Arc Voltage Control (AVC):-

Arc itself is a sensor, since it converts a measurement of length (arc gap) into an electrical signal (arc voltage). AVC compares the measured and desired arc voltages to determine the direction and speed at which the electrode should be moved. The difference expressed as voltage error signal is amplified to drive motors in a slide which supports the torch.

Powder Feeder:-

An inert gas is used to carry the powder onto the plasma. In PTA, argon is used as carrier gas. Fluidised bed system of feeding the powder is preferred. The system takes care of uniform flow of powder despite differences in densities in composite powders, such as, mechanically mixed WC plus Ni-base self-fluxing alloy (matrix) powders. Dual feeder system has been used successfully to form graded layers of required compositions, by controlling the feed rates of two different powders.

ID Torch for PTA Welding using Powder

For coating inside a bore or tubular products, the PTA torches available can work within an internal diameter of 35 mm and length up to 460 mm.

Process parameters & controls affecting deposit properties:-

Harris and Smith (29) used a two level, half replicate factorial design to study linear and first order interactive effects between the process parameters and quality features (ref Harris & Smith) and found direct correlation amongst process parameters like current, feed rate, travel speed, oscillation width and torch stand-off and the deposit qualities in terms of hardness, width, height and dilution. The control of torch stand-off (voltage), current, powder feed rate and travel speed leads to optimum deposit characteristics. The controls are achieved by presetting the independent variables before the start of the process. Some data on parameters controlling the deposit quality of Stellite6 powder in terms of dilution (30) are tabulated in Table 2.2.1. However, for individual application the optimum process control data are to be established by conducting trials, before going for mass production. PTA using powder is

more tolerant to variations in process parameters compared to GMAW or GTAW (30).

Current:-

The current is normally varied between 80 to 249 A, depending on the consumable feed rate, travel speed and the type of job. Higher current enables higher deposition rate, and thus improves productivity. However the use of higher current results in higher dilution (Table 2.2.1), distortion and overheating of the substrate. Therefore, it is necessary to find out the optimum current required to produce the acceptable levels of dilution, distortion and overheating of the base, combined with high productivity.

Feed Rate/Travel speed

Feed rate depends on current and travel speed. For a given deposit thickness and width, feed rate is determined by travel speed. Higher feed rates are used for higher travel speeds to produce required bead size (Table 2.2.1). For a particular feed rate and travel speed, the optimum current is to be found which would result in acceptable dilution limits.

The travel speed V_s (mm/s) and the diameter of circular surfacing layer, d (mm) are related as follows (31):-

$$V_s = \pi d/t, \text{ where } t = \text{surfacing time in seconds.}$$

Powder feed rate, g (g/min) is related to travel speed of V_s by the following equation:-

$$g = V_s \cdot h \cdot \rho / \eta,$$

where h = average height (mm) of the deposit per oscillation, ρ = density of the alloy (g/mm^3), and η = powder deposition efficiency

Dilution (32):-

For a given dimension of the deposit, the dilution increases with the increase in the current. In order to achieve the acceptable dilution level in a single layer deposit, the current need to be controlled to a minimum required value (Table 2.2.1). However, for a multilayered deposit, higher current can be used in building up the deposit thickness, excepting the top layer. For top layer, minimum required current for acceptable dilution level is used. The use of higher current shall result in the increase in productivity. In case of Stellite 6 coating on low carbon steel base, the dilution by iron results in decrease of the deposit hardness.

Tab.2.2.1 Process Parameters & Dilution in Stellite6 PTA Deposit

Deposit Area (mm ²)	Dilution (%)	Travel Speed (mm/s)	Current (A)	Powder Feed Rate(g/min)
7.5	5	4.9	163	17.5
	10	4	172	15
12.5	5	4.2	175	23
	10	2.7	185	17
	15	2.2	191	14
25	5	2.6	182	28.5
	10	1.8	194	18.0
	15	1.35	198	15.0

Bead Area: -

Larger size beads require more current and thus lead to more dilution. For example, in bead size less than 7.5 mm.sq., normally the dilution is restricted to 10% (Table 2.2.1). For large deposition areas, it is advisable to have multilayered deposit instead of a thick single bead. The higher current required to build up a thick layer shall result in more dilution in the deposited layer & distortion of the base structure. Due to overheating and slow cooling for large single bead size, the grains and the precipitated carbides become coarser. Also for large bead size, the wetting angle of 90 may lead to fusion defects across the bead. In multilayered deposit, the lower wetting angle of say 60 to 70 degrees allow more opportunity for a subsequent deposit to be fused onto a previous bead, thus reducing the possibilities of fusion defects.

Major Advantages of PTA :

Low Dilution (32)

In comparison to other welding processes, PTA using powder alloys produces very low dilution, i.e., very low pick-up of base material elements in the weld metal. Dilution in PTA deposit can be controlled within 5%, whereas in other welding processes, such as MMAW, the dilution in the first layer can be as high as 30%. With 30% dilution in each layer, three layers of weld deposits in MMAW shall result in the top layer with approximate dilution of 2.7%, i.e., within the compositional range of a single layer deposit from PTA. In MMAW, using 4mm diameter electrode, the three layers of deposits shall add up to 9 mm in thickness. Thus the top 3 mm layer of MMAW deposit

conforms to the required chemistry of the wear resistant weld overlay. In PTA, the specified composition of the wear resistant alloy can be retained in the first layer, thus allowing substantial savings in costly wear resistant material, energy and time.

Low HAZ:-

Lower HAZ in PTA deposit using powder alloys is possible due to lower heat input to the base metal. Thick deposits in other arc welding processes lead to longer depth of heat affected zone in base metal.

Weld deposition on difficult to weld metals:-

Due to low HAZ, low dilution and possibilities of making thin coating, PTA process has been successfully used to form crack-free weld overlay of high carbon highly alloyed cobalt base alloys on:-

- cast ferritic stainless steel, such as, CA6NM in critical hydroturbine components
- forged SS in engine valves
- forged ring of AISI410 in process control valves

Savings in Costly Wear Resistant Materials:

For a number of applications, such as tappet valves for passenger car, a thin layer of wear resistant material is required to be weld deposited on the seat area. It is possible to make a fraction of a millimeter thin deposit of expensive wear resistant powder (size 45-70 microns) materials by PTA. Also unlike other arc welding processes, the deposit retains the wear resistant properties of the Stellite powder used. Additionally unlike other arc processes no grooving is required to be formed for PTA deposition in the seat area of tappet valve. All these factors leads to enormous saving in materials.

High Productivity:-

Less welding time to build single layer deposit without filling the grooving and no subsequent elaborate finishing operation lead to very high productivity in PTA.

Coating Materials:-

A wide range of wear resistant alloys belonging to Fe-, Ni- and Co-bases are used to make weld overlays by PTA process. Coating materials are used in the form of spherical powders (approximate ASTM sieve size range is -100 to +325 mesh) with good flowability. The powder alloys are normally produced by gas atomization.

Metal matrix composites are produced by mechanically mixing required proportion metallic matrix powder(s) and hard carbides or by adding hard carbide powder in the molten metal pool created by plasma transferred arc. An

example of mechanically blended metal matrix carbide composite is a mixture of 50% self-fluxing Ni-Cr-B-Si-C alloy plus 50% tungsten carbide, both in the form of powder. The composite has been successfully used as PTA deposit for various applications, including tricone rock cutting bit, ID fan blade, sinter fan blade etc. For plastic extrusion screw, a wear resistant PTA deposit consisting of a mixture of high speed tool steel (matrix) and titanium carbide on the screw edges has found to improve substantially the life of the component. Another technique of forming composite is to melt the surface by PTA, while making controlled addition of hard carbides from a feeder to the molten pool. Improvement in wear resistant properties of light weight 5083 Al-alloy can be achieved by PTA melting of the surface with simultaneous addition of hard carbides (TiC, NbC).

Today almost 90% of Stellite & other wear resistant overlays on tappet valves, process control valves, hydroturbine components are carried out at OEM stage with automated PTA. In some nuclear valves it is mandatory to use only PTA process (29). Due to low heat input, the distortion in PTA process is less compared to other fusion welding processes. Selected coating materials, their nominal compositions and applications are listed in Table 2.2.2.

Typical Applications

Engine Valves (33,34):-

The wear properties of engine valves material depend on the type of fuel used, the duty cycle, stationary or mobile engine etc. The exhaust valves operate in severe environments of combustion products, especially the valve face area. The selection of valve materials is based on their corrosion and oxidation resistance properties in the high temperature combustion products of the specified fuel and operative conditions. However, the valve face needs extra protection against adhesive, abrasive and high temperature corrosive wear. In certain cases valve seat area needs extra coating. The commonly used coating materials for valve face are listed in Table 2.2.2. The commonly used valve materials include iron-base austenitic alloys, such as, 21-2N (0.55 C, 8.25 Mn, 20.35 Cr, 2.10 Ni, 0.3 N, rest Fe), 21-4N (0.52 C, 9.0 Mn, 21 Cr, 3.85 Ni, 0.44 N, rest Fe) and nickel base alloy like Inconel 751 (0.1 max C, 15.5 Cr, 0.95 Cb, 2.30 Ti, 1.20 Al, rest Ni).

In gasoline engines, for light duty applications, such as, automobiles and small utility engines, the exhaust valves operate in the range of 1350 to 1700°F (732 to 927°C). The valve materials are subjected to severe wear due to high temperature oxidation and corrosion. The materials like 21-4N and 21-2N mostly cater for this kind of requirements. With the current use of lead free gasoline, the corrosive wear due to formation of low melting compounds by deposited lead does not occur.

Table 2.2.2. Selected list of PTA alloys, compositions & applications

Alloys & Nominal Composition(wt%)	Weer/Applications
Iron base	
1.Ferritic SS AISI 410(0.04C,13Cr,4Ni) AISI 414(.03C,13Cr,5Ni,.14N)	Hot Corrosion /Con-Cast Rolls
2.Aust. SS AISI 309Cb(.08C,23Cr,14Ni,1.1Cb) AISI 316L(.03C,17Cr,12Ni,2.5Mo)	Cavitation-erosion/ Hydroturbine Pitting Corrosion/Chemical Equipments
3. HSS M42(1.1C,4Cr,.5Mo,14W,1V,8Co)	Hot hardness/Cold Shear Blades(Steel)
4.White CI Fe-2.4C,11.3Ni,24Cr,0.6Mo,1.2Si	Hot hardness, Thermal shock & Oxidation resistance /Concast Rolls, ID & Sinter Fan
Nickel base	
1.Ni-Fe-Cr *Incoloy 800(21Cr,39.5Fe,.35Ti, 35Al.)	Heat resistant/Carburising plant / Petrochemical equipments subjected to carburising
2.Ni-Cr *Inconel 625(22Cr,9Mo,3.5Cb., 32Al,.32Ti)	Corrosion & heat resistant/chemical, marine & pollution control equipment
3.Ni-Cr-Mo **Hastelloy 276(16Cr,16Mo,5Fe, 35V,3.5W),	ditto/Recovery of 'sour natural gas', heat exchanger, shear blade
4.Ni-Cr-Mo-Ti-Al ***Udimet 520(19Cr,6Mo, 12Co,3.5Ti,2 Al)	Creep resistant/Bar forging hammer, dies
5. Ni-Cr-Si-C (16Cr,0.5B,3.5Si,0.35C,17Fe)	Heat & corrosion resistant/Engine Valve
Cobalt base (Stellite****)	
1.Stellite 21 (.25C,1Si,27Cr,5.5Mo)	Corrosion & heat resistant/Forging dies, turbine components
2.Stellite 306(.4C,25Cr,2W,5Ni,6Cb)	-ditto-/ hydroturbine components
3.Stellite 6 (1C,1Si,28Cr,4W)	Engine, process control & nuclear valves, plastic extrusion screws
4.Stellite 12(1.4C,1.4Si,28Si,8W)	-ditto- higher hardness applications
5.Stellite 190(3.3C,26Cr,14.5W)	-ditto-/Drilling & mining equipments
Metal matrix Composite	
1.Ni-Cr-B-Si-C + WC	Hard coat on Tricone rock cutting bits
2.HSS(M2) + TiC	Hard coat on Plastic extrusion screws

*Trademark of Inco Alloys International,USA/ **Trademark of Hynes International Inc.,USA

*** Trademark of Special Metals Inc,USA****Trade mark of Cabot Corporation,USA

Heavy pitting due to high temperature oxidation and corrosion on the valve face can lead to escape of high velocity gas through the unseated gaps resulting in heavy erosive wear or burning of certain portion of the valve face. Erosive wear causing burning of valve face can also occur by deposited combustion product mechanically preventing the valve from properly seating on the head. Normally for light duty gasoline engine valves, the base material is capable of withstanding the environmental attack and thus no coating is

required. The lead free gasoline results in metal to metal contact in valve and valve seat due to the absence of intermediate layer of deposited lead. The high wear of valve seat area can be prevented by using suitable mating pair of coating materials with low adhesive wear (34).

The wear facing of the flange portion of the engine valves is necessary for engines designed for moderate to heavy duty using gasoline or diesel as fuel. Materials for the exhaust valves are same as that of light duty engines. The wear facing materials normally used include, Stellite 6 (480 HV), Stellite F or 32 (480 HV), and a Ni-Cr-Fe-Si-C alloy (425 HV) (33). The most important property of these materials is the retention of moderately high hardness at the temperature of operation. Since wear is inversely proportional to hardness, the materials retaining hardness at the operating temperature shall have excellent wear resistance (33). The variations in hot hardness values of Stellite 6 (Alloy 1), Stellite F or 32 (Alloy 2) and Ni 11(Ni-Cr-Si-Fe-C) (Alloy 3) alloys with increasing temperatures are shown in Fig. 2.2.3. The microstructures of the PTA deposits are shown in Fig. 2.2.4 (Stellite 6) and Fig. 2.2.5 (Ni-60). The stationary engines based on diesel or natural gas are characterised by large cylinders and slow speed. The exhaust valves of large-bore diesels are normally made from 21-4N, 21-2N, and Inconel 751. The wear resistant coating of materials, such as Stellite 6 on the flange area of valves minimises 'burning'. The 'burning' is caused by the presence of metallic salts from residual fuels and metallic ash from lubricating oils. Operators normally employ diesel engines as prime movers in locomotive and marine service as well as power plant operation (33).

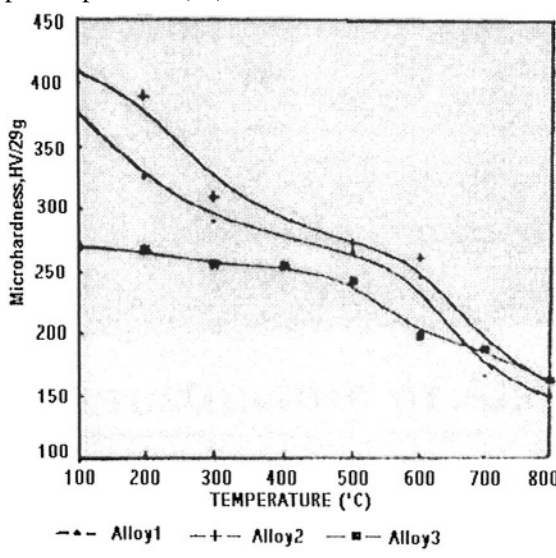


Fig.2.2.3. Hot hardness vs. temperature of nickel and cobalt base alloys deposited by PTA

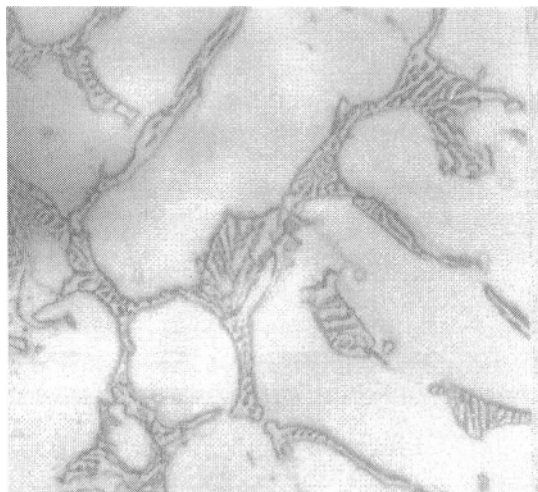


Fig 2.2.4 Microstructure of Stellite 6, PTA deposit

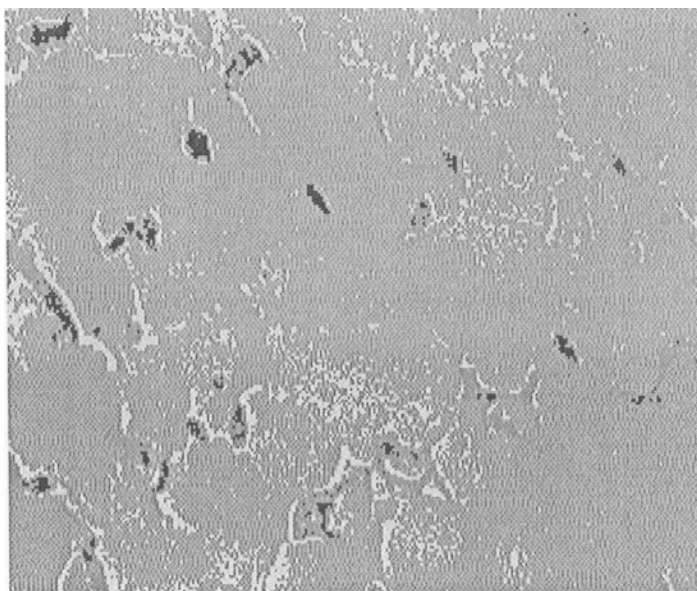


Fig 2.2.5 : Microstructure of a Ni-base alloy (Ni-60), PTA deposit, 1200X

In natural gas engines, heavy wear can occur in the valves and seat inserts. Since the natural gas burns with very little residue, the oxidized valves and inserts surfaces are in intimate contact with each other under high stress. In order to minimize wear, the recommended practice is to use high hardness

Stellites, such as Stellite 1 (670 HV) or Stellite 12 (500 HV) or Stellite 6 (480 HV) coatings on valve flange and also on the inserts (10). Natural gas engines are normally used in gas and oil fields, pipeline and irrigation service (34). The most widely used process for coating the valve face and seat areas is PTA using powder alloys materials (33).

Automated PTA systems are available for OEM valve facing of automotive engine valves. For other OEM applications including refurbishing the optimum deposition parameters need to be developed.

Process Control Valves:-

The sealing faces of the process control valves need to be surfaced by wear and corrosion resistant alloys. The alloys used include, Stellite 6, Inconel, Monel etc. The selection of the alloy depends on the wear environment in which the components need to work during operation. The most widely used process is PTA. The advantages claimed (31) over the conventional welding process include the followings:-

- Five times increase in productivity
- Seventy per cent less consumption in material
- Forty eight per cent reduction in cost
- Hundred to two hundred per cent improvement in service life using same hardfacing materials.

Rock Bit:-

Rolling cutter rock bits consists of three major components, namely, the cones, the bearing pins and bit body. All steel teeth cones need hardfacing or wearfacing in the gage surfaces. Wearfacing materials are also applied to the teeth depending on the intended usage of the cone. Wearfacing improves wear resistance to teeth but reduces resistance to chipping. Hence for hard formation cones, only gage is wearfaced and not the teeth. For soft formation cones usually both teeth and gage are wearfaced. The nose bearing area, as well as the thrust surface areas are hardfaced and ground to provide precision friction bearing surfaces. High hardness cobalt base alloy, such as, Stellite 1 or 190 is normally deposited in these areas by gas welding process. However, PTA deposit of a powder alloy composite containing Ni-alloy plus tungsten carbide has shown superior performance in comparison to gas welded Stellite in these application areas (35).

Continuous Casting Rollers (36):-

The rollers in the continuous casting process make contact with hot metal as well as cooling water spray. They are thus subjected to a combination of thermal fatigue, thermal shock, high temperature oxidation and wear. The commonly used surfacing materials for concast rollers is 12-14 % Cr- steels

weld overlays which are deposited with sub arc using metal cored tubular electrodes or open arc process. Both the processes lead to high dilution & coarse microstructure. Rolls of diameters at 200 mm or lower are difficult to built up in SAW without intermediate cooling due to excessive heat developed during welding. For smaller size rolls, PTA is superior process than currently used FCAW due to much less heat input and dilution. In order to increase the powder deposition rate of around 15 kg/hr, an high amperage torch of around 300 A was used.

A series of powder alloys (13 numbers) belonging to iron (includes 14% Cr-steels, Austenitic SS, Cast iron), nickel (Inconel, Hastelloy, Nimonic) and cobalt (Stellites) base were deposited by PTA. The hot hardness, oxidation resistance, thermal expansion coefficient and thermal shock properties of the weld deposits were evaluated. Of all these alloys, a white cast iron (Fe-2.4 C, 11.3 Ni, 24 Cr, 0.6 Mo, 1.2 Si) and Stellite F (Co-1.7 C, 22.7 Ni, 25.6 Cr, 12.3 W, 1.3 Si) are suggested as possible substitutes for the 13% Cr steel for this application.

Hydroturbine Components (35, 37)

The components such as valve seats, spindles, and cones are surfaced with stellites (St6, St21 and St306) by PTA process.

2.3.1 Transferred Arc-plasma Surface Treatment by Scanning (38)

The surface of a hardenable grade steel is heated by scanning the surface with an air arc plasma to austenitising temperature. Self quenching due to mass effect is not sufficient to form martensite even in medium carbon steel subjected to arc plasma scanning. Faster cooling by water jet shall result in the formation of hard martensite on the surface. The plasma current is controlled to achieve the required heating rate and the case depth. High intensity plasma arc leads to faster heating of the surface in comparison to that of induction or oxy-fuel flame processes.

2.4 Plasma Nitriding (10)

Glow discharge region of nitrogen containing plasma is used for nitriding. Nitrogen ions in the plasma stream striking the clean cathodic substrate promote not only nitriding the surface but also provide the heat necessary for the diffusion process. Plasma nitriding is carried out in a water cooled evacuated chamber (Fig. 2.3.1). Chamber surface forms the anode while work-pieces inside are connected to negative terminal. Design of the fixture containing large number of specimens should be such that there are enough gaps amongst them in order to avoid hollow cathode formation.

Chamber is grounded through a high resistance to prevent interference from the discharge by built up charges on the walls. Voltage across anode and

cathode varies between 500 to 1000 V. At electron volt of 1-10 eV and current density of $0.1 - 10 \text{ mA/cm}^2$, glow discharge occurs at a plasma density of $10^6 - 10^{14} \text{ cm}^{-3}$ (Fig. 2.3.2).

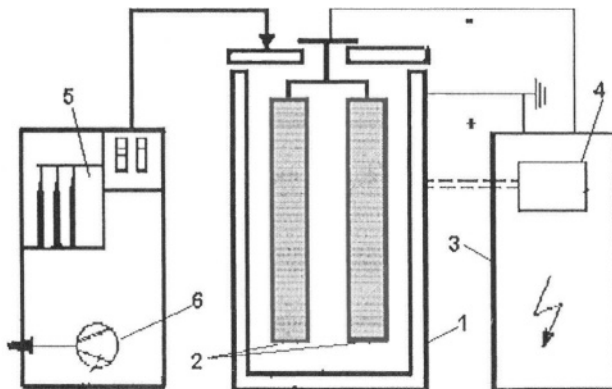


Fig.2.3.1 Plasma Nitriding System (Schematic)
 (Legends: 1= Vacuum furnace, 2=Workpiece, 3=Power pack & control, 4=Temperature controller, 5=Gas mix & control
 6 = Vacuum pump)

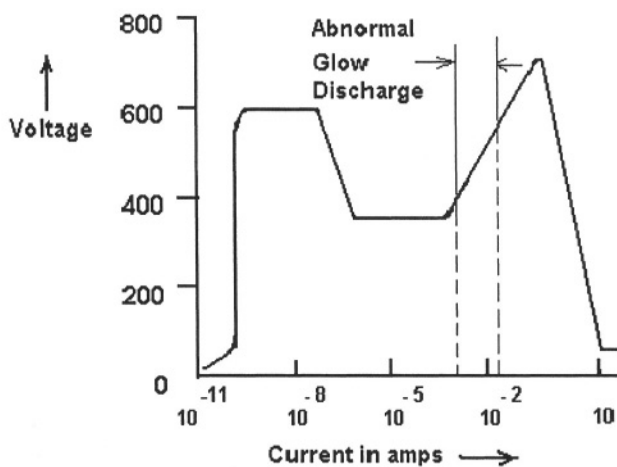


Fig.2.3.2 Current-Voltage Characteristics of Electric Discharge

Before abnormal glow discharge (Fig. 2.3.2), there is a normal glow discharge region marked by a fall in voltage to ~ 400 V. The voltage remains almost constant with the increasing current in normal glow discharge region. Beyond this region, steep increase in voltage is required to increase the current, and the discharge occurring under these conditions is known as abnormal glow

discharge. Nitrogen containing plasma formation in a vacuum of $\sim 10^{-2}$ - 10^{-5} torr and an applied voltage of ~ 500 volt leads to abnormal glow discharge (Fig. 2.3.2) region. Abnormal glow discharge plasma containing nitrogen results in nitriding of the components. During abnormal glow discharge, the current density is uniform everywhere in the cathode. The uniform current density on the cathode surface results in uniform heating, deposition and case depth of nitrided components.

Important factors influencing the glow discharge include (i) type of gas, (ii) gas pressure, (iii) electrode size & spacing and (iv) current & voltage condition (39). Different proportions of gases are mixed in a gas mixer and delivered at uniform pressure through gas manifold. Commonly used plasmagenic gases for nitriding are $N_2 + Ar$ or H_2 or $NH_3 + Ar$. Argon sputtering, prior to nitriding produces irregular clean surface which is found to be favorable to the formation of nitride layer. Nitriding of titanium was carried out by introducing nitrogen gas into chamber at 4 torr and using a subsidiary cathode to produce glow discharge at specimen temperature of 800–1000°C (39).

Process:-

After evacuating to 10^{-5} torr, the chamber is flooded with plasmagenic gas mixture to a pressure of 10^{-2} – 10^{-3} torr. The d.c power source is switched on and the voltage level is gradually increased to around 500 volts, when the glow of the discharge forms and covers the entire specimen, leaving a small dark region close to the cathode (specimen). Dark region corresponds to cathode fall region, where electron impact ionization is most prominent. The energetic nitrogen ions in plasma stream strike the specimen surface resulting in (i) the breakdown of passivating surface oxide layer, (ii) the rise in surface temperature to nitriding range (400-600°C) and (iii) mass transfer due to bombardment by nitrogen.

Glow discharge is maintained for a specified time depending on the temperature and the required case hardness & depth. Nitrided components are allowed to cool in the chamber.

Time for treatment at a particular temperature can be obtained from a plot of hardness against time. Hardness peak is obtained at optimum time. Shorter treatment period is required for higher temperature. With increasing temperature and time than the optimum, the hardness decreases due to coarsening of precipitates and grains.

Gas pressure in the chamber and the nitrogen content in the gas are also required to be optimized so as to achieve high hardness value of around 700 HV on nitrided surface.

Mechanism of plasma nitriding:-

The suggested mechanism of plasma nitriding is the formation of uniform layer of iron nitride on the surface through combination of sputtered iron atoms from cathode surface and nitrogen ions from plasma. Plasma process allows both bulk and grain boundary diffusion compared to only grain-boundary diffusion in gas nitriding. In plasma nitriding, it is possible to form single phase γ' or ϵ -nitride in contrast to mixed (γ' + ϵ) phase in conventional nitriding. White layer formed due to single phase γ' is comparatively more tough with minimum residual stress.

Microstructure of nitrided layer:-

The Fig. 2.3.3 a & b are the optical and SEM micrographs of glow discharge nitrided AISI 420 steel. The case depth is measured to be 61 microns. The XRD and XPS studies indicate the presence of predominantly hexagonal ϵ -Fe₃N phase in the microstructure. Also observed the presence of CrN and minor phase of Fe₄N in the microstructure (40). However, the XRD studies on plasma nitrided AISI 410 showed the presence of a mixture of γ' -Fe₄N and ϵ -Fe₃N (41).

Microhardness profile of nitrided specimen:-

The microhardness and N concentration profiles follow the same pattern. The microhardness is maximum (1400 HV) up to 60 micron beyond which there is a sharp decrease to the microhardness value of the base alloy at 80-90 micron (Fig. 2.3.4) (ref 40).

Plasma Nitriding Alloys:

White layer (0.005 – 0.01 mm) of γ' nitride (Fe₄N) can form on almost all types of alloy steels (heat treatable steel, nitriding steel, hot working steel, maraging steel etc). Presence of nitride forming elements, such as Cr, Al, Mo, W, V, Ti etc, leads to increase in the hardness of diffused layer to an extent depending on the type & amount of nitride formation.

Applications:-

The nitrided components possess excellent adhesive wear resistance, particularly to galling and scuffing, and have proved very successful in prolonging the life of dies & tools (punches, progression and press tools, dies and forms, slitting knives, plastic processing moulds and machine parts), automotive components (shift forks, rocker arms, tappets, cam shafts, discs & housing of rotary piston engines, cylinder liners, piston rings, crank shafts, gears, pinions, pinion shafts etc), forging dies, pressure bar pins & moulds, drive gears of rolling mills, cranes and turbine transmission.

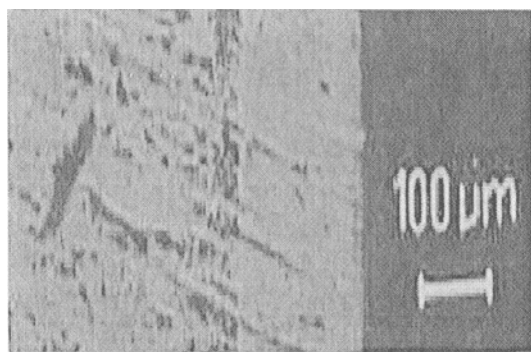


Fig.2.3.3a Optical microstructure of plasma nitrided steel

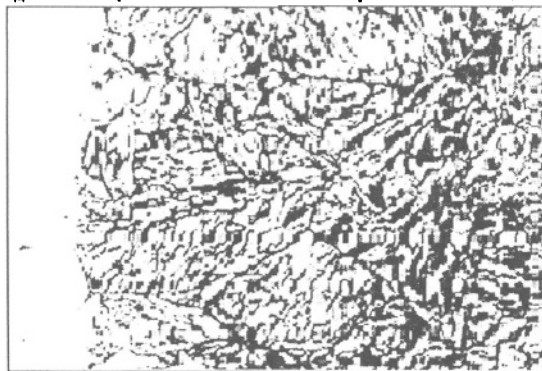


Fig.2.3.3b SEM picture of plasma nitrided steel; X3000
Total case depth of 61micron, first few microns with
different structure. (Permission to reproduce fig.
2.3.3a & b are obtained from authors of ref.40)

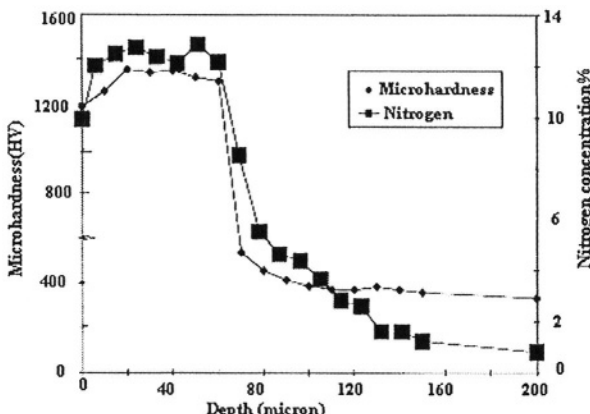


Fig.2.3.4 Microhardness and nitrogen concentration profile (Ref.40, permission to reproduce obtained from the authors)

2.5 Plasma Carburising (42, 43, 44) :

Plasma carburising is carried out in a vacuum furnace at 950-1050°C by diffusion of deposited carbon ions on the surface. The carbon ion containing plasma is produced by glow discharge in mixture of hydrocarbon plus nitrogen (for dilution).

Process:-

The schematic diagram of a plasma carburising system is shown in Fig. 2.4.1. The water-cooled vacuum chamber contains three compartments. The compartment on the left is connected to vacuum pumps and that on the right for quenching the carburised specimens. Middle compartment, which can be connected to either left or right ones, is used for plasma carburising. Carburising chamber contains anode, specimens as cathode and graphite heating elements. Specimens resting on a roller hearth are shifted after carburising for quenching to next chamber. Since the temperature required for carburising is almost 2-times that of nitriding, therefore separate arrangement is required to heat the specimen through graphite heating elements. Unlike nitriding, plasma is used only as a source of carbon. Once the required vacuum level is attained, the middle chamber is closed from both the sides. After heating the specimens to carburising temperature, methane (diluted with nitrogen) is introduced in the middle chamber. Methane is preferred to other carburizing gases, because plasma excitation enables it to provide a carburising gas yield of up to 80%. At an applied voltage in the abnormal glow discharge region, a thin glow from plasma surrounds the workpiece, causing increase in the carbon content on the surface layer. Specimens are quenched in oil immediately after carburising.

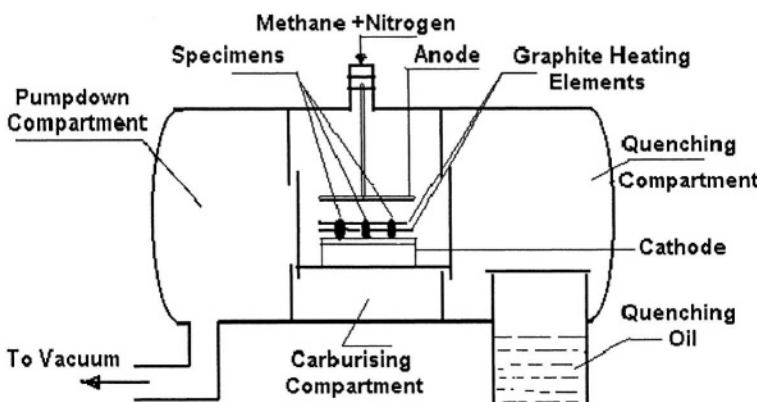


Fig.2.4.1 Plasma Carburising System (Schematic)

Advantages of Plasma over Conventional Carburising: A high carburising temperature of 1050°C in plasma process requires less time to develop the same case depth. For example, case depths of 2.5-3.0 mm can be achieved by low pressure plasma process in 20 hours, which is roughly half the time required by conventional process (43). The amount of carbon deposition on the surface depends on plasma current density, which can be controlled and monitored (43). As a result, it is possible to produce an uniform carburised layer with superior structure and excellent reproducibility.

High pressure gas quenching or ‘dry quenching’ of carburised components using inert gas as quenchant has gained popularity in recent years due to ecological and economic advantages over liquid quenching media. Emission of nonpolluting gas, clean surface of the component and equipment, reduced distortion of parts are some of the advantages cited in favor of high pressure quenching.

Plasma or glow discharge carburising has shorter cycle time, closer control of surface carbon and no part size limitation. Also there are no surface oxidation and less distortion than conventional processes. In plasma process, a simple mechanical masking is required to prevent carburising of any part of the component. The other three carburising techniques, viz, pack, gas & liquid require costly masking methods, such as copper plating or stop-off paste. Plasma process has been used successfully for partial or selective case hardening. For example, only the teeth of the steering-system pinion gears are plasma carburised leaving the gear tips and roots unhardened by masking with caps. The internal blind hole of a fuel injection nozzle is uniformly carburised leaving the outer surface masked by a sleeve during plasma carburising.

*Applications:-*Earlier restricted to aircraft industries due to high cost, plasma carburising is gaining popularity in automobile & other sectors as a major case hardening process for critical components.

Similar to carburising, nitriding & carbonitriding, plasma-assisted diffusion process for bonding has been used successfully (44).

2.6 Plasma Paste Boronizing (44, 45):-

In paste boronizing of stainless steel by plasma heating, a borax paste (30% B) is applied to stainless steel surface and then the component is heated in an argon plus hydrogen plasma. The diffusion of boron leads to the formation of a boron-enriched layer on the surface. The boronized surface layer contains precipitates of chromium boride and nickel borides. The processing time required for plasma is less than the conventional process to form boride layer of same thickness. The microhardness of 2000 HV can be obtained on the plasma borided surface.

2.7 Plasma Assisted Vapor Deposition (10, 46, 47, 48, 49):

The process consists of vaporizing and subsequent deposition of coating material from the vapour phase onto the substrate. When the evaporation of the coating material is carried out with high intensity beam, such as plasma, ions or electron or by electrical heating the process is known as Physical Vapor Deposition (PVD) process. Alternatively, volatile compound of the coating material in vapor phase at high temperature is allowed to decompose on the substrate so as to deposit the required elements or alloys on the surface. The alternative technique is known as Chemical Vapor Deposition (CVD) process. The list of coating materials includes metals, carbides, nitrides, carbonitrides and amorphous diamond (Table 2.6.1). The coating can be made of a single layer or a multiple layered deposit of same or different coating materials.

Tab.2.6.1 Some Coating Materials for Vapor Phase Deposition

Element	Carbide	Nitride	Carbonitride
Ti	TiC	TiN	TiCN
Ta	TaC	TaN	TaCN
Zr	ZrC	ZrN (TiZrN)	(Ti-Zr)CN
Cr	-	CrN	-
Al	-	TiAlN	-
Mo	-	-	-
W	WC	-	-
Hf	HfC	HfN	-
C	-	-	β C ₃ N ₄ -

2.7.1 Plasma assisted PVD:

Physical vapour deposition process is carried out by vaporizing the material to be deposited by evaporation, sputtering, or ion plating process and then condensing the vapor on substrate surface. Evaporation process can be carried out by heating the coating material by resistance, RF induction or by high energy beams like plasma. Ion plating is carried out with ion beams heating system. Evaporation technique produces PVD coating with lowest adhesion at highest deposition rate. A major disadvantage of sputtering technique, compared to evaporation and ion plating is the low deposition rate,

which does not exceeds $500 - 1000 \text{ A}^\circ$ per minute and only reaches $10,000 \text{ A}^\circ$ per minute with copper due to its good thermal conductivity. However with more recent magnetron & plasma sputtering processes higher deposition rates can be achieved.

The structure of the vacuum evaporated deposit (47, 48, 49, 50) depends on substrate temperature (Fig. 2.6.1). At substrate temperature less than 0.26 Tm (for oxides) or 0.3 Tm (for metals), where Tm being the melting temperature of the material, the structure of the deposit is fine grained and convex in shape (zone 1). At substrate temperature between 0.26 to 0.45 Tm (for oxides) and $0.3 - 0.45 \text{ Tm}$ (for metals), columnar structure results (zone 2). With further increase in the temperature above 0.45 Tm , a denser deposit with improved grain formation is achieved. (zone 3). The '3-zone' model has been established for many materials such as Ti, Ni, W, Al_2O_3 , ZrO_2 and TiC. The superior deposit purity is obtainable with shorter distance between substrate and evaporation source, lower residual gas pressure and higher evaporation and condensation rates.

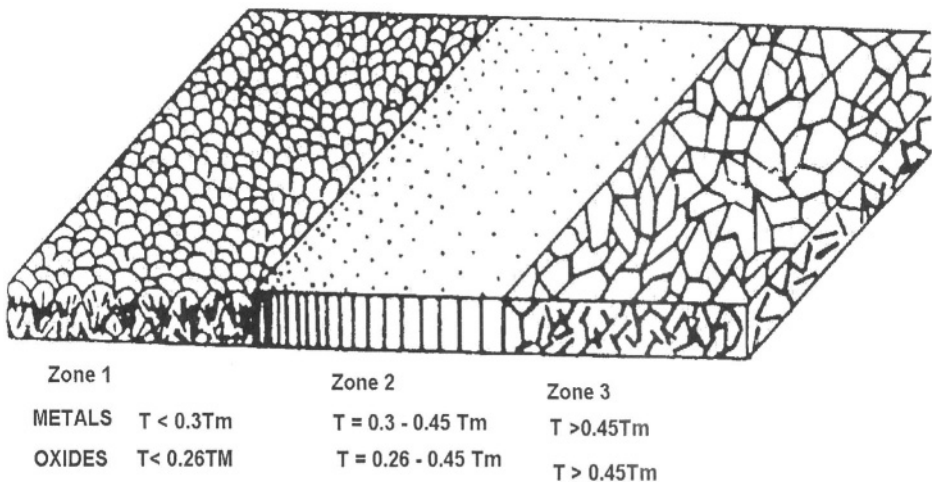


Fig. 2.6.1. Variation in Microstructure with Temperature in Vapor Phase Deposit (Schematic). T= Substrate Temperature and Tm = Melting Point.

Plasma Sputtering Deposition:

Production of sputtered coating utilises abnormal glow discharge phenomenon, like plasma nitriding, between the coating material (target) connected to cathode and the specimen as anode (Fig. 2.6.2). Sputtered coating is produced in a chamber evacuated to a vacuum of 10^{-5} torr and subsequently flooded with plasmagenic inert gas like argon to a pressure of $10^{-1} - 10^{-3}$ torr. Abnormal glow discharge occurs between the cathodic target

material (coating material) and the grounded substrate with applied voltage in the range of 100 V to several KV. Positively charged ions from plasma in the glow discharge strikes the negatively charged target with high energy at 1000 eV. The process disintegrates atoms or groups of atoms (molecules) from cathode surface and is known as 'sputtering'. The "knocked out" or "sputtered" materials from the target settle on the surface of substrate. Prior to coating operation, the surface can be cleaned by reversing the polarities, when the plasma produced by glow discharge cleans the substrate surface by removal of surface layers. Non-conductive materials, such as, refractory carbides, nitrides and oxides can not be deposited while using DC mode. Reactive DC sputtering or RF power source is used for non-conducting films. Gas occlusion (Ar) can occur in deposit using higher pressure. The gas occlusion and slow cooling rates are the principal limitations in DC or RF sputtering. These difficulties can be overcome in magnetron sputtering where higher sputtering rates can be obtained at lower pressure.

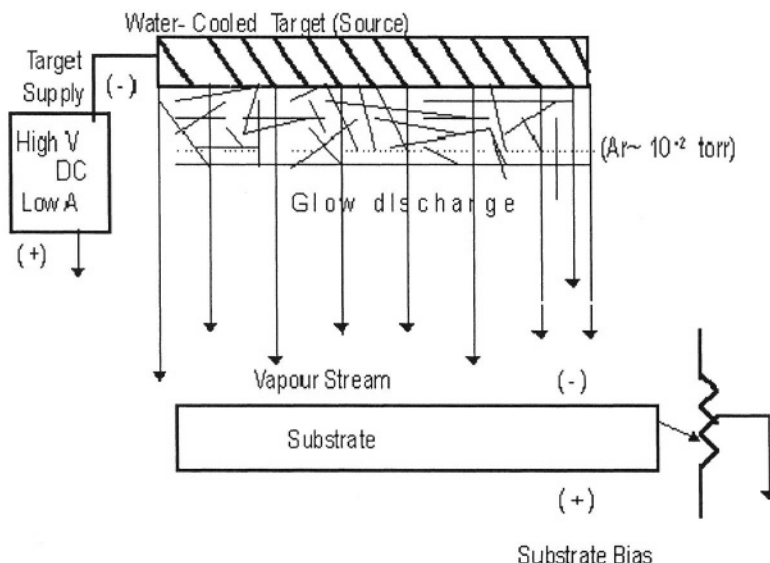


Fig.2.6.2 Schematic of DC Sputtering

Magnetron Plasma Sputtering:- In magnetron, electromagnetic field is designed to magnetise trapped electrons near cathode (sputtering target) resulting in enhanced ionisation of plasmagenic gas. The magnetron plasma, normally consists of ionised argon, is accelerated towards the target. The striking plasma stream causes sputtering from the target. The magnetron target can be cylindrical or planar (disc or rectangular) in shape. The magnetic field can be balanced or unbalanced. In a planar magnetron with a leakage magnetic field near the substrate is known as unbalanced magnetron. Normally more than one magnetron is used, preferably placed at alternate

ends with the substrate in the middle. This type of configuration leads to higher coating rates. Usually magnetrons are made with DC or RF biasing of the target. Recently bipolar single and dual magnetrons are also used. This has made possible to sputter insulating and multiple targets. In a bipolar power supplies, the voltage waveform changes between positive and negative with respect to reference. The negative bias does the sputtering (also charges the insulator surface positive) and while positive bias accelerates electrons and neutralizes the surface positive charge. In dual power supplies, two separate targets can be biased which enable reduction in sputter time & formation of new coatings. For example, TiAlN coating can be formed by sputtering from aluminum and titanium targets in a nitrogen atmosphere. The oxidation and wear resistance of Ti(C, N) coating is improved further by adding aluminum to the coating (51). In this case aluminum oxide layers form on the Ti(CN) during use at higher temperatures, which minimises diffusion of elements from or into the coatings. As a result, the diffusion wear, which represents one of the major wear mechanisms affecting cutting tools, is minimized. Apart from argon used for sputtering, another reactive gas, such as nitrogen can be introduced in order to form the desired coating (nitride with nitrogen). It has been observed that the use of a separate plasma environment ionizing the background gas results in the improvement in sputtering rate, coating formation rate and coating adhesion to substrate.

The density and structure of sputtered deposit are dependent on substrate temperature and deposition rate. Similar to evaporation method, the columnar deposit structure is observed at substrate temperature above 0.5 Tm. At substrate temperature above 0.7 Tm, equiaxed grains are observed. Sputtering is one of the most effective techniques for deposition of multilayer coatings, due to the followings:-

- Unlike other PVD processes, it permits transformation of original materials to the vapor form as a result of impact ablation of the target, without any intermediate liquid phase
- Less danger of decomposition than in the case of electron-beam induced evaporation (52)
- Sputtering is not limited by the melting point of the coating materials.
- Sputtered deposits have appreciably better adhesion than obtainable through other evaporation processes. The impingement of the sputtered high energy particles effects penetration into the surface of the substrate thus causing diffusion and improved adhesion of coating materials.
- Sputtering also enables multicomponent alloys of the correct composition to be deposited even at low temperatures by varying the partial pressure ratio between the reactive and process gases.

With plasma sputtering the deposition rates can be increased to ~250 micron per hour, which is lower by one order of magnitude than those obtainable with

evaporation process. The sputtering process has been used to produce segmented structures consisting of number of fine cracks perpendicular to the substrate surface (49). The network of small individual segments is expected to improve strain tolerances and thermal cycling life.

The level of nuclear plant exposure due to activated cobalt wear debris can be reduced by providing wear resistant coating on cobalt base materials. Multilayer chromium nitride ($\text{Cr-N}_{ss}/\text{Cr}_2\text{N}$) coatings consisting of chromium nitride (Cr_2N) top layer and solid solution of nitrogen in chromium (Cr-N_{ss}) as the base layer are produced by a reactive, unbalanced magnetron sputtering on cobalt base alloys, such as Haynes 25 and Stellite 3. This coating results in significant decrease in wear rates in nuclear applications (53).

Sputtering like other PVD processes is a “line of sight” process, hence the thickness of the deposit falls off towards the edge. Therefore to obtain uniform coating it is necessary to either move workpiece or steer the beam to required direction (54). Another development to eliminate ‘line of sight’ problem associated with PVD is the use of *Plasma Source Ion Implantation (PSII)* technique. In this process, the target to be implanted is placed directly in a low pressure (glow discharge) plasma source and to high negative potential with respect to chamber walls. Ions from the plasma are accelerated normal to the target surface across the plasma sheath. This eliminates not only line of sight problem, but also the problem of non-uniform dose retention in non-planar targets (54).

PVD Applications:- The commonly used coating materials are titanium nitride (TiN) & titanium carbide (TiC). Various combinations of coatings, like TiC + TiN or TiC + TiC(N) + TiC etc are also used to improve the tool life. A thin film of gold-coloured TiN coating improves wear resistant properties of cutting tools, plastic extrusion dies, moulds etc. PVD process can be carried out on tools after heat treatment or finished tools, provided the tempering has been carried out above the PVD process temperature employed. This permits use of this process to form a thin wear resistant coating on finished tools, made from heat treatable tool & die steels. As a matter of fact, new ISO/Euronorm grades of carburising steels with higher tempering temperatures ($>300^\circ\text{C}$) are increasingly being used for carburising gears and other dies & tools applications in order to enable TiN, TiC & diamond coating on the finished components (55).

2.7.2 *Plasma Assisted CVD (PCVD)*

A major drawback of CVD process is the requirement of high substrate temperature ($\sim 1000^\circ\text{C}$) for the deposition process. With the use of glow discharge plasma in chemical vapor deposition process, the substrate

temperature can be reduced to the same level as that of PVD coating, i.e., 150-200°C.

Process:

In this process, prior to deposition, hydrogen (plasmagenic gas) is introduced into the evacuated chamber and a dc glow discharge between the furnace wall and the substrate leads to formation of hydrogen plasma. Plasma stream containing hydrogen ions strike the substrate and increases surface temperature between 400-700°C. Reactive gases, methane (for TiC), or nitrogen (for TiN) are introduced to a total pressure of 4 torr. Uniform coating of TiN or TiC is obtained at deposition rates between 1-3 micron per hour.

Variables:

The chlorine content in TiN coating increases with decreasing temperature below 550°C and that of TiC coating below 475°C. Coating hardness decreases continuously with decreasing deposition temperature. Hardness of coatings with a chlorine content of less than 5 wt% are 3000 & 2000 HV for TiN & TiC respectively, and continues to decrease with increase chlorine content. TiN & TiC coatings formed by plasma assisted CVD have higher adhesive strength than similar coatings formed by ion plating and they have very good wear and seizure resistance.

Plasma enhanced chemical vapor deposition process (PECVD) has been used to deposit wear resistant coating of 100nm thick diamond like nanocomposites on miniature micro-electro-mechanical components. The film contains a diamond like network of C : H and a second network of Si : O with good adhesion to most substrates. The hardness of the film ranges from 9 to 17 Gpa with friction coefficient of about 0.5 in air at 30 to 50% relative humidity (56).

Thermal-plasma CVD, unlike conventional PCVD operation is not restricted in a reduced pressure. Thermal-plasma CVD has been used to form ceramic coatings at high deposition rates. It has been successfully used for deposition of diamond or diamond-like coatings (DLC).

Microwave-plasma CVD using gas mixtures of methane & hydrogen with additions of oxygen and carbon-di-oxide has been used to produce diamond film on silicon. Substrate temperature is at 870°C.

High Energy Intensified Plasma Assisted Processing (HEIPAP) unit employs three power supplies, viz, emission source for heating filament and DC-powered positive plate plus RF-powered substrate holder for generation of highly intense plasma. Nitrogen is used to form plasma containing nitrogen ions, which combine with sputtered aluminum atoms from the base to form

aluminum nitride on the substrate surface. Advantages claimed include the use of nontoxic nitrogen compared to toxic or flammable precursors required for CVD (57).

2.7.3 Vapor Phase Deposition Techniques for Diamond

A large number of thermally assisted processes or combinations are used for the low-pressure diamond deposition. The list of vapor phase diamond film deposition processes include the followings (ref. 58):-

1. Thermally activated CVD (TA-CVD) : These are high temperature processes.
 - i. Hot Filament/hot surfaces
 - ii. Laser heating
 - iii. Arc discharge and arc plasma jets
 - iv. Oxy-acetylene gas flame
2. Electric or electromagnetic gas discharge activation : These are mainly plasma activated chemical vapour deposition or PA-CVD processes.
 - i. Microwave or radio frequency gas discharge
 - ii. AC or DC glow discharge
 - iii. Plasma jet induced by RF/Microwave/DC
3. Combination of 1 and 2.
 - i. Hot filament plus Microwave.
 - ii. Hot filament plus DC discharge
 - iii. Hot Filament plus BIAS or in other words, electron assisted CVD.Excepting the processes involving plasma, others are discussed in the relevant chapters.

Types and formation of diamond coatings:- The chemistry & structure of the diamond coatings can vary widely, and accordingly the coatings are referred to as follows:

- i. hydrogenated amorphous carbon (α -C:H)
- ii. metal doped hydrogenated amorphous carbon (Me: α -C:H) and
- iii. Diamond-Like Carbon (DLC) which are carbon coating containing mixtures of diamond and graphite.

A mixture of methane and hydrogen is generally used in vapor deposition system to produce diamond coating. Hydrogen in it's atomic form tends to stabilise sp^3 bonding (diamond) and to eliminate sp^2 bonding (graphite). When an atomic hydrogen dominated plasma stream containing carbon strikes the prepared substrate surface, any graphite bonding is washed away leaving only high quality diamond (57). Silicon wafer substrate facilitates nucleation and growth of diamond. Silicon combines with hydrogen in hydrogen plasma to form SiH_4 , which on reaction with CH_4 forms β -SiC. Nanocrystals of β -SiC helps nucleation and growth of graphite (58). Polycrystalline diamond can be

grown by a variety of techniques, including PVD (55) and microwave plasma assisted CVD (46, 59) technique. Self-supporting polycrystalline diamond is usually allowed to grow on silicon substrates and removed chemically after growth. Wafers can be polished, processed and laser cut to required dimensions. High quality white transparent diamond containing virtually no graphite grows at a very slow rate. High growth rate is observed in the formation of 'black' diamond containing small amounts of graphite. While the former is required for electrical & optical applications, the latter is used for cutting tool inserts and heat spreaders.

Properties and Applications (ref 60):- Due to very strong chemical bonding, the hardness, molar density, thermal conductivity, sound velocity, and the elastic modulus are the highest of all known materials while its compressibility is the lowest. The dynamic friction coefficient of diamond is 0.05, a figure which is as low as that of Teflon and the lowest amongst the materials of interest. Diamond does not react to normal acids even at elevated temperatures. Hot chromic acid or a mixture of sulphuric and nitric is used to remove graphite from the surface of diamond. Molten hydroxides, the salt of oxy-acids, and some metals (Fe, Ni, Co etc) have some corrosive effect on diamond. At temperatures above 870°K diamond reacts with water vapor or CO₂. Diamond reacts chemically with metals like tungsten, titanium, tantalum and zirconium, to produce carbides at high temperatures. Diamond dissolves in white iron, cobalt, nickel, manganese and chromium at high temperatures. Due to dissolution reaction of diamond with iron at temperatures above 680°C, diamond tools are not suitable for machining operations of steels. Due to high hardness and low coefficient of friction, diamond is used as cutting tools. The cutting applications include nonferrous materials like aluminium & its alloys, copper & its alloys and ceramic materials like quartz, sapphire, Si₃N₄, SiC, WC etc.

Diamond or diamond like coating has the following advantages (55):

- permits use of less lubricants and the additives (less pollution of environment).
- improves load bearing capacity
- extends working life of the component
- allows use of cheaper, lighter base material.

Wear of a diamond coated carburised transmission component, e.g., low speed planetary gear system sun wheel under poor lubricating conditions, is less than 1/4th of that occurs in carburised component. Low wear in diamond coated component is due to low friction and high hardness of the coating (59).

Diamond coated high speed, highly loaded gears have shown fatigue limits of around 20% more than corresponding carburised materials. Since the fatigue life of both the through-hardened and carburised gears after diamond coating is similar, hence considerable cost saving is possible by the use of

through-hardened component. (55). In diesel fuel injection systems, emission control legislation has led to reduced lubricity of fuels and increased injection pressures, the use of diamond coatings has become the only possible technology to combat wear due to scuffing. It is possible to precisely control the formation & dimensions of thin diamond coating and thus can be used on components without any design change.

2.8 Vapor Phase Deposition of Amorphous Materials

Amorphous structures of crystalline materials can be produced by rapid cooling of the liquid during solidification or the vapor phase during condensation. The vapor condensation process is mainly used for producing required magnetic and electric properties in the amorphous materials. By rapid condensation from vapor phase at a cooling rate of more than 10^5 K/sec, the crystalline metals and alloys can form a deposit with amorphous or glassy structure. The atomic deposition process is estimated to produce “cooling rates” of around 10^{15} K/sec (61).

Plasma gun techniques have been used to produce amorphous materials (61). In one system, the substrate rotates and the plasma gun oscillates to cover a wider substrate area and thus reduce substrate heating. In another case, a gas jet at right angle to plasma sweeps away the hot plasma gas. Thick film of amorphous metal can be made by the plasma guns. Thickness of the film can be several millimeters. However with increase in thickness there is an increase in internal stress leading to formation of cracks and separation of deposits from substrate. Thicker films may contain 10-15% porosity.

Sputtering (62) has been used for production of amorphous metals. Parameters controlling structure & properties of the deposits include sputtering rate, the nature (d.c or r.f) and magnitude of substrate bias, the overall geometry of the system and the substrate temperature. Of equal importance is the composition and pressure of the atmosphere supporting the plasma. Significant amount of plasma gases (Ar or Ne) or reactive gases present as impurities may be present in the film and will affect the properties.

Magnetron Plasma Sputtering can result in high deposition rates of 1 micron per minute. The faster rates of deposition makes the use of sputtering for other applications than the thin film such as wear resistant coating.

Vacuum Evaporation where thermally vaporized atoms are allowed to condense on the substrate has been used to deposit amorphous metal film (63). The process can be carried out by heating the coating material by resistance, RF induction or by high energy beams like plasma, electron or ion. As with

sputtering the deposition rate, atmospheric composition & pressure and the substrate temperature are the important parameters determining the character of the film. The control of alloy composition in the deposit is difficult when only one molten alloy source is used due to differing vapor pressure of the constituent elements. Thus an independently controlled source for each of the components of the alloy provides the best compositional control. Even nominally pure metals, such as cobalt and chromium has been produced as thin film with amorphous structures by this technique (64).

Due to higher cooling rate and possibilities of codeposition of different elements in atomic scale, the condensation process can be used to form amorphous materials with following special features:

- a. Wide compositional range, for example almost nil solubility of Ni in liquid Ag-Ni alloy, it is possible to produce Ag-Ni amorphous alloy deposit with 13at% Ni solubility by sputtering. Also homogeneity range can be extended for certain compounds, such as, Nb_3Ge by sputtering (65).
- b. Difficult alloys, such as Cu-Sn, Cu-Ag and Au-Co can be produced in amorphous state by sputtering or evaporation but not by melt quench.
- c. Codeposition of elements in atomic scale can lead to formation of novel compositions. Sputter deposits of compositionally modulated amorphous film of Pd base/Fe-based materials with wavelength of the order of 20 \AA are produced. Some of the applications of wear and corrosion resistant amorphous metal coatings include tape recorder heads (metallic glasses with high permeability combined with high hardness) and razor blades (amorphous coating with superior corrosion resistance, high hardness and high elastic limits) (66).

2.9 Plasma Assisted Polymer Surface Modification

Vacuum Plasma Process (67) is used for cleaning and altering surface properties such as surface energy & adsorption of plastics, rubbers and natural fibers. Low temperature vacuum plasma process is preferred compared to other types of plasmas, such as flame (plasma flame energy causing damage), corona discharge (damage due to accumulation of electrical charge), or atmospheric ac (material damage due to high energy, also surface contamination by airborne particles) plasmas.

Process: The evacuated chamber is filled with inert gas at 13-65 Nm^{-2} . The specimens are placed between two electrodes connected to RF power source. Normally specimens are electrically insulated. With an applied voltage of 500 V, the generated plasma impinges on the specimens. At low specimen temperature of 40-120°C, the impact of inert gas molecules and ions in plasma results in non thermally activated changes in the surface (Fig. 2.9.1). Plasmas

can also generate radiation in the UV range. UV radiation can penetrate in polymer materials to a depth of about 10 micron causing chain scissions and cross linking.

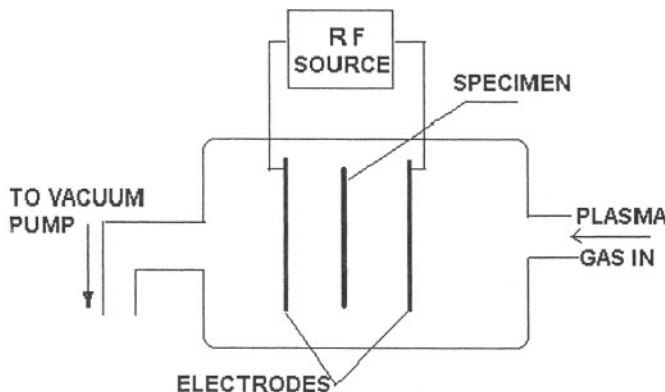


Fig.2.9.1 RF Plasma System for Polymer Surface Modification

Applications: Some examples of vacuum plasma treatments of automotive components include Polypropylene car bumpers, door mirror housings & dash boards before painting, ABS components before imprinting wood grain effect and PTFE for improved wettability and bonding. RF plasma (Fig. 2.9.1) is also used to deposit thin film on a wide range of materials, including metals, polymers, and carbon fibers.

Plasma Polymerisation (PP) of Surface (68, 69):- The process of depositing thin (<2 micron) pinhole-free polymeric film onto a wide range of metals, polymers & carbon fibre is known as plasma polymerisation. The plasma assisted polymerisation process is gaining popularity as a method for formation of a thin coating of a new kind of polymeric materials. The material constituting the coating is different from either conventional organic polymers or inorganic materials. Thus the plasma polymerisation process includes polymerisation of metallic or inorganic elements as well as organic materials. In conventional polymerisation process monomer molecules grow without losing identity. Plasma polymerisation is not a molecular growth process but an atomic process of building up a coating. The process is grouped as a plasma assisted CVD process.

Process:

The electric discharge is carried out by radio frequency (RF) or DC (or AC) or corona plasma in a reactor chamber. RF coupling can be inductive or

capacitive. The reactor chambers can be tubular or bell jar or rotating drum type. The three systems for plasma polymerisation are as follows;—

- Inductive Coupling using a tubular chamber,
- DC (or AC) plasma using a bell jar
- Corona reactor with rotating drum

The schematic diagram of plasma polymerisation in a tubular chamber by electrodeless induction coupling is shown in Fig. 2.9.2. Monomer may be fed directly in the plasma or can be mixed with a carrier gas and introduced in the plasma glow area.

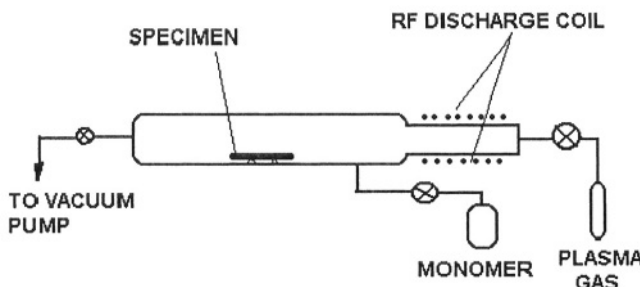


Fig.2.9.2 RF Plasma Tubular Reactor for Polymerisation(schematic)

Fig. 2.9.3 is a schematic diagram of using internal parallel plate electrode in a bell jar for plasma polymerisation in high frequency (50-2450 MHz) DC or AC glow discharge. In DC discharge, polymer film forms mainly on the cathode. In AC, the polymerisation occurs on both the electrode surfaces. The substrate, when placed in between the two electrodes, good deposition can be obtained.

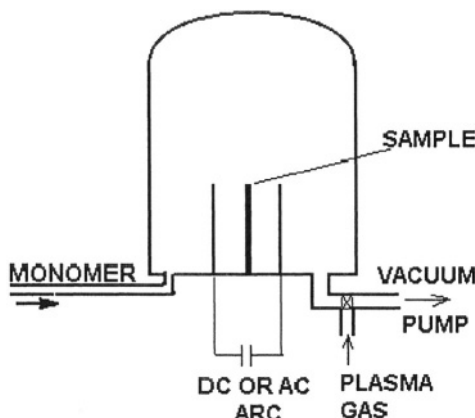


Fig.2.9.3. Plasma Polymerisation in a Bell Jar with DC or Ac Arc

Polymerisation process is controlled by several variables, including, the shape of the chamber, the size of electrodes, the distance between electrodes, frequency used etc. Some parameters require adjustment during the run such as monomer flow rate, pressure in the system and the power delivered. When the gas is static, the rate of polymer deposition increases as the initial monomer pressure is increased. For a fixed monomer pressure the polymerisation rate increases with increase in discharge power. Deposition rate can be increased by cooling the electrodes. The monomer is fed continuously in the bell jar with or without carrier gas. The flow-through mode reduces build up of the contaminants.

By controlling the chemical group present in the PP, it should be possible to tailor very accurately properties such as adhesion. In normal PP process, the chemistry of PP depends on the ratio of plasma's electrical power (P) and the flow rate of organic vapour (f). For developing a film with good physical properties a high P/f is required. But the use of high ratio results in increasingly random distribution of chemical group in PP. In order to overcome this problem and to produce controlled chemistry PP using low P/f ratio, the technique of plasma **copolymerisation** has been developed (70). In the copolymerisation process, the organic precursors are mixed with a hydrocarbon diluent, which allows accurate control on the chemistry of plasma copolymer (PCP) produced. Some of the advantages of plasma polymerisation are listed as follows:-

- Deposit is obtained in partial vacuum and therefore very clean, dust free high purity film forms on desired substrate.
- Very thin, flawless & uniform film (even few angstroms) is obtained at a short deposition time with substrate maintained at ambient temperature. The film has been used as protective coating against corrosion & wear. Coating of fluorinated compounds can improve mechanical & contact wear resistance of the surface. Twin coating of methyl-methacrylate formed by using metal electrode discharge at 6 KHz serves as good protective coating against corrosion. Surface modification technology involving PP has been used also in tissue culture engineering.

Summary

Plasma or the fourth stage of matter has been used for almost all the major thermally assisted surface engineering techniques & applications. No other heat source has been used so extensively as plasma because of its wide range of power (1 to 5×10^6 W) and the power density, which are utilized as plasma flame for thermal spraying, plasma transferred arc for weld overlay, glow discharge plasma for nitriding and carburizing, magnetron plasma sputtering for vapor phase deposition, non-transferred plasma scan for transformation

hardening, concentrated plasma beam for amorphous metal coating, plasma CVD for diamond coating, and low powered plasma for plasma polymerization and co-polymerization. Some of these unique features in plasma assisted surface engineering processes are highlighted in the summary.

In thermal spraying atmospheric and vacuum *plasma flame spray* processes together cover almost all the surface engineering applications requiring deposits of a wide spectrum of materials, such as, metals, ceramics, polymers and composites for coatings on similar or dissimilar substrate materials. In addition to conventional materials, special composite materials, such as, BN + NiCrFe + Al, AlSi + McrAlY + Polymer + Lubricant are developed to take care of critical wear problems. Variants of the spray system include different anode designs, atmospheric conditions, pressures and power ratings. The versatile surface engineering process along with important materials and major applications has been given due coverage in this chapter.

Plasma transferred arc welding with powder materials as consumable is an unique fusion weld overlay process, producing high integrity coatings of wear resistant alloys and metal-matrix composites with very low dilution and HAZ. Fully automated process with torches in the range of 10amps to 300amps are used to cover a wide spectrum of applications ranging from small tappet valve's face (2 gm of powder) to big concast roller (several kilograms of powder). Very low dilution requires only a single layer to develop fully the wear resistant surface thus making PTAW with powder consumable as the most techno-economically viable weld overlay process. Some of the critical applications such as nuclear valves & governor shaft in hydroturbines it is almost mandatory to use PTAW.

Glow discharge plasma is used for diffusion processes such as nitriding and carburizing. Plasma nitriding can produce a tougher single phase white layer compared to less tough two phase white layer possible in conventional nitriding. It is a well-established surface engineering process with a wide range of applications. Plasma carburizing is a costly process mainly developed for aircraft industry.

With dual power source and two targets, *magnetron plasma sputtering* is used to produce newer coatings, such as TiAlN or TiAl(CN) which resist diffusion wear of coated cutting tools by forming diffusion barrier layer of Al₂O₃ during usage. Unlike other PVD processes, in sputtering vapor forms directly without any intermediate liquid and thus less chance of decomposition before deposition.

Gas discharge plasma (induced by microwave or radio frequency), *glow discharge plasma* (AC or DC), and *plasma jet* (induced by RF/microwave/DC) are used to produce vapor phase (PA-CVD) diamond film

deposition. Diamond has extremely low dynamic coefficient of friction (0.005, same as Teflon) and compressibility while it's hardness, thermal conductivity, elastic modulus are the highest of all known materials. Extremely low wear of diamond coatings is due to these unique properties of diamond.

Tab.2.10. Summary of Plasma Assisted Surface Engineering Processes

Surface Engineering Methods	Plasma Assisted Processes	Major Applications
Thermal spray	Non-transferred arc plasma spray	Aeroengine, automotive engine, boiler tubes, MG cylinders
Weld overlay	Transferred arc plasma welding	Automotive & process control valves, hydroturbine spindles
Diffusion	Carburizing, nitriding by glow discharge	Aeroengine & automotive components, tools & dies
Transformation hardening	Plasma beam scan	Dies & tools
Vapor phase deposition	Magnetron plasma sputtering PACVD by glow discharge	Hard TiCN coating on tools & dies Diamond coating on tools
Amorphous metal deposition	Vapor phase deposition	Tape recorder head, razor blades
Polymer surface modifications	Plasma polymerisation & copolymerisation	Wear & corrosion resistant surface/coatings on metals

References:-

1. Michael A. Lieberman & Alan J. Lichtenberg, Principles of Plasma Discharges & Material Processing, Wiley Intersciences, 1994.
2. D.L. Book, NRL Plasma Foundry (Revised), Naval Research Laboratory, Washington, DC.
3. B.M. Smirnov, Introduction to Plasma Physics, Mir Publisher, Moscow, 1977
4. R.F. Smart & J.A. Catherall, Plasma Spraying, Mills & Boon Ltd, London
5. L.K. Leshchinskiy & S.S. Samotugin, WJ, January, 2001, Welding Research Supplement 25s-30s
6. R. Chattopadhyay, Sem. on 'Advances in Surface Treatment of Metals', Bhabha Atomic Research Centre, Bombay, 14-16 Oct, 1987, p540-544.
7. R. Chattopadhyay, Proc. Int Conf. on Welding Technology, Univ. of Roorkee, Roorkee, India, Sept. 1988, III-57-61
8. R. Chattopadhyay, Proc. Disc. Meet on Surf. Modification Tech of Materials, 3-5 Dec, 1992, Indira Gandhi Centre for Atomic Research, Kalpakkam, India. p80-111.
9. S. Sampath and H. Herman, p1-8, in "Thermal Spray Technologies New Ideas & Processes", Ed. D.L. Houck, ASM Int, 1989
10. R. Chattopadhyay, Surface Wear- Analysis, Treatment & Prevention, book published by ASM International, July, 2001
11. E. Hayes, Jr and David P. Thun, Development of a thermally efficient paper machine Yankee dryer coating, Second Nat. Conf. on Thermal Spray, 31 Oct.-2 Nov., 1985, Long Beach, CA, ASM, p21-26
12. G.M. Herterick, WJ, Feb, '87, p 27-30
13. ASM Engineered Materials Reference Book, ASM Int., 1989, p165
14. I. Kvernes, Coating of Diesel Engine Components, a paper from book on "Coatings for High Temperature Applications" Ed. E. Lang, Applied Science Publishers Ltd, England, 1982, p361-394
15. Ingrad Kvernes, "In-service performance of ceramic and metallic coatings in diesel engines", SAE Technical paper no.860888, 1986, p1-12
16. H. Fukutome, H. Shimizu, N. Yamashita and Y. Shimizu, Proc. ITSC'95, Kobe, May, 1995, p21-25
17. Houck, D.L. and W. Whisenant, Proc. Nat. Therm. Spray Conf., Orlando, Fl, Sept, 1987, p55-61
18. G. Barbezat, S. Keller and K.H. Wegner, ITSC'95, Kobe, p 9-13
19. M.G. Gemmill, Materials for Power industries, Metals & Materials, Dec, 1985, p759-763
20. E.J. Morgan-Warren, Welding and Metal Fabrication, Jan/Feb, 1992, p25-31
21. J.R. Nicholls and D.J. Stephenson, Metals & Materials, March, 1991, p. 156-163

22. J.T. Prater, J.W. Patten, D.D. Hayes and R.W. Moss, Proc 2nd conf 'Advance materials for alternate fuel capable heat engines, 1982, Ed. J W Fairbanks and J. Stringer, (Report no 2639SR, 7/29-43, Palo Alto, CA, EPRI, 1981)
23. J. Wigren et.al, Proc.ITSC'95, Kobe, 1995, p113-118
24. J.R. Nicolls et. al., in "European Research on Materials Substitution"(Eds I.V. Mitchell, H. Nosbueh), 1988, 295-307, Elsevier, London
25. F. Ghasripoor, R. Schmid and M. Dorfman: Abradables improve gas turbine efficiency, Materials World, July 1997, p328-330
26. James D. Cotton, Larry P. Clark and Henry R. Phelps, AM& P, May, 2002, p 25-28
27. Dagobert Fleming, Stainless Steel Europe, Dec, 1990, Vol 2, issue 7, p27.
28. Mike Sammons, WJ, May 2000, p35-39.
29. Harris & B.L. Smith, Met. Construction, 1983, Nov, p 661-666
30. D.T. Spencer, A. Patel, J.H. Nixon, and S. Grainger, Surface Engineering, June, 1987, p25-34
31. Zhan Zu-bao, Micro-beam plasma arc powder surfacing, ITSC'86, Sept. 8-12, Montreal, Canada, p727-736
32. R. Chattopadhyay & P.A. Kammer, Study of Dilution of Overlays, 3rd Int. Conf. on Trends in Welding Research, 1-5 June, 1992, Gatlinburg, TN, ASM Int. & AWS, p 455-460
33. R. Chattopadhyay, Wear Resistant Plasma Transferred Arc Coating on Engine Valve, Proc. Int. Thermal Spray Conference'95, Kobe, Japan, Seminar on Automobile Industry, p31-34
34. James M. Cherrie and Edward T. Vicha, New Automotive Poppet Valve Materials, Source Book on Wear Control Technology, ASM, 1978, p447-449.
35. R. Chattopadhyay, Wear studies of PTA deposited powder alloys for critical applications, Internal report, EWAC Alloys Ltd, 1989.
36. H. Hellen & Others, Material Development for PTA Surfacing of Rollers for Continuous Casting, Proc. Int. Thermal Spray Conference'92, 28 May-5 June, 1992, Orlando, Florida, USA p 893-897
37. R Chattopadhyay, High Silt Wear of Hydroturbine Runners, Proc. Int. Conf. on Wear of Materials, 1993, San Francisco, Part B, American Society of Mechanical Engineers, p1040-1044.
38. A.Y.M. Domboaskii and A.V. Brover, Metall. Sci. Heat Treat, July 1999,41(1-2), 12-15
39. B.C. Mohanty, Disc. Meet on Surface Modification Tech of Materials, 3-5 Dec, 1992, Indira Gandhi Centre for Atomic Research, Kalpakkam, India, p 80-111.
40. Private Communication, P.I. John, Institute of Plasma Research, Gandhinagar, India

- 41 M.F. Danke, F.J. Worzala, *J. Sci. Forum*, 1992, 102-104, 259
- 42 William J. Girwood, *Forecast, Adv. Mat. & Processes*, 1993, 1, p178.
- 43 Rob Neale, *Mat. World*, 1999, May, p272
- 44 P. Jewsbury, *Materials Forum*, 1986, 9(3), 179-181.
- 45 S.V. Lee & Y.K. Jee, *Surf. Coat. Tech*, 1999, Feb, 112(1-3), p71-77.
- 46 J.A. Thornton, 19th Sampe-Symposium, Los Angeles, 1974
- 47 R.F. Bunshah, Ed., *Handbook of Deposition Technologies for Films & Coatings*, 2nd edition, Noyes Publications, Park Ridge, NJ, 1994
- 48 H.D. Steffans, 9th Int Conf. on Thermal Spraying, The Hague, May, 1980, 19-30
- 49 J.W. Patten, *Proc. Conf. Met. Coatings*, San Diego, April, 1980, CA, Vol II, p 463
- 50 B.A. Mochan & A.V. Demchiskin, *Metalloved*, 1969, 28, p653
- 51 O. Knoteck, W. Bosch, & T. Leyendecker, *Proc. 11th Plansee-Seminar*, Reutte/Tyool, 1985
- 52 R. Nimmagadda and R.F. Bunshah, *Journ. Vac. Sci. Tech.*, 1976, 13, 532
- 53 Brian V. Cockeram, *Adv. Mat. & Processes*, 2000, April, p47-50
- 54 J.R. Conrad & others, *Surf. & Coating Tech.*, 1988, 39, p927.
- 55 Andy Bloyce, *Mat. World*, 2000, 3, p13-14.
- 56 Somuri Prasad, Todd Christenson, and Mike Dugger, 'Tribological coatings for Ligaments', *AM&P*, Dec.2002, p30-33
- 57 W. Ahmed, D. Tither and Eugene de Silva, *Mat. World*, 2, 1997, p92-93.
- 58 B. Lux & R. Haubner, *Low Pressure Synthesis of Superhard Coatings*, R M & H M, Sept, 1989, p158-173.
- 59 Chris Beck & Masood Ahmed, *Mat. World*, Feb, 1998, 81-83
- 60 S. Tung & Others, *CVD diamond films nucleation & growth*, *Materials Science & Engineering*, 25, 1999, p123-154.
- 61 D.E. Polk, B.C. Geissen and F.S. Gardener, 'State-of the-Art and Prospects for Magnetic, Electronic and Mechanical Applications of Amorphous Metals, *Rapid Solidification Technology, Source Book*, Ed. R.L. Ashbrook, *ASM*, 1983, 278-285).
- 62 Donald E. Polk & Bill C.Giessen, *Overview of Principles and Applications*, p213-247
- 63 K. Sinha, B.C. Giessen, and D.E. Polk, in *Treatise in Solid State Chemistry*, vol 3, Ed. N.B. Hanny, *Plenum Press*, New York, NY, 1976, p1
- 64 P.K. Keung and J.G. Wright, *Phil. Mag*, vol 30, 1974, p 994
- 65 J.R. Gavaler, *J. Appl. Phys. Letter*, 23, 480, 1973.
- 66 Global Report, 'Japan active in surface modification R&D', *Adv. Mat & Processes*, 1990, 2, 13-15
- 67 Peter Rawlinson, *Mat. Worlds*, 1999, 5, p 276-277

- 68 H. Yasuda, *Plasma Polymerisation*, Academic Press, London, 1985.
- 69 A.J. Beck & Others, *Mat. World*, 1998, 2, p70-72.
- 70 A. J. Beck & Others, *Materials World*, Feb, 1988, p70-72

This page intentionally left blank

Chapter 3

ION BEAM PROCESSES

3.0 Introduction

Similar to plasma, ion beam has been used for vapor phase deposition of coating materials. Also an unique surface modification process of implanting the ions of the desired elements in the surface layer has number of applications. Ion implantation is an ‘atomic level’ surface modification process, where the structure of near-surface region is altered to produce a new phase while the part dimension remains same. Both the processes are to be covered in this chapter.

3.1 Ion Source

The available sources for generating ions include (a) RF discharge plasma, (b) DC discharge plasma and (c) Surface ionization by application of heat.

Ion beam equipment consists of an ion source and the extraction-cum-acceleration system for ions. The plasma source for production of ions is comprised of a heated filament cathode, anode and a confining magnetic field. The ions are removed from the plasma by extractor grids. The escape of electrons is prevented by suppressor grids. The ions extracted from the plasma source drift through a field free space to reach the substrate (Fig. 3.1). Amongst the ion assisted surface modification processes the most important one is ion implantation followed by vapor phase deposition (PVD).

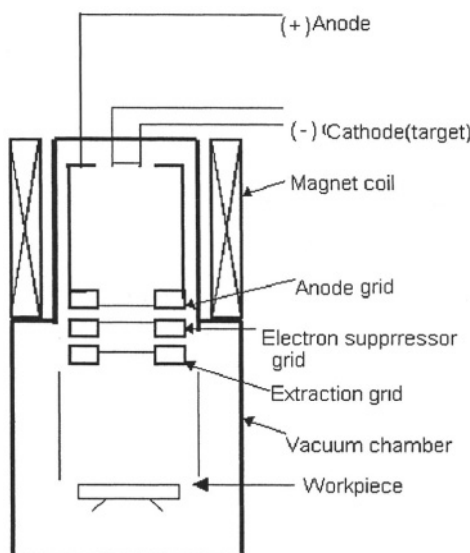


Fig.3.1.Schematic of Ion Plating System

Comparison of PVD with Thermal Spraying

In both PVD and thermal spraying processes, it is possible to use a wide range of coating and substrate materials (Table 3.1). For example, metals, ceramics, plastics or composites are used either as substrate or coating materials. The lamellar spray deposits in thermal spraying being parallel to the surface possess superior resistance to mechanical stress and strain compared to that of the columnar PVD deposit, which are perpendicular to the surface. The bonding to substrate in both the processes is mechanical in nature.

Tab.3.1.Comparison between PVD & Thermal Spraying

Items	Thermal Spraying	VD
1.Equipment Cost	Cheap/Moderate/Expensive	High,viable for large lot size
2.Deposition Rate	High	Low
3. Coating Thickness	High	Low
4.Microstructure	Lamellar, i.e, ll to surface Can withstand stresses Substrate unaffected	Columnar,i.e, \perp to surface Can't withstand stresses Substrate unaffected
5.Surface Roughness	As sprayed rough surface	Reflective mirror finish
6.Deposit Purity	High(vacuum plasma)/ Moderate	High
7.Substrate Material	Any solid surface	Any solid surface
8. Coating material	Metal/ceramic/plastic	Metal/ceramic/composites

3.2 Ion Beam Assisted Vapor Deposition Processes

Glow discharge argon plasma process :

The glow discharge argon plasma has been used to clean substrate and make surface rough as well as to deposit evaporated coating material (1). The good adherence to substrate is ensured by cleaning and roughening the substrate surface by glow discharge argon plasma. The process combines the advantages of high deposition rates in the evaporation technique with those of sputtering, i.e., formation of dense deposit with good adherence to the substrate.

Ion sputtering

In sputtering the source is cathode and the substrate is anode. In this process, the positively charged argon ions from the plasma strikes the negatively biased coating source with energies up to 1000 eV. The individual

atoms are ejected from the cathode surface by ion bombardment. The process is known as sputtering. The sputtered material flux deposits on the substrate, which is connected to negative terminal. Non conductive materials can not be deposited by glow discharge mode. Reactive dc sputtering or radio frequency (rf) power sources can be used for non-conductive coatings. The substrate can be sputter cleaned by reversing the polarity to obtain better coating adhesion. Ion beam sputtering has also been used to produce a thin coating of diamond at a low growth rate of 0.3 to 0.4 micron per hour (2).

Ion plating, ion vapour plating (IVP), or ion vapour deposition (FVD)

In ion plating, the substrate receives an opposite bias. A high voltage (3-5 KV) bias DC source is used for biasing the substrate negative with respect to vapor phase. Thus the ion plating is essentially a PVD process in a soft vacuum ($1\text{-}10^{-1}\text{Nm}^{-2}$) with evaporant depositing onto substrates held at a high negative potential between 3-5 KV. Ion vapor plating results from deposition of a small number of ions and a large number of neutrals with an average energy of 100eV. Because of the high energy, the ions & neutrals can get implanted to small depths of around 50 Å. The structure of ion plated coating is similar to that of sputtering, viz, 3-zone model depending on the pressure and substrate temperature (Fig. 2.6.1 in Chapter 2).

The advantages of ion plating includes excellent adhesion due to implanted graded interface, good throwing power, dense deposit and plating possible on any material (metal, ceramic & plastic). Unlike electroplating there is no effluent disposal problem and risk of hydrogen embrittlement of the deposit in ion plating.

Uniform coating thickness is observed in ion-plated surfaces including corners, recesses, holes and undercut portions due to relatively high pressure ($10^{-2} - 10^{-3}\text{ m bar}$) involved in the plating. However the shadow effect still persists and job rotation is required for overcoming the problem.

Ion beam assisted deposition process (IBAD)

In this process, the use of steered-arc cathode as an ion source leads to significantly higher deposition rates compared to existing planar magnetron cathodes. The deposited atoms get mixed with the matrix forming graded interface layer of novel, non-equilibrium composition with good adherence to substrate. Improved IBAD produces adherent, ductile films having low porosity and fine grained structure at deposition temperatures below those of conventional CVD processes (3). The hardness and wear resistance of titanium nitride films grown by IBAD can be controlled by the ratio of ion-to-atom arrival rates. The factors affecting coating performance include, coating

thickness, microstructure, hardness, chemistry, orientation of the coating, coating to substrate bonding and also the strength of substrate material.

3.2.1 Types of Coatings

The ion beam processes are used for deposition of various materials, such as, pure metals (e.g., chromium), elements (e.g., oxygen), ceramics (e.g., titanium nitride) and intermetallics (e.g., nickel aluminide) for forming wear and corrosion resistant coatings. Ion plating is a favored process compared to polluting electrochemical process of hard chrome plating. Similarly ion beam process of oxygen deposition on aluminum has replaced anodising in several applications. Process has also been used to produce wear-resistant films on parts such as cutting tools and gas-turbine blades.

Hard chromium coating (4)

The chromium coating of 5 to 10 micron (0.0002" to 0.0004") thickness and high hardness can be obtained by ion plating at a low temperature of 65°C resulting in no distortion in the coated component. The chromium can be directly deposited on the substrate without any intermediate layer of copper or nickel.

Hardness of chromium coating in this process has been found to be 1200 Knoop (2 gf), compared to 750 Knoop of electroplated hard chromium, 950 Knoop for baked hard Cr-plating, 988 Knoop for Ni plus hard Cr-plating and 589 Knoop for electroless Ni-plating. The coatings are harder than conventionally plated chromium because they are fully dense, hydrogen free, and compressively loaded. The thin coating replicate substrate surface finish, thus eliminating the need to costly grinding and lapping to match the original finish. There is no alteration of bulk material properties due to low temperature of 65°C employed during coating.

The environment friendly ion plating process of hard chromium coating eliminates the use of chemical plating solutions and the toxic wastes generated in the process.

Application areas include gears, bearings, valves, pump impellers, pistons and shafts. The batch process used is capable of handling jobs up to 305 mm (12") in diameter and up to 180 mm (7") long (4).

Anodising, aluminium and titanium coating

Thin coating of oxygen on pure aluminum and high strength aluminum alloys by ion vapor deposition process is replacing anodising, hard anodising and conversion coating systems. Also commercial aluminum is plated on to

steel and titanium fasteners for use in aircraft and spacecraft replacing previously used Cd coating.

Diffusion coating

NiCrAlY plating has been applied on aeroengine components for protection against high temperature oxidation and corrosion. Ion plated diffusion barrier coating of Ni-13Al has been used at the interface of a high chromium containing overlay coating and a Ni-base superalloy substrate in aeroengine. The gamma prime diffusion barrier decreases the diffusion rates of elements like chromium and aluminum from the protective layer to substrate at the high operating temperatures used in modern aeroengines (5). For example, the diffusion coefficients (cm^2 per sec) of chromium and aluminum at 1150°C without the barrier layer are 8×10^{-9} and 2.5×10^{-9} respectively. With the diffusion barrier these values are decreased to 6×10^{-10} and 5×10^{-10} for aluminum and chromium respectively (4). The decrease in diffusion rates are much more at lower operating temperatures.

TiN coating and tool materials

The partially ionised titanium and nitrogen in the vapor formed in the low pressure argon/nitrogen atmosphere are positively charged. The ions are attracted towards the negatively biased workpiece, where they react to form TiN at a temperature of around 400°C . Therefore the tool steels, which are tempered above 450°C are ideal for TiN coating using PVD, such as high speed tool steels HSS, D2, and H13. Both ferritic/martensitic and austenitic stainless steels, such as AISI 429, 304, 316 are suitable for TiN coating. The AISI 420 grade is used for plastic moulding and the austenitic type is used where lubricants are not permitted, for example food processing equipments and chemical plants.

Applications in Industries

Tooling

Reactive ion plated TiN on the flutes of twist drills made from M7 HSS material has caused an increase in drill life of up to 50 times than that of the uncoated drills of same material (6). Apart from coating thickness and properties, the performance of the drill depends on drilling conditions and work-tool combinations. A linear relationship between coating thickness and drill life was found (6). The TiN coating delays the occurrence of both crater and margin wear and also greatly reduces the extent of flank wear. The progress of wear follow the familiar pattern of high initial wear with an

intermediate slow and steady wear followed by final stage of accelerated wear (7).

The cutting tool segments are the first to use PVD and in Japan, where the adoption has been most rapid, some 90% of gear cutting tools are now coated (8). It can be highly beneficial to go for a higher grade of tool steel, such as, high speed steels (HSS), which will economically provide an inherently longer life in the first place and have that extra multiplied several times by the relatively low cost treatment (8).

The TiN coated cemented tungsten carbides are increasingly being used because of the retention of sharp edge by PVD treatment. The high temperature operation required in CVD coating tends to round off the corners (8).

Metal Forming (8)

The adhesive wear resistance of metal forming tools and punches is significantly improved by TiN coating. With TiN coating, it is possible to prolong the life of hot and cold work tool steels by four to ten times than that of the original uncoated tools. The increase in total price of the tool by such treatment is only around 15% (8).

Plastic Molding & Extrusion (8)

The current practice is to add highly abrasive fillers amounting to around 50% to plastic materials in forming the components. This shall result in severe wear of the forming tools. The present practice is to coat the surface of forming tools such as moulds, hot runners, extruder screws, calibration dies, and other wearing parts with either ion plating or ion implantation. There is a significant improvement in the wear resistance properties of these tools.

In the mould, the draft angle of 2° for a plain surface and 6° for a textured surface is required to enable release of the formed product. The release is improved by TiN coating and ion implantation, so that the draft angles can be reduced and process cycle times can be made shorter by faster mould release. For some plastic moulding, large forming tool is built from a combination of small segments. The use of TiN coating prevents the segments from getting cold welded.

Automotive (8)

The titanium alloys with high strength to weight ratio are ideally suited for automotive applications due to increase in payload combined with the decrease in dead load. However their use in such applications could not be made due to poor abrasive and adhesive wear resistance properties. Titanium

nitride coating and ion implantation have both resulted in dramatic improvements in wear resistance properties of titanium alloys. The TiN coating is now a part of established practice for use in parts for gearboxes, wheel hubs, differentials and steering racks in Formula One racing cars.

Another interesting automotive application is the use of light weight and strong titanium as engine valves leading to better fuel economy. The titanium alloy stem rod can be friction welded to stainless steel seat. The poor wear resistance properties of stem made from titanium alloy can be improved by TiN coating.

Aerospace (8)

For prolonged smooth operation of space crafts, the conventional 'wet' lubricants are found to be not suitable in the high vacuum. However the ion beam coating of TiN provides a 'dry', hard, smooth and maintenance free surface that can survive operations under severe wear situation.

Nuclear (8)

In order to eliminate contamination, lubricants and other organic materials are excluded from being used in nuclear areas. Here again, the low adhesive wear of TiN coating is utilised. The stainless steel screw threads, nuts and studs are coated with TiN for quick and easy release without the use of any anti-seize compound. The same treatment is used for stainless steel or alloy fasteners used in critical areas of operations involving high temperatures and pressures.

Advantages of Ion Beam Assisted PVD Coating

- The ability to clean the surface by the ion beam and the high energy at which the coating material strikes the clean substrate shall result in excellent coating adhesion.
- The dense coating chemistry is controllable and is also reproducible.
- A wide range of coating materials, such as, metals and ceramics can be deposited on substrate made of similar or dissimilar materials.
- It is possible to coat multiple materials in different layers.
- Uniform coating thickness can be obtained due to gas scattering and the ability to rotate the component.
- It is possible to obtain surface finish equals to that of the substrate, thus eliminating finish machining.
- Low temperature of operation below 500°C can be carried out on tempered & finished high speed tool steels and similar materials having the tempering temperature above coating temperature.

Designing of the Coating (8)

Some of the key points in designing the PVD coatings are as follows:-

- The depth of the blind hole should not be more than twice the diameter for coating the full depth. However the through holes can be 4 to 5 times the diameter in depth.
- Substrate material should be selected so as not to temper below around 400°C. Low temperature systems are available but can be used with some sacrifice in coating adherence and structure, particularly when treating larger parts or components.
- Materials containing a significant quantity of volatile material like zinc is to be avoided. The volatility of zinc at these temperatures and in vacuum shall create serious contamination problem.
- The performance of the coating is normally the same for thickness from 2 to 4 micron. It is easier to control the process, and made cheaper and more productive if the coating thickness variation is kept within these limits including the specified tolerances.
- For most PVD systems, there is limitation in the size of the component to be treated. Typical equipments in commercial use will accept either items up to 600 by 600 by 400 mm or cylindrical items up to 700 mm long by 200 mm diameter. Some machines can treat up to 3 m long components.
- For larger items, it is necessary to ensure sufficient preheating of the component, and proper cleaning of holes and crevices before the coating is applied.

3.2.2 Dual IBAD (9)

In this process, physical vapour deposition (PVD) via electron beam evaporation of metals and metalloids onto the substrate is combined with simultaneous ion-beam bombardment from an ion source. The simultaneous ion-stitching densifies the synthesized film and improves the adherence between the film and substrate. The adhesive bonding to substrate can be improved by using an intermediate composition (graded coating) or a suitable material with good adherence to both the substrate and top coat.

Excellent adhesion of metals, polymers and ceramics can be obtained without the need of excessive high temperature. Compounds like ZrO_2 and DLC are grown by introducing reactive ion beams concurrently with the evaporated species. When producing high ductility high temperature tribological coatings, such as Al_2O_3 , ZrO_2 , silicon nitride, and boron nitride, the use of IBAD substantially reduces the impurity content, by eliminating the porous, columnar microstructure commonly seen in low-temperature deposition. The applications of dual IBAD for various surface treatment functions are listed in Table 3.2. The list of wear and corrosion resistance

IBAD coatings include hard dry wear resistant carbides, nitrides and oxides, lubricating materials such as silver, lead, molybdenum sulphide and tungsten sulphide, diffusion barrier coatings of alumina, palladium, platinum, rhenium and titanium nitride, corrosion resistant passive film of chromium, tantalum and molybdenum and oxidation resistant coating of MCrAlY, platinum and silicon carbide.

Tab.3.2. Some Dual IBAD Applications

Function	Dual IBAD coatings
Wear (dry)	Hard coating (TiN, TiC, CrN, Cr ₂ O ₃ , I-BN)
Wear lubrication	Ag, Pb, MoS ₂ , WS ₂
Diffusion barrier	Al ₂ O ₃ , Pd, Pt, Rh, TiN
Corrosion	Passive film (Cr, Ta, Mo)
Oxidation	MCrAlY, Pt, SiC

A crystalline TiB₂ coating of hardness 3340 kgf/mm² has been obtained with 10 KeV Ar+ bombardment (9).

3.3 Ion Implantation

Ions are implanted at different doses by exposure to the accelerated ions. The atomic species to be implanted are first ionised and then accelerated to energies of around 90-150 KeV. The striking ions penetrate the surface of the material and form an ion enriched layer. The depth of penetration is controlled by the atomic numbers & masses of both the ions & target atoms and the rate of energy transfer. The energy transfer depends on dose, energy and temperature. The implantation of ions into target materials can lead to the production of amorphous or metastable alloys. The mobile ions during implantation form new alloy precipitates with target atoms. The precipitation produces high density of point defects developing compressive stresses (10). The generation of compressive stress on the surface shall result in improvement in fatigue life of the component.

Ion implantation is an 'atomic level' surface modification process, where the structure of near-surface region is altered to produce a new phase while the part dimension remains same. Ion implantation process has been carried out on metals, ceramics and polymer in improving the wear & corrosion resistance of the treated surfaces.

Microstructure & Wear of Nitrogen Implanted Austenitic Stainless Steel

One of the recent methods of improving the wear resistance of austenitic stainless surface without impairing corrosion resistance properties is through the implantation of nitrogen ions. The effectiveness of improving wear resistance depends on ion implantation conditions. For example, with 40 KeV energy and at a sample temperature of 25°C during implantation, the best results are obtained after a dose of 2×10^{17} N ion/cm² implantation (11). An increase in temperature during implantation is a favorable factor (12). The friction coefficient of AISI 304 stainless steel does not show any significant change due to ion implantation. The friction coefficient varies from 0.1 to 0.2 in lubricated test (13) and in between 0.6 to 0.7 in dry test (10) for both untreated and ion implanted AISI 304 regardless of ion implantation conditions. On the other hand the ion implantation of AISI 304 results in a decrease of wear rate by a factor of 20 or more (12, 13, 14, 15, 16, 17, 18).

Scanning electron microscopic observations of worn surfaces of non-implanted AISI 304 show severe wear and large plastic deformation in comparison to mild wear and small deformation in implanted material (11, 13, 19). The microstructure of the nitrogen ion implanted AISI 304 consists of α' -martensite plus mixed nitrides (or carbonitrides) of hexagonal (ϵ -type) and orthorhombic (ξ -type) (18). Additionally the presence of deformed austenite is reported to be found in the microstructure (19). The transmission electron micrograph of a nitrogen ion implanted surface indicates the presence of highly oriented nitrides (11). After nitrogen ion implantation of 2×10^{17} ions cm⁻², on AISI304 steel, the TEM micrograph (11) of the surface layer is mainly composed of highly oriented mixed nitrides (Fig. 3.3.1).

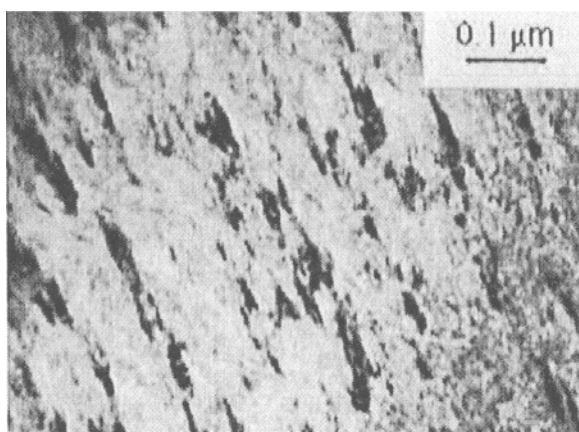


Fig.3.3.1 TEM micrograph of nitrogen ion implanted AISI 304 stainless steel (ref.11, S. Fayeulle, Proc. Int. Conf. on 'Wear of Materials', 1987, p17, permitted to reproduce by The American Society of Mechanical Engineers, copyright, 1987)

The mechanism of the increased wear resistance by ion implantation has thus been explained as due to (i) high hardness of superficial layers by martensite transformation and nitride formation (14), and (ii) tough nitrogen stabilised austenitic phase not transforming to a brittle strain induced martensite (17, 20). The effectiveness of ion implantation in retaining wear resistance of the sub-surface, i.e., exposed surface after removal of implanted layers, is explained as due to diffusion of nitrogen into the substrate (16).

Examples of ion implantations in metals & alloys include nitrogen ion in aluminum, (21, 22, 23), nitrogen & boron in HSLA steel (24), nitrogen and/or boron in stainless steel (25, 26) and tool steels (26). Nitrogen ion implanted surface of aluminum forms hard nitride at high doses and nitrogen diffused layer with low doses (23). The nitrided surface in steel can contain up to 50 atomic percent of nitrogen which is nearly five times the nitrogen than that obtained in ion nitriding, producing an equivalent hardness of 85 HRC. The multielement process, such as, implantation of both nitrogen and boron improves vastly surface hardness and lubricity and thus wear resistance (26). The hardness of implanted (B+N) surface of high speed steels (M-series) is found to be in the range of 3000 to 4000 VPN. With a fraction of the costs required for diamond or diamond like coatings, ion implantation can result in a coating surface with wear resistance similar to that of diamond. Chromium, nickel & other metals can be implanted to produce corrosion resistant surface in steel. Ion implantation of Ti or Y on alumina improves wear resistance due to abrasion at the onset of amorphisation and that due to friction after amorphisation.

Advantages of the process:-The advantages of ion implantation process over other similar surface modification techniques include the followings (26):-

- It is a low temperature process ($>300^{\circ}\text{F}$), hence no distortion of treated parts occurs in comparatively low temperature process like nitriding.
- It is an atomic level treatment on the near-surface, hence no chance of delamination or peeling of the modified surface.
- It does not result in the growth, build-up or a rolled edge like vapor deposition processes (CVD, PVD).
- It eliminates problems associated with elastic modulus mismatch between hard coating and soft substrate materials.
- It results in high miscibilities of implanted elements, much more than equilibrium solubilities. For example nitrogen implanted steel contains 5 times more nitrogen than gas nitrided case. Boron implanted steel contains up to 50% boron.

Limitations of the process (26): The main limitations are as follows:-

- Equipment size limits the size of the parts to be treated.
- It is a line of sight process which limits its ability to treat certain geometries such as deep holes. However, the newly developed, plasma source ion implantation is a not a line of sight process and can be used for deep holes.
- The interstitial elements like nitrogen and boron in implanted components can diffuse inwards from the surface at a high operating temperature resulting in deterioration of both the surface and the core properties. For example, implanted nitrogen diffuses at approximately 370°C (700°F) in tool steels and 595°C (1100°F) in tungsten carbide. However for substitutional elements like chromium and nickel appreciable diffusion occur only at higher temperatures (>600°C).

Applications: Ion implantation process has been used to modify surface properties of metals, ceramics, plastics and polymers.

Metallic Materials:- The list of ion nitrided metallic materials includes stainless steels, tool steels, chromium coatings, aluminum and titanium. The main application areas are mold cavities, prostheses, cutting/ forming tools and bearings.

Mold Cavities: The wear resistance properties of hard chrome plated injection mold cavities are vastly improved by nitrogen ion implantations. High concentration of nitrogen at the surface produces high compressive stresses, which not only improves the fatigue resistance but also closes the microcracks inherent in the hard chrome plating. Also implanted nitrogen combines with chromium to form extremely hard (>80 HRC) chrome nitrides. Both effects produce a surface with very high resistance to abrasive and adhesive wear. By implantation the lubricity of the chrome plated surface is improved. The nitrogen content of the titanium nitride coated die can be increased by ion implantation resulting in further improvement in wear properties.

Cutting and Forming Tools:

Ion implantation of nitrogen plus boron has increased wear life of the tools used to cut abrasive composites such as aluminum honeycomb, polycarbonate and aramid fibers by five to ten times than that of untreated tools (26). Some of the examples include routers, hoggers, end mills, saw blades, slotting saws, and valve stem cutters. A 400% improvement in cutter

life was achieved by using ion implanted high speed steel cutter used in aircraft components such as bulkheads, wing flaps and tips, and radomes. The nitrogen implanted AISI D2 dies are used to form 40,000 flanges from 2mm (008") hot rolled steel for use in automobile transmissions (26). There is a 80-fold improvement in the die life.

Other applications where implanted dies have shown good performance include the punches for deep drawing casings for rocket and shell grenades from 3.2 mm (0.125") thick hot-rolled AISI4140 steel. The nitrogen implanted punches are used successfully to form 60,000 parts.

The chrome plated punches after nitrogen implantation could be used to produce 116000 parts compared to 12000 parts produced by untreated dies (26).

Bearings

Ion implantation improves vastly the performance of bearings used for aerospace applications. Nitrogen ion implantation of AISI 440C stainless steel bearings increases hardness by 300% and reduces dry sliding friction by a factor of three. The implantation of chromium in AISI 52100 or M50 bearing steels results in a surface with corrosion resistance similar to AISI 440C. Implanting metals like gold, platinum, iridium or tantalum can lead to dramatic improvement in the service life of bearings in critical application areas (26).

Prostheses

The frictional wear of cobalt and titanium base alloys used for artificial hips and knees is high while working in contact with ultrahigh molecular weight polyethylene (UHMWPE). Ion implantation can reduce the frictional wear of metallic surface in this application. Similar benefits can be derived by ion implantation in other biomedical devices, such as, cardiovascular components, dental prostheses, and pedicle screws (26).

Ceramics

Implanted ions in tungsten carbides lead to increase in hardness and lubricity, thus improving the wear and galling resistance of the treated surface. The use of implanted tungsten carbide blanking punches and dies has resulted in 60% increase in the number of parts produced between tool sharpenings (26).

Polymers & Carbon-based Materials

An ion implantation technology based on high-dose ion implantation followed by special oxidative treatment together produce graded oxide base coating on surfaces of polymers and carbon-based materials (27). The coating protects polymers and composites from excessive wear due to erosion in FAO (fast atomic oxygen) fluxes of space environment in low Earth orbits. The coating process consists of two stages. In the first stage, high doses of low- or medium energy ions of specially selected elements, such as, Si, Al, Si+Al, are implanted. The surface enriched with the implanted element in a carbonised or graphitised original surface is produced. The implantation energy for a oxide-coating thickness of 50-100 nm is in the range of 20-50 KeV, using ion dose in the range of 10^{16} – 10^{17} ions /cm². The second stage consists of treatment in an oxidative environment including exposure to fast atomic oxygen (kinetic energy of 2-5 eV) flux (23). Both high-current monoenergetic ion beams and metal-vacuum/vapour arc ion can be used for producing the coating. The graded coating produced by ion implantation takes care of the mismatch in the coefficients of thermal expansion between base and coating materials and thus reduces the risk of thermal spalling. The silicon and aluminum oxide coatings on polymer or composites provide resistance to oxidation in highly oxidative environments, such as atomic oxygen, ozone, oxygen plasmas and erosion due to fast moving particles to spacecrafts.

Ion implantation is a line-of sight process and parts need to be manipulated towards the beams. Moreover the maximum doses retained by the target are governed by the angle of incidence of the beam.

It appears that the less expensive and more convenient plasma sources are likely to replace the elaborate accelerators being used for implantation of N, B, O etc in non-semiconductor surfaces (28, 29).

3.3.1 Plasma Source Ion Implantation

In this process the specimen is placed in a low pressure glow discharge plasma field containing desired ionic species and then pulsed to a very high negative voltage. The pulsing accelerates the ions and leads to implantation of the ions onto the specimen surface. With the ions implanted in a thin layer (sub-micron) on the surface, there is no dimensional change of the component in ion implantation. One of the major advantages of plasma source ion implantation is that it is not a line of sight process and the plasma uniformly covers the object to be implanted.

3.3.2 Reactive Ion Sputtered Coating (26)

Thin films of coating materials can be formed by ion sputtering on the substrate. High sputtering losses prevent the use of ion implantation to form

coating. However in reactive ion sputtering system developed, there is virtually zero sputtering loss. Without any loss of implanted material, the successive layers of sputtered ions form a dense adherent layer of the coating.

Reactive ion implantation process has been used to form a sputtered film of zirconium oxide, 1 to 5 μm (40 to 200 micro-in) thick, on metal surface. The coating is highly adherent due to interfacial substrate containing a mixture of both coating and substrate materials. The conventional thermal spraying or CVD processes for deposition of ceramic coatings normally produce a sharp interface with either side having almost cent percent of coating or substrate materials. The resultant adhesive bonding between the two materials is thus quite weak, if no bond coat is applied (26).

A 3-step sputtering process is used to develop DLHC coating on bearing steel samples as follows (30):-

- The surface is sputter cleaned with approximately 2mA cm^2 argon ion beam from 1 KeV ion source, for 30 minutes,
- A 0.2 μm amorphous-silicon-hydrocarbon (a-SiHC) interfacing bonding layer is reactively sputter-coated onto the steel surface, which shall provide good adherence to both top DLHC layer and the steel substrate
- Finally a layer of DLHC is formed by bombarding with 450 eV carbonaceous molecular ions using methane as ion source.

Raman spectra peaks of DLHC film indicate the presence of amorphous carbon, disordered graphite and very small crystalline graphite. Although no strong evidence of four-fold (diamond) bonding is indicated in the spectra, it does suggest a durable DLHC film. DLHC layer has 3-fold interface with hexagonal plane of graphite. The bond angle disorder and small crystalline size has resulted in a very rigid lattice with the strength of a three-fold bonds in the DLHC layer (30).

The reactively sputtered coated DLHC coatings on bearing steels, such as AISI M-50, 52100,4118, and 440C steels, are found to improve substantially the rolling contact fatigue lives of bearing steels (30,31). However repeated stressing of the coating causes it to revert back from a hard amorphous-carbon to soft lubricating graphite.

Ion beam sputtering has been used for texturing, etching and simultaneous deposition and etching (32). Ion beam source is used to sputter-texture surfaces of ceramics, metals and plastics by forming conical or ridge like microstructures. Rough surface is highly adherent to bonding and develops compressive residual stress on the surface. In simultaneous deposition and etching, an argon beam hits a carbon target and deposits carbon atoms onto a substrate. The substrate is selectively masked with carbon. The balance of etching and deposition processes due to striking carbon ions results in buildup

of carbon on the mask and deep etching of the rest of substrate. The technique can produce infinite-life sputter mask and high aspect ratio electronics microstructures.

3.4 Ion Beam Assisted EBPVD (33)

In EBPVD, high energy electron beams are used to vaporize the coating materials and the vapor is directed onto substrate surface. By attaching an ion beam source to EBPVD, the following additional benefits over that of EBPVD are claimed to have been obtained (27):

- Produces more dense coating with better adherence to substrate,
- Possible to deposit textured coatings, which are preferred for microelectronics, optics and high wear applications such as, cutting tools,
- Possible to change internal stresses developed at the surface from tensile to beneficial compressive by ion bombardment with energies ranging from 10 to 100 eV (34).
- Possible to clean the substrate thus improving bonding

Superior bonding of the vacuum deposited dense coating occurs on the surface cleaned by high energy beams. The dense, adherent thermal barrier coatings are reported to have increased the life of the components by a factor of two (33) compared to that of plasma sprayed coatings of same materials. Thermal barrier coatings of insulating ceramic oxides, such as stabilised ZrO_2 , are mainly used to protect the metallic surface against excessive heat, high temperature corrosion, oxidation and wear. The performance of PVD coated tools with TiC, TiN, TiAlN, TiZrN materials can be further enhanced by using ion-beam assisted PVD (33).

References

1. L.A. Bucklow, Surface Journal, 1977, 4, 3-9
2. A. Ueno, K. Wasa, 1st Int. Conf. Diamond Sci. Techn., Oct., 24-26, 1988, Tokyo, Japan, 1-08, pp36-37.
3. Helmut Lammermann and Gerhard Kienel: Adv. Mat. & Processes, 1991, 12, 18-23.
4. Arnold H. Deutchman, Ion beam helps deposit hard-chromium coatings, Adv. Mat. & Processes, 1, 1991, p21
5. J.R. Nicholls and D.J. Stephenson, Metals and Materials, March, 1991, p156-163
6. R.L. Hatschek, Coatings, Revolution in HSS Tools", American Machining, March, 1983, pp129-144

7. C.T. Young and S.K. Rhee, Wear processes of TiN coated drills, Proc. Wear of Materials, April 5-9, 1987, Houston, Texas, ASME, vol 2, p543-550
8. B. Garside and R. Sanderson, Engineer's guide to advanced surface engineering, Metals and Materials, March, 1991, p165-168.
9. Bruce Haywood, Adv. .Mat. & Processes, 1990, 12, 35
10. N.E.W. Hartley, Thin Solid Films, 1979, 64, 177-190
11. S. Fayeulle, The microstructural study of the friction and wear behaviour of a nitrogen implanted austenitic stainless steel, Proc. Int. Conf. on Wear of Materials, Houston, Texas, 1987, Ed. K.C. Ludema, ASME, vol1, p13-22
12. P.D. Goode and I.J.R. Baumvol, Nucl. Intr. Meth, 1981, 189, 161-168
13. I.L. Singer, R.A. Jeffries in 'Ion implantation & ion beam processing of materials' Ed. G.K. Hubler & others, North-Holland, New York, 1984, p667-672.
14. F.G. Yost, S.T. Picraux, D.M. Follstadt, et. al, Thin Solid Films, 1983, 107, 287-295
15. W.C. Oliver, R. Hutchings and J.B. Pethica, Met. Trans.A, 1984, 15A, 2221-2229.
16. H. Dimigen et.al, Mat. Sci. Eng., 1985, 69, 181.
17. A.K. Suri, R. Nimmagadda and R.F. Bunshah, Thin Solid Films, 1979, 64, p.191.
18. A. Cavalleri et.al, Scripta Met, 1986, 20, 37-42.
19. R.G. Vardeman, R.N. Bolster and I.L. Singer in 'Metastable Materials Formation by Ion Implantation, Ed., S.T. Picrauk and W.J. Choyke, North -Holland, NY, 1982,p269
20. I.L. Singer, Appl. Surf. Sc. 1984, 18,26-62
21. S. Lucas, G. Terwagne, M. Piette and F. Bodart, Nucl. Instrum. Methods, B59/60, 1991,925;
22. S Ohira & M. Iwaki, Nucl. Instrum. Methods, 1987, B19/20, 162.,
23. U.M. Mhatre, D.C. Kothari and others, Disc. Meet on Surface Modific, Tech. of Mats, 3-5dec, 1992 IGCAR, Kalpakkam, India, p395-415
24. R. Krishnamurthy & H.V. Somasundar, Adv. Surfc. Treat, of Met., 1987, p. 326-329, BARC, Bombay, India.
25. S.T. Picraux. S.M. Myers, D.M. Foolstaet, Thin Solid Films, 1979, 63, p1-2) etc.
26. Brain Holtkam, Adv. Materials & Processes, 12, 1993, p45-47
27. Jacob Kleiman, Zelina Iskanderova and Roderick C Tennyson, Adv. Mat & Process, 1998, 4,26-29
28. J.R. Conrad et. al, Surf. & Coating Tech, 1988, 36, 927
29. F.J. Worzala et al, Proc. Int. Conf. on Tool Materials, Chicago, Sept, 1987
30. Ronghua Wei and Paul J. Wilbur & others, ' Rolling contact fatigue wear characteristics of diamond like coatings on steels 'Proc. Conf. on 'Wear of

Materials', Part A, San Francisco, CA, April 13-16, 1993, p558-568, Elsevier Sequor, Lausanne

- 31. R. Wei, P.J. Wilbur and F.M. Kustas, A rolling contact fatigue study of hard carbon coated M-50 steel, ASME J. trib., 1992, 114(2), p298-303
- 32. Bruce A. Banks, Advance Materials & Processes, 12, 1993, p22-25.
- 33. Joginder Singh, Adv. Mat. & Processes, 12, 1996, p27-28
- 34. Joginder Singh and Douglas E. Wolfe, Adv. Matrls. & Processes, April, 2002, p39-42.

Chapter 4

ELECTRON BEAM PROCESSES

4.0 Introduction

The high energy electron beam has been used to vaporize or melt the wear resistant materials and to deposit the vapor or molten phase onto the surface of the substrate. The process using electron beam to evaporate the coating material and subsequently deposit onto the work-piece is known as physical vapor deposition (PVD) process. The electron beam physical vapor deposition process (EBPVD) is one of the most widely used techniques for coating turbine aerofoil (blades and vanes) components. The rapid cooling of the deposited vapor phase may lead to amorphous material formation. The rapid surface melting and solidification via directed energy from electron beam can be used to develop rapidly cooled microstructures, including metallic glass on the surface. Electron beam welding has limited applications for weld surfacing. Electron beams have been used for polymerization of polymers and vulcanization of elastomers (rubbers). The most popular surfacing process using electron beam is the physical vapor deposition (EBPVD) of wear resistant materials.

4.1 Electron Beam

Thermionic emission from a heated cathode leads to generation of electrons, which are simultaneously shaped into beams and accelerated towards anode by precisely configured grid or bias cup. At gun operating voltages of 25 – 200 KV, the beams are accelerated to 30-70% of the velocity of light. The generation of the beams is to be carried in a vacuum chamber. Electromagnetic lenses are used to converge and focus the beams (Fig. 4.0). The rate of thermal energy input onto the coating material surface depends on the number of striking electrons, the velocity and the spot size. The commercially available systems cover 25 to 200 KV and 50-1000 mA, with the capabilities of focusing the beams to spot diameters of 0.25–0.76 mm. The maximum power density obtainable with commercial systems is 1.55×10^4 W/mm².

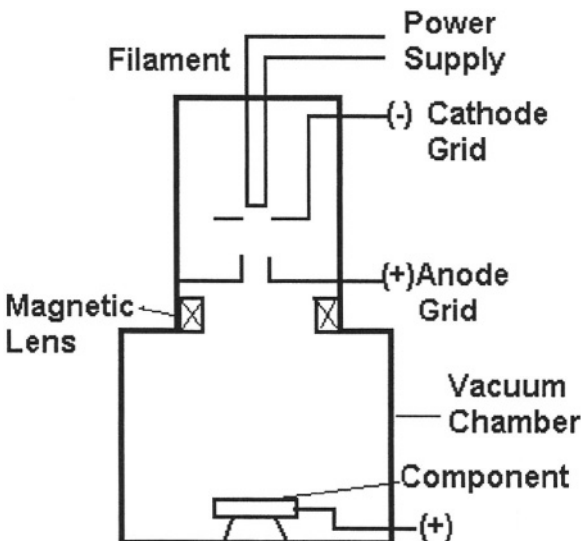


Fig.4.0 Electron Beam Gun

4.2 Electron Beam Assisted Physical Vapor Deposition (EBPVD)

In this process, the focused electron beams are used to vaporize the wear resistant material in a vacuum chamber. The parts to be coated are manipulated within the vapor cloud. The condensation of the vapor on the substrate surface results in coating formation. The term physical vapor deposition refers to deposition of metals by transport of vapor in vacuum without the need for a chemical reaction (1). In physical vapor deposition process the substrate preheating is normally limited to low temperatures. Due to low deposition temperature there is no alteration in the bulk properties of the substrate materials. It is also possible to deposit hard coating on low melting point materials, by this process such as diamond on polymers. By maintaining a low substrate temperature, it is possible to form deposit with amorphous or metallic glass structure.

Process

The coating material kept in a water-cooled copper crucible is evaporated by the thermal energy of directed electron beams from the electron guns (Fig. 4.1.0). The level of molten material in the crucible is controlled by a laser based system. The vapor clouds coming in contact with the parts to be coated form the deposit of the coating material. The components to be coated are

preheated directly by oscillating electron beam guns or indirectly through graphite plating. The preheating is carried out in vacuum in the same chamber or in a separate vacuum chamber. The parts are rotated within the vapor cloud during deposition process. The rotation of the components ensures uniform coverage as the EBPVD is primarily a line-of sight process. The water cooled copper condensation shield captures any metal vapor that fails to condense on the parts. The process is carried out in a vacuum environment of 10^{-2} to 10^{-4} Nm⁻² pressure (2).

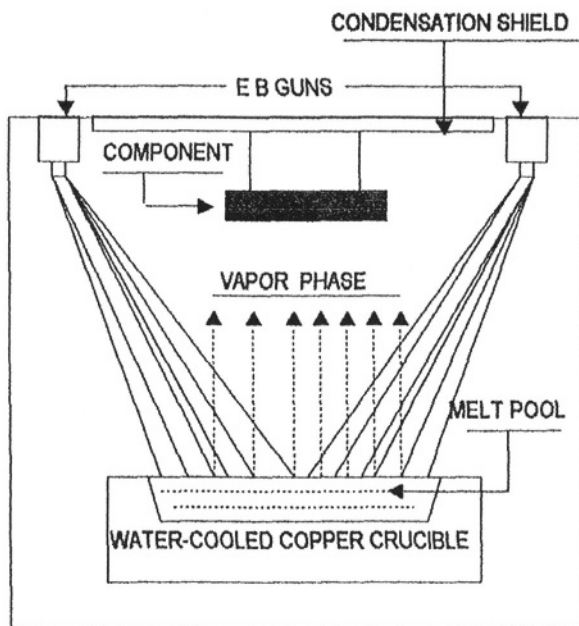


Fig. 4.1.0 : EBPVD Coating System with Multiple Electron Guns(Schematic)

The progressive deposition from vapor phase leads to the growth of as-deposited material perpendicular to substrate. In the columnar grains unbonded interface or separation between two adjacent colonies known as 'leader defect' is often present, particularly as the coating grows in convex curved surfaces due to shadowing effects (Fig. 4.1.1).

High deposition temperatures shall result in increased surface diffusivity which reduces the leaders. It also allows certain minimal interdiffusion between the coating and substrate during the short processing time ensuring good adhesion. The spallation is rarely a problem with EBPVD coating, with a properly cleaned substrate. The deposition rates in this process often exceeds 1 to 150 μm per minute and the total coating thickness ranges from one micron to more than two centimeters (3). The high rate of deposition

makes it possible to obtain a throughput of some 500 standard sized parts in an 8 hour shift (4).



Fig.4.1.1 EBPVD coating with leaders defect

Post-coating diffusion treatment (5)

Diffusion treatment of the coating shall result in interdiffusion and better bonding and removal of leader defect. The as-deposited microstructure of EBPVD coating of Co-19Cr-12Al-0.3Y on a Ni-base superalloy is shown in Fig. 4.1.2a (5). The diffusion treatment removes the leader defects and also forms an interdiffusion zone at the interface of coating and substrate (Fig. 4.1.2b) (ref. 5).

The high aluminium content in the coating results in the precipitation of β -CoAl in the matrix. Limited interdiffusion occurring during coating and post-coating heat treatment does not make any significant alteration in the structure and composition of the coatings across the thickness, excepting in the small interdiffusion zone, where both the structure and composition undergo major changes. Deposit composition may differ from the coating material due to differences in vapor pressure of elements in an alloy. Thus the coating material composition is to be adjusted to produce desired composition in the deposit. With the advanced techniques, a range of elements with different vapor pressure can be evaporated from a single source. The leaders or gaps between columnar deposit can lead to premature failure due to environmental attack and by thermal fatigue cracking. Apart from diffusion treatment, the leaders can also be closed by techniques, such as, glass bead peening and laser glazing. In the EBPVD process of depositing thermal barrier coating of stabilized zirconia plus a bond coat on aeroengine

components, it is possible to produce a number of fine cracks perpendicular to substrate (4). The segmented network improves the cyclic life of the coating.

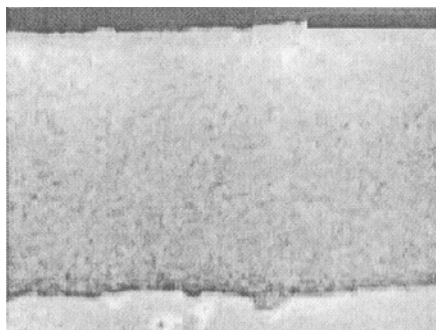


Fig.4.1.2a.EBPVD coating of MCrAlY on Ni-base superalloy,X500

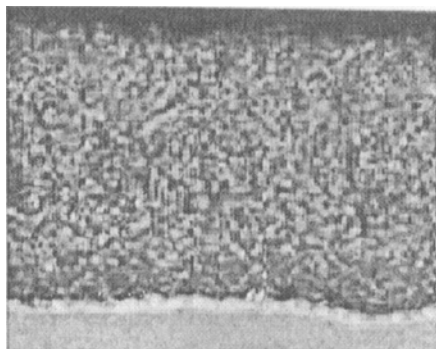


Fig.4.1.2b.EBPVD MCrAlY coating on Ni-base alloy,after diffusion heat treatment,X500

(Ref.5 reproduced from book on 'Superalloy II,
by permission of John Wiley & Sons
Copyright © 1987.)

Advantages of EBPVD (3):-

- The process flexibility allows control of composition in the deposit. The composition control can be achieved through independent evaporation of multiple ingots. It is possible to make multilayered coatings of different materials, such as, ceramic and metallic layers.
- Microstructure control is possible. By frequent interruption of the deposition process it was possible to form fresh nucleation sites and avoid continuous columnar grain formation. Coating has uniform microstructure.
- Surface finish of the coating is excellent.

*Applications:**Aluminium Coated Steel Strip*

A plant for coating aluminum on steel strip has been reported (6) to have achieved a high evaporation rate of up to 100 kg per hour at a high beam power of more than 300 kW in continuous operation of 100 hours. The aluminum coated steel strips are used in packaging industries to replace costly tin plated steel strips.

Gas turbine

A major application of EBPVD is the thermal barrier coating on aeroengine turbine components. Following combustion, the highly oxidising hot gases enter the turbine at a temperature, which is 200°C or more than the melting point of the superalloy. The temperature of the gas entering the turbine is known as TET. Massive amount of cooling air is blown through the components to cool them below the melting point of the superalloy. A significant reduction in specific fuel consumption can be achieved only by increasing the gas temperature at turbine-section inlet throats. The continued demand for increased power and improved specific fuel consumption has resulted in progressive increase in TET over last three decades. In new generation of civil aircraft, TET exceeds 1800°K on take-off (7) and metallic structures of superalloys are expected to withstand temperatures of up to 1200°C (2190°F). At such high TET, no uncoated rotor or stator blade can possibly last long. Additionally the hot gases are highly corrosive. EBPVD process is used to deposit several layers of coatings of different materials on aerofoil to protect the components at high TET. A typical coating sequence is as follows: -

- i. Multicomponent MCrAlY Coating Layer:- The coatings for the turbine blades are designed to protect the surface against wear due to high temperature oxidation, hot corrosion and erosion from particles in the combustion products. However, the coating material should be suitable for use with the blade materials, which are normally nickel base superalloys. At the high operational temperatures in service, there should be low diffusivity of elements constituting the coating so as to form a very thin diffusion zone. Also the diffusion process should not adversely affect the fatigue, creep or fracture resistance properties of the blade material during coating process or in service. The coating should be easily removable to facilitate part repair (8). The multicomponent system such as, MCrAlY, (where base metal M= Fe, Co, Ni) has been found to satisfy the coating requirement of the turbine blades.

The normally accepted practice for coating is to use conventional EBPVD, or plasma-assisted EBPVD or low pressure plasma spray. The

EBPVD generally produces higher quality coatings. Plasma spray technique has the equipment cost advantage. The film thickness of 0.1 to 0.2 mm (0.004 to 0.008 in.) is generally adequate (8). In the EB PVD process (8) for deposition of MCrAlY, the substrate must be heated rapidly to a high temperature and maintain the temperature during deposition. The high deposition temperature ensures formation of dense structure, which is required to provide adequate resistance to hot corrosion and oxidation by hot gas. The rapid heating of the substrate is necessary to avoid overheating and recrystallisation. The actual preheating temperature depends on the alloy composition. In the case of a nickel base superalloy substrate the preheat temperature is reported as 960 to 980°C (1760 to 1795°F). The time required to heat the substrate surface to this temperature should be less than 6 minutes (8). The temperature should be maintained within $\pm 10^\circ\text{C}$. The preheating is carried out in a separate chamber under vacuum. The surface temperature of the molten evaporant is to be held constant during evaporation. Also the evaporant material is to be continuously added to the crucible in order to maintain equilibrium conditions. The coating chamber contains two or three EB guns, each with beam power rating of 200kW maximum. A water cooled copper crucible contains the evaporant and a laser-based system is used to regulate the level of molten material in the crucible. The coating thickness of 0.1 to 0.2 mm (0.004 to 0.008 in.) is deposited in about 10 minutes time. The corresponding coating rate is 1 micron per second (40 micro-inch per sec).

A typical composition of MCrAlY is 20 Cr, 10 Al, 0.3 Y and rest M(Fe, Co, Ni, Co). Depending on the composition, the tolerances are specified for the individual elements. For example, in a NiCoCrAlY deposit, the acceptable tolerance range for chromium, aluminum, and yttrium are 80%, 60% and 60% respectively. In otherwords, if the specified chromium content in NiCoCrAlY is 16 to 22%, then the production coating will contain approximately 16.5 to 21.5% Cr.

Normally diffusion coating of aluminides (e.g., NiAl) or platinum-aluminide is used as bond coat before MCrAlY deposition by EBPVD. The diffusion bond coat layer is around 10 micron (Fig. 4.1.1).

ii. Thermal barrier coating:- The blade life is further extended by applying a heat insulating top coat. The function of the insulating layer is to primarily act as an insulator so as to form a barrier for heat flow to base metal, and thus prevent base material temperature from increasing beyond acceptable limit. This is done by applying a coating of insulating ceramic material on the metal surface. The coating is known as thermal barrier coating (TBC). Normally Y_2O_3 -stabilised ZrO_2 is used for this purpose. The temperature difference between surface and at the base of TBC layer can be as high as

150°C. The coating material is capable of providing resistance to high temperature oxidation and hot corrosion. The TBC layer also reduces thermal shock loads on the blades by reducing the effect of ambient temperature fluctuations. The Y_2O_3 -stabilised ZrO_2 containing 7% Y_2O_3 is deposited by the same process as that of depositing MCrAlY. The raw material used are Y_2O_3 and ZrO_2 . The partial dissociation of oxides results in oxygen deficiency, which is compensated by adding controlled amount of oxygen during coating. Smaller crucibles are used to cope with high evaporation temperatures of the refractory oxides and the EB gun capabilities. Additionally, a thin layer of alumina is to be formed on MCrAlY, which acts as 'glue' for adhesion of ceramic to MCrAlY. The insulating alumina layer is formed by diffusing out aluminum from the MCrAlY coating to the surface, where it is converted to the oxide. The growth of the oxide film is self-limiting, ie., it becomes extremely slow once it reaches a certain thickness. The intermediate film of around 10 micron thick provides additional oxidation resistance (9). The advantage of using LPPS to deposit alumina is the ability to add Hf or other elements, which enhance the adhesion of alumina scale, a factor critical to the life of EBPVD deposited thermal barrier coating. The spalling of ceramic coating occurs due to growth of alumina 'glue' region resulting in the development of increased stress at the interface. Recently developed bond coat materials based on platinum has shown improved life during thermal cycling (9).

The multilayer coating of different materials on aeroengine turbine blade is shown in Fig. 4.1.3. The thickness of the first layer on the substrate is around 10micron. The diffusion zone provides good adhesive bonding of CoCrAlY to the substrate. The thickness of the corrosion and oxidation resistance layer of CoCrAlY is around 100micron. Another diffusion layer on the top of CoCrAlY has a thickness of approximately 5 micron. The diffusion layer acts as a bond coat between top Y_2O_3 stabilised ZrO_2 layer and substrate containing CoCrAlY. The top thermal barrier coating (TBC) layer is around 250 micron thick (8).

Tools (10,11)

The improvements in tool life to the extent of 100% to 400% are obtained by hard, wear resistant EBPVD coatings of TiC, TiN and TiAlN (10). EBPVD coatings of TiCN, TiAlN and CrN are developed (11) to cater for the needs of specific tooling applications. The new coatings have replaced TiN in areas where their comparative performance is superior to TiN. The golden colored TiN coatings (2-5 micron) of hardness of 2200 HV are widely used in metal cutting and forming industries. The TiCN coating has both high hardness (~3000 HV) and toughness, but lower oxidation temperature (400 vs

600°C) in comparison to that of TiN. Therefore the TiCN coating is used for interrupted cutting tools, such as milling, where the tool temperature rise is less and high toughness prevents tool breakage. The titanium aluminum nitride (TiAlN) coating is hard, tough and capable of withstanding high temperature. Therefore the TiAlN coating is recommended for high speed tooling, requiring less lubricants or for dry machining. An additional lubricious carbon based coating on TiAlN layer can minimize heat generation through reduced friction (11).

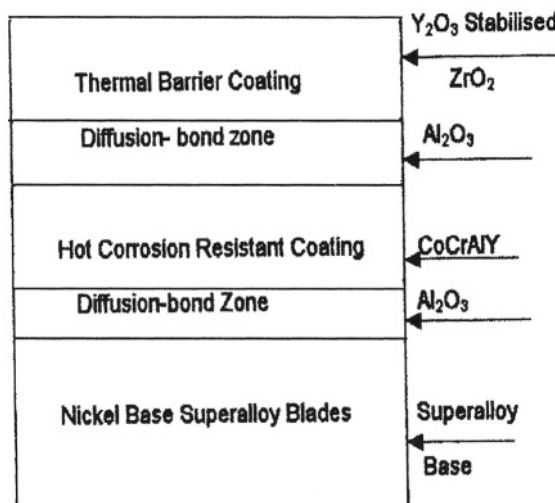


Fig 4.1.3 Schematic diagram of a multi-layer coating to prevent hot corrosion and oxidation in turbine blade

Low Friction Mixed DLC-WC Coating for Automobile Industry (11)

A high hardness (1000 HV), low coefficient of friction (~0.5 against steel), carbon based diamond like coating containing WC has found a large number of applications. The low deposition temperature of 160 to 200°C, allows the coating to be used on a large number of engineering steels, including carburized steels without getting tempered during coating process. The coating structure consists of lamellar structure of amorphous carbon containing tungsten carbide precipitates (11). An interesting application is the plungers in the diesel fuel injection systems (11). In order to cope with stricter emission regulations, the injection pressure in the fuel injection system has been increased significantly thus reducing the clearances between, for example, plungers and barrels. The reduced clearance has increased the scuffing problem. The mixed C-WC coating on plunger has found to provide solution to scuffing problem. The transmission performance of carburized gears in poorly lubricated environments can be improved by the use of C-WC

coating. The pitting fatigue resistance of the coated carburized gear is increased by 10-15% compared to that of uncoated gear (11).

Frictional Wear Resistant Silver/Molybdenum Coating (12)

Advanced heat engines and gas turbines require coatings to withstand high temperature harsh tribological conditions. Silver has been used as solid lubricant in high temperature applications (13,14) due to its high conductivity (no hot spot formation due to quick dissipation of frictional heat), low shear strength (can serve as a self-sacrificed layer) and high chemical inertness. Molybdenum and molybdenum sulphide (MoS_2) coatings are used extensively as anti-scuffing and friction reducing agents (14). The simultaneous electron beam evaporation of silver and molybdenum, which are not miscible in liquid state, produces nano-crystalline structures onto steel substrate at room temperature. The co-deposited thin film contains a mixture of crystalline silver (69%) and molybdenum (31%). The nano-crystals are in the size range of 8 to 47 nm. In wear tests, the film provided lowest friction during the first 10 hour of sliding compared to other samples such as bare steel substrate, pure molybdenum coating, or molybdenum rich (66% Mo, 34% Ag) films. The wear resistance in terms of wear depth measurements can be increased by 25 to 27% in comparison to the base steel materials. The improved wear resistant characteristic of the silver rich molybdenum film is ascribed as due to the formation of a nano-crystalline binary mixture by EBPVD deposition process.

Graded EBPVD Coating

The large differences in thermal properties, such as, thermal coefficient of expansion and thermal conductivity, between metallic and ceramic materials, can lead to failure of pure ceramic coating on the metallic component during thermal cycling. The coating integrity is impaired by such drastic change in coating properties at the coating interface between metal and ceramic. In such a situation, it is advisable to have a multilayer coating, where increasing percentages of ceramic materials are added to each successive layer till the ceramic composition is reached. The number of layers and the amount of additions in each layer are to be decided based on overall coating thickness limitation. In EBPVD, the coating composition can be altered by manipulating the evaporating material compositions or by independent evaporation of materials from multiple ingots. The process has thus the flexibility to form graded coatings. The gradual change in properties across the graded coating results in improved resistance to spalling during thermal cycling of the coated component.

Amorphous Deposit by EBPVD

In the condensation process, the vaporized material is condensed on a surface maintained at a temperature well below that of configurational freezing. Thus the potential for novel metastable structure formation is much greater in condensation where the quench rates are much higher than melt quenching. The quench rate for condensation from vapor phase is 10^{-12} whereas in 'splat' cooling it is 10^8 (15). Also in contrast with melt quenching, there should be no limit on the compositional ranges of solid solutions formable by condensation. Thus, it should be possible to co-deposit over the entire composition range of elements with limited liquid state miscibility. It is now well established that the component variety and composition ranges of alloys which form amorphous solids are much wider in condensation than melt quenching. For example, Cu-Sn (16), Cu-Ag (17), and Au-Co (17) are vapor or sputter co-deposited, but not melt-quenched, in amorphous solid forms. The amorphous metal coatings possess excellent corrosion resistant properties due to the absence of grains in the structure.

Plasma assisted EBPVD

A plasma assisted electron beam evaporation process has been developed for producing coatings with improved density. In this process, positive ions are produced and accelerated via use of a supplementary electrode and the application of bias voltage to the parts (1). The film condensation rates remain similar to conventional vacuum evaporation but the coatings are much denser and thus more resistant to hot-gas corrosion encountered in gas turbine blade application. The plasma-assisted technique has been successfully used to deposit hard coatings on metal sheet (1).

4.3 Electron Beam Welding (18)

The high energy electron beam when focused onto the consumables results in the formation of fused weld overlay on the substrate surface. The electron beam welding can be performed in high vacuum ($<1 \times 10^{-3}$ mm, Hg), medium vacuum ($\sim 1 \times 10^{-2}$ to 1×10^{-1} mm Hg) and in non-vacuum (NVEB). In NVEB, the electron beam is shielded with inert gas, such as, helium, which also acts partially as a shielding gas for the molten metal pool. EBW is a preferred process compared to others for precision applications involving exotic materials with stringent weld requirements because of the ability to:-

- melt materials reactive to traces of atmospheric gases in the vacuum chamber
- locally melt high-temperature materials without preheat allowing formation of small, precisely controlled weld pools

- melt highly conductive materials and also materials highly reflective to laser beam
- weld very thin and very thick materials due to wide range of controls. The main limitations are the object size restriction (due to chamber size) and high cost. NVEB, or medium vacuum can be used for non exotic materials retaining most of the advantages of EBW, in applications, such as, automobile gears, steering column, and also for bandsaws and hacksaws.

References

1. D.G. Teer, Coatings for high temperature applications, Ed. by E. Lang, Applied Science Publishers, p79, 1983
2. R. Nicholls and D.J. Stephenson, Metals & Materials, March, 1991, p156-163
3. Joginder Singh and Douglas E. Wolfe, Adv. Materials & Processes, April, 2002, p 39- 42
4. D.H. Boone, Proc. Conf. "Materials Coating Techniques", Neuilly-sur-Seine, AGARD, 1980
5. John H. Wood and Edward H. Goldman, *Protective Coatings*, an article in the book, Superalloy II, p359-385, Copyright © 1987 by John Wiley & Sons,
6. A.V. Thakur, Workshop on, Beams and Ions, Bhabha Atomic research Centre, Bombay, India, 31 Jan-Feb 2, 1990, p47
7. D.H. Boone & J.W. Fairbanks, Specialised cleaning, Finishing and Coating Processes, Conf. Proc, Los Angeles, CA, ASM, Feb, 1980, p357
8. Helmut Lammermann, and Gerhard Kienel, 'PVD Coatings for Aircraft Turbine Blades', AM&P, 12/91, 18-23
9. Rodney Wing, Mat. World, March, 2000, p10-12
10. Joginder Singh, Adv. Mats. & Processes, 12, 1996, 27-28
11. Andy Bloyce, 'Engineering PVD Coatings Beyond Titanium Nitride, Coatings', October, 2000, bulletin published by the Thermal Spraying and Surface Engineering Association, UK
12. S.C. Tung, Microstructures and tribological characteristics of electron-beam co-deposited Ag//Mo thin film coatings, WOM, April 13-16, SanFrancisco, CA, ptB, Elsevier, p 763-771
13. F.P. Bowden & D. Tabor, The Friction and Lubrication of Solids, Part 1, Oxford University Press, London, 1964.
14. U. Buran & others, Plasma sprayed coatings on piston rings – state of development and application potential, Proc. Int. Conf on Surface Modification and Coatings, October, Toronto, Canada, 1985, paper no 8512-023

15. D. Urnbull, Metastable structures in metallurgy, Rapid Solidification Technology Source Book, ASM, 1983 p30-43
16. W. Buckel and R. Hilsch, Z. Phys., 1954, vol 138, p109
17. S. Mader and A.S. Nowick, Appl. Phys., Letters, vol 7, p57, 1965
18. Frank Smith and John Milewski, Welding Journal, June, 2001, p43-46

This page intentionally left blank

Chapter 5

MICROWAVE ASSISTED SURFACE MODIFICATION PROCESSES

5.0 Introduction

Electromagnetic waves with wavelength in between radiowave & infrared and frequencies higher than radiowave are known as microwaves or millimeter waves. Microwave heating of a material depends on the *loss factor*, which is the product of dielectric constant of the material and its loss tangent. Materials with loss factor in the range of 1 to 100 are suitable for microwave heating. Surface heating can occur in materials with high loss factors. Loss factor varies with the frequency and temperature and can be changed by altering the state of a material through different processes such as powdering, compacting, heating or melting. An insulator, which is transparent to microwave at room temperature can get easily melted by absorbing microwave at elevated temperatures. Microwaves are used in CVD deposition of diamond coating, surface diffusion and sintering of surface deposit.

5.1 Formation and Properties of Microwave

Light is considered as a component of the *electromagnetic spectrum* (Fig. 5.1). Electromagnetic waves move with the same speed as that of the light, i.e., $c = 2.997924 \times 10^8$ meters/sec, in the free space. Different types of rays differ in wavelength, frequency and photon energy. The labeled regions in Fig. 5.1 represent frequency and wavelength intervals. Microwaves (radar waves) or MM-waves (1), are defined as the electromagnetic radiation spectrum at frequency range between 3×10^9 to 3×10^{11} c/s, wavelength of 10^{-1} to 10^{-3} m and photon energy of 10^{-5} to 10^{-3} eV. All such regions overlap. For example, radiation of wavelength 10^{-3} can be produced by either microwave techniques (microwave oscillators) or by infrared techniques (incandescent sources). Microwave frequency bands are designated by alphabets (Table 5.1.0). Microwaves are typically in higher frequency regions than RF. Above ~ 1 GHz is microwave. Higher frequencies of ~ 300 GHz are called millimeter waves or far-infrared waves (terahertz = infrared). There is a lot of overlap in the terminology between the fields.

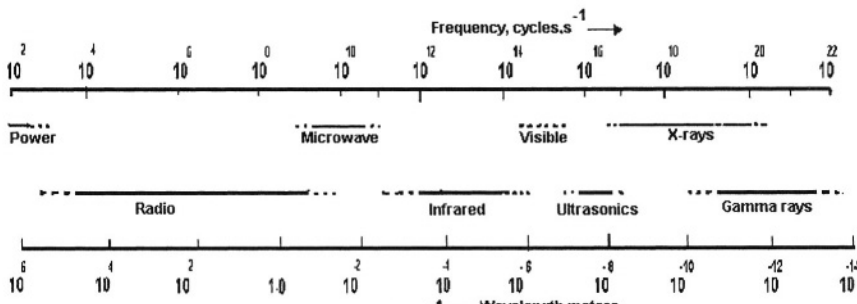


Fig.5.1.1 Electromagnetic Spectrum (logarithmic scale)

Tab 5.1.0 :Microwave Frequency Bands

Letter	Frequency band (GHz)	Wavelength band in vacuum(cm)
L	0.390 - 1.550	76.9 - 19.3
S	1.550 - 5.200	19.3 - 5.77
X	5.200 - 10.900	5.77 - 2.75
K	10.900 -36.000	2.75 - 0.834
Q	36.000 -46.00	0.834 -0.652
V	46.000 -56.000	0.652 -0.536
W	56.000 - 100.000	0.536 - 0.300

An important characteristic of electromagnetic wave is that it can transport energy from point to point. The rate of energy flow per unit area in a plane electromagnetic wave is described by a vector \mathbf{S} , called Poynting vector, as follows:-

$$\mathbf{S} = \frac{1}{\mu} (\mathbf{E} \cdot \mathbf{B})$$

\mathbf{S} is expressed in watts/m², and the direction of \mathbf{S} gives the direction in which the energy moves. \mathbf{E} and \mathbf{B} are the instantaneous values of the electric and magnetic field vectors. μ is equal to magnetic flux per amp-m or expressed as weber /amps-m.

Microwave heating per unit area follows Poynting vector, and it's integration denotes the heat produced ($I^2 R$, where I = current) over the whole area. For example, the rate at which energy flows into a resistor (R) through a cylindrical surface can be calculated by integrating Poynting vector over the surface as follows:

$$\int \mathbf{S} \cdot d\mathbf{A} = I^2 R, \text{ where } d\mathbf{A} \text{ is the element of area of the cylindrical surface.}$$

Most metals absorb photons with wavelengths shorter than infrared radiation ($\lambda_{\text{microwave}} < \lambda_{\text{infrared}}$) (Fig. 5.1). The power absorbed by the striking microwave passes through a maximum when plotted against conductivity. Microwaves possess the unique property of transferring heat neither to conductor nor to insulator but materials within the middle conductivity range, such as, water (Fig. 5.2).

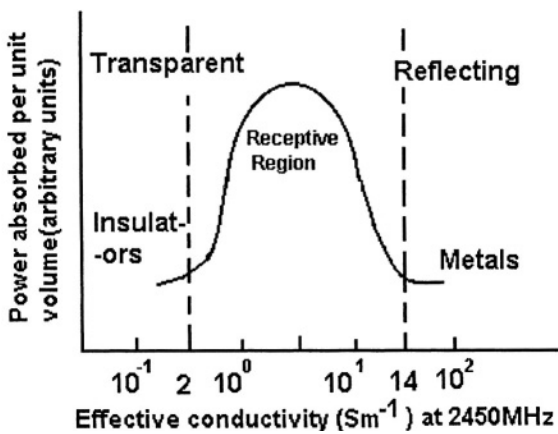


Fig.5.2 Microwave energy absorption vs effective conductivity

[Ref.2, Reproduced from *Materials World*, Nov. 1989, p633-639, the journal of the Institute of Materials, Minerals & Mining, (formerly the Institute of Materials) London, UK]

Energy absorption of material from microwave can be described by **loss factor**. Loss factor (2) is the product of dielectric constant of the material and its loss tangent. Low loss factor material cannot be effectively heated, whereas surface heating can occur in materials with the high loss factors. Materials with loss factor in the range of 1 to 100 are suitable for microwave heating (Fig. 5.2). Loss factor varies with the frequency and temperature. The effective conductivity can be varied widely by changing the state of a material through different processes such as powdering, compacting, heating or melting, and thus altering the microwave absorption capability. An insulator, which is transparent to microwave at room temperature can get easily melted by absorbing microwave at elevated temperatures.

Mechanisms suggested to explain heat generation by microwave includes followings (2):

- Dipole rotation in polar water molecules is the best-known mechanism. Rapid changes in the direction of magnetic field (4900 million times/ sec in a domestic microwave oven) leads to

oscillation of polar molecules at the same rate causing generation of high heat in the material.

- ii. Ohmic heating from induced current or arc generated between charged particles
- iii. Magnetic materials interacting with the magnetic field component

Heat is generated throughout the bulk of the component by microwave and not by conduction from heat generated at the surface. Microwaves are used mainly for communications (Radar) and heating. Selected frequency bands are allotted for these two major applications in each country. For example in Australia, two heating frequency ranges are designated, viz., 2450 MHz for all domestic and many commercial purposes and 915 MHz for the remaining commercial applications (2).

Microwave generation & transmission

Microwaves consist of electric and magnetic components directly combined with each other. For generation of microwaves high frequency electro-magnetic fields are required.

Earlier systems for generation of microwaves were based on vacuum devices like Klystrons, magnetron and travelling wave tubes. However, solid state (semiconductor) types of amplifiers and generators are now available at relatively high power levels and at frequencies up to 300 GHz. Microwave generation requires high frequency electromagnetic fields. Generated microwaves are transmitted onto the material to be heated by wave guides with their respective tuners, or by absorbers via special wave-guide radiators.

Microwave heating requires a magnetic field. The mechanism for coupling is the resonance frequency of the cyclotron motion of the electrons around the magnetic field line. For example, 2.45 GHz which is the frequency used in microwave ovens couples to electrons at about 850 Gauss. This is obtainable nowadays by using rare-earth permanent magnets. The coupling is very good and produces high ionization and high plasma density of 10^{11} cm^{-3} .

5.2 Microwave Assisted Plasma CVD Process (3, 4)

Microwave Plasma CVD

In addition to DC plasma, two other types of plasma with widely different frequencies are microwave and radio frequency (RF) plasma. The excitation frequency of microwave plasma is typically 2.45 GHz, while that of RF plasma is 13.56 MHz. The unique property of microwave plasma is the capability to oscillate electrons at microwave frequency. As a result of electrons colliding with gas atoms and molecules, high ionization fractions

are generated. Microwave plasma is often said to have 'hot' electrons and 'cool' ions and neutrals.

It has been observed that the concentration of atomic hydrogen could be increased by the use of a DC plasma established by an electrical discharge (5). The plasma therefore has been considered as another method to dissociate molecular hydrogen into atomic hydrogen and activate hydrocarbon radicals into promoting diamond formation. The temperature for the formation of diamond coating can be reduced substantially by using microwave in plasma CVD coating. Diamond growth requires an environment in which a high rate of graphite etching occurs. Two regions of microwave plasma actively etch graphite are :

- i. centre of the plasma ball and
- ii. region just under plasma.

The second region provides conditions for low temperature crystallization of diamond. In order to obtain high crystallization rate, two possible solutions are:

- i. Substrate is placed under the plasma ball.
- ii. Plasma is extended down stream by means of a coaxial waveguide.

The waveguide can be made of a strip (or rod) of graphite or metal and shall extend the outer layer of plasma ball. Microwave oscillations shall be transferred along the waveguide with the plasma. A schematic diagram of microwave assisted CVD process for diamond film formation is shown in Fig. 5.3. Microwaves enter into the reaction chamber through waveguides. The microwaves proceeds through a silica window into the plasma enhanced CVD process chamber. The reactive gas mixture methane plus hydrogen entering from the top is allowed to interact with microwave plasma. The size of the luminous plasma ball will increase with increasing microwave power. Diamond films have been grown with the edge of the luminous plasma located about 2 cm higher than the substrate. The substrate need not be in immediate contact with the luminous glow for diamond to grow via microwave plasma. Uniform diamond films with substrate diameters of up to 4 inch can be deposited using this system.

Temperature of substrate at reaction zone was found as 800-1000°C by optical pyrometer and 400°C by infra-red pyrometer. The coating thickness of 1-2 micron per hour was obtained with substrate (glass, metal or ceramic) at around 800°C. In MWCVD system, by applying negative bias to the substrate during nucleation, it has been possible to enhance nucleation rate to a density as high as $10^9 - 10^{10} \text{ cm}^{-2}$ on silicon (6) and silicon carbide surfaces (7). The high growth rates are achieved on polished surface, i.e., without any scratching.

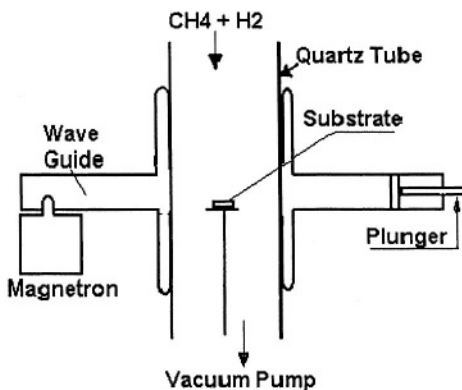


Fig.5.3. Schematic of Microwave CVD Process

Microwave plasma assisted CVD has been used to produce wear resistant coating of not only diamond but also other ceramic materials, esp., for small cutting and milling tools.

Electron-Cyclotron Resonance Microwave Plasma CVD

The electron cyclotron resonance microwave plasma (ECR-MP-CVD) has been used to synthesize diamond film, since ECR-MP generates high density plasma ($>10^{11} \text{ cm}^{-3}$), which is favorable for diamond growth. ECR-MP-CVD has been used to obtain uniform films at substrate temperatures as low as 300°C (8). However due to extremely low pressure of the ECR process (10⁻⁴ – 10⁻² Torr), diamond growth rate is extremely low. Therefore this method cannot be used for industrial production.

5.3 Microwave assisted surface diffusion (2)

- i. Carburising:-Experiments have been conducted for case hardening of low carbon steel by carburising in microwave assisted diffusion of carbon at the surface from carburising atmosphere.
- ii. Diffusion of substitutional elements:- The concentration of substitutional elements like Mn, Ni, Cr, Al etc at the surface layer can be increased by microwave assisted surface diffusion process. Surface alloying can convert the surface of a low carbon steel to nonmagnetic austenitic structure (Mn, Ni), or formation of corrosion & oxidation resistant (Cr) layer or high temperature oxidation resistant (Al) case.

Steep diffusion composition gradients were found in these experiments.

5.4 Microwave Sintering

Microwave heating has been used to sinter ceramic oxides & carbides. Microwave sintering of metallic materials have also been carried out (9). The sintering of thermally sprayed carbides (WC + Co) and oxides (Al-, Ti-, Cr- & Zr – oxides and mixed oxides) for development of dense wear resistant coatings is yet to be explored. The increase in density due to sintering shall result in higher hardness and the corresponding improvement in wear resistance properties of the ceramic & composite coatings. The closure of open pores by sintering can lead to the improvement in high temperature oxidation & corrosion resistance of coatings.

5.5 Fused Ceramic Surfacing by Microwave (10, 11)

By focusing microwaves of 122 mm long on a 1mm spot on the surface of the materials such as, ceramics, concrete, and glass, which absorb microwaves (but not on metals, which reflects microwave), it is possible to produce sufficiently intense microwave energy for melting the spot. The area is rapidly heated because of “thermal run-away effect”. The material at the hot spot absorbs more microwave energy due to increased temperature. The cascading effect of higher energy absorption with increasing temperature leads to the development of extremely high temperature in a small volume (10). Similar to laser, the microwave can be used to modify the surface properties by rapid melting of small localized wearprone area, followed by rapid cooling due to mass effect of the bulk material on removal of heat source. Utsumi & others (11) has reported the formation of crack free fused ceramic coating (titanium diboride) by melting applied ceramic paste layer by laser beam (see section 6.8). The microwave can be used to preferentially melt the ceramic layer to form a hard wear resistant coating similar to that obtained by Utsumi & others (11). Also the microwave can be used to close the open pores in thermal spray ceramics to prevent the ingress of fluid corrosive chemicals.

References

1. D.T. Emerson, The work of Jagdish Chandra Bose : 100 Years of MM-wave research, IEEE-MIT-S Int. Microwave Symp Digest, vol 2, 1997, 8-13 June, Denever, CO, pp 553-556
2. B.P. Barnsley, Microwave Processing of Materials,, Materials World, Nov, 1989, p633-636
3. Y. Mitsuda et al, J. of Matrl. Sci., 1987, 1557-1562
4. S. Tong Lee & others, CVD diamond films : nucleation and growth, Mat. Sci. & Engineering, 1999, 25, 123-154

5. B.V. Spitsyn, L.L. Bovilov, B.V. Derjagnin, J. Crystal Growth, 1981, 52, p219
6. S. Yugo, T. Kanai, T. Kimura, T. Muto, Appl. Phys. Lett, 1991, 58, 1036
7. B.R. Stoner, J.T. Glass, Appl. Phys. Lett, 1992, 60, 698
8. D. Mantei & others, Jap. Journ. of Appl. Physc., 1996, 35, 2516
9. D. Agarwal, Material World, Nov., 1999, 672-673
10. Eli Jerby, 'Microwave Drill Melts Holes in Concrete, Ceramics, Glass', Advanced Materials & Processes, February, 2003, p17-18. Also private communication.
11. A Utsumi, J. Matsuda, M. Yonneda, M. Katsumura and T. Araki: Int. Thermal Spraying Conf. Kobe, 1995, 325-330.

Chapter 6

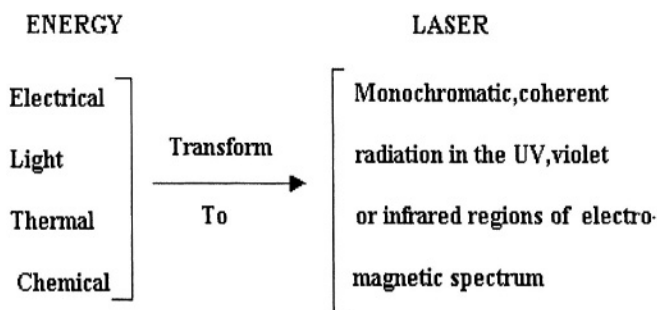
LASER ASSISTED SURFACE ENGINEERING PROCESSES

6.0 Introduction

The concentrated source of heat obtained from the light amplified by stimulated emission of radiation or LASER has been used extensively for various surface engineering processes. The three main types of laser used in surface modification processes include solid (Nd-YAG), gas (CO_2) and high power diode lasers. The list of processes using laser as a heat source includes surface hardening, melting and amorphous phase formation, alloying, surface coating by welding, vapor phase deposition and thermal spraying. In addition to formation and properties of laser, use of laser in various surface engineering processes and the major industrial applications are to be discussed in this chapter.

6.1 Formation & Properties of Laser

LASER is the light (L) amplified (A) by stimulated (S) emission (E) of radiation (R) producing high energy parallel beams at specific wavelength. Energy in different forms can be converted to produce laser (Table 6.1.0):



Tab.6.1.0.Laser formation from other forms of energy

A laser device consists of optical pumping to excite the light quantum from lasing element and a resonator or optical cavity for light amplification.

6.1.1 Lasing Elements

Lasing or light emitting elements can be solid (including semiconductors), liquid, or gas.

Solid lasing elements: The list of solid elements includes ruby, erbium garnet, neodymium – doped glass etc. $\text{Al}_2\text{O}_3\text{-Na}$ garnet doped with neodymium has power output up to 1 kW in continuous wave (CW) or up to 50 MW in pulsed operation.

Liquid lasing elements: List includes some dyes and neodymium oxide containing solution. Inorganic liquid lasing solutions have similar capabilities as that of solids. However, liquids exceed solids in terms of pulse power output due to their large volume of lasing element.

Gas lasing element: Gases normally used include hydrogen, nitrogen, argon and carbon-di-oxide. Gas laser has the most wide spectrum of radiations and highest power output in CW operation in conjunction with high efficiency. Commercial CO_2 lasers use a gas mixture comprising of 10% CO_2 , (lasing gas), 78% He (for heat dissipation) and 12% nitrogen (to increase efficiency).

Single Crystal or Semiconductor Lasing Elements: The list of single crystals or semiconductors used as lasing elements include gallium and indium arsenide, alloys of Cd, Se and S. An example of single crystal semiconductor or diode laser is the use of n-doped GaAs single crystals with extremely high purity as lasing element. Lightweight semiconductor lasers consume less energy while operating at a very high efficiency (70%).

Excimer laser is also a gas laser which uses mostly a combination of inert gas halides, such as xenon chloride. These dimer gas molecules only exist as short lived excited states and therefore the excimer laser is operated on a pulsed basis.

6.1.2 Pumping Systems

Pumping system supplies energy to excite and emit light from lasing element. The pumping systems are developed to suit the lasing elements. Examples of pumping systems for different types of lasing elements are as follows:-

Solid state and liquid lasers: These are usually optically pumped by a flash tube.

Gas Lasers: The gas lasers are pumped by gas discharges.

Semiconductor lasers: Energy of current traversing the p-n junction is utilised for pumping.

The laser can be operated in the continuous wave (CW) or pulsed mode, depending on the energy capability of pumping system.

6.1.3 Techniques For Laser Formation (1, 2, 3, 4, 5)

Laser from Solid Lasing Element (1, 2): The solid lasing element like Nd-YAG is normally used in the form of a cylindrical bar of 150 mm long and 9mm diameter. The parallel ends are ground flat to close tolerance, polished to optical finish and silvered to make reflective surfaces. Excitation or optical pumping of the Nd-YAG crystal is carried out by a krypton or xenon lamp (Fig. 6.1.1). By combining a number of rods, high power YAG lasers can be produced. For example, by combining single rod 600W systems, it has been possible to develop a high powered two-rod 1.2 kW system or a three-rod 1.8 kW system or a four-rod 2.4 kW system in CW mode. The poor beam quality of high power Nd-YAG laser can be improved by either changing the geometry of lasing medium from rod to slab or by aperturing the beam. The negative aspects of the slab or rectangular laser include high cost of growing and finishing the crystal to the precision required, its limited sources, and its limited durability.

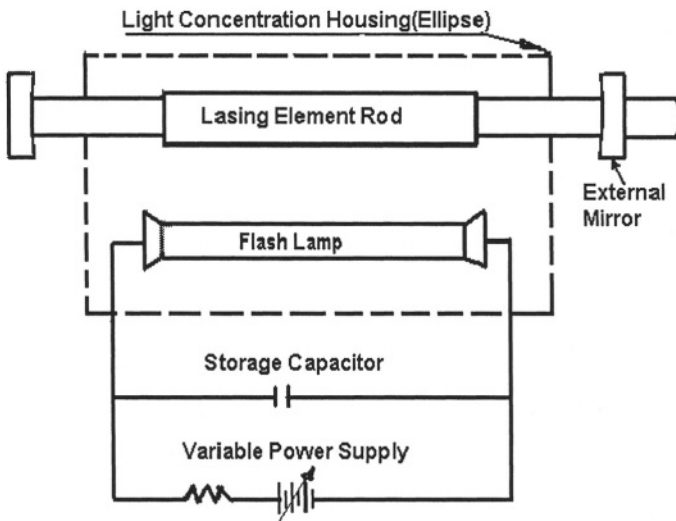


Fig.6.1.1. Schematic of a Nd-YAG Laser System

Power output depends on excitation method. In continuous excitation (CW), xenon lamp excitation can produce power up to 10 W, whereas krypton

lamp produces up to 100 W or more. Intermittent pumping is carried out in pulse mode by using a pulsed power supply to drive the flash lamp. In pulse mode, the power output pattern shows a number of spikes of varying heights or peak power levels despite similar duration of each spike. Average power produced by Nd-YAG in pulse mode is in the range of 10 to 100 W. The flash lamps, which need frequent replacements, are being substituted by an array of diode lasers. The diode lasers improve the pumping efficiency by matching the absorption spectrum of neodymium. A diode pumped Nd-YAG laser can develop up to 6 kW power.

Gas laser (1, 2) : In CO_2 laser, a gas mixture consisting of 10% CO_2 , 78% He and 12% nitrogen is optically pumped (CO_2 molecules excited) by glow discharge (Fig. 6.1.2). In a high efficiency CO_2 laser, around 80% of the electrical power input dissipates as heat through the gas with the resultant increase in the gas temperature. Laser action ceases if the gas becomes very hot. Therefore the gas temperature is to be maintained within 200-250°C by adapting suitable cooling system. The lasing gas is cooled either by *convective cooling through heat exchangers* with the help of a suitable gas circulated through blower or by *removal of heat by diffusion* through the glass wall to the circulating water in the jacket placed surrounding the tube, called 'diffusion cooled'.

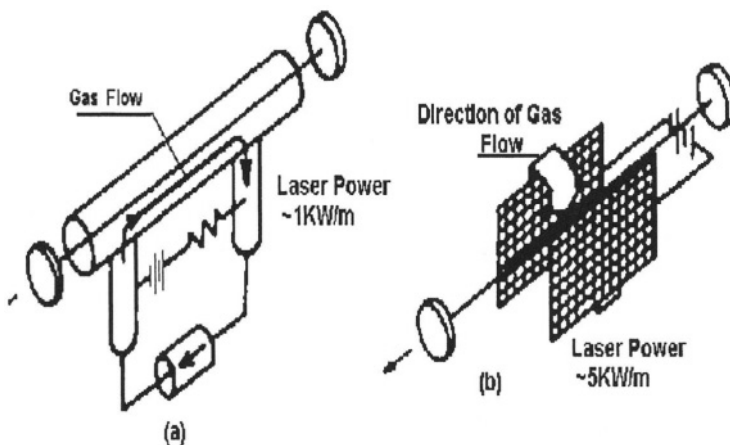


Fig 6.1.2. Convective Flow CO_2 Laser (a) Axial Gas Flow and (b) Transverse Gas Flow

Convective cooled CO_2 lasers

The convective cooling technique is used for most of the high power CO_2 lasers in multi-kilowatt range. In this system the laser gas is circulated through

the discharge zone and then through heat exchangers at high speeds with the help of a circulating blower. The laser power (PL) can be increased by increasing the gas flow velocity or mass flow rate (M) as follows (6):-

$$PL = 120 M \text{ Watts, where } M \text{ is a mass flow rate in g/s}$$

Gas heating is controlled by continuous flow of gas mixture through the optical cavity area and therefore the CO_2 lasers are usually described according to the direction of gas flow with respect to the direction of optical oscillation, such as, slow axial flow (SAF), fast axial flow (FAF) or transverse flow (TF).

Axial Flow:-In this system (Fig. 6.1.2a), convectively cooled gas flows parallel to the direction of discharge and optical oscillation. SAF is the simplest gas laser. In a more efficient heat exchange system in FAF, higher output power obtained in comparison to SAF. FAF in CW mode can produce 500-1000 W/m.

Transverse Flow:- In TF, gas is circulated across the discharge & optical path (Fig. 6.1.2b). The long optical path & short resonator structure make possible to produce higher output power of 1-25 KW (CW) in compact TF system.

Diffusion cooled extended electrode CO_2 lasers:

The conventional system of diffusion cooling through the circulating water outside the glass tube becomes less effective with the increase in tube diameter unless there is a corresponding increase in laser gas pressure so as to maintain the product of the laser gas pressure and the discharge tube diameter at a fixed value of around 25-30 Torr-cm. By increasing discharge tube length, the maximum power available is about 50-60W/m. For materials processing high power output in kilowatt range is required. The diffusion cooled lasers are scaled up to kilowatt range by increasing the active length and then placing several discharge tubes optically in series or parallel configurations. In commercial units using series configuration, power output up to around 1kW is possible. In parallel discharge tubes, the units with power outputs of up to 10 kW are available.

A new concept of increasing power output in diffusion cooled CO_2 laser is through formation of stable and uniform discharge between two extended electrodes (7).

The water cooled two plane (flat plates) or coaxial cylindrical electrodes with larger electrode areas are used to increase power output in few kilowatt range. Lasers of this type are usually excited by RF discharge instead of DC discharge. With the availability of compact solid state base RF power supply, this type of CO_2 laser in kilowatt range is gaining popularity. However the

planar or coaxial system of extended electrodes requires specially designed optical resonator to produce good quality beam suitable for material processing.

Intensity distribution in a plane perpendicular to the propagation of a cylindrically symmetric beam is classified by its transverse electromagnetic mode, TEM_{pl} , where p & l refer to the number of radial and angular modes. The subscripts refer to the allowed oscillation (standing electromagnetic waves) in two orthogonal directions in a plane transverse to the axis of optical cavity. TEM_{oo} mode means only one orientation of the beam and the beam intensity follows Gaussian distribution pattern about a central peak. TEM_{oo} can be focussed to the smallest size with largest depth of focus.

High Power Direct Diode Lasers (HPDDL) (3, 4, 8)

Low efficiency of Nd-YAG laser is ascribed as due to very wide spectrum of optical flash/arc lamp radiation not fully utilized in laser excitation. Earlier attempts to improve the efficiency of solid state Nd-YAG laser by diode pumping laser of appropriate wavelength resulted in an efficiency of as high as 20%.

Recent development of high power direct diode laser (HPDDL) also known as semiconductor lasers with very high energy conversion efficiency (40 to 50%) has for the first time led to the production of compact, modular and highly efficient laser heating systems. HPDDL systems are not only economic alternatives to conventional lasers but also to other heat sources, such as, plasma, electron beam or ion beam, which are used for thermally assisted surface modification processes (3).

The basic material for diode laser is high purity n-doped GaAs single crystal. Thin wafers of around 350micron thick and 2.0 (50.8 mm) to 3.0 (76.4 mm) inches diameters are sliced from the crystal. The layered structure is generated by CVD process and epitaxial growth. By carefully scratching, the wafer is broken into small individual diodes. At the edges multilayer mirrors are deposited in order to form a resonator. A few milliwatts of light can be generated from such unit.

In order to develop higher power, several single elements are integrated into one semiconductor element. The unit is known as 'laser bar' with dimensions of around 1000 micron \times 600 micron \times 115 micron of which 600micron is the resonator length.

The shape of the light generation area leads to special light emitting characteristics, such as a high divergence in the direction of the pn-junction ('fast axis') and a low divergence but wide emitting 'stripe' in the other ('slow axis') direction. To bring the divergent beams in useful form, a lenslet array is close coupled to a two dimensional array of laser diodes. The other axis ('slow axis') is not collimated and allowed to diverge. The beam thus produced has a

very high intensity profile along the long axis and a Gaussian profile perpendicular to the line along the short axis (3, 8).

For developing high current required for high power laser, it is necessary to remove the resultant excess heat generated in the small laser bars. With proper cooling systems, the efficiencies for conversion from electrical to optical power are vastly improved to 40% to even above 50%. Earlier microchannel cooling technology based on silicon anisotropic etching is now replaced by heat sinks containing a network of small copper channels with cross section around 300 micron \times 300 micron. The water circulation at a rate of 0.5 litre per minute through copper microchannels located underneath the laser bars can generate laser power of up to 50 W or even higher without causing damage to laser bar (4). The stacked diode laser with several elements on top of each other can deliver up to 1 kW. The coolant flows through the heat sinks in a parallel configuration.

For further increase in power, 2 or even 3 can be combined by stripe mirrors to fill in the aperture. Single or combined stacks can be further directed onto the same optical path by polarization coupling, or wavelength coupling so as to deliver 5 to 6 kW laser power from a laser head of typically not larger than a shoe box (4, 8).

The Fig. 6.1.3 is a schematic diagram of a multiple diode lasers, which are stacked in such a fashion so as to emit a linear beam shape (8). Multiple applications are shown along the beam directions.

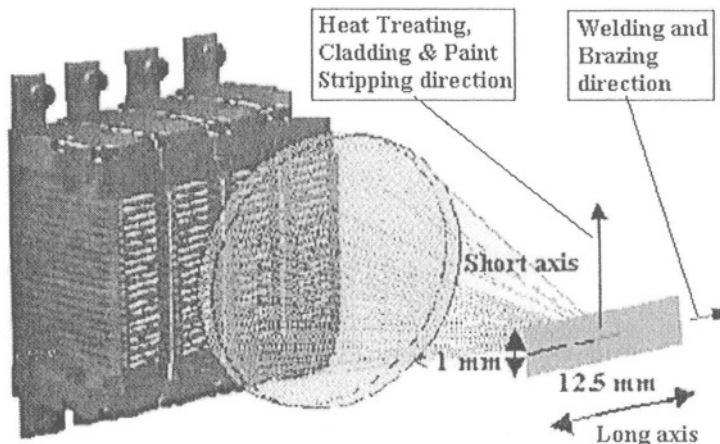


Fig.6.1.3. Multiple diodes laser system & the resulting linear beam shape for different applications (ref.8. Adopted from an article by Tim Nancy in Welding Journal, June, 2001, p28-30, with permission from American Welding Society)

Excimer Laser:

The inert gas halides lasing elements in excimer laser produce wavelengths in ultra violet spectrum ranging from 0.193 micron for ArF to 0.351 micron for XeF. In recent times efforts are being made to increase the repetition rates and peak powers so as to make use of the excimer laser in material processing. The average power in kilowatt range is being developed. With pulse time as low as a few nanoseconds it is possible to obtain high peak power in excimer laser. Laser- material coupling is better in the ultraviolet region, thus enabling excimer laser to process materials more efficiently.

6.1.4 Laser Focusing

The parallel laser beams are focused onto a small area of the workpiece in order to produce intense heat effect of the concentrated beam on the striking surface area. The power density generated on the workpiece surface by striking beam is directly proportional to beam power (P) and inversely on the square of the divergence (O) and the square of the focal length of the lens (F) being used, as follows:

$$\text{Power Density} \propto P / O^2 \cdot F^2$$

Laser beams are electromagnetic radiation in UV and infrared regions. Focusing of the laser beams therefore requires optical components, such as, polariser, grating, lenses (conical, spherical), mirror (flat, cylindrical), prism, beam splitter axicone lenses etc. Rotating and cylindrical mirrors are used for heat treating internal surfaces of cylinders.

Low power solid state laser systems employ normally transmissive style optics (lenses) to focus the beam on the workpiece. The zinc selenide (ZnSe) and potassium chloride (KCl) blanks are used as transmissive optics. High power gas lasers generally make use of reflective optics (mirrors) for beam focusing. Reflective mirrors are normally highly polished, water cooled metals (Cu) or coated (Au or Mo coating) metals surfaces. The schematic diagram of a focusing system for surface modification is shown in Fig. 6.1.4. Transmission of short wavelength laser beams, such as, diode and Nd-YAG up to 1 kW total flux can be carried out by fiber optics and higher power by lenses and mirrors. The long wavelength CO₂ is transmitted by mirrors. A single laser source can be used for a number of workstations with the help of beam shuttles.

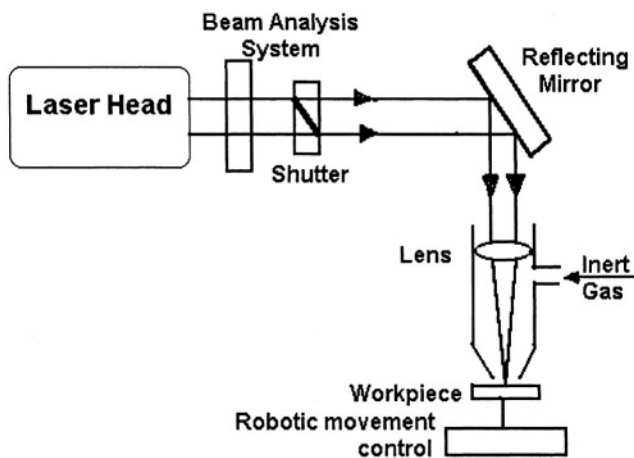


Fig.6.1.4 Laser beam focussing system for surface modification

6.1.5 Variables Affecting the Laser Assisted Processes

Radiation Characteristics : Following characteristics of the radiation affect beam properties.

Wavelength : Wavelength of excimer laser is the shortest (0.2-0.4 micron), followed by that due to diode (0.8 – 1.0 micron) and slightly higher value of YAG (1.06 micron) compared to very long wavelength of CO₂ (10.6 micron) (Table 6.1.1). Shorter wavelength beams produce higher energy density. It is possible to guide the short wave length lasers produced by Nd-YAG and diode by optical fibers and lenses and also mirrors. However the long wavelength CO₂ laser can be guided by only mirrors.

Absorptivity : The absorptivity of laser beam increases with the decrease in wavelength. Absorptivity at metal surfaces by CO₂ laser is mere 10-12% compared to that of 25-30% by Nd-YAG and 30% by diode laser.

Divergence: Power density varies inversely as square of beam divergence. Lower beam divergence can lead to large increase in energy density

Tab.6.1.1 Comparison of Laser Properties(1,2,3,4.)

Properties	Nd-YAG	CO2	Excimer	HP ¹ Diode#
Wavelength(micron)	1.06	10.6	0.19-0.4	0.8 — 1.0
Laser output Power (CW Watts)	50--1000	50-45,000	1000	several kW
Size of laser head	10 ⁻¹ m ³	1m ³		10 ⁻⁵ m ³
Av. Intensity(VW/cc)	10 ⁵ -10 ⁹	10 ⁶ - 10 ⁸		10 ³ -10 ⁵
Absorptivity at metal Surface(%)	25-30	10-12		30
Efficiency (%)	1 -3(20)*	5-15	<2.5	30-50
Price (\$/W)	200-600	150-300	300-900	100-300
Maintenance Periods	200hrs	1000hrs	---	M ² Free
Beam Guidance**	M/L/F	M		M/L/F
Pulsed	20J/pulse	<150J/pulse	<150Wav	
a. Pulse length	1-10ms	50ns-100μs	1-80ns	
b. Repetition rate	10 Hz	0.1-1000Hz	1- 500 Hz	
c. Beam diameter	5-10mm	10-50mm	2x4 -25x30mm	
d. Beam divergence	5-10mrad	1-3mrad	2-6mrad	

HP¹=High Power,*with appropriate wavelength diode laser pumping; **M=mirrors/
L=Lenses/F=Fibers; M² =Maintenance

Beam Diameter: Beam diameter varies directly with the wavelength. Smaller beam diameter improves power density.

Focal Length: The square of focal length is inversely proportional to the power density. Therefore a slight decrease in focal length can cause large increase in power density. However in practice there is a limit up to which the focal length can be reduced since longer focal length is preferred for many applications.

Interaction time: Total energy delivered to the workpiece is given by the product of the power in the beam (P) and the interaction time (t). The time of interaction in pulsed laser is the pulse duration. In CW mode the relative speed of motion between the laser beam and workpiece determines the interaction time.

CW or Pulse mode: TEM₀₀, with Gaussian distribution of power in the wave is ideal for welding, cutting and thicker hard cases. Higher order mixed modes are suitable for surface modification processes.

Commercially available lasers have outputs in the range of 10-100 J and repetition rates of 0.25 Hz at an average power of 25 kW (9).

New developments in these areas include followings:-

- square and linear beams helping in speed and uniformity
- pulsing at higher rates or oscillating beams to avoid the disadvantages of plasma formation.
- feedback control for power and beam quality.

Materials Characteristics (1):

Reflectance & Absorptivity of Materials:- For laser applications the materials can be classified as conductors (metals), insulators (ceramics) and semiconductors. In order to improve poor absorptivity of metals, it may be necessary to resort to one or other of the following techniques:

- i. Roughen the surface by mechanical means, such as, grit blasting or chemical etching
- ii. Apply laser beam absorbent coatings, such as carbon soots or ceramic (Al_2O_3) or Zn-phosphate etc
- iii. Use superimposed pulse and CW lasers.

Ceramics possess the capabilities of absorbing large quantity of beams at the surface.

In semiconductors with low impurity concentrations, laser radiation produces electron-hole pairs whose recombination generates heat and heat transfer to core takes place by conduction.

Thermal diffusivity: Metals being good conductor, the heat dissipation through the bulk is fast. This enables formation of amorphous metals on the surface by rapidly melting a thin layer of the surface by laser and fast cooling by the bulk on withdrawal of heat source. Good conductors like Cu posses higher diffusivity ($1.1^2 \text{ cm}^2 \text{ s}^{-1}$) than steel ($0.15 \text{ cm}^2 \text{ s}^{-1}$). Ceramics, being poor conductor, the heat gets concentrated at the point of application resulting in melting and evaporation. This phenomenon is used to milling & turning of hard ceramic materials like SIALON.

Heat of fusion & evaporation: The required heat input for fusing and vaporizing depends on the latent heat of transformation and heat required to reach the transformation temperature of the material. The intense heat of the focused laser beam leads to rapid fusion and evaporation from the surface.

6.2 Laser Assisted Surface Modification Processes

Advanced laser assisted surface modification processes include the followings:-

1. Lasershot Peening
2. Transformation Hardening
3. Surface melting (RSP)
4. Surface Alloying
5. Surface Ablation
6. Fusion of Thermal Spraying Coatings
7. Laser assisted Vapor Deposition Process
8. Weld Overlay
9. Laser Spraying
10. Direct Material Deposition by Laser

The thermal energy of laser beam is used to heat, melt or vaporize the materials. The basic phase transitions occurring in various processes include evaporation, melting or fusion, and changes in crystal form. The total heat required for phase transformation is the summation of heat required to raise the material to the transformation temperature and the latent heat for the transformation (chapter 1, section 1.4.1).

With the increasing energy input, the material transforms from solid to liquid to vapor phase (ref. 9) (Fig. 6.2.1). The energy input being a product of beam power density (W/min) and interaction time (min), higher power density is required for shorter interaction time. The laser beam can be focused to a very small spot size thus providing concentrated high intensity heat energy. The shorter interaction time of high intensity laser beam has been utilized to bring about changes in surface properties without affecting the bulk material properties. The mass effect of cool bulk material can result in the formation of amorphous metals by rapid solidification from liquid and vapor phases. High intensity beams are also used for peening the surface layer. Low surface temperature due to short interaction time in peening results in the development of deformation induced high compressive residual stress on the surface.

Intense heat source improves productivity of coating processes such as welding and vapor phase deposition by cutting down the interaction time.

1. Lasershot Peening (10)

Similar to peening by high velocity shots, the laser beam has been used to produce the similar effects on the surface. Laser peening system needs a power level approaching 1 KW, and an energy ~100 J per pulse, with a pulse duration of 10 ns. Recently developed Nd doped phosphate glass slabs and a master oscillator/power amplifier with wavefront correction by phase conjunction provide the required combinations of high energy, short pulse and high repetition rates for shotpeening.

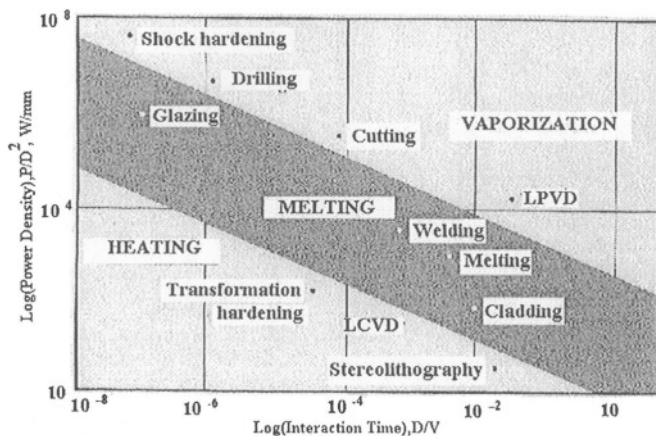


Fig.8.2.1 Laser Processing Zones Based on Power Density and Interaction Time
(Permitted to reproduce from book by William Steen on 'Laser Materials Processing' Ch8, page 173, fig 8.1, 1991, by Springer Verlag GmbH & Co.KG, Germany)

Laser peening technique involves the generation of tampered plasmas at the component's surface. High laser intensities of 200 Jcm^{-2} in a pulse duration of 30 ns can generate shock pressure of up to 10^5 atmospheres when absorbed on a metal surface.

The lasershot peening can induce residual compressive stress on the surface to an amount equivalent to that produced by conventional process i.e., approximately 60% of tensile strength of the material. The process is capable of producing compressive residual stress at a greater depth than that of conventional peening without any significant change in surface finish. Deep residual stress is important for safety of critical items such as compressor and turbine blades. An important additional benefit of lasershot peening is the prevention of crack growth.

2. Transformation Hardening

Solid state transformation from soft annealed or normalised to hard non-equilibrium structure by short thermal cycling can produce a hard shallow case. In rapid heating the transformation temperature of the steel shifts to a higher value than that at equilibrium due to temperature hysteresis. Also due to short treatment time at transformation temperature, there is hardly any opportunity for carbide to dissolve in the austenite formed at the expense of ferrite. In pure iron while heating the transformation of α to γ occurs by a diffusionless shear at about 920°C , and gives rise to acicular austenite (11). In the presence of carbide, austenite is nucleated at the carbide/matrix interfaces at temperatures between Ac_1 and Ac_3 . The new γ grains grow consuming the α and dissolving carbides until impingement occurs. After impingement the

austenite grain growth occurs (12). Even with rapid heating rates, the same mode of transformation persists (13). However during the short austenitising time allowed most of the carbides remain undissolved and the newly formed austenite grains can hardly grow. Finer austenite grains lead to formation of finer ferrites on cooling (14).

The low carbon lath martensites formed on rapid cooling possess lower hardness but higher strength and toughness than that of the corresponding high carbon twinned martensite. There is a significant improvement in strength and toughness by rapid heating and cooling cycles due to the formation of fine grains (15). With the cooling rate exceeding that of the critical cooling rate for the composition of the steel employed, the austenite shall transform into hard martensite on cooling through Ms (martensite start transformation temperature) to Mf (martensite finish transformation or 100%martensite formation temperature) temperature region.

The transformation to fine grained martensitic structure can be accomplished by rapidly scanning the surface regions with a low power density laser beam of the order of 1 KW cm^{-2} . Rapid cooling of the thin heated surface occurs due to mass effect of the bulk. With very fast cooling rates, the finer structure produced is both strong (martensitic) and tough (fine grained). The system enables formation of high strength, tough, wear resistant surfaces in irregular shapes or sections, difficult locations and selected sites, without any appreciable distortion. The process has found commercial applications in producing discrete hardened patterns on machined components of different shapes and sizes.

In rebuilding of rolling mill rolls, electroslag process is used in preference to submerged arc welding resulting in lesser quantities of harmful subsurface inclusion thus improving fatigue life (ref. Ch.12). The surface properties of electroslag weld overlay can be further improved through transformation hardening by laser heating (16) to produce hard wear resistant working surface.

3. Laser Melting

The possibility of rapid melting of surface layer by laser beam followed by fast cooling by the remaining cool mass of the bulk phase has led to development of unique properties in the rapidly solidified surface layer including the formation of metallic glass.

Rapid Solidification Process (RSP) (17)

The thin surface layer when melted by focusing a high intensity beam and the heat source is withdrawn, solidifies rapidly to form non-equilibrium structures due to mass effect of the bulk material. Depending on the cooling

rates rapid solidification from liquid state can result in the formation of following three types of metastable metals and alloys (17).

Supersaturated Solid Solutions: If the cooling rate is sufficiently high enough to prevent nucleation and growth of a second phase, solute atoms is retained in the parent lattice in excess of equilibrium concentration. For example, the solubility of Mg in aluminum is increased from 18.9 to 37 at% by liquid quenching and that of Al in magnesium from 11.6 to 23%. Liquid quenching can result in complete solubility in certain systems such as, Cu-Ag, Ga Sb-Ge and others.

Non-equilibrium Crystalline phases:- Rapid quenching from liquid, can lead to the formation of a crystalline phase which does not exist under equilibrium conditions. Examples of such occurrences include formation of simple cubic crystals by liquid quenching of Au-Te and Pb-Sb alloys.

Surface can be melted and cooled to produce non-equilibrium high temperature structure in the melted area. For example, cast iron cam surface is hardened by first preheating to 400°C and then melted uniformly to a depth of 1mm in less than 10s using a laser beam of width 14 mm and power 13.5 kW (18). On self quenching due to mass effect, hard wear resistant ledeburitic structure is formed. Ledeburite is the eutectic mixture of austenite & carbide (Fig. 1.4.3, Ch 1). A hard wear resistant case is thus formed by laser melting of a ductile cast iron cam surface.

Amorphous Phases:- The crystallization process can be suppressed by more rapid quenching from melt, vapor or solution provided certain kinetic and structural conditions are satisfied. The resulting unstable phases are characterized by the absence of long range order in the atomic arrangement beyond nearest neighbors, and are therefore in amorphous state. The suppression of nucleation by rapid quenching of the liquid until the alloy reaches glass transition temperature (T_g) has been used for glass or amorphous metal forming. The glass forming tendencies (GFT) of alloys has been defined in terms of their reduced glass transition temperature (T_{gr}), which is a ratio of the glass transition temperature (T_g) to the liquid temperature of the alloy (T_m). As the ratio increases the critical cooling rate to produce an amorphous structure decreases. The values of $T_{gr} > 0.45$ have been observed for present known metallic glasses (19, 20). The critical cooling rate (T_c) is an important processing parameter. There is almost a monatomic increase in $\log_n T_c$ with decreasing T_{gr} (20).

Heat flow model for the rapid solidification of surface layer (21) Recent availability of high power directed energy sources such as electron or laser beams has led to the development of rapid melting and solidification

techniques in which bulk (semi-infinite) substrate in intimate contact with the molten layer acts as a quenching medium. The exact cooling rates during solidification require estimates of heat transfer coefficients between the melt and substrate. In this case, the heat transfer coefficient between the two surfaces tends to infinity and the maximum achievable cooling rate is a function of the thickness of the molten surface region. Average cooling rate can increase by one or two orders of magnitude as the melt thickness (deposit thickness) is decreased by one order of magnitude. The required cooling rates depending on alloy systems can vary widely in the range of 10^4 – 10^{16} K per sec. Higher cooling rates are achieved by increasing the heat flux and reducing dwell time of the incident beam.

Most of the experiments with the directed energy source, such as the continuous CO₂ laser involve scanning the source over the surface of the substrate. A schematic diagram by Kou et.al. (22) on laser beam interaction geometry with the substrate during rapid surface melting and solidification is illustrated in Fig. 6.2.2. In Fig. 6.2.2, a semi-infinite substrate is subjected to a high intensity heat flux directed over a circular region on its bounding surface and moving with a constant velocity, U in the positive y-direction in a Cartesian coordinate system. The three main variables in the process are absorbed heat flux q, the radius of circular region a, and the velocity of the moving flux U. The three variables can be combined into two independent variables qa and Ua or U/q. In other words, the dimensionless temperature distribution in the liquid-metal pool and the solid substrate remain the same as long as the products qa and Ua or U/q are kept constant while the individual values of the three variables are varied. The melt depth, Z_{max} depends directly on q and inversely on U. In order to heat at a faster rate over a larger traverse area both q and U are kept high. The corresponding Z_{max} becomes low allowing rapid solidification.

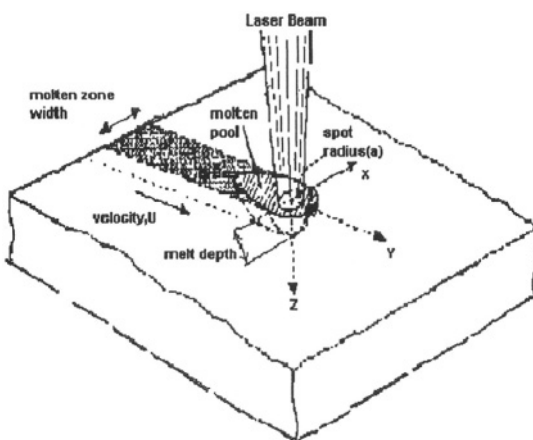


Fig.6.2.2 : Schematic illustration of laser beam-substrate interface geometry during rapid surface melting and solidification

(Ref.22. Reproduced by permission from ASM International, OH44073-0002)

Therefore in this process of rapid melting and solidification of surface using directed high energy beam, the high cooling rates are achieved only at the expense of high absorbed heat fluxes per unit time, reduced heat affected zone and melt depths.

Alloy systems forming metallic glass:

The list of major systems forming metallic glass by melt quench technique includes:-

- Pd-Si, Co-P, Fe-P-C, Ni-P-B systems with metals (late transition metals, such as, Fe, Co, Ni or noble metal like Pd) plus 15-25 at% metalloid, and
- M + M' system (M = early transition metals, like Sc, Ti, V and M' = late transition), such as, Ti-Ni, Nb-Ni, Ta-Ni systems where the second metal concentration varies over a range of 30-65 at% depending on the elements forming the systems.

Properties of amorphous metals:

Three important properties in the metallic glasses are high ultimate tensile strength, excellent corrosion resistance and ferromagnetic properties. Some of the amorphous alloys, such as, Pd-Si, Fe-Ni, Fe-B, Fe-B-C systems exhibit very high tensile strength combined with high compressive and bending ductility. The metallic glass composition $\text{Fe}_{80}\text{B}_{20}$ alloy has reported to have very high ultimate tensile strength of 370 kg/mm^2 (23). High microhardness values in the range of 750 to 850 VPH are found on the metallic glass surfaces in Fe-Cr, Fe-V, Fe-Ti system depending on the concentration of second element.

The metallic glass case has excellent corrosion resistance due to chemical homogeneity & absence of grain boundaries and crystalline defects and thus the absence of local electrochemical potential difference. The rate of pitting attack in $1 \text{ M H}_2\text{SO}_4 + 0.5 \text{ NaCl}$ at 300 mV for 18/8 stainless steel has been found to be two orders of magnitude higher than that of amorphous $\text{Fe}_{70}\text{Cr}_{10}\text{P}_{13}\text{C}_{07}$ (24).

The absence of directional anisotropy in an amorphous structure results in very high permeabilities and low energy losses. The combination of very high permeabilities and high hardness makes metallic glasses useful for tape recorder heads. Amorphous metals possessing high hardness, high elastic limit and superior corrosion resistance are used as razor blades.

Laser Assisted Commercial RSP Process:

Snow, et. al, (25) described a **LASERGLAZE™** process in which controlled laser surface melting followed by rapid self quenching resulted in forming amorphous structure in thin layer where a cooling rate of up to 10^6 C/s were obtained. The thin molten layer can be formed *in situ* on metal

surface by short high energy laser pulses. The fast cooling rate due to mass effect transforms the molten layer to metallic glass (26).

In rapid solidification process (RSP), the fast cooling rates of more than $\sim 10^4$ C/s ($\sim 10^6$ C/s) is normally employed. Bloembergen (27) has shown that it is possible to obtain a quench rate as high as 10^{13} to 10^{14} K/s from high energy laser pulses in the picosecond range through increased heat flux and reduced dwell time of the incident radiation. In order to produce high cooling rates required to form amorphous metal, the corresponding thickness of the molten surface region is proportionately reduced. In the laser fusing & rapid cooling process, therefore only a thin surface layer of amorphous glassy structure can be produced. In thicker section or at lower cooling rates, quenched layer transforms into solid solution with extended solubility, ultra-fine eutectic, and refined dendritic structure.

LASERGLAZE™ process has also been used for surface alloying (Fig. 6.2.3; ref 25). Surface alloying is achieved either by pre-placement of alloying materials before laser melting or by continuous feeding the alloying materials at the point of impingement of the laser beam. Alloying material can be used in the form of powder or wire. Pre-placement method has been used for hardfacing of selected wear prone surface areas. The continuous feed method can be used both for hardfacing and to produce rapidly solidified structure in the surface to near-net shapes.

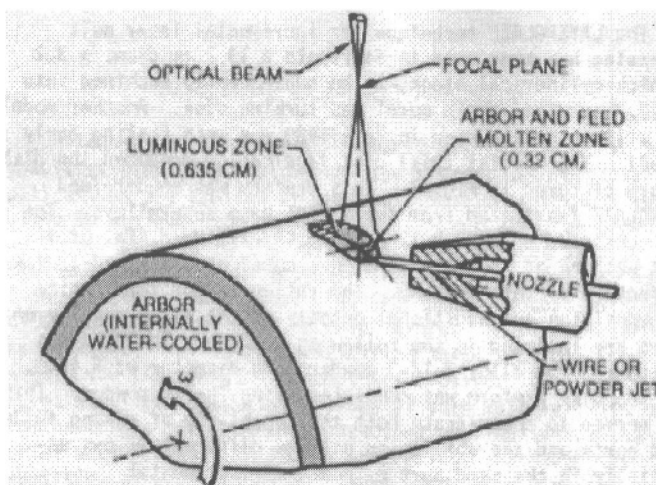


Fig. 6.2.3 : Schematic of Laserglaze process for thick coating deposition from powder or wire feed.(Ref.25 .Permitted to reproduce by ASM-International, OH44073-0002)

4. Laser Surface Alloying

Surface melting accompanied by additions of alloying elements, known as laser alloying allows the surface composition to be altered without altering the bulk material chemistry, thus producing wear and corrosion resistance surface (Table 6.2.1). In an AlSiCu, surface alloyed with 19.6 at% Ni, the intermetallic phases, such as Al_3Ni , Al_3Ni_2 , and AlNi are formed (28). The brittle intermetallics retain their hardness properties at elevated temperatures. By adding 25 at% Ni a surface hardness of 900-1000 HV can be obtained (28).

Tab 6.2.1: Some Examples of Laser Surface Alloying

Base Material	Additions	Surface Phase(s)	Surface Properties
Al-Alloys AlSi19Cu	19.5at%Ni	Al_3Ni , Al_3Ni_2 , AlNi	High HV at high T°C due Ni-aluminides
	25at%Ni	Brittle TCP	V. High HV 900-1000HV
	SiC	Metal-matrix + SiC	High HV
Ti-Alloys Ti-6Al-1V	N BN	TiN Boronized	1350 HV High HV
Low C-steel α or γ -SS High C Steel	Fe-Cr Fe-Cr,Fe-Ni HSS Fe-Mo Fe-Mo	α + Cr>11% γ (18 Cr8Ni) Mo-W-Cr-V-C +martensite Mo \geq 2% Mo-Carbide	Ferritic SS Austenitic SS High HV Resist pitting High HV

The addition of SiC to Al-alloy surface through laser surface alloying results in the formation of hard wear resistant Al-SiC composite coating (1). Laser alloying of copper with chromium increases significantly the microhardness and wear resistance of the surface (29).

The chromium (>11%) addition to low carbon steel leads to formation of ferritic stainless steel surface with excellent corrosion resistance. The laser alloying of the low carbon steel surface with nickel (Ni = 8) and chromium (Cr = 18), results in the formation of 18/8 austenitic steel surface. Addition of around 2% Mo or more to ferritic or austenitic stainless steels shall make them resistant to pitting type of corrosion. Since molybdenum is a ferrite former, high molybdenum containing austenitic stainless steels contain higher nickel.

The addition of Ni plus Mo to austenitic stainless steel surface are mostly carried out by depositing Ni + Mo by sputter deposition or plasma spraying and subsequently fusing the deposited layer by CO₂ laser. The Ni-Mo layer has also been deposited by electroplating and fused by pulsed Nd:YAG laser(30). By laser fusing the electroplated deposit, the depths of alloying in the range of 40.5 to 359.1 μ with concentrations in the range of 12.1 to 27.9 wt% Ni and 1.6 to 6.1 Mo were obtained. Fine microcracks associated with laser fusing were completely eliminated by maintaining the specimen at 983 \pm 10 K during the fusion treatment (30, 31).

The alloying addition of HSS to the low carbon steel shall result in a good cutting surface (31). The addition of molybdenum to high carbon steel and cast iron leads to vast improvement in abrasive wear properties.

The addition of refractory materials like tungsten carbide in steel, aluminium oxide in aluminum during laser surface melting leads to the formation of hard wear resistant composites. A thin layer of laser deposited titanium metal on zirconia acts as solid lubricant and thus improve frictional wear properties.

Laser Nitriding:

The surface melting of titanium in a nitrogen atmosphere leads to hard titanium nitride formation at the surface. The stream of reactive nitrogen gas along with an inert carrier gas like argon is allowed to strike the laser molten surface layer (28). The formation of hard wear resistant TiN phase leads to the development of excellent adhesive wear resistance properties at the surface of titanium metal components. The applications of laser nitrided titanium alloys in automotive and aerospace industries include tappets, gear box components, turbine blades, and landing gears.

Laser boronizing of Ti-6Al-4V with pre-placed BN has been reported to form hard wear resistant coating (1).

5. Laser Ablation

Pulsed laser ablation of high flux nitrogen on graphite surface leads to the formation of β -C₃N₄. It has not been possible to measure the hardness of β -C₃N₄ coating. However from binding energy considerations the hardness of carbon nitride is estimated to be comparable or greater than diamond (32). In an attempt to form β -C₃N₄, Zhang et.al. (33) used a beam of atomic nitrogen to react with the carbon plume formed by laser irradiation of graphite target. However they found the formation of C₂N instead of β -C₃N₄.

Laser ablation is normally used to strip paint coating. A 6 KW CW laser has been reported to have been used for stripping paint coating of aircraft (27). The coating was vaporized by 6 J pulses of 30 microseconds duration and

1 KHz frequency, without any damage to the substrate. Environmental friendly method eliminates use of toxic chemicals.

6. Laser Fusion of Thermal Sprayed Deposits

Metals and alloys deposited by thermal spraying are normally fused by oxyacetylene flame or induction heating. Ceramic and ceramic based composites with higher fusion temperatures compared to metals and alloys are difficult to melt in the oxy-fuel flame and these non-conductors cannot be fused by induction heating.

Laser fusion & glazing systems are extensively used for surface fusion and closure of open pores of the thermally sprayed ceramics and related composites respectively. The non-reflective ceramics at the surface have capabilities of absorbing large quantity of laser beams. Ceramics being poor conductor, the laser heat gets concentrated at the point of application resulting in melting of the sprayed surface layer. The closer of surface pores prevents ingress of corrosive chemicals & vapors and therefore improves the corrosion resistance of the surface.

Four types of ceramic oxides and their modified or combined forms are used commonly for thermal sprayings. They are aluminium oxide, titanium oxide, chromium oxide and zirconium oxide. The list of extensively used ceramic and composites include stabilized ZrO_2 , WC-Co, BN-Ni and Cr_3C_2 -NiCrBSi.

Adamski and McPhenson (34) reported the use of two continuous CO_2 lasers at 600 and 1200 watts to fuse thin layers of several plasma sprayed ceramic coating of Al_2O_3 , Y_2O_3 -stabilised ZrO_2 . The specimen mounted on a high speed turn table, and the laser beam scanned across the whole surface, using the following parameters:

- i. Pass overlap ~ 66%
- ii. Scan rate (mm/s) = 0.2 to 0.8 for 600 w, & 1.0-1.6mm/s, for 1200 w;
- iii. Rev/s = 2-8 for 600 w and 10-16 for 1200 w.

Bhatt and others (35) reported improvement in high temperature oxidation resistance by laser treatment of plasma-sprayed NiCrAlY coating on a superalloy substrate. They used a CO_2 laser of 200 – 300 w and a power density of 10^6 w/cm^2 and optical spot size of 125 micron.

Rapid solidification of the laser fused metallic thermal spray deposit layer leads to the formation wear and corrosion resistant alloy with metallic glass structure at the surface. Thin layer of amorphous alloy has superior corrosion resistance properties compared to normal crystalline alloy coating of the same composition.

7. Laser assisted vapour deposition

For physical vapor phase deposition (PVD), laser ablated vapor phase of the target is allowed to deposit on prepared substrate surface. In CVD process, a reactive atmosphere is used for the ablated vapor to react thus leading to the deposition of reaction product on the substrate. Excimer lasers have played a significant role in vapor deposition processes, particularly in multi-layered laser forming operations due to their ability to ablate whole molecules without destroying stoichiometry. In pulsed laser deposition process the formation of particulates can cause a serious problem (36).

Laser CVD diamond coating

Laser assisted chemical vapour deposition (CVD) process has been used to deposit hard wear resistant diamond film (37). Laser is used to thermally activate the carbon deposition process through cracking of hydrocarbon in a mixture of hydrocarbon and hydrogen (Fig. 6.2.4). The following two reactions proceed simultaneously:-

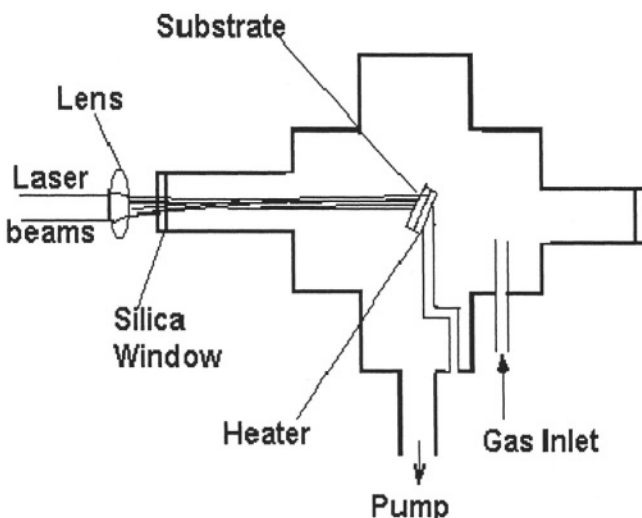


Fig.6.2.4.Laser-CVD for C-deposition process

- *decomposition reaction* and the chemical vapor deposition on substrate surface by pyrolytic hydrocarbon decomposition.
- *etching reaction* by the atomic hydrogen to prevent the formation of all other solid compounds except diamond.

Diamond coatings on metals are produced by using a combination of wavelengths, from excimer to CO_2 lasers. Diamond like coatings (DLC) are produced from various targets, including polybutadiene (38). A layer of

aluminum nitride coat on the substrate can avoid nondiamond phase formation during CVD deposition of diamond (39). AlN-diamond composite films are deposited on bearing steels, low carbon steel and other materials by using pulsed laser deposition of AlN followed by hot filament CVD for diamond.

8. Laser Welding (40, 41, 42)

Laser beam welding (LBW) is a fusion welding process, where a concentrated beam of coherent, monochromatic light beam is focused on area to be welded. Laser welding has normally been carried out with solid state Nd-YAG laser or CO₂ gas laser, or more recently with diode laser depending on the energy capabilities of pumping systems. The laser can be operated in the continuous wave or pulsed mode. Shielding gas is provided to prevent oxidation of molten weld pool. Filler metals are used in the overlay process.

A continuous wave CO₂ laser with power output up to 6.0 kW was used for laser welding using 1.2 mm diameter wire consumable. The laser beam was focused using a parabolic mirror to a focal length of 150 mm. The beam power delivered to workpiece was calibrated using a black body absorption device. The laser beam was focused to depth of 1.00 mm below the workpiece surface. The continuous laser welding system, including welding head, wire feed arrangement, shielding gas feeding arrangement etc., is shown in Fig. 6.2.5. The matching consumables were used to join pipes continuously.

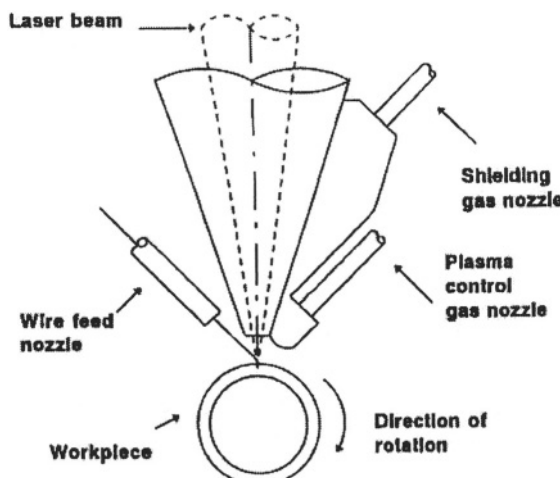


Fig.6.2.5,Laser welding nozzle and wire feed arrangement

Ref.40, Z.Sun & T.Moisto, Proc. 3rd Int. Conf. on Trends in Welding Sci. & Tech., 1992, permitted to reproduce by ASM-International, Materials Park, OH44073-0002.

A comparison has been made amongst laser, plasma and GTA (TIG) welding processes for joining AISI347 (Cb stabilised 18 Cr-9 Ni) austenitic steel to 13 CrMo44 (1 Cr-0.4 Mo) ferritic low alloy steel, with or without Inconel 625 (Ni-22Cr-9Mo-3.7Cb) as filler metal (40). The welding parameters are given in the Table 6.2.2. Laser welding is found to produce lower heat-affected zone (HAZ) width and less distortion in comparison to other two processes (Table 6.2.3). The axial shrinkage in the tube to tube joints made by laser welding is about one-half and one-quarter of those made by plasma and GTAW respectively.

Tab.6.2.2 Welding Parameters for Laser, Plasma, & GTA Welding(40)

Laser beam welding LA LF	Plasma arc welding				TIG welding, TF		
	PA	PF	First	Second			
Power (kW)	3.5	3.5	Current (A)	145	145	Current (A)	120
Air gap	0	0.2	Air gap (mm)	0	0	Voltage (V)	9.0
Wire feed rate (mm/min)	0	112	Wire feed rate (mm/min)	0	162	Wire feed rate (mm/min)	160
Heat input (kJ/mm)	0.1	0.1	Heat input (kJ/mm)	0.5	0.5	Heat input (kJ/mm)	0.54
Speed (mm/min)	125	125	Speed (mm/min)	320	320	Speed (mm/min)	90
Plasma control gas (He) (l/min)	0	0	Plasma control gas (Ar+H ₂)	2.2	2.2	-	-
Shielding gas (He) (l/min)	32	32	Shielding gas	15	15	Shielding gas	8
							8

Note: LA & PA are Autogenous laser and plasma welding respectively; LF, PF, & TF are laser, plasma, & gas-tungsten welding respectively.

Tab.6.2.3. Comparison of Laser, Plasma & GTA welding(40)

PROPERTIES	LA	LF	PA	PF	TF
HAZ Width (mm)	1.0	0.9	4.3	4.6	5.7
Weld Hardness (HV0.3)	453	179	309	155	166
Axial shrinkage (mm)	1.8	2.2	3.9	4.2	0.86
Welding time ratio	1	1	3	3	20
Material required (ratio, if L=1)	1	1	6	6	10

Despite heavy investment, the factors favorable for laser welding include high speed welding (1/3rd time needed for plasma welding and 20 times faster than GTAW welding), reduced material usage (1/6th of plasma and 1/10th of GTA welding), reduced manpower and elimination of grooving preparation

Applications of Laser Weld Overlaying:- The wear resistant consumable materials meant for cladding are in the form of wire, powder, or foil. The normally used consumables on steel substrates include iron, nickel and cobalt based hardfacing alloys as well as some of the metal matrix composites containing carbides. The alloys are delivered in the weld zone using a CNC delivery system. The cladding operation is carried out by laser fusing the consumable onto the substrate surface. Due to low dilution, the wear and corrosion resistant properties of the deposited material can be obtained in a single layer of laser welded deposit.

Naval Applications : A good number of applications has recently been developed for US Navy for laser cladding and welding (42). Iron, nickel and cobalt base alloys are used. Procedures are or being qualified for the weld cladding of diesel cooling pump shafts, steam valve seats, aircraft carrier catapult components and aluminum torpedo shell sections. The laser process has been selected due to low dilution and heat input resulting in “near pure” deposition of material with minimum thermal or dimensional impact on the structure.

Engine & Process Control Valves : The current practice for hardfacing the seat area of the tappet valves is to use GTAW or PTAW process. Due to low dilution plasma transferred arc welding (PTAW) is more widely accepted practice compared to GTAW (43). The dilution in laser welding can be controlled at a lower level than PTAW and thus can be more gainfully used for this and other hardfacing applications (43, 44). The alloys normally used for valve seat applications include Stellite 6 (Co-27Cr-4W-1C), or a lower cobalt version Stellite 32 or F (Co-25 Cr-11.8W-22Ni-1.75C) or a nickel base alloy of nominal composition Ni-16.7Cr-3.5Si-0.45C-17Fe. A Ni-base self fluxing alloy (Ni-0.65C-3.15B -4.4Si-14Cr-4Fe) has also been recommended for nuclear applications.

Laser cladding of cobalt base material for valves

The laser weld overlay of Stellite6 powder was carried out on HY80 steel surface to make 0.04" (1.016 mm) thick deposit (45). A 1.8 kW YAG-laser with beam spot size of 0.02"(0.508 mm) was used to fuse the powder fed at 12g/m (0.2 g/s), while the linear (XY) motion of the component was controlled at 18 ipm (7.62 mm/s). Argon was used as shielding gas and the job was preheated to 240°C. The surface hardness of the weld overlay was 47

HRC. The HAZ was 0.03" (0.762 mm) thick with a hardness of 23 HRC. The same cladding operation could be carried out on AISI 4130 steel with similar results by using 2.5 kW CO₂ laser. The YAG laser is thus proved to be more economic in terms of power consumption (45). Because of low dilution the use of PTA process is mandatory for stellitizing nuclear valves (46). The laser cladding is likely to be an ideal process for such applications.

Laser cladding with iron base materials for valves

The approximate composition of one of the iron base substitutes for Stellite6 is 1.3 C, 3.0 Si, 25 Cr, 0.4 W, 1.8 Mo, 8 Ni, 11 Mn, 0.5 V and remainder Fe. The cobalt free composition is particularly suited for nuclear applications. A 10 kW CO₂ laser was used to deposit a similar composition iron base alloy on mild steel substrate by delivering a mechanical mixture of the elemental powders forming the alloy from a powder feeder. Argon and helium were used as carrier gas for the powder delivered at the laser-substrate interaction point. The rapid heating and cooling cycles in laser processing led to fine microstructures. A combination of fine grains and precipitates of MC, M₇C₃ and M₆C types of carbides in the microstructure resulted in coating with optimum combination of microhardness and wear resistance properties (47). With a preheating temperature of 484°C with specific energy input for the process was 9,447 kJ/cm² (47).

Laser cladding of valves with nickel base materials

The laser cladding of Ni-0.65C-3.15B-4.4Si-14Cr-4Fe was carried out with a 2.5 kW laser (44) on a medium carbon steel surface. The coating material was injected in powder form at a constant rate and shrouded by inert gas at the molten pool formed by striking laser beam. The powder was fed at a rate of 60g/min. The travel speed of the sample under the laser beam was 60cm/min. The substrate was in the form of a rotating disc.

The microstructure of laser melted deposit consists of very fine discrete precipitates of carbides (e.g. M₇C₃), borides (e.g. CrB) and silicides (Ni₅Si₂) uniformly distributed in the nickel matrix. Also the amount of eutectic present in the structure is large. This avoids the formation of shrinkage cavities.

Due to uniform distribution of fine hard particles in the matrix, the hardness of the laser clad deposit may reach 1000 HV. The average hardness of laser melted alloy is found to be nearly double than that of the same alloy deposited by plasma melting.

Hydroturbine Components:-

The base material for the hydroturbine is cast ferritic stainless steel conforming to CA6NM. A good number of critical components in a hydroturbine are coated with different grades of stellites. Normal arc welding of CA6NM with Stellite 6 results in the weld getting enriched by around 30%

iron and the base by 0.3% C. Both the high carbon containing CA6NM substrate and high iron containing Stellite are highly susceptible to cracking while cooling from welding temperature. Low dilution in PTA welding makes it an acceptable process for overlaying Stellite 6 onto CA6NM. For the same alloy combination, laser welding shall result in less dilution, narrower HAZ, higher deposit hardness than PTAW. Laser welding is therefore an ideal process for deposition of Stellite 6 on CA6NM. The PTA deposit of Stellite6 has been found to reduce substantially the erosive wear of hydroturbine runner blades in high silt containing river water (48). The laser weld cladding can possibly improve the life of the blades further than that achievable with PTA welding.

Steam Turbine Blades (45)

The standard practice of a reputed turbine manufacturer is laser cladding with a hardfacing alloy for protecting the leading edges of steam turbine blades from water (steam) erosion. The hardfacing materials normally used to minimize erosive wear are Stellite 6 and Stellite 21. The cladding on blades (nearly 4ft long) is carried with powder deposition of the cladding alloy ahead of the laser beam, while the blade being manipulated in a 3-axes of motion.

Gas turbine Blades (45)

The wear prone areas in the gas turbine blade include, leading edges, notch regions and blade tips. The nickel alloy blades are coated with laser weld deposit of wear resistant cobalt base alloy (Stellite) powders. Notch region was reported to have been coated in a four axis workstation where the beam of a 6kW laser fuses the powder alloy in 8 to 10 seconds. For turbine blade tips, a single pass from a 5 kW laser was found sufficient to fuse the deposited alloy powder. With automation, as many as 20 blades per hour can be processed. The cladding of shroud-abutment faces of a 60 blade wheel of a aeroengine has been carried out by a 5kW laser, with 3-axis motion from the 5-axis workstation and a special powder-feed system to deliver the powder to the required spots. The very low dilution is responsible for high hardness even at 0.06" depths in laser cladding compared to that of GTAW deposit. The hardness of laser clad surface is 53 HRC, compared to that of 40 HRC in GTAW deposit surface. By minimizing heat input, the clad thickness was precisely controlled thus drastically reducing subsequent finishing operations.

Refurbishing Aircraft Engine Components (45)

The vision generated programming has been used to refurbish aircraft engine turbine and compressor blades, knife edge seals and certain rotary seals by laser cladding with unique powder feeding system. The powder and laser beam are allowed to travel coaxially through a single nozzle permitting the nozzle to follow complex paths delivering the powder and fusing the

same. The path programme, laser power, powder-feed rates and machine speed are determined from a photograph of the workpiece taken by the vision system. The actual working system includes a main conveyor for loading/unloading, smaller conveyors for alternately positioning blades beneath the vision camera and the 1.7 kW laser head, a dual camera-vision computer, dual powder feeder and the NC. The linear traverse for each axis is 24" (0.6096 m) at a speed of 200 ipm (84.66 mm/s). Positioning accuracy is $\pm 0.005"$ (0.127 mm), with $\pm 0.003"$ (0.0762 mm) repeatability. The maximum conveyor load is limited to 100 lb (45.45 kg).

ID Weld Overlay (45)

The purpose of cladding the internal diameter of pipes with wear resistant materials is to minimize wear due to materials transported through the pipes. The internal diameter across the length of a 4ft (1.2182 m) long and 4" (101.6 mm) internal diameter stainless steel pipe has been laser clad with chromium carbide. The laser beam was projected inside one end of the pipe and focused from a flat suspended mirror. The powder was delivered beneath the beam impingement line and the pipe was simultaneously rotated and translated. In order to salvage a costly undersize, thin walled, 2 ft diameter stainless steel gate valve, the laser cladding of one face was carried out with the valve material.

Boiler Tubes

The fossil fuel fired boiler tubes are subjected to corrosive wear due to high sulfur in the fuel. The corrosive wear of the tubes can be minimized by coating the outside surface with corrosion resistant alloys, such as, Fe-Cr-Al-C and Ni-Cr. The boiler tubes are normally coated with these alloys by using a suitable thermal spray process, such as, plasma, arc or flame spray. However the bond strength of the mechanically bonded thermally sprayed powder deposit is limited to a maximum of 10,000 psi and the deposit is porous. The presence of large number of pores reduces the thermal conductivity of the deposited layer, thus reducing heat transfer to the boiler water. Also the ingress of corrosive combustion products in fluid form may cause early detachment of the coating. With laser fusion cladding, a dense welded coating of corrosion resistant material forms on the boiler tube surface resulting in higher heat transfer efficiency and longer life compared to thermal sprayed deposits of same materials.

In a fossil fuel fired utility power plants, boiler panels of approximately 1ft (0.3048 m) to 4 ft (1.2192 m) wide and 20 to 30 ft (6.096 to 9.144) long has been laser clad (45). The panels consists of a series of 1.25 to 2.50" diameter steel tubes connected to each other at their mid-points along their length by flat webs of steel about $\frac{1}{2}"$ (12.7 mm) wide. The laser cladding of one entire side of the panels is carried out with corrosion resistant Fe-Cr-Al-C

or Ni-Cr alloys. The clad thickness ranges from 0.030" (0.762 mm) to 0.060" (1.524 mm). One single pass at 12-15 kW and 10 to 15 ipm (4.23 to 6.35 mm/s) is normally sufficient for the flats, but three to four passes are usually required at each tube.

Laser Tempering of Laser Weld (49)

One of the major disadvantages in laser welding is the faster rate of cooling leading to the formation of non equilibrium structure of low toughness. In order to reduce brittleness and thus to improve toughness of the weld it is necessary to temper the weld overlay. Laser tempering of laser weld immediately after the welding has advantages over the conventional furnace tempering process in terms of cost reduction and time saving. Laser welding and tempering of AISI 4130 steel were carried out by 4 kW fast transverse flow continuous CO₂ laser with an optical lens of 175 mm in focal length. Following welding the laser weld was tempered by multipass scanning of defocused beam. The defocused beam with lower energy density is used for scanning the surface pass by pass so that no surface melting occurs during the tempering process. Tempering effect through full thickness is achieved by successive defocused beam scanning and by adjusting the relevant process parameters. The toughness of the weld bead was almost fully recovered by laser tempering.

Plasma Arc Augmented Laser Welding (PALW)

In this process, the constricted arc of a PTA system is allowed to strike at the point where laser beam impinges the surface. The high heat developed due to simultaneous heating by laser plus arc causes rapid fusion of the surface material. Advantages claimed for the process includes increased welding speed and decreased cooling rates compared to laser welding. PTA system can be retrofitted to most beam delivery system to enhance the heat development capability at a fraction of the cost involved for an equivalent capacity laser (50).

Induction assisted Laser Welding (51)

Induction preheating allows weld deposition to be made on difficult to weld materials like HSS as substrate or Stellite deposits on AISI410 alloys, without any crack formation. The thin laser deposit cools at a very fast rate and in the case of welds can lead to brittle non-equilibrium structure, which along with the stress developed during cooling can cause crack formation in the deposit. The induction preheating of substrate is carried out to a predetermined temperature so as to form the equilibrium structure with lower residual stress. The induction post-weld heat treatment (PWHT) reduces the thermal and transformation stresses developed during cooling of the weld metal.

Fused Ceramic Surfacing by Laser Welding (52)

A thin layer of titanium diboride deposit on metallic substrate after fusing by laser beam was allowed to cool fast. The high cooling rate leads to the formation of a metastable phase containing the weld deposit diluted with substrate metallic material. Since the Nd-YAG laser beams can be transported through fibre optics, hence it is possible to fuse deposit at remote locations. The process consists of fusing by laser beam a thin (~150 μm) spray deposited precursor (Ti_2B powder mixed with water soluble organic binder) layer on a low carbon steel surface. A 2 KW Nd-YAG continuous wave laser, operating at 1.5 KW at a transverse speed of 200 cm/min and configured to provide a beam length in TEM_{01} mode was used to fuse the Ti_2B layer (51). A thin layer of substrate also gets melted making the total coating thickness as 200 μm . An uniform, continuous, adherent & crack-free titanium-diboride coating has excellent wear and hot corrosion resistance properties. The hardness of the coating ranges from 700 to 1300 VPN. Applications as wear resistant coating include grinding bodies, bearings, sandblasting equipment, and rock drilling equipments. Excellent corrosion resistance against molten aluminum and cryolite (fused mixed fluorides) is made use as coatings for the inert cathodes in Hall-Heroult cells for aluminium production. Also used as coating for pipes carrying molten metal or thermocouples for measurement of molten alloy temperature.

9. Laser Spraying (53)

The use of laser beam for thermal spraying is a comparatively new development. A 5 kW continuous wave CO_2 laser beam has used to melt titanium wire and the resultant gas stream containing molten metal particles was sprayed on steel substrate (52). In nitrogen atmosphere the sprayed deposit consisted of titanium nitride.

Process (52)

A 5 kW CO_2 continuous wave laser beam is focused by ZnSe lens onto a titanium wire at the exit point from the nozzle of the spray gun (Fig. 6.2.6). The spray gun consists of a central outlet for wire feeding and two coaxial ring nozzles for the flow of spray gases. High pressure (around 500 kPa) argon and nitrogen emerging from the coaxial nozzles are used to atomise the molten wire and to spray the molten droplets onto the prepared substrate surface. In order to maintain steady flow rate of fine molten particles onto the substrate, the spray parameters such as laser power, wire feed rate type of gas and gas pressure are to be controlled. The normal procedure involves finding of minimum laser power required to form a steady flow of atomized molten particles at a particular wire feed rate and for a given a spray gas pressure. For example, laser power of minimum 3 kW is used for melting and spraying

titanium at a wire feed rate of 33 mm/s, and a gas pressure of 500 kPa. A five layer gradient coating of Ti-TiN was formed by using different volume proportions of the argon and nitrogen in the gas mixtures for each layer. Argon was used for the formation of titanium base layer followed by nitrogen additions of 25% (volume), 50% and 75% in the gas mixture for the formation of successive layers with increasing nitride contents. Pure nitrogen is used to form fully titanium nitride layer in the top coat. The spray velocity can be increased by additional supply of high pressure inert gas or by combining with plasma. The five layer gradient deposit of titanium nitride has been found to have excellent thermal shock resistance and recommended for use as thermal barrier coating (51).

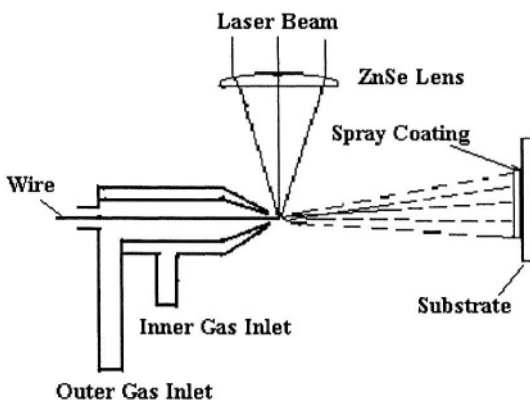


Fig.6.2.6.Laser Spraying (Schematic)

A 1 kW CO₂ laser spray unit combined with a microfeeder has been used for thermal spraying of ceramics (54). The technique is useful for thin coating of materials with deposit chemistry same as that of sprayed powder materials. In contrast to vacuum deposition and sputtering methods, the crystal structure obtained in the coating is the same as that of the original powder. Laser can also be used to clean and prepare the surface before plasma spraying. It is possible to remove the top contaminated layer of the substrate by laser ablation, thus providing a clean surface for thermal spray deposition process. The process is superior to degreasing and grit blasting, where the retention of residual grit particles on the surface can result in poor adhesion of coating to substrate. The laser ablation cleaning is particularly useful in vacuum plasma spraying, where both surface preparation and spraying operation can be carried out in the vacuum chamber. It has been possible to prepare ideal substrate surface with surgical cleanliness by laser ablation in vacuum plasma spraying.

The low pressure plasma spraying of titanium and subsequent laser fusion in nitrogen atmosphere lead to the formation of TiN-Ti coating of hardness

over 1200 HV (55). A 40 kW plasma spray unit was used with nitrogen as plasma gas. For laser fusion a 1 kW CO₂ laser was used. The nitrogen pressure inside the chamber was at 1.3×10^4 Pa.

10. Direct Metal Deposition (DMD) by Laser (56)

In DMD, the metal or metal matrix composite powder is transported through inert carrier gas onto the substrate surface, where a focused laser beam melts the powder material. Hardfacing operation is carried out in an inert atmosphere enclosure. A high intensity 2.4 kW CO₂ laser is used. The operation is carried out in a CNC workstation according to the geometry given in the CAD file. The process is capable of depositing a layer of 0.005" (0.127 mm) with tolerances in the order of 0.0002" (0.005 mm). The cooling rate during solidification of the thin deposits is extremely high and is in the order of 10^3 to 10^6 °C per sec, which results in very fine grains to glassy structure. The list of powder materials includes hardfacing alloys like tool steels, stainless steels, Ni-base alloys (Inconel), Co-base alloys (Stellite), pure metal like copper, hard metal matrix composites like tungsten carbides and titanium diboride. *Laser forming* is a process of building up designed structure by multi-layered laser deposits onto a skeleton of the required design. For example, structural components of military aircrafts using titanium alloys (Ti-Al-V, Ti-Al-Sn-Zr-Mo, Ti-V-Fe-Al, etc) can be built up by using a high power 14 kW CO₂ laser producing layered deposits through CNC system following a tool path generated directly from a 3D solid model.

Laser based direct fabrication (57):

It is possible to fabricate directly the shapes without the use of molds with laser based processes. There are number of terms to describe this technological innovation, such as, rapid manufacturing (RM), flexible fabrication (FF), and solid free-form fabrication (SFF). Similar to laser surfacing, parts are initially formed by depositing a small volume of materials and then building the part with successive layers. Appropriate selection of the composition gradients provides opportunity to adjust properties as a function of position creating functionally graded materials. Different positions in the same component can be developed to possess different wear resistant properties as required for a specific application.

Summary

After plasma most widely used beam for surface engineering is laser. Two important drawbacks of laser are high capital cost and high running cost due to low power conversion efficiency (1-3% for solid laser and 5-15% for carbon-di-oxide laser). However with the developments of high power direct

diode laser (HPDDL) with 40-50% efficiency the use of laser in surface engineering is expected to grow further. The list of laser assisted surface engineering processes include lasershot peening, transformation hardening, surface alloying, surface ablation, fusion of thermally sprayed coating, vapor deposition, weld overlaying, thermal spraying and direct material deposition and fabrication processes. Some unique application areas in laser assisted surface engineering include the production of :

- Lasershot peened surfaces in critical components, such as compressors and turbine blades with vastly improved fatigue properties
- Ultra hard surface with $\beta\text{-C}_3\text{N}_4$ (hardness more than diamond) by pulsed laser ablation
- Metallic glass surface by laser glazing. RSP can also result in the formation of non-equilibrium phases with unique compositions and properties
- Alloyed or composite surfaces with excellent wear and corrosion resistance by surface alloying

Another important development is the use of laser deposition technique for rapid manufacturing (RM), or flexible fabrication (FF) process.

References

1. A.K. Nath, Seminar on 'Applications of Lasers in Engineering Industries', Mumbai, February 10, 2001, ASM Int. (India Chapter) & Indian Institute of Metals, p8-15.
2. Welding Handbook, vol 3, Welding Processes, Chapter 22, Laser Beam Welding, p 713-738, American Welding Society, 8th edition, 1991.
3. C.M. Cook, J.M. Haake, M.S. Zediker, M.D. Crydermann, High Power Direct Diode Laser Application and Advanced Processes, a paper presented at International Congress on Applied Lasers and Electron Optics, ICALEO 2000, Dearborn, MI, USA
4. Friedrich Bachmann, High power kW-range diode lasers for direct material processing, XIII Int. Symp. on Gas Flow & Chemical Lasers-High Power Laser Conf., p1-9, Florence, Italy, Sept 18-22, 2000
5. G.L. Goswami, 'Applications of Lasers in Engineering Industries, Mumbai, February 10, 2001, ASM Int. (India Chapter) & Indian Institute of Metals, p32-55
6. A.K. Nath & others, "Development of a high power transverse CO₂ laser for material processing", Proc. ECLAT, '96, Sept 16-18, 1996, Stuttgart, Germany
7. D.R. Hall and H.J. Baker, 'Area scaling boosts CO₂ laser performance', Laser Focus World, 25, 77, 1989

8. Tim Nacey, Diode Laser Offer Welding Advantages, WJ, June, 2001, p28-30.
9. Laser Material Processing by W. M. Stern, Springer-Verlag, New York 1991
10. Graham Hammersley, Materials World, May, 99, 281-2.
11. K.J. Albutt and S. Garber, JISI, 1966, 204, 1217
12. J. Nutting, JISI, Centenary Issue, June, 1969, p872-893
13. H.W. Paxton, Sym. on transformation and Hardenability in Steels, 3; 1967, Michigan, Climax molybdenum Co
14. W.E. Duckworth, Met. Rev, Metals and Materials, 1968, 13(128), 145
15. P. Chakraborty, R. Chattopadhyay. & S.S. Bhatnagar, Grain Refinement by Short Austenitising Treatment, Trans. I.I.M, Dec., 1970
16. Pavel Blaskovic, Manufacture and rebuilding of rolling mill rolls by surfacing and laser processing, Symp. on Joining Materials for 2000 AD, Tiruchirapalli, India, 12-14 Dec., 1991, Indian Institute of Welding
17. C.C. Tsuei, Electrical & Magnetic Properties of Rapidly Quenched Metals, p260-275, 'Rapid Solidification Technology Source Book, Ed. R.L. Ashbrook, ASM, 1983.
18. John C Ion, Metals & Materials, Sept, 1992, 485
19. H.A. Davies, Physics and Chemistry of Glasses, vol 17
20. Donald E. Polk & Bill C. Giessen, Overview of Principles and Applications, p213-247, 'Rapid Solidification Technology Source Book, Ed. R.L. Ashbrook, ASM, 1983
21. R. Mehrabian, *ibid*, p168-209.
22. S. Kou, S.C. Hsu and R. Mehrabian, Met. Trans., 1981, 12B, 33
23. L.A. Davies, R. Ray, C.P. Chou and R.C. O'Handley, Scripta Met., vol 10, 1976, p541.
24. K. Hashimoto and T. Masumoto, Material Science Engineering, vol 23, 1976, p285.
25. D.B. Snow, E.M. Breinan and B.H. Kear, Rapid Solidification Processing of Superalloys using High Power Laser, 'Rapid Solidification Technology, Source Book', Ed. R.L. Ashbrook ASM, 1983, p138-152
26. D Turnbull, Rapid Solidification Technology; Source Book, *ibid*, p30
27. N. Bloembergen, Laser-Solid Interaction and Laser Processing; Ed. S. D. Ferris and others, A.I.P. Conf. Proc, vol 50, pp1-10, 1979
28. B.L. Mordike, Lasers in Engineering, 1995, vol4, pp 187-200
29. I. Manna, J. Dutta Mazumdar, U.K. Chatterjee, and A.K. Nath "Laser Surface Engineering of copper with chromium for enhanced wear resistance", Scripta Materialia, 35, 3, 405, 1996
30. Dilip Kumar, A.K. Grover, A.L. Pappachan, G.L. Goswami, G.B. Kale and M.K. Totlani, Lasers in Engineering, 1998, vol 7, pp103-117
31. G.L. Goswami, D. Kumar and Others, Control of defects during laser surface alloying, Surface Engineering, 1999, vol. 15, No. 1, p.65-70.

32. M. Leiber, *Adv. Mat. & Process.*, 1993, (10), 16
33. Z.J. Zhang et.al., *Mater. Sci. & Eng.*, A209, 1996, 5
34. A. Adamski and R. McPhenson, *Int. Thermal Spraying Conf.* 1986, Montreal, Canada, p555
35. H. Bhatt, R.A. Zatoski, Herman, R.J. Coyle, *Int. Thermal Spraying Conf.* 1983, p21
36. D.B. Chrisey and G.K. Hubler (ed.), *Pulsed Laser Deposition of Thin Films*, Wiley, New York, 1994
37. K Kitahama & others, *Appl Phys Letter*, vol 49, no 11 (1986) p537
38. M. Ouyang, *Met. al., Mat. Sci.& Engg.*, 1996, B39, 228
39. V.P Godbole, et.al., *Mat. Sci. & Engg.*, 1996, B39, 153
40. Z. Sun & T. Moisio, *Proc. 3rd Int. Conf. on Trends in Welding Science & Technology*, Gatlingburg, USA, ASM Int./AWS, 1-5 June, 1992, p433-438.
41. Paul Denney, *WJ*, March, 2001, p47-50
42. N. Blundell, *MW*, 1998, 9, p537-538
43. R. Chattopadhyay & P.A. Kammer, *3rd Int. Conf. on Trends in Welding Science & Technology*, ASM/AWS, 1-5 June, 1992, Gatlinburg, Tennessee, USA
44. M. Durrand-Charre, M.C. Sahour and A.B. Vannes, Metallurgical structure of a hard facing laser deposit, *RM & HM*, Sept., 1986, p192-195
45. *Laser Technology, Sp. Report 814 on "CO₂ & YAG Lasers tackle tough tasks"* by John A. Vaccari, *American Machinist*, March, 1992, p37-48
46. P. Harris and B.L. Smith, *Metal Construction*, November, 1983, p661-666.
47. S.K. Chaudhuri, J. Choi and J. Mazumder, *Symp. on Joining of Materials for 2000 AD*, Tiruchirapalli, India, 12-14 Dec, 1991, Indian Institute of Welding
48. R. Chattopadhyay, *High Silt Wear of Hydroturbine Runners*, *Int. Conf. on Wear of Materials*, 1993, Part B, ASME, p1040-1044
49. J.N. Aoh & others, *Int. Trends in Welding Science & Technology*, Ed. S.A. David & J.M. Vitek, *Proc of Conf. held at Gatlingburg, TN*, June 1-5, 1992, ASM-Int, p649-653
50. Anatoly Khersonsky & Houston Lee, *AM&P*, April, 2000, p39-41
51. Arvind Agarwal & Narendra B. Dahotre, *AM&P*, April, 2000, p43-45
52. A Utsumi, J. Matsuda, M. Yoneda, M. Katsumura and T. Araki: *Int. Thermal Spraying Conf. Kobe*, 1995, 325-330.
53. Tim Heston, *WJ*, July, 2000, p98 & 105
54. F. Uchiyama, et.al., *ITSC'92*, May 28-June 5, 1992, Orlando, Florida, ASM international, p105-110
55. A Ohmori & others, *Spraying of TiN by a combined laser and low pressure plasma spray system*, *ITSC'92*, May 28-June 5, 1992, Orlando, Florida, ASM international, p201-206

56. Eric J. Whitney, John E. Smugeresky & David M. Keicher, Laser-Based Direct Fabrication, ASM Handbook, vol 7, Powder Metals, Technologies & Applications, 1998, p433-435.
57. David Abbot, Materials World, June 1999, p328-330.

Chapter 7

SOLAR ENERGY FOR SURFACE MODIFICATIONS

7.0 Introduction

The direct solar beam can be concentrated and focused onto the surface to be heated. The small spot size of focused beam can generate very high intensity heat capable of fusing even high melting point refractory materials in seconds. The heat generation by solar beam and its applications in various surface engineering processes are described in this chapter.

7.1 Solar Heating

The use of direct solar beams for thermal treatment is probably the most economic energy efficient process for surface modification. Similar to other high energy beams, such as laser, electron, the solar rays can be focused as concentrated high heat intensity beams into a small spot size onto the work-piece surface. Solar radiation, used for heating covers a wide spectrum of wavelength including near ultraviolet (305 nm) through visible (700 nm) to near infra-red (~2500 nm). Many materials absorb visible radiation better than infra red. The solar processing utilizes direct sunlight, which is reflected once or twice resulting in losses of 5 to 10 % per reflection, giving an energy utilization efficiency as high as 90%-95%. In converting heat obtained from burning fossil fuel to electricity and again electrical energy into light, the process efficiency can be as low as 9% for high pressure arc lamp and 4% for CO₂ laser. Therefore the most economic source of energy with high utilization factor is the solar energy. For surface modification of materials, a properly designed solar heating furnace is used.

7.1.1 Solar Furnace (1)

Solar furnace is designed to collect solar beams throughout the day and to focus the concentrated beam onto the surface to be heat treated. A vacuum chamber with provision for maintaining controlled atmosphere is used for heat treatment of materials prone to oxidation & scaling. In a solar furnace, radiation from the sun is collected & concentrated through primary (a series of hexagonal mirrors) and secondary (attenuator with vertically opposed two plate design) concentrators and focused on the area to be heated. The

schematic block diagram of the components making a solar furnace is indicated in Fig. 7.1.1.

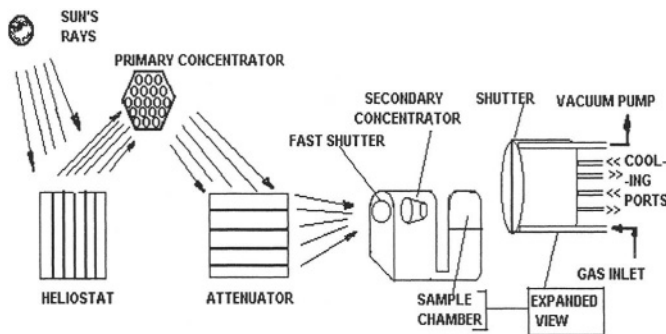


FIG 7.1.1.DIRECT SOLAR BEAM HEATING SYSTEM(SCHEMATIC)

Various components of a solar furnace and their functions are as follows:-

- i. Heliostat:- This equipment is mirror driven by clockwork to reflect sunlight in fixed direction. With changing direction of sun during the 12 hour cycle, mirror rotates to reflect maximum light at any point of time.
- ii. Primary Concentrator: A series of spherical mirrors packed in a hexagonal shape to face the beams. Mirrors are ground to required radius of curvature and have aluminum coating. In the solar furnace at SERI (ref 1), the beam can be focused on a 100mm diameter circle containing 94% energy. The flux distribution is of Gaussian shape with a peak flux of 2.5 MW/m^2
- iii. Attenuator: This piece of equipment consists of vertically opposite plates for trimming the light emerging from top and bottom concentrator facets.
- iv. Shutter:- The guillotine type shutter is air-actuated and can be operated manually or through computer.
- v. Secondary Concentrator:- The lens configuration is so chosen as to provide the flux range suitable for the application.
- vi. Sample Chamber:- The chamber with a quartz window for allowing incoming beam to be focused onto the sample surface. There is provision for evacuation and filling up with required gas mixture for maintaining controlled atmosphere. The back side of the sample can be cooled by air or water circulation.

With a flexible system optics, it is possible to change the beam pattern for accommodating irregular shape parts and the focal length to reduce damage to optical elements by sputtering or outgassing of target materials. Also

configuration of secondary concentrator can be altered to provide flux range appropriate to the application. Solar radiation can be concentrated to produce peak power of about 16 MW/m^2 with a single imaging concentrator and to 100 MW/m^2 by non-imaging concentrators in media with refraction indices more than unity.

Solar furnaces can be used for heating the materials at very fast rates. The time to reach the melting point of material when exposed to an absorbed solar flux of 20 MW/m^2 is listed in Table 7.1.1. The listed materials include metals and ceramics.

Tab.7.1.1. Heating Rates In Solar Furnace for Selected Materials (ref.1)

Materials	Melting Temp °C (T _m)	Time to reach T _m (s)
Metals		
Al	660	0.42
Cu	1083	3.21
Ni	1453	1.03
Steel	1535	0.79
Ceramic Oxides		
Silica	1720	0.014
Titania	1870	0.044
Alumina	2050	1.00
Zirconia	2900	0.089
Carbides		
Titanium carbide	3200	9.14
Colombium carbide	3500	0.86
Zirconium carbide	3540	0.112
Silicon Carbide	3830	0.56
Nitrides		
Silicon nitride	1900	0.059
Aluminium nitride	2200	1.320
Boron nitride	3000	0.545
Titanium nitride	3200	0.611

Ref.1. James T. Stanley, Clark L. Fields & Ronald Pitts,
Adv. Matl. & Processes, 12 1990, p16-21, permitted to
reproduce by ASM-International, Materials Park, OH, USA

Metals :

The time required to reach the melting temperatures of some selected metals are indicated in Table 7.1.1. The heat input required to reach the melting temperature is calculated by multiplying specific heat (C) of the metal by atomic weight (m) and the temperature difference between room temperature and the melting point (ΔT). The calculated heat input ($C.m.\Delta T$) requirements for the metals are indicated in Table 7.1.2. Tungsten requires highest heat, followed by iron and the least heat is required for aluminium (Table 7.1.2). Accordingly, time required for reaching the melting point with a fixed solar heat source increases from aluminium (0.42s) to iron (0.79s) and maximum time is required for tungsten (9.8s). The ratios of the time periods required by different metals to reach the respective melting temperatures against that of aluminium are indicated as "Time Ratio" column in Table 7.1.1. Actual and calculated (ideal) values for tungsten showed large difference. Due to high conductivity and density the actual time required for reaching the melting point of tungsten is much higher than the calculated value (Table 7.1.2).

Tab 7.1.2 Calculated & actual time to reach the melting point(1,2,3)

Materials	Specific heat Cp Cal/g°C	Atomic weight g/mol	Melting Point °C	Heat Input to M.pt Cal/mol	Time Ratio		Thermal Conductivity (w/mK)x10 ²
					Ideal	Actual	
Metals							
Al	0.215	27.0	660	3831	1	1	2.344
Fe	0.1047	56.0	1535	8995	2.34	1.88	0.745
W	0.0321	184	3407	20123	5.26	23.33	1.657
Ceramics							
Molar specific heat							
Limiting value (Cal/mol°C)							
Si ₃ N ₄	6.0		1900	11,400	0.92	0.059	0.09
Al ₂ O ₃	6.0		2050	12,300	1	1	0.26
SiC	6.0		3830	22,980	1.87	2.0	1.00

Ceramic-

Refractory oxides with low thermal conductivity and superior heat absorption capabilities require less time than metal for reaching similar temperatures. For example, to reach fusion temperature of silica (1720°C) and zirconia (2900°C) require 0.014s and 0.089 s respectively (Table 7.1.1).

However some of the oxides due to their comparatively lower heat absorption and retention properties may require slightly longer time. Similar trends are observed for carbides and nitrides (Table 7.1.2). The heat required to reach the melting temperature was calculated by multiplying the limiting constant value of molar specific heat ($3 R = 6 \text{ cal/mol}^\circ\text{C}$) by the melting temperature. In this case also, Si_3N_4 with low thermal conductivity requires much less time to reach the melting point than that calculated (Table 7.1.2). Many materials absorb visible radiation better than infra red hence for solar heating no special coating is required.

7.2 Solar Hardening

The selective case hardening of AISI4340 steel to a depth of 1-2mm has been achieved by using a solar flux of 2 MW/m^2 and scan speed of 0.5 mm/sec. The hardness scan across the transformation hardened zone shows a gradual change in hardness from case to soft core (Fig. 7.2.1). The heat affected zone can extend by another 4.0 - 5.0 mm beyond the hardened case.

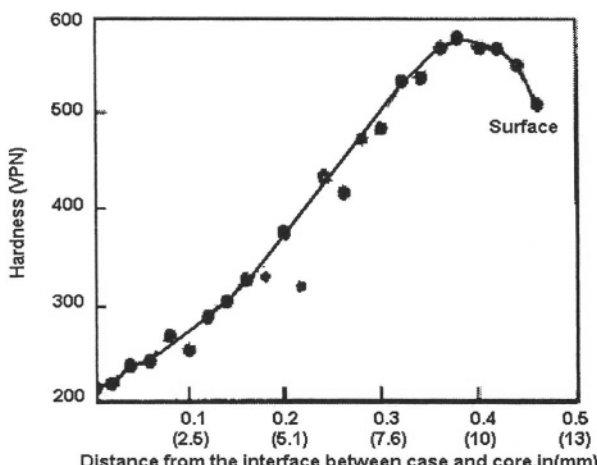


Fig.7.2.1 Microhardness depth profile of AISI 4340 steel surface hardened by solar flux

(Adopted from ref.1, Adv. Materials & Processes, 12, 1990, p17, ASM-International, Materials Park, OH 44073-0002)

7.3 Sunbeam Fusing (1)

Fusion of materials deposited on the surface can be carried out at extremely fast rates. Post coating fusion by solar energy can be carried out on following deposits:-

Thermal spray coatings:

The thermally sprayed metals, alloys and metal matrix composites are porous in nature. The coated layer is mechanically bonded to substrate with a low adhesive bond strength. For applications requiring dense deposits with good metallurgical bonding, the total thickness of the deposit is fused.

The thermally sprayed coating of Ni-Cr-B on AISI 4340 steel (Fig. 7.2.2A), AISI 316 stainless steel on AISI1040 steel (Fig. 7.2.2B), and WC-6Co on AISI1040 steel are successfully fused by solar beam to form dense fused overlay, metallurgically bonded to substrate. The lamellar structure of thermal spray deposits are replaced by dendritic structures of the fused coatings. The fusion of thermal spray porous deposit has been fused with sunbeam without any crack formation as normally observed in laser fusion process.

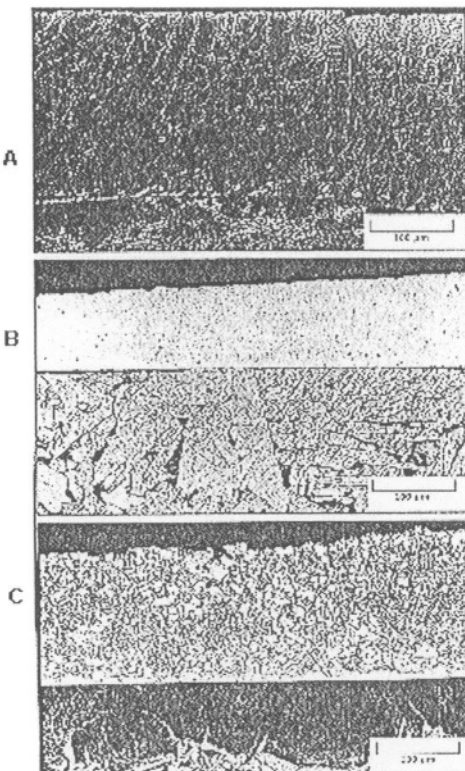


Fig 7.2.2 : Microstructures of fused coatings formed by solar beam melting of preapplied powder coatings. A. Self fluxing Ni-Cr-B alloy on AISI 4340; B. Stainless steel AISI 316 on AISI 1040; C. WC-6Co on AISI 1040 (Ref 1, Adv. Materials & Processes, 12, 1990, p18, ASM-International, Materials Park, OH44073-0002)

The ingress of hot corrosive fluids through open pores at the surface of thermally sprayed coating may lead to spalling of the coated layer. For ceramic deposits, mostly the fusion of top layer is required to close the open pores.

Thin layered deposits :

Due to rapid heating by solar beam, the substrate remains cool. As soon as the heat source is removed the material cools fast due to mass effect. If the cooling rate exceeds 10^4 $^{\circ}\text{C/sec}$ then the amorphous metal (glassy structure) is formed.

Layered PVD deposit:

Layered deposits of aluminum and nickel by PVD process, when fused forms intermetallic compound, nickel aluminide by exothermic reaction. Nickel aluminide possesses excellent creep resistance properties.

Fusion of coating applied by processes, such as, slip casting can be carried out by solar beam.

References:

1. James T. Stanley, Clark L. Fields & J. Ronald Pitts, *Adv. Materials. & Processes*, 12, 1990, p16-21. ASM-International, Materials Park, OH
2. *Metal Handbook*, Desk edition, Second edition, 1998, ASM International; Thermal conductivities of metals, page 68.
3. *ASM Engineered Materials Reference Handbook*, 1989, ASM International, Ceramics, p 151-195.

This page intentionally left blank

Chapter 8

COMBUSTION PROCESSES FOR SURFACE MODIFICATION

8.0 Introduction

The combustion processes are used in surface engineering to generate inert or endothermic gas (for bright annealing), reactive gas (for carburizing), & reducing gas (for DLC), flame (thermal spraying or fusing), or high velocity flame (HVOF/HVAF/HVIF). Higher limits of combustion are achieved by recently developed pulse combustion technique. The various surface engineering processes based on combustion technology and the industrial applications are to be discussed in this chapter.

8.1 Heat & Flame Generated by Oxy-Fuel Combustion Processes

The combustion is a process of burning a substance by combining with oxygen. Easily combustible products are fuels in the form of solid (e.g., coal), liquid (e.g., kerosene) and gas (e.g., natural gas). Almost complete combustion is possible with gas, followed by atomised liquid fuel. For heat treatment of metals, the preferred fuel is normally gas followed by liquid fuel. The combustion of fuel leads to the production of heat, flame and combustion products.

Amongst the combustion products, hot flame and gas are used for various surface engineering processes. The gas produced by combustion of fuel can be made neutral, reducing and carburizing depending on the fuel/oxygen ratio and the combustion conditions. Reactive gases are used to enrich the substrate surface with the elements such as carbon and nitrogen. The hot flame formed by combustion of fuel, such as acetylene and oxygen at the tip of torch nozzle has an outer high temperature oxidizing zone, followed by lower temperature reducing feather and an inner cone. The outer hot zone is used for fusion of thermal spray deposit and welding.

Hot flame with higher velocity is used for thermal spraying. Extremely high velocity flames, i.e., the flame velocities exceeding than that of the sound, are produced by combustion of fuel gas or oil (kerosene) in a similar manner to that employed in jet engines in a specially designed torch. The high velocity oxy-fuel flame (HVOF) is used to produce high integrity coating on aeroengine components by thermal spraying. Heat developed by combustion of some common fuel gases and the corresponding flame temperatures are listed in Table 8.0.1 (ref. 1).

Table 8.0.1: Heat and flame temperature developed by combustion of common fuel gas

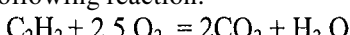
Fuel gas	O ₂ / Fuel Ratio	Flame temperature ⁽¹⁾ °C	Heat of combustion ⁽²⁾ MJ/m ³
Acetylene	2.5	3087	55
Propane	5.0	2585	104
Natural Gas ³	2.0	2538	37
MPS ⁴	4.0	2927	91
Propylene	4.5	2900	89
Hydrogen	0.5	2660	12

(Legend:- 1= neutral flame temperature, 2=total value, 3=mainly methane,

4=methylacetylene propadiene + saturated hydrocarbon).

Ref 1, Welding Hand Book, AWS, Vol1, Ch11, p352. Reproduced by permission from American Welding Society.

Ideal ratio of oxygen : acetylene(fuel) is 2.5:1 for complete combustion is derived from the following reaction:-



However excess oxygen or air than that indicated in the ideal ratio, is required for complete combustion.

Flame temperature & velocity depend on the degree of combustion for a given amount of fuel and the flame is termed as oxidizing, neutral and reducing depending on the proportions of CO₂, O₂ and CO.

Combustion intensity or “specific flame output” of a flame is a product of heat (J/m³) of combustion and flame velocity (m/s) for a specific mixture of gas and oxygen. Highest combustion intensity is found in acetylene compared to methane (natural gas), propane and hydrogen. Acetylene is therefore a preferred gas for gas welding and also for thermal spray processes.

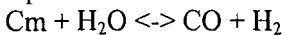
Pulse combustion-a new development (2) :- Recently developed pulse combustion technology consists of combining acoustic waves within a combustion chamber to create a resonating system under which combustion is allowed to occur. At resonating frequency of 20-1000 Hz, acoustic pressure waves cause gas & materials in the combustion chamber to oscillate rapidly resulting in efficient burning of fuel, hotter & cleaner flames, improved mass & heat transfer and also reduces emissions of hydrocarbon, CO, & NO_x. The pulse combustion system reduces the energy consumption by half than that for conventional processes. The key to the success of such a system has been attributed to the design of the heating chamber which allows stable resonating

combustion. Flame produced in pulse combustion technique is not continuous but discrete flamelets that are ignited on the hot remaining gases of previous flamelets. The short flame pulses result in significantly higher heat production than the conventional burner system accompanied by lesser quantity of reducing gas in the exhaust. Pulse combustion systems can lead to a NO_x emission level as low as 2-3 ng per Joule of useful heat, compared to current legal levels (in Australia) of 40 ng per Joule. The value is much lower than the latest legal emission limits for California at 9ng per Joule (2)

8.1.1 Surface Modification Processes by Furnace Atmosphere Control

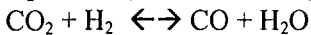
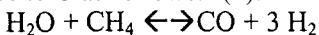
Furnace atmosphere control is required to retain surface chemistry or to alter the composition during elevated temperature treatments. Some of the examples are as follows:-

1. Bright annealing of steel strips: For continuous bright annealing of CRCA (cold rolled close annealed) steel strips, an endothermic atmosphere containing nitrogen plus 4% CO (3) is used. CRCA strips with bright surface finish are used extensively for car bodies, refrigerators and washing machines. Recent developments in high integrity annealing of steel strips (CRCA), include use of 100% hydrogen as furnace atmosphere. The use of high thermal conductivity & strong reducing agent like hydrogen instead of CO plus N_2 has considerably reduced the thermal cycling time with consequent improvement in productivity by 26% and cost reduction of 11% (3)
2. Removal of carbon from surface layer: Addition of H_2O vapor to reducing atmosphere removes carbon from the surface layer:-

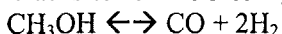


The process is used to produce soft magnetic materials.

3. Addition of carbon to surface layer (gas carburizing):- The carbon is deposited on steel surface due to breakdown of methane(hydrocarbon) by reaction with H_2O and subsequent catalytic decomposition of CO at the surface to C as follows:- (4):-



Carburizing atmosphere requires CO >15%, which is produced by partial combustion of hydrocarbon in an endothermic generator. However, following fuel price hike in seventies, synthetic atmospheres based on methanol + N_2 , ethanol + $\text{H}_2\text{O} + \text{N}_2$ or isopropanol + $\text{H}_2\text{O} + \text{N}_2$ have gained popularity as alternative to endothermic generators (5). Methanol at 750°C cracks to form CO & H_2 in the 1:2 ratio, as follows:



The carbon transfer rate in endothermic and synthetic substitutes remains at $1.2\text{-}1.3 \times 10^5$. Hydrogen intake in a component carburized by carrier gas produced in a outside generator using a mixture of methanol-nitrogen-propane was less than 5 ppm compared to more than 20 ppm hydrogen in the component after carburizing directly in the furnace with the same gas mixture (6). The use of 2-stage carburizing process employing hydrocarbon (first stage) and carbon monoxide (second stage) results in faster mass transfer across solid/gas interface and avoid superficial oxidation normally found in conventional gas carburizing (7).

4. Addition of nitrogen to surface: Ammonia added to the furnace atmosphere decomposes to form atomic nitrogen as follows:-

$$\text{NH}_3 \leftrightarrow 2\text{N} + 3\text{H}_2$$

Atomic nitrogen diffuses in the substrate surface to form nitrided case. Reverse reaction can be used to remove nitrogen from surface. Reverse reaction can be utilised to remove nitrogen from surface.

8.2 Normal to Moderate Capacity Flame Spray/Fusion Systems

Spray systems

Low velocity oxyacetylene torches are used for spraying self-fluxing low fusion temperature Ni alloys, bronzes, Zn and Al. Higher thermal capacity torches are required for high melting point materials, such as, ceramics and composite powders and for spraying on large components, such as, larger diameter shafts, drying rolls for paper and carbide plants. However, the flame temperature and velocity of moderately high capacity torches (~60,000 Btu per hour) are not high enough to form as-sprayed dense coating with good bonding to substrate, esp, for ceramic and composites.

Spray Fuse System

In this process thermally sprayed deposits are fused by a specially designed oxyacetylene torch. Simultaneous spray and fusion processes can also be carried by the same torch, if the job is of small size. For large jobs such as conveyor rolls for steel plants, spraying and fusing are carried out at two different stages. The compositions, hardness values and applications of selected self-fluxing alloys are indicated in Table 8.1.1. In these alloys, the fluxing agents, such as B & Si are added to reduce fusion temperatures in the range of 950°C –1050°C, to increase deposit hardness up to 62HRC, and to form a thin slag coverage. Chromium is added to improve corrosion and oxidation resistance and to increase hardness through carbide & boride formation.

The spray fusion process is essentially a brazing operation in which the base metal does not get molten. The coating has been applied to carbon, alloy & stainless steels, cast iron, Ni-alloys and Co-alloys. Hardenable grade steels

need slow cooling to prevent formation of martensite and cracks. Vacuum brazing of sprayed surface deposit is carried out for difficult to braze weld parent metals like stainless steels, nickel base super alloys like Inconel 718 containing highly oxidizable Al & Ti. The basic advantages of the process include almost nil dilution, good metallurgical bond of the coating with wide range of hardness, corrosion and wear resistant properties

Tab.8.1.1. Compositions of Selected Ni- and Co-base Self Fluxing Alloys

Alloys	Chemical composition, wt%								Hardness	Applications
	Cr	Si	B	Fe	C	Ni	Co	Other		
Ni 1	0-5.0	3.0-3.5	1.0-1.5	1.0-1.5	0-0.2	bal	25.0-30.0	Glass mold
Ni 2	7.0-10.0	3.0-4.0	1.5-2.2	3.0-4.0	0.2-0.4	bal	36.0-42.0	LMM rolls
Ni 3	10.0-12.0	3.0-4.0	1.8-2.5	3.5-4.5	0.4-0.6	bal	46.0-52.0	Plunger
Ni 4	13.0-17.0	4.0-5.0	3.0-3.5	4.0-4.5	0.5-0.8	bal	56.0-62.0	Wear ring
C 5	5.0-6.0	1.5-2.0	0.9-1.2	1.8-2.3	0.2-0.3	bal	...	WC 50.0	60.0-65.0	Tricone bit
Co 6	24.0	2.5	1.5	1.5	1.0	12.0	bal	...	44.0-48.0	Cane cutting
Co 12	2.4	2.5	1.5	1.5	1.0	12.0	bal	...	50.0-55.0	Knives
bal, balance. LMM, light merchant mill										

The process can be automated by simply motorizing the torch traverse. For cylindrical objects, like rolls are rotated symmetrically while, the torch making deposits moves across at a controlled speed to build and fuse the required coating thickness. High thermal capacity torches are required for thick coating on large components.

Applications include automated processes such as conveyor rolls (8), compressor plungers (9) and glass molds, and others like, off-shore control valve (galling and H₂S corrosion in sour wells), ID fan blades (particle erosion) (10), wheel-burns (impact adhesion wear) on rail road rails (11), wear rings (galling) in pumps etc.

Self Fluxing Tungsten Carbide Composite-

A mechanical mixture of fine tungsten particles (<75 micron) and a self fluxing nickel base powder alloy can produce spray fused coatings (0.25 to 3.0 mm) with excellent resistance to abrasive and erosive wear. The deposit microstructure consists of uniformly distributed unmolten angular carbides in a nickel alloy base matrix (Fig.8.1.1). Major application areas include rock drill bits, ID fan blades, and diamond tool matrix.

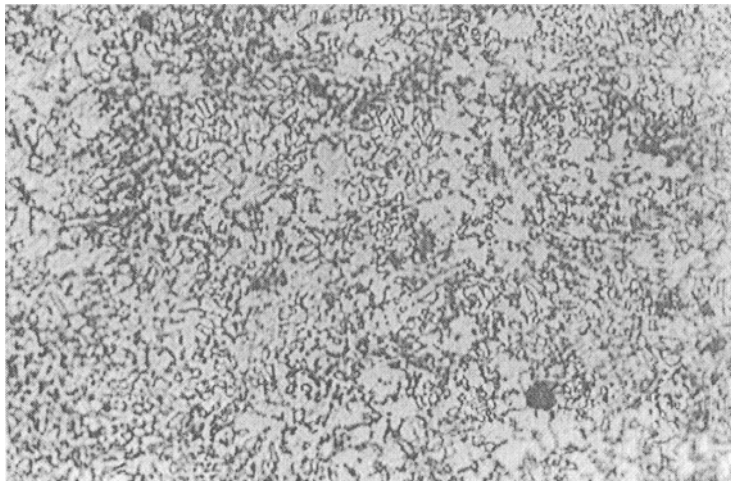


Fig.8.1.1. Microstructure of flame fused composite(C5) alloy

Some of the major application details are as follows:-

Light Merchant Mill Rolls (8)

The conveyor rolls of light merchant mills are required to carry hot steel strips. The hollow mild steel rolls are coated with a Ni-Cr-B-Si-C self-fluxing alloy of hardness 40-45 HRC. An automated 2-stage process of spraying followed by fusing of deposit has been used. Burners are placed across the length of the roll to maintain high surface temperature. High surface temperature reduces dwell time of the fusion torch and thus improves productivity.

Compressor Plunger (9)

An automated spray fusion process has been used to deposit Ni-3 alloy to a coating thickness of ~1.5 mm, in comparison to maximum deposit thickness of 0.25 mm for hard chrome plating in previous practice. The process is non-polluting compared to highly polluting chromium plating. For compressor plunger, the fused surface needs finishing by grinding to 0.45 micron.

Roll cavity forming on spray fuse overlay

In this process, required thickness of alloy Ni-3 is deposited in the oversize die cavity of a roll mounted in a lathe. A steel die of the required cavity shape is mounted on the tool post of the lathe. The die is pressed onto the semisolid layer of spray fuse deposit of the rotating roll resulting in the formation of coated die cavity of required dimensions. The spray fuse coating leads to substantial improvement in the performance of forming rolls in steel plants.

Torch fusion of tungsten carbide composite gas welding rod

Large angular grains (>4000 micron or 0.16 micro-inch) of tungsten carbide are made into a rod by using copper-base brazing alloys. The deposition of the rod material by oxyacetylene torch fusion process leads to melting of copper base matrix, leaving undissolved massive angular carbides brazed onto the cutting edges of components such as, rock drills, oil drills, sand mixer blades and oil well fishing tools. In 3-body abrasion wear tests, the respective wear factors of deposits containing WC + W₂C (2112 HV) and WC (1278 HV) are around 2.5 and 1.1 times compared to that of Cr-Mo cast iron as 1. For superior performance the presence of W₂C is required. (12).

8.2.1 High Velocity Flame Spraying:

Detonation Gun (D-Gun) Systems

Detonation gun was the first high velocity oxy-flame torch developed in Russia & by Union Carbide in USA. In the detonation gun process, measured quantities of oxygen, nitrogen and powder are detonated by a timed spark inside a water cooled barrel (1 m length × 25 mm diameter). Due to the special geometry of the vessel, the initial subsonic flame formed by the spark detonation develops into a high temperature supersonic detonation wave and emerges through the nozzle at a supersonic speed along with the suspended powder particles (Fig. 8.2.0). Thus the detonation creates a high speed gas stream at 4500°C which instantly heats the particles and propels them at velocities up to 800 ms⁻¹ (2640 ms⁻¹) onto the prepared substrate. The whole process is repeated 4-8 times per second with intermediate purging by nitrogen. The D-Gun process is therefore like an intermittent high velocity oxy-fuel (HVOF) system, with limited chamber pressure and the flame velocity in comparison to HVOF. The high velocity of the impacted molten or semi molten particles leads to higher density, bond strength and hardness of coatings consisting of wear resistant refractory material like WC-Co, CrC-NiCr, Al₂O₃, TiO₂, Cr₂O₃ and ZrO₂.

HVOF/HVAF Spraying:

High velocity oxy-fuel flame (HVOF) spraying process consists of spraying powder particles of coating material through high velocity (velocity >1 mach), high temperature jet formed by combustion in a specially designed gun. During the passage through the high temperature flame the powder particles become molten or semimolten before striking the substrate surface. The process using air for combustion is known as HVAF.

In the conventional oxy-acetylene flame spray torch, the flame is ignited at the exit point of the combustible gas mixture, i.e., at the tip of the nozzle. In such a torch design, it is not possible to accelerate the flame formed outside

the torch. In the high velocity system (Fig. 8.2.1) oxygen (or air) and fuel are ignited under pressures in an enclosed volume or chamber and resulting high temperature and pressure developed in the enclosed space allow the combustion product to escape thorough an orifice at extremely high velocity.

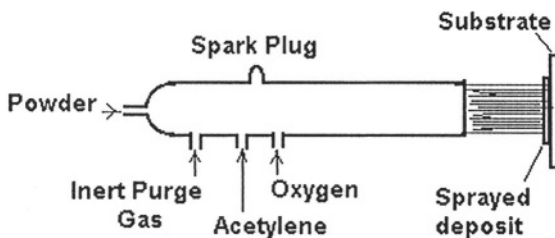


Fig 8.2.0.Schematic Diagram of D-Gun Spraying

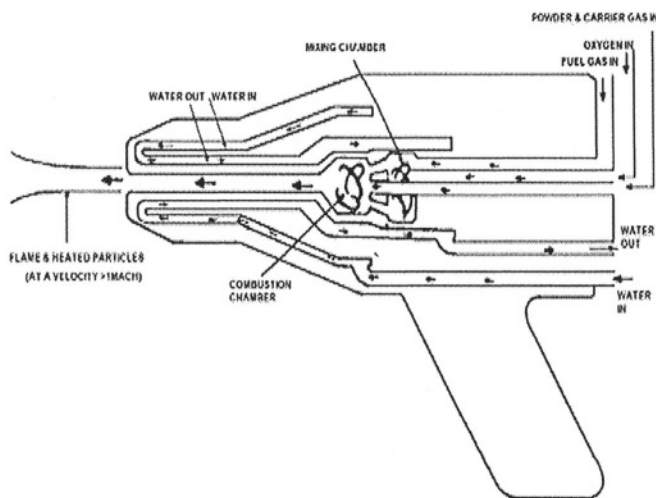


Fig.8.2.1:HVOF SYSTEM

Earlier high velocity systems had severe limitations with respect to coating thickness particularly with respect to hard carbides and other ceramic deposits. The thickness of deposit was limited to 1.27 mm due to tensile residual stresses developing in the coating. The tensile residual stress increases with thickness and hardness of the coatings, hence the limitations on thickness of hard coatings. Also the deposition rate was rather low at 2.25 kg / hour.

The development of HVOF with higher gas jet velocity (~1.5 times than that of earlier system), has made it possible to overcome the limitations associated with earlier systems. The higher velocities are achieved by using a superior combustion design, similar to that of rocket engine technology. The combustion is carried out at a chamber pressure of around 150 psig. The generated hypersonic gas velocities are in the range of 1370-2200 m/s (4520 – 7200 ft/sec). The powder coating material is introduced inside the combustion chamber. The molten or semimolten powder particles in the hot jet stream are found to have velocities in the range of 480-1190 m/s (1584 – 3927 ft/sec). In the same gas stream, the smallest particles (10 μm) reaches high velocity of 1190 m/sec, while the coarser fraction (50 μm) may reach a low velocity of 480 m/sec. The gas jet temperature is in the range of 1650-2760°C, depending on the type of fuel gas used. The high pressure, high energy technology, permits continuous application of coating with superior properties than that of other similar processes, such as D-Gun and plasma.

Burners

Two basic types of burner designs are used. These are throat combustion and chamber combustion burners. The advantages of chamber burner over that of the throat burners include higher particle velocity and more particle heating because of

- a larger diameter combustion chamber allows higher throughput and the resulting increased chamber pressure causes the gas and particle velocity to rise.
- longer passage of the flame along with the powder through longer barrel length without air contamination.

Fuels & Oxy-fuel Ratio

The list of fuels used for HVOF includes propylene, acetylene, propane, hydrogen, MAPP & kerosene. The jet temperature and velocity depend on the type of fuel and oxygen to fuel ratios. The maximum velocities are obtained in the stoichiometric to a slightly fuel-lean range. There is a substantial decrease in velocity (13 to 15%) in fuel rich (incomplete combustion) and fuel-lean (cooling effect of excess oxygen) regions.

Particle Feeding

Different burner designs allow injection of powder particles at different locations. Powder particles can be fed axially at the one end of the burner or radially injected inside the chamber. With radial injection it is possible to achieve at least twice the spray rate per unit energy compared to the axial feeding. Also in radial injection, the particles are more uniformly distributed within emerging jet than axial injection, and thus providing a flatter coating profile

Standoff distance

The particles in the emerging jet continue to be at maximum velocity and temperature up to a distance of 1 meter from the barrel exit. The particle velocity and temperature are found to be constant within 0.25 to 1.0 meter from the torch nozzle exit (13). The standoff distance of the substrate from the nozzle exit should therefore be maintained within the range of 0.25 to 1.0 meter in order to obtain satisfactory coating properties.

Particle size

The smaller particles attain higher velocities and thus strike the substrate sooner than larger particle. The larger particles with lower velocities allow them to stay longer in the jet and thus get heated to similar extent as finer particles before striking the substrate. However the very small particles (~10 micron) have the tendency to follow the decaying gas velocity and temperature after leaving the barrel. Normal particle size range of the powder used is therefore limited in the range of 20 to 50 micron.

Velocity

The high velocity jet results in shorter in-flight exposure to atmosphere, reduced mixing of air with the jet, lower ultimate particle temperatures compared to plasma, and higher kinetic energy [\propto mass \times (velocity) 2] of the particles impacting onto the substrate. The benefits accrued due to high velocity and high kinetic energy includes coatings with less porosity (superior corrosion resistance), high density (high hardness wear resistance), higher adhesive bonding to substrate and interparticle cohesive bonding (less spalling tendency), compositional uniformity, thicker coating and smooth as-sprayed surface. With increased velocity, the spray rates has increased to around 3-4 times than that of earlier systems. Increased velocity produced coating with compressive instead of tensile residual stress. Development of tensile residual stress in the coating reduces the fatigue life and excessive stress can cause coating to spall. On the other hand, the compressive residual stress improves fatigue life and reduces the spalling tendency. It is possible to make coatings of up to 3.2 mm of hard materials with the higher velocity HVOF.

Microstructural Characteristics of a typical HVOF deposit of WC-Co

The tungsten carbide compound, W₂C with a hardness of 3200 Knoop, possesses superior wear resistance properties compared to that of WC with hardness of 1500 Knoop. However, for thermal spraying, a mixture of WC and W₂C is used along with cobalt binder.

The decarburization and decomposition of tungsten carbides are minimized by controlling flame temperature and velocity. Both the high energy plasma (HEP) using at or above 80 KW plasma gun and HVOF are used for the deposition process. The higher velocity in HVOF leads to less

decomposition of carbide compared to air plasma and thus more carbides are found in the microstructure (Fig. 8.2.2) of HVOF sprayed deposit than that of plasma. In both the high energy processes, it was found that the dissociated tungsten and carbon react with cobalt and the molten product on deposition solidifies as amorphous material. The post-coating heat treatment (860°C) in an inert atmosphere resulted into recrystallisation of the amorphous product into eta-carbides ($\text{Co}_2\text{W}_4\text{C}$ & $\text{Co}_6\text{W}_6\text{C}$) with vastly improved wear properties (14).

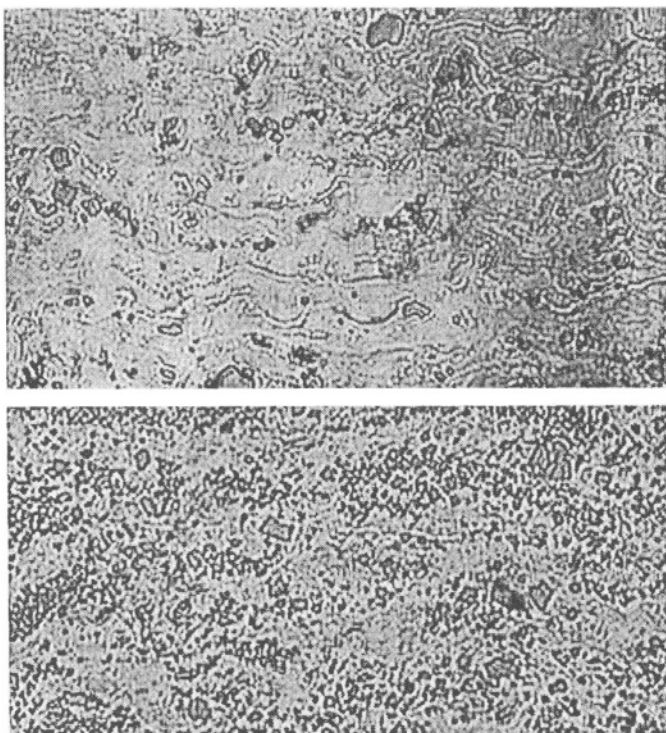


Fig 8.2.2. Microstructures of thermally sprayed WC-Co powder X500; 80KW Plasma (top) and HVOF (bottom) sprayed (Ref. 14, Journal of Thermal Spray Technology, vol 1 (2), 1992, page 149, fig. 2. Permitted to reproduce by ASM International, Materials Park, OH, USA)

HVOF applications : HVOF has replaced plasma in several application areas due to denser coatings with superior bond strength values. Applications list includes piston ring (Mo or Mo+Ni-Cr-B-Si-C) & crown (Y_2O_3 -stabilised ZrO_2) in auto-engines, CAPL & CGL hearth rolls ($\text{CoCrAlY}-\text{Y}_2\text{O}_3/\text{CrB}_2$), and sink rolls (WC-Co) in steel plants, boiler tubes ($\text{CrC}+\text{NiCr}$) in thermal power

plants, thermal barrier (Y_2O_3 -stabilised ZrO_2), oxidation resistant (NiCrAlY), abrasion resistant (WC-Co) coatings in gas turbine components.

8.2.2 Hyper Velocity Impact Fusion (HVIF) (15,16)

In recent times, high velocity flame spray system, such as HVOF, has gained popularity due to its capability in producing high quality tungsten carbide coatings. The coating quality is superior to that produced by plasma spray process in terms of density and hardness. Further increase in jet velocity shall result in the formation of still better quality of coating. The process using high pressure combustion system resulting in high kinetic energies of the particles and thus releasing high heat energy on impact to the substrate has been termed as hyper velocity impact fusion or HVIF system.

A rocket type HVIF burner is used in which the fuel burns in oxygen (or air) at high pressure (150-1200 psi or 1034-8274 Pa) and the hot combustion products expand to supersonic velocity through the converging-diverging nozzle section (Fig. 8.2.3). Higher is the combustion pressure larger is the temperature drop on the jet on emerging from the torch nozzle. The choice of using air or oxygen for hypervelocity depends on the combustion pressure. Hyper velocity air fuel (HVAF) can be used up to a combustion pressure of around 150 psi (1034 Pa). For combustion pressure in the range of 150-1200 psi (1034-8274 Pa), a combination of HVAF and HVOF, i.e., oxygen enriched air is to be used. To compensate for substantial temperature drop in very high pressure region, pure oxygen (HVOF) is to be used for combustion above 1200 psi (8274 Pa).

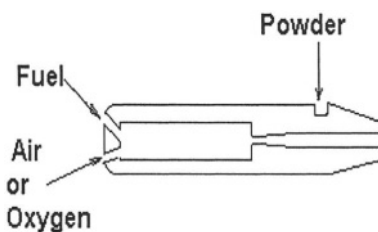


Fig.8.2.3. Schematic of HVIF Burner

The temperature normally drops below the melting point of the sprayed powder material. However the kinetic energy of the impacting particles generates sufficient heat to fuse the particles onto the substrate surface. For example in HVAF system for spraying 316 grade stainless powder, while operating at a chamber pressure of 70psi (482Pa) on combustion results in a temperature of 3500°F (1927°C), which in expanded hypersonic jet is reduced to 2625°F (1440°C). The jet temperature is therefore below the melting point

of stainless steel. In a long expansion nozzle producing a jet velocity of around 4780 ft/sec (1457 m/sec) from the combustion, the particle impact velocity in the expanded jet is around 2500 ft/sec (758 m/sec). The kinetic energy, on 100% conversion efficiency basis, leads to an enthalpy increase of 125 Btu/lb (290 J/gm) of stainless steel. With a specific heat of 0.12, the impacting stainless steel particles at 2625°F require only a fraction of the heat energy to reach fusion temperature. The fused micron size particles solidify rapidly on the substrate surface. Rapid solidification & deposition processes provide very little scope, if any, for decomposition, alloying or oxidation of the coating material. The coating is essentially 100% dense. Successful examples involving HVIF process for deposition, include 88/12 WC-Co and AISI 316 grade stainless steel. HVAF (air + fuel) system at 70psig combustion pressure and 12 inch stand-off distance resulted in dense deposit of 88/12 WC-Co composite. The hardness of the deposited composite was found as 1778 Knoop. Under similar operating conditions, 100% dense deposit of 316 stainless steel was obtained. The microhardness of the deposit was found to be 352 VPN (100 g). Lower hardness of the stainless steel deposit indicates low oxide content.

High Velocity Impact Forging is a process somewhere in between conventional HVOF and cold gas- dynamic spray method (CGSM) from Russia (17). In this process, combustion pressure above 200 lb/in² (1379 Pa) is used. The preferred pressure with pure oxygen is above 600 lb/in² in order to obtain the expanded jet temperature down to 2700F. However for low melting point metal & alloys water is added to the jet to cool the particles so that they do not get hot and melt. Both powder and wire can be used in this process. Copper, aluminium, Inconel 625 and WC/Co coatings were produced by this process with better density and less porosity compared to other spray processes. In CGSM process, the gas jet is heated by resistance in the absence of combustion.

8.3 Hot Chemical Gas Flame for Diamond Film Deposition (TA-CVD) (18,19,20,21):-

An outstanding new method for diamond film deposition is the use of oxyacetylene flame at atmospheric pressure. The growth rate is as high as 100-200 $\mu\text{m}/\text{hour}$. However the temperature for deposition is around 800 to 1000°C. The nucleation density has been found to be maximum at ~1000 K (11) at fixed oxygen/acetylene ratio. Hirose (18) successfully manufactured diamond from an oxy-acetylene flame under atmospheric conditions with high growth rates of 100-150 $\mu\text{m}/\text{hour}$. Other workers (19, 20, 21) reported further progress on the cheap process of forming tribological coating of diamond film.

Process (22)

The oxyacetylene flame formed by combustion of oxygen and acetylene at the tip of the torch nozzle consists of three zones, namely, outer oxidizing cone, followed by reducing feather (length = L) and inner cone (length = L - D) (Fig. 8.3.1). The specimen is placed at a distance, H from the nozzle tip in the reducing feather of the flame. The substrate is cooled indirectly by placing on a large water cooled copper box during deposition. The oxygen and acetylene gases used for this purpose are of 98% purity. The process is carried out with a torch of 0.9 to 1.0 mm nozzle orifice using a flame of reducing feather (L) length of 16 to 21 mm, produced by combustion of oxygen and acetylene at a flow rate in the ratio (O_2/C_2H_2) of approximately 1. The variables affecting the deposition process are as follows:-

- Gas flow ratio*:- The optimum gas flow ratio of oxygen /acetylene(R) is found to be in the range of 0.99 to 1.01. The reducing feather length (L) varies from 16 to 21 mm in the optimum gas flow range. With R below 0.99, the graphite growth is preferred, while the length of reducing flame tends to become either too short or non-existent at $R > 1.01$.

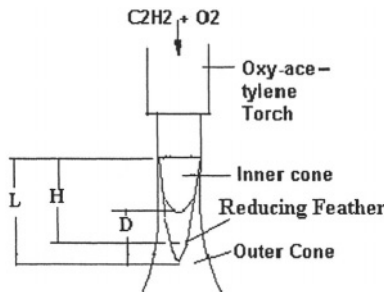


Fig.8.3.1 Oxyacetylene Flame Process for Diamond Coatings

- Substrate pretreatment*:- The substrate surface is scratched with fine diamond paste and then cleaned ultrasonically. A dense and continuous diamond film forms on the scratched surface. No diamond film formation occurs on polished surface. Of the two suitable substrate materials, silicon and molybdenum, it has been observed that the diamond film formation is easier on silicon than that on molybdenum. Fig. 8.3.2 shows the diamond crystals grown on a molybdenum substrate for 36 minute (21).
- Substrate position with respect to flame*:- Diamond film could be grown on the entire length of the reducing feather (D) but decreases with the deposition distance, H. The maximum deposition is observed at H nearer to 8mm and then decreases rapidly to half the rate at H = 11.
- Substrate temperature and distribution*:- The reasonable growth rate has been found to occur at substrate temperature in the range of 800 to

1000°C. Imperfect contact of the substrate material with water-cooled base results in different growth rates and an inhomogeneous diamond film.

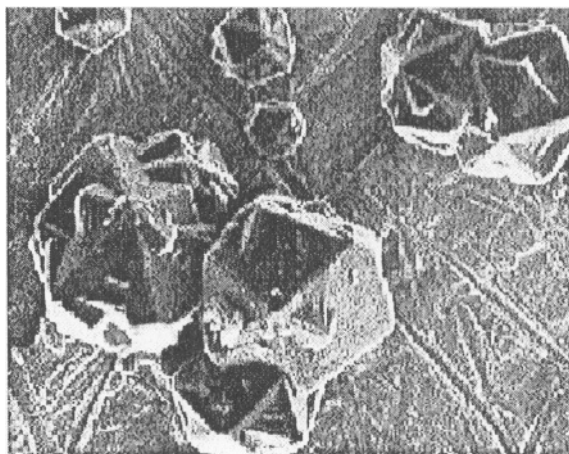


Fig 8.3.2. SEM structure of diamond grown on Mo; X1000
(Ref.21, *Journal of Thermal Spray Technology*, vol1,(2), 1992
1992, ASM International ©, Materials Park, Ohio, page 114,
fig.8)

Properties and Applications (ref. 22):-

Extremely high hardness and very low coefficient of friction make the diamond suitable for a number of applications, including, cutting tools (for nonferrous materials, ceramic materials etc), drills and dies. The properties and applications of diamond film are discussed in chapter 2 section 2.5.

8.4 Flame Assisted Vapor Deposition (FAVD) Process:-

Flame assisted deposition process involving both spray pyrolysis and flame synthesis has been used to deposit thermal barrier coating materials, such as, Y_2O_3 -stabilised ZrO_2 on turbine components made from superalloys. The process involves spraying an atomised precursor solution across a flame source in open atmosphere. The flame provides the thermal environment for the combustion, decomposition and/or chemical reactions of the droplets near the heated substrate surface resulting in the formation of stable coatings. Deposition at a temperature of 800°C produces dense, continuous columnar structure without any microcracks (23).

References

1. Welding Hand Book, Vol 1, Ch 11, p 352, American Welding Society
2. David Proctor, Mat. World, March, 200, 17-18
3. R. Chattopadhyay, Gas Composition Control of Endothermic Atmosphere in Continuous Annealing Furnace for Bright Annealing, Internal Report, Tube Investment of India, 1977.
4. P. Stratton, Mat. World, May, 1999, 269-271.
5. Alan J. Hick, The Met. & Materials Technologists, 1983, July, pp325-340.
6. F. Hoffman, T. Linkewitz and P. Mayr, Hart-Tech. Mitt, Jan-Feb, 1999, 54(1) 10-14. (in German)
7. J. Dulcy, P. Bilger and D. Zimmermann, Metall. Italapril. 1999, 91(4), 33-44 (in English).
8. R. Chattopadhyay, Development of spray fused coating for steel plant conveyor rolls in Light Merchant Mill, Seminar on “ Recent developments in Hot Strip Mills”, Tata Iron & Steel Co, Jamshedpur, 1990.
9. R. Chattopadhyay, Recent developments in Thermal Spraying, an invited talk by ASM International (India Chapter), 1986.
10. R. Chattopadhyay, Seminar on Wear in Steelplants, organised by Indian Institute of Metals & Inter-steel Tribology Committee, Bokaro Steel City, India, Feb., 1986.
11. R. Chattopadhyay, Development of spray fused coating alloy and technique for *in situ* repair of wheel burns, Presentation made at Railway Design and Standard Organisation, Lucknow, India 1992.
12. R. Chattopadhyay, Surface Wear-Analysis, Treatment, and Prevention, ASM International, 2001.
13. M.L. Thorpe and H.J. Richter, J. of Thermal Spray Tech., vol 1(2), June, 1992, 161-170
14. J. Nerz, B. Kushner, and A. Rotolico, J. of Thermal Spray Technology, vol 1(2), March 1992, p147-152
15. J.A. Browning, J. Th. Spray Tech., 1992, vol 1(4), Dec, 289; ITSC, 1992, p123-125 ASM Int.
16. M. Dvorak. & J.A. Brownings, ITSC'95, Kobe, Japan
17. Bob Irving, WJ, Feb, 2000, p42-43.
18. Y. Hirose, 1st Int. Conf. Diamond Sci & Techn., 24-26 Oct, 1988, Tokyo, Japan, 1-09, pp.38-39
19. M. Murakawa, et.al, *ibid*, P33-13, pp.208-209.
- 20: M.A. Golozar et.al., Diamond & Related Materials, vol. 1, Nos, 2-4, 262-266, 1992
21. H.C. Chio & Others, Journ of Thermal Spray Technology, vol 1(2), June, 1992, p111-115

22. S. Tung Lee & others, CVD diamond films : nucleation and growth, Materials Science and Engineering, 25, 1999, p123-154
23. K.L. Choy, 1997 High Temperature Surf. Eng. Conf., Edinburgh, Scotland, 233-25 Sept, Institute of Materials, UK.

This page intentionally left blank

Chapter 9

FRICITION WELD SURFACING

9.0 Introduction

Friction stir weld overlay process consists of material transfer from consumable rod (wear resistant material) to substrate through adhesive wear process by the heat generated in the frictional process between two rotating surfaces under applied load. Solid phase bonding process has been utilized for producing weld overlay of wear resistant materials. Solid phase welding produces strong joint without the defects associated with fusion welding. The process has been used for joining difficult to weld materials, including joining metals to ceramics.

9.1 Principle of Friction & Frictional Heat (1, 2)

When a solid surface is pressed against another, the ratio of the maximum force of static friction (F_s) to that of normal force (N) is called the coefficient of static friction (μ_s). The relation between the tangential force of friction (F_s) and normal force ($N \tan \alpha$) is as follows:-

$$F_s \leq N \tan \alpha \leq N \mu_s$$

where $\mu_s = \tan \alpha$ is called coefficient of friction of rest (or of static friction), and angle α is the angle of friction of rest (or angle of repose). Similarly the ratio of the force of kinetic friction (F_k) to that of normal force (N) is called the coefficient of kinetic friction (μ_k) and expressed as follows:-

$$F_k = N \mu_k$$

both μ_s and μ_k are dimensionless constants and the actual values depend on the nature of both the surfaces in contact in dry sliding, and also on lubricant for lubricated sliding. Other variables affecting coefficient of friction include atmospheric dust, humidity, oxide film, surface finish, velocity of sliding, temperature, vibration and contamination.

The extent of material removal by adhesion of similar mating components is dependent on the sliding velocity and the applied force. For a mild steel pin rotated on a hardened and tempered steel disc (Fig. 9.1), an empirical material removal mechanism map by adhesive or frictional wear (2) processes is shown in Fig. 9.2. In this map, the values of normalized pressure W_n , (equal to nominal pressure divided by the surface hardness and area) are plotted

against the corresponding normalized velocity U_n , (sliding velocity divided by velocity of heat flow) data as axes with contours showing values of V_n (volume loss per unit area of surface per unit distance slid). Also included in the wear map is the value of sliding velocity, U in m/s. In Fig. 9.2, W_n is plotted against U_n and with line contours (where appropriate) indicate the value of V_n (2). W_n ranges from 10^{-5} to 10 and U_n ranges from 10^{-2} to 10^5 . When two surfaces slide together, most of the work done against friction is turned into heat. The frictional heat generated at the tiny contact areas, i.e., the asperities is a function of the normalized pressure, W_n and normalized velocity U_n . The heat generated per unit area, q is given by the following relationship (2):-

$$q = \frac{\mu W U}{A_n} \quad \text{Eq.9.1.}$$

Where q = heat generated per unit area per second in J/m^2s , W = normal force on the pin, U = sliding velocity, A_n = nominal (apparent) contact area of wearing surface.

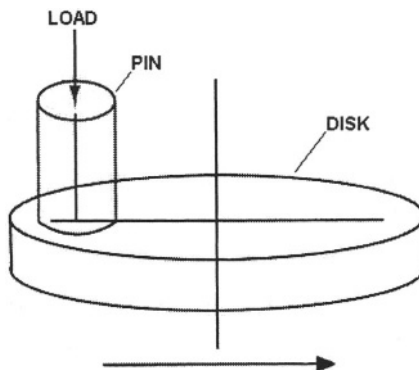


FIG.9.1 Pin-on-disk adhesive(frictional) wear test set-up

The four main regions (2) of the wear map (Fig. 9.2) includes:

- Oxidation-dominated wear ($W_n = 10^{-5}$ to $10^{-3.5}$ & also higher pressure ranges)
- Deformation or delamination wear ($W_n = 10^{-3.5}$ - $10^{-2.5}$)
- Melt dominated wear ($W_n = 10^{-2.5}$ - 0.4)
- Siezure ($W_n > 0.4$)

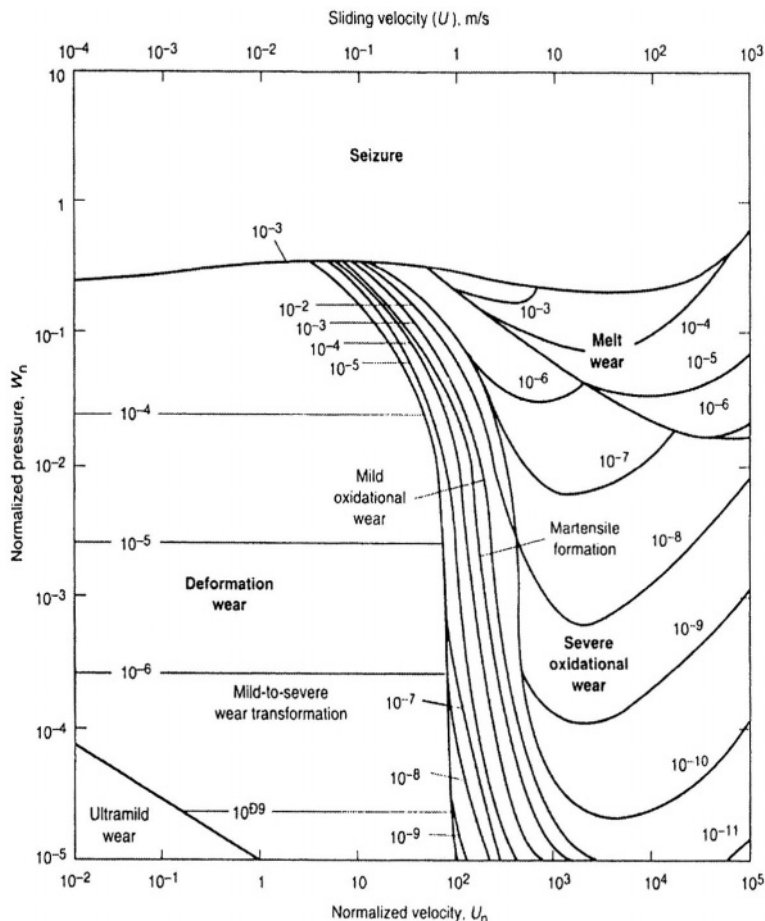


Fig. 9.2 Frictional Wear Characteristics (Map); Wear of Pin Material in Pin-on-Disk Tests

(ref. 22. S.C.Lim & M.F. Ashby: Wear Mechanism Maps, *Acta Metall.*, Overview No.55, vol 35, No.1, Fig. 27, p21, Copyright© 1987 Pergamon Journals Ltd. Reproduced with permission from Elsevier.)

At sliding velocities below 0.1m/s, surface heating being low, the effect of frictional force ($W_n = 10^{-3.5} - 10^{-2.5}$) is to deform the metal surface and shearing it in the sliding direction (3, 4). Deformation occurs mainly in the pin head interfacing with the larger disk and the material from the pin is transferred to the disc by deformation wear at a rate stipulated in Archard's law (5) as follows:-

$$\text{Wear} = k_A \cdot W_n$$

where, k_A is the Archard wear coefficient (typical value 10^{-5} to 10^{-3}). Deformation wear under same pressure can increase from 10^{-5} to 10^{-2} with the increase in sliding velocity from 0.1 to 1.0m/s (Fig. 9.2). The seizure or galling occurs when the pin plastically indents the disk, i.e. at $W_n = 0.4$ over the entire range of U_n (Fig. 9.2). The seizure can cause removal of the heated and thus softer pin material to the disc. The removal of pin material by melting will occur only when the power dissipated against friction, $\mu F U / A_n$, per unit area of the pin exceeds a critical value. The melt area is clearly defined by a triangular field in the top right of the Fig. 9.2. Energy generated by friction has been utilized for weld deposition of wear resistant materials through solid state bonding. Similar to adhesive wear the relative motion between two surfaces under pressure produces deformation & heat by frictional forces causing removal of deformed and heated softer material from one surface and forming strong adhesive bond with the other mating surface. The relative motion dislodges the locally heated bonded material from one of the surfaces (consumable) and is retained by other surface (substrate).

9.2.Friction Surfacing (6, 7)

Friction surfacing is a comparatively new technique. The process is similar to pin and disk arrangement in Fig. 9.1. It consists of rotating the coating material in the form of a rod under pressure on the substrate, and due to the frictional heat developed, a layer of 1.0-2.0 mm thick coating material can get transferred on to the substrate surface (Fig. 9.3).

Process

The basic steps in the process, based on the principle of adhesive or frictional wear, includes the following (Fig. 9.3)

- i One of the workpieces (consumable rod) should be rotating while the other held stationary. In frictional surfacing, with the rotational motion, a relative motion in a direction perpendicular to the axis of rotation (X-direction) is added to the consumable.
- ii. After appropriate rotational speed (S) is reached, the consumable rod surface is allowed to make contact with the substrate surface. An axial pressure (W) is applied on the rod.
- iii. Frictional heat generated at the sliding interfaces under pressure increases the temperature in near surface region and results in strong adhesive bonding amongst points. The bonded metal soon is sheared from the rod and retained by the substrate surface. With continued sliding under pressure, the increase in the torque and interfacial temperature result in the transfer of larger fragments until a continuous layer of plasticized metal forms on the substrate surface. A thin film of liquid may form at the interface.

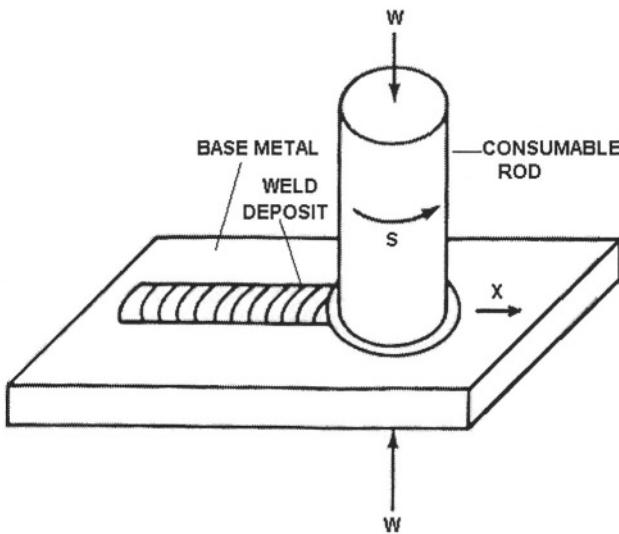


Fig.9.3.Friction Surface Welding Process (Schematic)

Process Variables

The basic process of frictional heat generation and bonding depend on two main variables, namely, speed (S) and pressure (W) (eq.9.1).

Speed

One of the basic conditions for frictional or adhesive wear is to have relative motion between two sliding surfaces. The objective of rotating consumable rod is to produce a relative velocity at the sliding interface. For rotating solid rod, the velocity varies linearly from zero at the center to a maximum at the periphery. The less heat generation due to lower velocities at the central region may result in no bonding of these areas with the substrate. An optimum velocity should result in uniform bonding of the whole section. Lower velocities with their shorter heating times are used for dissimilar metal combinations in order to minimize the possibilities of brittle intermetallic compound formation.

Pressure

The applied pressure is directly proportional to the amount of heat generated (eq. 9.1). Pressure is used both for generating frictional heat and for forging. Heating pressure should be high enough for intimate interfacial contact and to generate required heat for adhesion to take place with minimum of axial shrinkage. Low pressure limits heating with little or no axial shrinkage. High pressure results in local heating to high temperature and

rapid axial shrinkage. For a given pressure during the heating phase, axial shortening is more at low speed than at high speed.

Heating Time

Heating time is the time required at a particular pressure and a velocity to generate sufficient frictional heat for adhesion to take place. Excessive heating time impairs the quality and reduces productivity. Inadequate heating time results in uneven heating as well as unbonded areas at the interface. At the center of the rotating bar, low surface speed may generate inadequate frictional heat. Longer heating time results in thermal diffusion from the outer portion of the sliding surface to interior leading to uniform bonding across the section.

Surface Preparation:-

In order to obtain proper weld quality and consistency, the fraying surfaces should be free from dirt, oxide, or scale, grease, oil, or other foreign materials. In addition fraying surfaces should mate together with very little gap. If the surfaces are not perpendicular to the axis of rotation, joint mismatch may result. For best results, the squareness should be within 0.010 in/in. (0.01 mm/mm) of joint diameter.

Structure and Properties of Friction Weld Overlays

The microstructure of the friction welded overlay is similar to that of the structure resulting from elevated temperature deformation. Several microstructurally distinct regions are observed in friction weld areas (Fig. 9.4) including the *stir zone* across the interface, the heat-and deformation-affected zone (HDAZ) or thermo-mechanically affected zone (TMAZ) below the stir zone and a true heat-affected zone (HAZ) below HDAZ. Stir zone is normally a hot worked region with appreciable grain growth due to high temperature. A thin layer of interfacing area in the stir zone may get molten depending on the heat generated at the interface. Diffusion of alloying elements can occur across the interface for longer welding time, forming a diffused layer. Diffusion in dissimilar material welding may result in the formation of brittle intermetallic phase. Proper welding conditions should usually minimize undesired diffusion or intermetallic phase formation. The thermo-mechanically affected zone in aluminum alloys showed flow lines and other indications of deformation in friction weld after cooling to room temperature (8). In friction welded mild steel, there was no indication of deformation, presumably due to allotropic transformations occurring during cooling (9). Heat affected zone (HAZ) may show grain growth and in hardenable steel may produce non-equilibrium structures due to rapid cooling. Hardenable steel should therefore be welded with a relatively long heating time to achieve slower cooling rates. The short heating time below melting temperatures leads

to very little alteration in the amount and distribution of different phases present in the material in non-hardenable alloys.

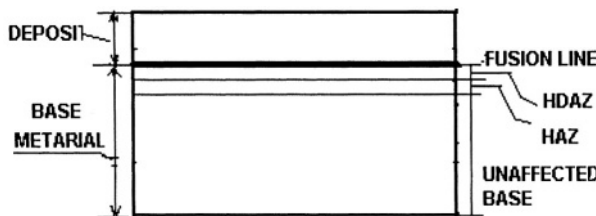


Fig.9.4 : Microstructural zones in friction stir weld (Schematic)

Advantages of friction welding include followings:-

- i. No flux or shielding gas is required.
- ii. Environmentally clean process does not produce any arc, spark, fumes etc
- iii. Surface cleanliness is not as significant since friction welding tends to disrupt and displace surface film.
- iv. Narrow HAZ.
- v. No process defects as associated with fusion welding. The solid phase bonding process in friction surfacing results in superior metallurgical structure at the interface compared to cast structure in fusion weld.
- vi. Suitable for dissimilar materials since no fusion is involved.
- vii. Most cases weld strength is stronger than weaker of the two materials joined.
- viii. Process can be automated.

Limitations of the process include:-

- i. In general, one workpiece should have an axis of symmetry and be capable of being rotated about the axis. This is not a problem in weld overlaying with consumable in the form of a straight rod or bar of uniform diameter.
- ii. Preparation and aligning may be critical

Friction welding of metal to metal:-

The solid state joining process can be used to join difficult to weld materials as well as ceramic or composites to metal. The process has been used to deposit wear resistant alloys, such as, stainless steels, high speed steels, Ni-Cr-Cb alloys, Co-Cr-W-C (Stellites) etc. on any weldable or non weldable steel surface. Commercially available rods of the wear resistant

alloys can be used. The process has been used to build wear prone areas of industrial knives, valves, pump components, plastic extrusion machines etc, with wear resistant alloys.

Friction welding of ceramic to metal:-

Four different ceramic materials such as alumina, zirconia (MgO-PSZ), silicon carbide and silicon nitride in the form of rods (10 mm dia and 50 mm length) were friction welded to an aluminum alloy (Al-SiMgMn alloy). The welding parameters used include, speed of rotation at 1500 to 5000 rpm, friction pressure 20-80 MPa, forge pressure 30-150 MPa, and friction time of 0.5-1.5 seconds (10). The edge geometry of the joint in the vicinity of the interface (flash) was found to have strong influence on the joint strength. The joint strength can be improved by optimization of joint geometry and welding parameters. The bond strengths for different ceramic material layers varied from 300 MPa for Al_2O_3 , through 350 MPa for SiC & 500 MPa for PSZ to a maximum of 600 MPa for Si_3N_4 (10). Ceramic surfacing of metallic materials leads to high hardness, insulating surfaces suitable for use in high temperature corrosive atmospheres.

Friction welding of composites to metals

Friction welding of Al-14% SiC particulate composite to 2648 Al is reported to have a bond strength of 380 N/mm² (11). The joining of two workpieces are done by friction welding. SiC-particulate reinforced aluminium alloys possess high hardness, wear resistance low thermal coefficient of expansion and good thermal conductivity. The composites are welded to high strength aluminum alloys for transportation industry applications including airframe structure, front disc brake rotors, turbocharger impellers, missile bodies and aircraft wing skins.

References

1. R. Chattopadhyay, 'Surface Wear, Analysis, Treatment, & Prevention', ASM International, 2001, Chapter 2, Friction/Wear.
2. S.C. Lim & M.F. Ashby, Wear Mechanism Maps, *Acta Metall. Overview* No.55, vol 35, No.1, 1987, p1-24
3. N.P. Suh, *Wear*, **25**, 111, 1973.
4. D.A. Rigney, Proc. int. conf. fundamentals of tribology, MIT, Cambridge, MA, p119, MIT press, Cambridge, MA, 1978
5. J.F. Archard, *J. Appld. Physics*, **24**, 981, 1953
6. G.M. Bedford, *Met. & Materials*, Nov, 1990, p702
7. *Welding Handbook*, volume2, Eighth edition, Chapter 23, Friction Welding, p740-762, American Welding Society.
8. L.E. Murr & others, *Journal of Materials Science*, 1998, 33, 1243-1251

9. T.J. Lienert & others, WJ, Jan, 2003, p1- 9
10. R. Weiss, WJ, March, 1998, Welding Research Supplement, 115s-122s.
11. M.B.D. Ellis & others, Materials World, 1996, 12(8), 415-417.

This page intentionally left blank

Chapter 10

INDUCTION SURFACE MODIFICATION PROCESSES

10.0 Introduction

The induction heating system has been successfully used for surface engineering processes such as hardening and fusing of alloys deposited by thermal spraying. These processes are to be discussed in the light of recent developments.

10.1 Induction Heating of the Surface

A steel component when placed in an induction coil or inductor, and a high frequency (10,000 to 500,000 cycles per second) alternating current is sent through the coil, the component gets heated primarily from the resistance to flow of currents created by induced voltage, i.e., eddy current losses and secondly from the hysteresis losses from rapidly alternating magnetic field if the part is magnetic. Plain carbon and alloy steels get most rapidly heated below the Curie point, where they are ferromagnetic and less above this temperature.

A medium frequency (180 Hz to 50 kHz) solid-state induction heating system is used for surface hardening. The heat developed by induction concentrates on the surface of the component. The depth of heating is proportional to the inverse square root of the frequency of alternating current in the coil. High frequency system has the depth of flux penetration up to ~8 mm, while the low frequency variety can heat up to a depth of 100 mm (1). Depth of flux penetration also depends on the temperature and on the holding time. For example, the current penetration in steel at 800°C is 0.8 mm and for 450°C is 5.5 mm at 10 Hz. The current penetration depths in room temperature for steel with frequencies at 450 Hz and 10 Hz are 0.05 mm & 0.25 mm respectively (2).

The selection of frequency depends on section size and the case depth. For example, a frequency of 10,000 Hz is used to produce case depth of 1.29-1.54 mm (0.051-0.10") in section sizes of 25.4 – 50.8 mm (1-2"), at a power density (kW/square inch or cm of surface exposed to inductor) of 1.55 kW/cm² (10 kW/in²). To produce case depths of 2.56 – 5.08 mm (0.101-0.20") in section sizes of 19.05-50.8 mm (3/4-2") requires a frequency of 3000 Hz at power densities of 2.33 kW/cm² (15 kW/in²) for 2.56 mm, and 1.55 kW/cm² (10 kW/in²) for 5.08 mm (3).

The heat penetration towards interior shall depend on the time of holding at a particular temperature and frequency. High frequency current path at surface is determined by the nearness of the return flow path. The easiest and probably the best method to reduce the air return path is to place the coil in close proximity to the job. The “proximity effect” improves induction heating efficiency by reducing the resistance to magnetic flux lines as they travel through the air. However, this technique reduces the path lengths between the drive coil and the specimen but does not help reduce the path lengths for the flux which must go around the coil. The air path reluctance in induction heating set-up can be reduced by the use of a high permeability magnetic material as flux concentrator. The effectiveness of a flux concentrator depends on the resultant flux path of a particular design. Examples of magnetic flux concentrator materials include silicon steel laminations, ferrites and iron powder composites. Lower reluctance of flux concentrator compared to that of air path which it replaces, reduces the total reluctance of the magnetic circuit. Another benefit which can be derived by using a flux concentrator is the ability to focus flux generation and therefore the heat in selected areas of the substrate surface.

10.2 Induction Hardening

The induction heating of the surface layer of hardenable grade steel to austenitising temperature followed by rapid cooling results in the formation of hard martensite in the heated layer. High hardness wear resistant case of required depth can therefore be formed on the surface by induction hardening, while the bulk remains mostly unaffected.

Transformation Hardening in Steel

The time-temperature-transformation (TTT) curves indicates the time for transformation of austenite to pearlite or bainite while held at a particular temperature. At temperatures above nose portion, austenite transforms to pearlite and below the nose bainite is formed. The time required at a particular temperature for the isothermal transformation to start (e.g. P_s) is obtained from the left curve. The right-TTT curve indicates the time for complete transformation (e.g., P_f) at a particular temperature. The amount of transformation depends on the holding time at transformation temperature.

Martensite forms only on continuous cooling, starting at M_s and finishing at M_f . The continuous cooling transformation diagram (CCT) of a 0.8% C-steel is superimposed on the TTT-curve of the same steel in Fig. 10.1. As indicated in the diagram for transformation to martensite continuous cooling is required at fast rate (above 40°C/s for 0.8% C-steel), and the material need to be cooled below M_s (martensite start forming temperature). However for 100% martensite formation in a 0.8% C-steel, a minimum cooling rate of

140°C/s is required and the material need to be cooled below M_f (martensite formation finish temperature) (Fig. 10.1). The minimum cooling rate for 100% martensite formation is known as the critical cooling rate for the steel. The TTT curves are different for different compositions, so also the critical cooling rates required to form martensite. The cooling medium is selected based on the critical cooling rate of the steel.

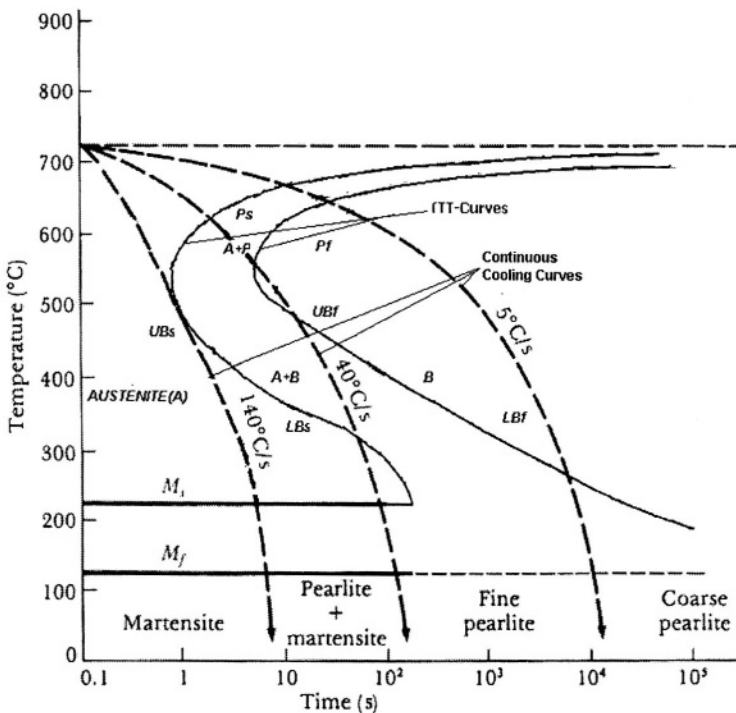


Fig.10.1.Time-Temperature-Transformation(TTT) Curves of 0.8%C-Steel. Continuous-Cooling-Transformation(CCT) Curves superimposed on TTT

Most of the alloying elements including carbon shift the TTT-curve to the right, thus decreasing the critical cooling rates required to form martensite in high alloy and high carbon steels. However most of these alloying additions also lowers M_s and increases the gap between M_s and M_f thus requiring sub-zero cooling for complete transformation of gamma to martensite. Sub-zero cooling is also employed to transform retained austenite to martensite in steel quenched above M_f temperature.

Quenching severity of the medium increases in the following order:-

Oil → Oil(VA)* → H₂O → H₂O(VA)* → Brine → Brine(VA)*
 (VA)* = Violent Agitation

High hardenability high alloy steels, such as HSS, require slow cooling rates, and are therefore quenched in oil. Low carbon alloy steels on the other hand may require high cooling rates, such as quenching in water. Higher quenching severity develops high stresses and can lead to distortion and crack formation in the component.

The heating rate is very rapid in induction process compared to conventional heating. In high alloyed steel, the carbides in the microstructure cannot get into solution at the short holding time. If high alloy steel is to be subjected to induction case hardening, the component needs to be solution treated prior to induction heating.

The hardness of the fully martensitic case depends on the carbon content and can vary between 52 HRC to 62 HRC. Due to fast heating rate and short holding time, induction hardening can produce very fine grain size in the transformed structure (4).

Case hardness, depth and microstructure:-

The hardness of the case is normally around 55 HRC. The actual case depth is the depth to which almost 100% martensite is formed in the structure. However effective case depth can extend up to the point where around 50% martensite has formed (Fig. 10.2).

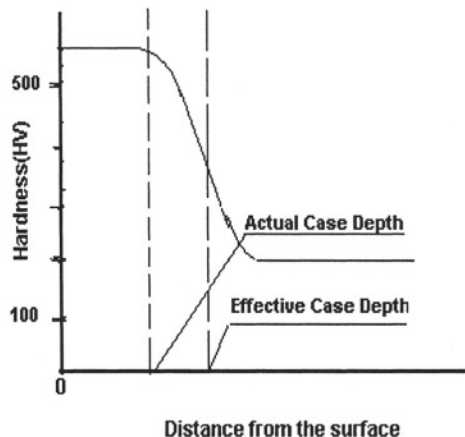


Fig. 10.2 : Effective and actual case depth in induction hardened surface (schematic)

Applications

Induction hardening system can be used to harden selected portion of a component. For example, pin bearing surfaces of V6 crankshafts of Mercedes-Benz are surface hardened by positioning transformer/inductors at

precise location (5). The flux concentrator has been used for efficient induction heating in case hardening of a number of automotive components. Some of the items are as follows (6):-

- i. *long shaft* :-case-harden up to a depth of ~6.4 mm depth (254 mm dia) of a long shaft in a single shot by using less than 200 KW power,
- ii. *torque transmitting component* :-selectively case harden fillet area but not the snap ring groove of a torque transmitting component
- iii. *valve seat* :-harden valve seat area
- iv. *rocker arm*:- harden rocker arm tip.

The induction hardening requires that the coil to be positioned closely and precisely symmetrical to the workpiece, particularly, at high frequencies, thus restricting process flexibility.

10.2.1 Induction Hardening of Cast Iron Surface (3)

Grey cast iron castings can be surface hardened by austenitizing at a temperature of 35°C (100°F) above A1 (transformation temperature) of the given composition and subsequent quenching in molten salt, oil or water soluble polymers. The transformation temperature (A1) of an unalloyed cast iron is approximately determined as:- $A1^{\circ}C = 730 + 28 (\%Si) - 25 (\%Mn)$. The combined carbon content of the grey iron should be in the range of 0.5 to 0.7%. Similarly ductile iron surface can be selectively hardened by induction heating to austenitising temperature of 845–925°C, depending on composition of the casting and then quenching in oil. The hardness of the wear resistant surface is 480 HV.

10.3 Induction Fusing:-

The spray deposit coatings of ferromagnetic materials can be fused by induction heating. Self-fluxing nickel & cobalt base alloys can be fused to form a dense and uniform wear resistant coating by induction heating of sprayed deposit. The thick (upto 3.0 mm maximum) thermally sprayed deposits can be fused rapidly by heating to fusion temperature of the deposit. The fusion temperatures of the self-fluxing alloys are in the range of 950–1150°C. The process has also been used in fusing coated layer in the internal diameter of hollow cylindrical components, esp., of small diameter.

Process

An automated induction fusion set-up with temperature sensing by infrared thermometer and the feedback signal to control induction output is shown in Fig. 10.3. In the two step spray and fusion process, the first step consists of spraying the powder alloy through suitable oxy-acetylene torch

followed by fusing the deposited layer by induction heating. Cylindrical objects like shafts, spindles or rolls are rotated, while the induction coil moves across the length fusing the sprayed coating. The axial movement of the induction coil and the speed at which the shaft is rotated are regulated to ensure proper fusion of the coated layer. The oxyacetylene torch sprayed coating (1.5 mm thick) of a high hardness Ni-alloy (Ni-16 Cr-4 B-4 Si-3 Mo-2.5 Fe-3 Cu-0.5 C) on a 22 mm dia \times 600 mm length steel bar was fused by induction heating using a power input of 15-50 kW and frequency of 2.0 kHz at a holding time of 60s (7). The sprayed coating is heated to point between solidus and liquidus and the proper fusing temperature is visually judged by noting when the surface attains a highly reflective, glassy appearance. Heating beyond the point produces too much liquid phase and is likely to induce shrinkage voids and to cause run-off of the coating. Rapid heating rates in induction fusion process leads to less fluxing and thus produces less slag and less loss in B & Si.

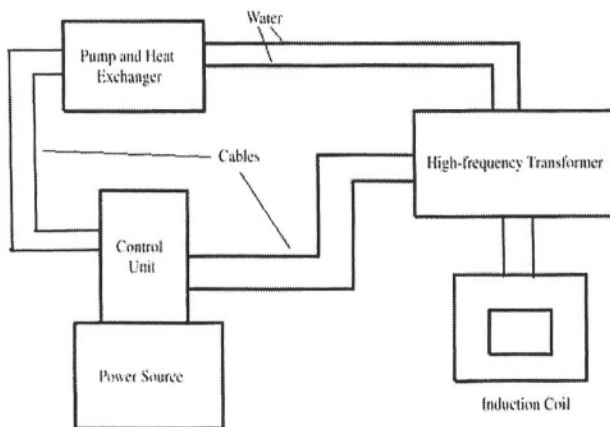


Fig.10.3 Automated Induction Fusing System

Properties

By induction fusion lamellar structure of sprayed deposits (Fig. 10.4a) is replaced by fine grains and carbide plus boride precipitates (Fig. 10.4b). The fused coating forms a diffusion bonded layer at the interface with substrate (Fig. 10.4c). The boron and silicon are added to nickel base alloy to act as fluxing agent, also to decrease the fusion temperature of the alloy and to increase hardness & wear resistance. Rapid fusion by induction leads to less loss of boron and silicon & less slag formation and less overheating in comparison to flame (oxy-acetylene) and furnace fusion processes. The induction fusion process thus results in deposit with higher hardness, lower

porosities and better surface finish (Table 10.1) in comparison to other two processes (7).

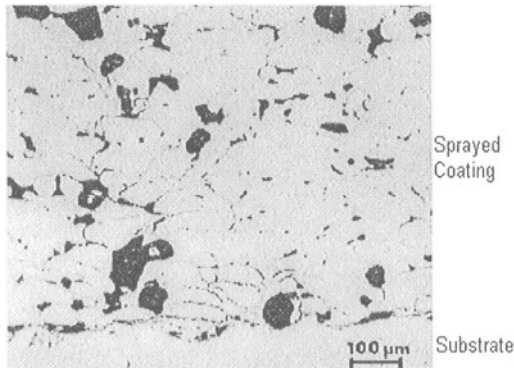


Fig 10.4a.Thermal spray coating of Ni-Cr-B-Si-C on steel

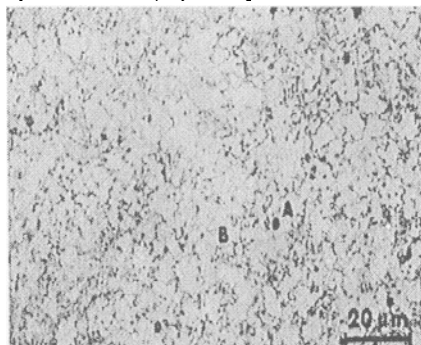


Fig 10.4b.Induction fused sprayed Ni-Cr-B-Si coating

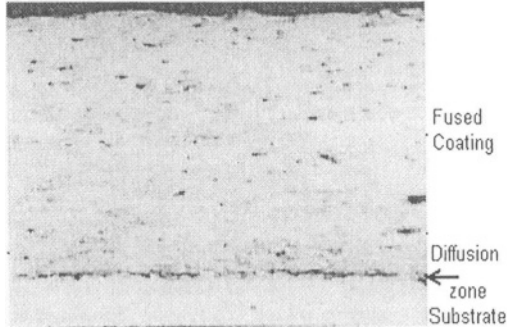


Fig 10.4c.Fused coating and diffusion zone

The application areas include fusion of coatings on shafts, spindles, plungers, conveyor rolls, wear rings etc. Induction fusing of thermally sprayed Ni-Cr and Ni-Cr + CrC coatings on worn boiler tubes have been recommended in order to improve the thermal conductivity of the coatings. To minimize corrosive wear due to high sulfur coal in boiler tubes normal

practice is to use a suitable thermal spray system to deposit Ni-Cr powder on the worn areas in the boiler *in situ*. For high ash erosion, a composite powder alloy of high hardness, such as, Ni-Cr+CrC is deposited *in situ* on the worn tubes. However the sprayed powder deposits are porous and bonded mechanically to the substrate. By induction fusing the deposits become dense and get diffusion bonded to the substrate. Both the thermal conductivity and the bond strength of the coating improve leading to increase in wear life of the boiler tubes.

Tab.10.1 Properties of Ni-Cr-B-Si-C-alloy fused by different processes

Fusion Process	Hardness HV	Porosity (%)	Surface Roughnes (μm)
Induction	750 - 800	0.5 - 1.5	3 - 6
Flame	650 - 750	1.0-2.5	3 - 8
Furnace	630-670	1.0-2.0	10 -13

The developments in induction heating (1) includes, uniform magnetic heating (UMH) and infra red fiber optics for temperature measurements. The UMH depends on the hysteresis loss in a high intensity magnetic field and has found applications in through heating of components. However the potential applications include fusing of low fusion temperature self-fluxing alloy deposits on large section. Another development is the use of infrared (IR) fibre-optic temperature measurement system to monitor temperature of moving, difficult to reach objects like push rods during induction heating and just before quenching.

10.4 Inductive coupled RF Plasma:

In this process, a quartz tube enclosed by RF-coil is evacuated and filled with argon (or suitable plasmagenic gas). With the application of appropriate electro-magnetic field, the plasmagenic gas is ionized and the circulating current begins to form the plasma. The inductive plasma has been used to produce high quality thermal spray deposit (8) plasma nitriding (9) diamond film deposition (10).

References

1. Paul J. Spencer, Mat. World, Aug, 1988, p470-471
2. High-Frequency Welding, Welding Handbook, 8th ed., vol 2, ch20, p652-669, 1991, American Welding Society
3. Induction Hardening and Tempering, Metals Handbook, Desk Edition, p1008-1011
4. P.K. Chakraborty, R. Chattopadhyay & S.S. Bhatnagar, Tran. Ind. Inst. of Metals, Dec, 1970
5. Rob Madeira, Heat. Treating, Supplement to Adv. Mat, & Processes, ASM-International, 2000, 6, pH9.
6. J.S. LaMonte and MR. Black, Heat Treating, June, 1989, p330-331, ASM-International
7. N. Takasaki, A. Tomiguchi, Y. Sochi and A. Ohmori, Fusing of sprayed Ni-base coatings by induction heating, Proc. of Int. Thermal Spray Conf., 28-May-5 June, 1992, Orlando, Florida, ASM-International p273-278
8. M. Magome, Properties of RF plasma sprayed coatings, *ibid*, p111-116
9. El-Hossary, F, et al, Surface Engineering, 1988, vol 4, no 2, p150-154.
10. S. Matsumato, et al, Appl. Phys. Lett., vol 51, no 10, 1987, 737-739.

This page intentionally left blank

Chapter 11

SURFACING BY SPARK DEPOSITION PROCESS

11.0 Introduction

Like arc, spark from capacitor discharge has been used to deposit material onto the surface of the component. The process has been found particularly useful to form a thin wear resistant coating of hard materials like tungsten carbide on tools.

11.1 Capacitor Discharge or Spark Deposition Process (1)

The capacitor discharge welding derives its heat from the dc spark power produced by the rapid discharge of electrical energy stored in a bank of capacitors. The process uses an electrostatic storage system as a power source in which the weld energy is stored in capacitors of high capacity. The spark is a transient electric discharge through the intervening space between the two electrically connected terminals, such as a carbide rod and the work piece in an electric discharge machining (EDM). The process of deposition of material in thin layer by spark discharge weld deposition process has been carried out by reversing the polarity of a electric discharge machining (EDM) or spark erosion machine (2,3). The spark discharge occurs when the applied voltage between the carbide and the base metal is large enough to cause a breakdown in the medium leading to an electrically conducting spark channel. The gap between the electrode and workpiece or the spark gap is the required applied voltage or breakdown voltage. The breakdown voltage is established by connecting the electrode terminals to a capacitor charged from a power source. The discharge can be repeated rapidly to deposit minute amount of material with each discharge (Fig. 11.1). The penetration of spark in the substrate is so shallow that there is very little mixing of the deposited material with the base metal. Therefore the process can be used to deposit hard carbides on difficult to weld metal surface. The thin overlay of hard material is deposited in a very short welding time, and therefore flux or shielding is not normally required to prevent weld metal contamination from air. A strong metallurgical bond forms between the deposit and base metal. The process has been used widely for wear facing with difficult to weld hard materials as well as correcting machining errors.

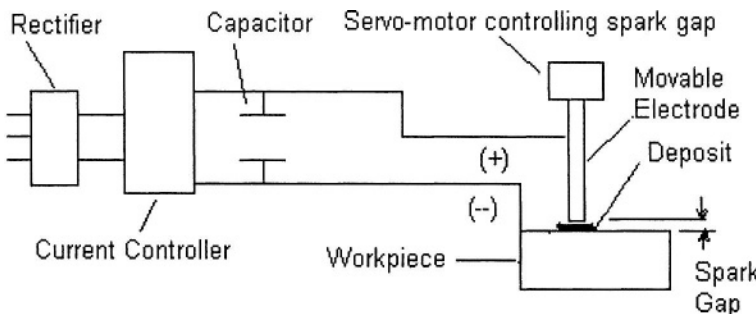


Fig.11.1 Spark Deposition System (Schematic)

Energy stored in a Capacitor :-

A charged capacitor (also known as condenser) can hold charge measured in *farads*, and its ability to store the charge is called *capacitance*. Farad is a large unit and most capacitors are rated in microfarads or less ($1\text{ microfarad} = 10^{-6}$ farads; $1\text{ picofarad} = 10^{-12}$ farad). The energy (E) stored in a capacitor is expressed as (4):-

$$E = \frac{1}{2} CV^2$$

where C = capacitance in farads, V = applied potential difference in volts, and the corresponding energy value of E in joules. The same quantum of energy is discharged during spark deposition through the spark gap. With the increase in applied potential difference energy input shows large increase ($\propto V^2$). The increase in capacitance (by connecting in parallel) leads to proportional increase in energy content. The calculated energy outputs in capacitor with higher applied voltages and capacitance values are indicated in Table 11.1. Higher energies lead to larger quantities of material transfer from the consumable electrode to substrate.

Process:

The equipment for spark deposition is the same as that used in spark machining, however with reversed polarity (Fig. 11.1). The hard material, such as tungsten carbide is in the form of around 3.2 mm (~1/8") diameter sintered rod. The rod is used as a consumable electrode and connected to the positive terminal and the workpiece is connected to the negative terminal. The discharge (or spark) occurs when the potential difference between the rod and the workpiece is large enough to cause a breakdown in the medium between the two electrodes. The breakdown potential is established by connecting the

electrodes to the terminals of a capacitor charged from a power source (Fig. 11.1). In such a situation, an electrically conductive spark channel is established between the electrodes causing material transfer from consumable electrode to substrate with each spark. The spacing between the electrode and the substrate is critical. The gap is adjusted by a servomechanism controlling the feed rate of the consumable electrode. The discharge is repeated in rapid succession till the required coating thickness is obtained. Each time a small quantity of material from consumable electrode is deposited on the substrate. In practice the rate is normally varied by changing the number of discharge per second or the energy per discharge. For example, the spark discharge transfer of carbide to produce a thin layer of adherent deposit on the substrate surface has been made through the use of a carbide rod (1/8" diameter, WC + 12% Co) which makes and breaks contacts with the substrate at a rate of 120 cps by the use of a vibrator. The vibrator is held in hand and is traversed over the substrate surface.

With the increased energy per unit of time, i.e., higher voltage and higher capacitance, the deposition rate as well as the surface roughness increases rapidly (Table 11.1). To deposit a thickness of 0.102 mm, the energy input required is at the rate of 0.3676 Joules per millimeter of thickness. For a coating thickness of 0.203 mm the energy required is at the rate of 0.9458 Joules per millimeter or almost three times than that required for building half the thickness. The energy required for building up a coating thickness of 0.508 mm is 1.6687 Joules or the energy required per 1 mm build up is 3.285 Joules, which is nine times the rate required to produce first 0.1 mm thick deposit. Thus the energy per mm build up increases rapidly with the coating thickness. The process is normally used for thin coatings of approximately within 0.5 mm. Surface roughness of the coating increases rapidly with higher energy input (Table 11.1). Thin deposit layers (0.10 mm thick) using low energy (50 V and 30 microfarads as C) shall result in fine surface finish of the coating (Table 11.1). The process is applicable to all materials which are sufficiently good conductors of electricity.

Table 11.1. POWER INPUT VS. DEPOSITION CHARACTERISTICS IN SPARK DISCHARGE PROCESS

Potential (V)	Capacitance microfarads	Stored Energy		Thickness (mm)	Surface Finish of Deposit
		Joules	Btu $\times 10^{-4}$		
150	150	1.6687	16	0.508	Coarse
80	60	0.192	1.82	0.203	Medium
50	30	0.0375	0.4	0.102	Fine

11.2 Applications

The spark discharge technique has been used to make deposits containing titanium, chromium, and tantalum carbides and ultrafine diamond particles (5). The spark deposition of fused materials is normally made onto a substrate maintained at ambient temperature. The deposition of tungsten carbide can improve tool life several fold. Instead of WC rod, the use of a graphite rod can increase the carbon content of the surface, and due to very high rate of cooling, a thin layer of deposit transforms to martensite. Although cutting tool wear can occur at both rake and clearance side of cutting edges, the carbide impregnation at the rake face of milling cutter and end mills of around 2-4mm width is sufficient to improve the wear life of the tools. Similarly the flutes of taps and drills, top surface of dies and the ends of punches are carbide impregnated to improve wear life. An interesting application of welding by a capacitor discharge process consists of joining wear resistant Al + SiC particulate composite to high strength aluminum alloy (6), for use in transportation industries.

References

1. R. Chatopadhyay, Surface Wear, Analysis, Treatment, and Protection, a book published by ASM international, 2001, p196-197.
2. R. Chatopadhyay, Wear resistant carbide deposition by reversing polarity in EDM, Internal report 5/1978, TI Diamond Chains, India.
3. R. Chatopadhyay, Internal report, 11/1993; Spark discharge deposition of stainless steel by reversing polarity in EDM for rectifying machining error in gas turbine component at Gas Turbine Research Establishment, Bangalore, India.
4. Edward Hughes, Electrical Technology, 7th edition, 1995, Longman Scientific & Technical, England, Ch5, p88.
5. Levashov. et. al., P/M Literature Review, Met. Powder Rep., Jan 1994, p42
6. J.H. Develtian, WJ, 1987, 66(6), 33-39.

Chapter 12

ARC ASSISTED ADVANCED SURFACE ENGINEERING PROCESSES

12.0 Introduction

Weld overlay by arc welding is an well established process for engineering the surface properties of the material. The process is particularly useful for depositing metallic and metal matrix composite materials with a wide range of properties to resist severe wear due to heat (Stellite, Inconel), abrasion (alloyed white cast iron), impact plus adhesion (Hadfield manganese steels), corrosion (Monel, stainless steels) & erosion (Stellite). The advanced automated processes, such as pulsed GMAW, pulsed GTAW, plasma transferred arc welding (PTAW) are used to overlay wear resistant deposits. For thicker deposits, SAW & ESW are used. The list of advanced power supply systems includes the use of inverter to control wave form & to produce high frequency AC and the use of thyristor control in pulsed GMA welding requiring higher currents. The use of inverter has made it possible to produce small portable welding units. The optical radiation from a high powered arc lamp has been used as heat source for surface modification. Also the heat of the arc has been used for thermal spraying. The surface modification processes based on the heat derived from arc are discussed in this chapter.

12.1 Arc Phenomena in Welding and Developments

Arc welding deposition process involves low-voltage, high-current arc between electrode and the substrate. Hence the first requirement is to reduce the utility input power voltage of 110 (or 120), 220 (or 240), 440 (or 480) volts to suitable output voltage in the range of 20-80 V. Transformer is normally used to reduce the voltage. However the solid state inverter is fast replacing transformer. Power source can be of constant voltage, constant current or constant current/voltage type. However, this kind of classification based on static volt-amp characteristic is not really valid in cases like pulsed current welding, where dynamic volt- amp relation exists. In the pulsing system, constant voltage power source is close to constant voltage output but current output is not nearer to current source. Solid state devices are available to provide power in pulses over a broad range of frequencies.

Advances in the power supply devices:

The automated GMAW, GTAW, SAW and the more recent processes like PAW (plasma arc welding) are widely used for the deposition of weld overlay. During the last three decades there has been a number of important developments in the area of welding power supply. An important development in the area of power supply devices is the use of inverter (1) to control wave form and to produce high frequency AC. Inverter is a circuit which makes use of solid state devices (SCR or transistors) to convert DC into high frequency (1 kHz to 50 kHz) AC. Conventional welding power source uses transformer with the line frequency of 50 or 60 Hz.

Chronologically, developments in this area followed the following trend:-

- In the period earlier to seventies, the electromagnetic amplifiers were used to control current output in the welding power supply units. In seventies, the introduction of thyristor control for dc-power supplies led to improved power output characteristics. Thyristors are capable of switching at variable intervals up to 360 Hz during an alternating current-wave half cycle. Thyristor control was used in pulsed GMA welding processes requiring higher currents.
- The solid state or transistor controls were introduced in early eighties. Transistor control with faster response time led to replacement of thyristor control in most of GMA (excepting some CO₂ shielded GMA) and GTA processes. With both electro-magnetic amplifier and thyristor, it was possible to phase control the wave form in low frequency range (~up to 330 Hz). With this limited frequency range it was not possible to control the arc plasma or filler metal transfer. Only some of the characteristic properties of the weld pool, such as, pool geometry, heat input and cooling rate could be controlled. In transistor, the control frequencies can be increased up to ~400 Hz in chopper, ~40 kHz in analog and 100 kHz in invertor modes of operations in the welding power supplies. Chopper & analog modes allow limited control of arc plasma, filler metal transfer, and weld pool. With the inverter it is possible to control arc plasma (behavior of starting arc, arc strike/restrike), weld pool (including weld metal flow, refining of grain size) and filler metal transfer (includes short circuit transfer and spatter). Advanced techniques used for wave form control have resulted in the following benefits over the conventional methods.
- *Improved Arc Strike:* Earlier method using inductance in power source led to unstable arc strike. With the recent waveform control, instant arc strike possible in GMAW, while in GTAW improve arc strike resulted in less electrode consumption.
- *Short circuit current regulation* by waveform control has resulted in less spatter and stable short circuit with higher speed of welding in GMAW.

- *Pulse current control* in advanced system resulted in deep penetration in GTAW and prevention of porosity and less spatter in GMAW. Ratio of electronegative/electropositive control in modern system makes deep penetration with reduced electrode consumption without the necessity of HF re-strike in GTAW possible. In GMAW the same controls lead to increase wire melting rate and permits penetration control.
- *Inverters* offer many possibilities, their applications are, however, limited to lower output and thus can not be used for high amps range of welding. For higher current ranges, alternative to the inverter is secondary pulsed and conventional sources (2). Although inverters are in use since late 1980, improvements made in last few years have made possible some inverters to approach the reliability levels to that of conventional power source (3).

The arc fusion processes for surfacing moderately thin layer of wear resistant materials include, GMAW, GTAW and PAW (plasma arc welding). These three processes are low current fusion welding techniques, which are used extensively for surfacing applications. The high current weld cladding operations are carried out by using SAW (submerged arc welding) and ESW (electroslag welding) processes. Since all these processes can be mechanized and computer controlled, it is possible to produce consistent quality products at a high rate of production. GMAW & GTAW processes along with torches employed are shown in Fig. 12.1.1 & Fig. 12.1.2 respectively.

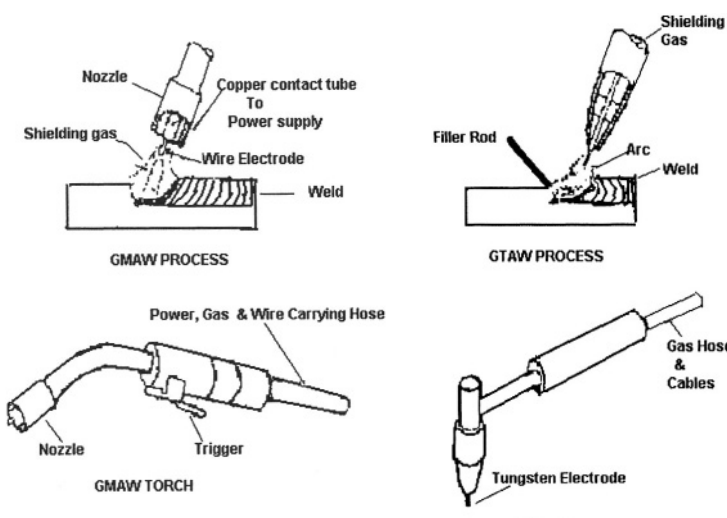


Fig.12.1.1 Gas Metal Arc Welding

Fig.12.1.2 Gas Tungsten Arc Welding

12.1.1 Gas Tungsten Arc Welding (GTAW)

In the gas tungsten arc welding (GTAW) process, the heat of the arc between a non-consumable tungsten electrode and base material is used to fuse the filler metal and the interface regions of two components to be joined (Fig. 12.1.2). The process can be made autogenous, i.e., can be used to join two surfaces without any filler metal. A shielding gas is provided to protect the molten metal from reacting with the atmosphere. The shielding gas is argon, helium or a mixture of the two gases. For weld surfacing, the consumables are in the form of continuous solid wire for ductile materials or in the form of rods (3.2 to 4mm dia) for harder materials, such as Stellites. GTAW process can be used to produce defect & spatter free high quality welds. The process allows precise control of the two main variables viz. heat source and filler metal. The weld penetration in the root pass is possible to control in GTAW. Almost all metals including dissimilar metals are welded by this process. The process can be made fully automatic producing high quality deposits of wear resistant materials with lower dilution than MMAW or GMAW. However, the deposition rates are lower than consumable electrode processes, making it more expensive for heavy deposition or joining thicker sections. DC, electrode negative technique is used for deep penetration and faster weld speed. Helium is a preferred gas for mechanised welding. The AC source provides cathodic cleaning of refractory oxides from the surfaces of reactive metals like Al and Mg. The repair welding procedures like the half bead, butterbead-temperbead and six layer GTAW techniques have been developed to produce refined and tempered microstructure for in-situ weld repairs (4). Refined microstructure of the weld, similar to 'temper-bead' can be obtained by pulsed GTAW. Low pulse frequencies and low welding speeds are required for obtaining necessary microstructural refinement (5). Pulsed GTAW has been found to be superior to half bead or butterbead-temperbead procedures adopted during repair welding.

Advantages of pulsed GTAW are follows (5):

- i. Weld deposit height can be kept at lower levels. It is easier to control and vary welding speed in pulsed GTAW and thus impose control on deposit layer height than that possible in normal GTAW. It is necessary to control the deposit layer height to a lower level in order to achieve both grain refinement and tempering..
- ii. The effective microstructural refinement can be obtained in single weld pass.
- iii. It is possible to weld hardenable steels without preheat due to inherent tempering effects of pulsing during welding.
- iv. Residual stress is lowered due to transformation plasticity effects of multiple cycling causing phase transformations on heating and cooling.

The main disadvantage in the use of pulsed GTAW to produce refined microstructures is the low productivity. Two other problem areas indicated in this practice, which are to be attended, include: prevention of overtempered soft layers formation in a multilayered deposit, and adoption of special procedures for weld starts and weld stop regions.

Applications:-

Valves:-

The preferred practice today is to use PTA for wear resistant coating on automotive engine valves. GTAW process is used mostly for heavy built-up, such as marine engine diesel valves, process control valves etc. The list of hardfacing alloys include cobalt base alloys such as Stellites for engine valves, nickel base (e.g., monel), cobalt base (e.g. Stellites), iron base (e.g. stainless steels) for process control valves.

Nimonic weld overlay on bar forging hammer:

The bar forging hammers are made of die steel (0.56 C, 1.1 Cr, 0.5 Mo, 1.7 Ni, 0.1 V) over which the weld overlay of Nomonic alloy (18.73 Cr, 12 Co, 5.8 Mo, 1.0 W, 1.7 Al, 2.86 Ti, Rest Ni) is made by GTAW process (6). The Nomonic type of alloys are capable of retaining high strength at the operating temperatures of the hammers (~850°C), due to the presence of gamma prime phase (nickel aluminide). As a matter of fact the yield strength of gamma prime phase increases with the increase in temperature up to the operating temperature of the hammer. However due to loss of aluminium and titanium in the electrode during welding arc transfer the preferred process for making weld overlay of Nomonic alloy is GTAW. In order to minimize the difference in the thermal expansion characteristics of the top f.c.c alloy (Nomonic) and the b.c.c substrate, it is necessary to have a buffer layer of Inconel 600, with thermal expansion characteristics intermediate between the f.c.c and b.c.c alloys. Most of the thickness build up is carried out with Inconel 600. A layer of Hastelloy C276 (C < 0.04, 16 Cr, 16 Mo, 4 W, Co > 2.5) is deposited in between Nomonic top layer and Inconel base layer to take care of dilution effect. The graded weld overlay deposits were found very effective in minimizing wear of bar forging hammers (6).

12.1.2 Gas Metal Arc Welding

In the gas metal arc process (GMAW) an arc between the electrode in the form of continuous wire and the substrate results in weld pool formation. The protective gas is fed externally (Fig. 12.1.1). The metal transfer from electrode to base in GMAW can occur by short circuit transfer, globular transfer, or spray transfer process. The type of transfer depends on various factors

including amount & type of welding current, electrode diameter, composition, electrode extension and shielding gas.

- i. Short circuit transfer mode:- In this process small, rapidly solidified weld pools are formed on electrodes touching the base metal or previous weld metal. In this transfer process lowest electrode diameters and welding currents are used. The spray transfer mode is suitable for out-of-position welding, joining thin sections, and bridging large root opening. As the electrode makes contact with the base the current starts increasing. The increase of current should be high enough to heat the electrode and ensure metal transfer. However, the current increase should be kept at minimum to avoid spatter caused by violent separation of metal drops. The current increase rate is controlled by adjustment of the inductance in the power source. In welding carbon and low alloy steels, a low spatter and good penetration can be obtained by using a mixture of argon and CO₂. The addition of helium to argon improves penetration in nonferrous metals.
- ii. Globular transfer mode:- At an average current of slightly higher than that used for short circuit transfer, globular droplets, with diameter larger than electrode diameter are transferred from electrode to base metal. The globular transfer mode requires high voltage to avoid spatter. High voltage, however leads to lack of fusion and insufficient penetration thus severely limiting the use of globular transfer mode in production applications.
- iii. Spray transfer mode:- At current above a critical value (called transition current), the transfer of highly directed stream of discrete droplets of metals in the form of spray occurs. The spray is accelerated axially by arc forces across the arc gap. Below the transition current, transfer mode becomes globular. The transition current depends on liquid metal surface tension & melting point, electrode diameter & extension and shielding gas. For electrode diameter of 1.1 mm, and shielding gas composition of 98% argon + 2% oxygen, the transition currents for mild steel and stainless steel electrodes are 220 and 225 amps respectively. Spray transfer mode can be used to weld almost any metal and alloy. However, thin sheets cannot be welded in this high current mode. Also overhead and vertical positions are difficult to weld in this mode. To overcome position and thickness limitations, specially designed power supply units producing controlled waveforms & frequencies that 'pulse' the welding current have been developed. The simplest power supply unit of this type, provides single frequency of pulsing (60-120 pps) with independent control of the background & pulsing current levels. More

sophisticated units, called *synergic*, automatically provide optimum characteristics.

Typical deposition rates during various transfer processes in GMAW are indicated in Table 12.1.1. The process is suitable for automated, repetitive weld overlay requirements. The shielding gas can be argon, helium, argon + helium, argon + CO₂, or argon + helium + CO₂, depending on the alloys. For weld surfacing by GMAW the consumable is in the form of a continuous wire, typically 1.2 to 1.6 mm diameter. One variation of GMAW is the use of tubular electrode containing metallic alloying elements (Metal cored electrode) plus deoxidants in powder form in the core. During the deposition process, the metal cored electrodes require external inert gas shielding. Another variation is the use of tubular wire containing fluxes inside. The flux cored wire (FCAW) generates shielding gas viz., carbon-dioxide, by decomposition of carbonates during welding. The deposition efficiency of the tubular electrode process is approximately equal to one and half times than that of manual metal arc welding. The benefits associated with high deposition efficiency include shorter arcing time, less total welding time and lower labor cost.

Tab.12.1.1 .Typical deposition rates in
Gas Metal Arc Welding(GMAW)

Process	Deposition(Kg/hr)
Spray transfer	5
Globular transfer	4
Pulse transfer	4
Dip transfer	3

Applications

For ductile materials, such as stainless steels, both the solid wire and the tubular versions are available. Only tubular wire are available for deposition of harder and difficult to be drawn into wire consumables such as Stellites. The tubular wires are used extensively for repair and resurfacing of railway crossings, crushing hammers in cement plant, coal crushing hammers in power plants and concast rolls in steel plants.

Cladding of superheater tubes in incinerators and coal-fired power plants:

The use of GMAW & GTAW for weld cladding of superheater tubes in incinerators of “waste-to-energy plants” and coal-fired power plants has been

reported (7). The tubes of 2.5-3 inch (63.5-76.2 mm) outside diameter are weld clad with Inconel® 625 with pulsed GMA welding and the weld is subsequently made smooth with a GTAW torch. Also used is Hastelloy C22. The dilution does not exceed 10%. GMAW-deposit contains distinct ridges and valleys and the clad surfaces tends to crack when bent for superheater pendants in boiler industries. With GTAW torch following, the remelting of the overlay leads to near-constant cladding thickness usually within a tolerance of 0.070" (1.778 mm). Water flows through the tube at a temperature of 100-110°F (37.77-43.33°C) throughout the welding operation. The tube life is reported to be twice than that of unclad tube.

Concast Roller:-

The SAW process for weld cladding of caster rolls makes use of metal cored tubular wire (8). The high heat required to melt wire and flux combination in the sub arc process results in fast heating of rolls enabling non-stop weld cladding of only large diameter rolls. For economical refurbishing and the production of rolls with 200 mm diameter or smaller, the FCAW process is recommended (9). The process requiring lower heat input leads to less dilution and distortion in comparison to SAW. Also a special nitrogen containing 400-N series of open arc welding wires developed to take care of basic problems associated with higher carbon containing ferritic stainless steels, such as AISI420. These are as follows:-

- Reducing carbon to 0.03–0.04 thus reducing extensive carbide precipitation, which may otherwise cause weld-decay and softening of the ferrite matrix. Addition of nitrogen improves high temperature strength and wear resistance.
- Low Ms temperature of ~200°C of the low carbon nitrogen containing 400 N series in comparison to 300–350°C of normal 400 series, allows use of low preheat and interpass temperature for welding in the austenitic range and results in faster cooling. The faster cooling results in tougher ferritic structure (9).

Repair weld overlay in nuclear reactor (10):-

The intergranular stress corrosion cracks were observed in nuclear reactor components, including the reactor tanks when inspected ultrasonically. The attempt to repair in-tank cracks by GTA weld overlay technique resulted in additional cracking in the HAZ of the repair welds. The additional cracking due to helium embrittlement is caused by the combined effect of ${}^4\text{He}$ that exists within the reactor tank walls (${}^4\text{He}$ is produced by the reaction of thermal neutron with nickel and boron), the heat input due to GTAW process, and the weld shrinkage stresses. The helium induced cracking tendency can be minimized by a low heat input GMA overlay process using AISI 304 austenitic stainless steel as consumable on the same substrate material. The

low heat input GMA produces limited changes in microstructure and helium distribution as compared to GTA weld material.

12.1.3 Plasma Arc Welding with Rod/Wire

The process is same as plasma transferred arc welding as discussed in Chapter 2. In this case, the consumable in the form of a rod or wire, is fed into the hot plasma column, resulting in weld pool formation by simultaneous fusion of the consumable and the substrate surface. The process is similar to GTAW. However the process has several distinct advantages over GTAW and GMAW using similar wire consumables. The plasma torch is unique in that the tungsten electrode is enclosed by the copper anode, and the argon gas is passed through the intervening space. This produces a hotter, more directionally stable arc column than that produced by GTAW or GMAW. Also by enclosing, the electrode is protected from fouling (a common problem in GTAW) and permits a longer workpiece-to-electrode (standoff) distance, and allows an additional benefit of reduced sensitivity to changes in welding distance (11). A secondary power supply maintains a pilot arc between the electrode and the orifice body that assists arc transfer at the start of the weld cycle. HF source is used to start the arc. The primary factors affecting heat input are the type of shielding gas, arc distance, welding current, plasma gas flow rate and welding rate or speed. Another important parameter is the arc column shape, which is determined by the orifice diameter.

Applications (11)

Exhaust Valves

A tubular wire of an iron base alloy (1.8 C, 0.8 Si, 10 Ni, 25 Cr, 5.5 Mo, bal Fe) has been developed (11) as a cheaper substitute to satellites for exhaust valve application. The alloy has similar corrosion and wear resistance to that of Stellites (12). The exhaust valve welding set-up (Fig. 12.1.3) consists of plasma arc welding torch, a water-cooled copper block fixture for supporting the valve, a motor to produce circular motion to the fixture along its axis, and a wire feeder. Power supply to the torch is programmable with controls on current upslope while starting and downslope when finishing the operation. Once set, the gap or voltage between the torch and the substrate can be maintained constant through sensing and adjusting the gap by automatic voltage control (AVC) unit. The oscillator can be used to control the bead shape and size. The whole process is made automated and a preprogrammed operation can be run by a single operator. By selecting optimum welding parameters, the poor overlap quality (radial cracks and blowholes), which is problem in GTAW process, can be avoided in plasma arc process for the same alloy.

A comparison amongst weld surfacing processes, such as GMAW, GTAW & PTAW is made in Table 12.1.2. Pulsed GMAW has been used in this comparison. The deposition rate of 1.3 kg, similar to that of PTAW using powder can be obtained in GMAW with 1.6 mm diameter electrode. The use of smaller diameter wires reduces deposition rates. Larger diameters requiring higher currents shall result in higher dilution. In GTAW, a deposition rate of 0.8 kg is achieved by using bare rods of 3.5 to 4.0mm diameters. In GMAW, melting occurs by direct arcing of electrode with the base metal, hence process power required is less than that of the other two processes, i.e., GTAW & PTAW. In GTAW & PTAW, consumables are melted by heat of the arc formed between a non consumable electrode and the base. However PTAW using consumables in the form of powder requires less power to melt compared to that of GTAW using cast rods. The deposition efficiency in PTAW is low due to loss of powder alloys falling outside the plasma plume. In the absence of spatter and other losses, GTAW has the highest deposition efficiency. At similar deposition rates, it is possible to get minimum dilution with PTAW compared to other two processes. The unique advantage of GMAW over the other two processes is the possibility of weld surfacing in all positions.

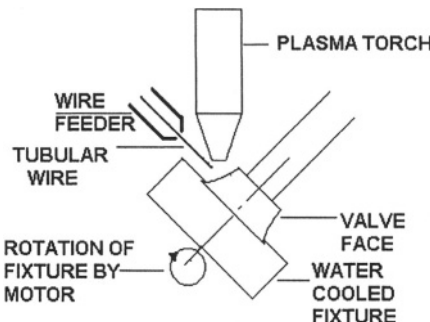


FIG.12.1.3.PLASMA ARC DEPOSITION BY CORED WIRE ON EXHAUST VALVE FACE(SCHEMATIC)

Bore Surfacing and Comparison of GMAW/GTAW/PTAW :-

Internal bore of pipes carrying corrosive or erosive fluid or slurry are quite often required to be clad with wear and corrosion resistant materials. The equipments available commercially can be used to overlay minimum bore diameters of less than 1 inch (<25 mm). It is possible to modify the torch belonging to any one of the processes, such as, GTAW, GMAW and PTAW for surfacing internal diameter of tubular structure. The main advantage of GMAW is use of consumable electrode and thus, unlike GTAW extra provision for electrode for feeding consumable rod or wire is not required in

the compact ID torch system. In PTAW, powder is feed through an internal bore in the torch. For thicker single layer deposit GMAW is superior to PTAW in bore surfacing. Lower dilutions can be attained by using reverse polarity soft plasma arc (13). For precise thin layer with very low dilution powder fed PTAW is the best process for bore surfacing. It is possible to weld deposit in smaller diameter bores in GMAW & PTAW in comparison to GTAW (Table 12.1.2). Application areas include weld overlaying with wear and corrosion resistant alloys for complicated valves and forgings such as well head Christmas trees.

Tab.12.1.2 Comparison of Weld Surfacing by GTA, GMA & PTA Processes

PROPERTIES	PULSED GMAW	GTAW	PTAW
1.Deposition Rate (Kg/hr/100A)	1.3 (1.6mm dia)	0.8(rod)	1.1(powder)
2.Process Power per Kg deposited (MJ/Kg)	5	9	7
3.Deposition Efficiency	98%	99-100%	90-95%
4.Current Range(A)	50-350	90-220	80-240
5.Dilution Achievable(%)	5-20%	7- 20%	2-15%
6.Surfacing Position	All	Flat	Flat
7.ID Surfacing Capabilities (bore diax length in mm)	20x2000	200x450	20x450

The ID torch (Fig. 12.1.4) can be completely automated with digital readout of weld head position and digital surface speed control to build not only complete bore surface but also worn section in the bore. For example a gas cooler shell from offshore oil rig has been weld cladded with Inconel 625, the main bore by automatic GMAW and the branches and nozzles by automatic GTAW (14).

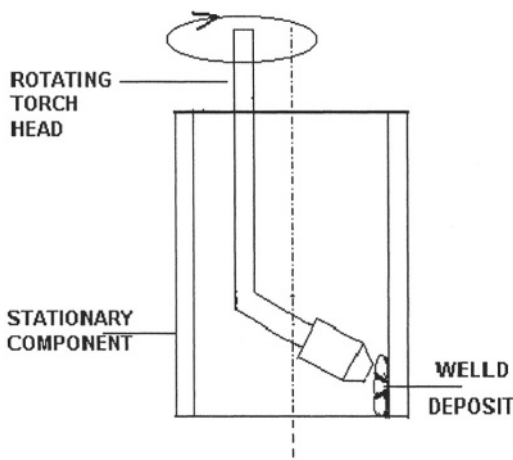


FIG.12.1.4.GMAW ID TORCH SYSTEM

12.1.4 Submerged Arc Welding (SAW) Process:-

SAW has been used for applications requiring heavy deposition. In this process, the arc is established between a consumable electrode and base metal submerged in the fusible flux material. (Fig. 12.1.5). Powder alloys can be added along with the flux. The consumable electrode is in the form of wire or strip. In SAW, very high deposition rates can be achieved by using current up to 2000 amps, in ac or dc mode using single or multiple wires or strips as consumable electrodes. The flux stabilizes the arc, provides slag coverage, and also controls the properties of deposits.

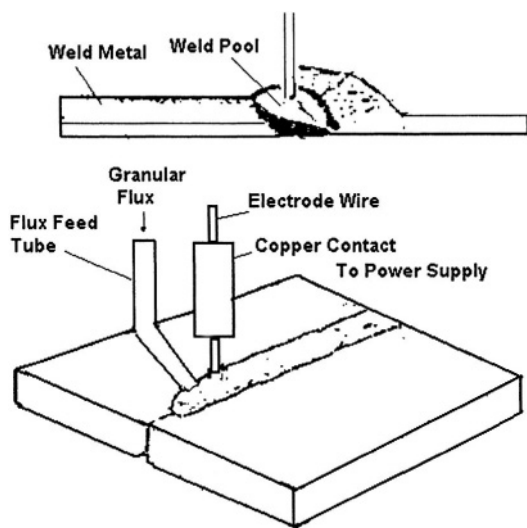


Fig.12.1.5 Submerged Arc Welding Process (Schematic)

Recently the process has been used to deposit various alloys by feeding powder alloys in the weld zone. The bulk welding process utilises the existing heat produced by SAW to melt powders and thereby increases deposition rates. In this process, a powder composition that matches the feed wire composition is used. Powder metal to wire ratio can be as high as 2:1. Advantages claimed for this process are as follows (15):-

- 2 to 3 times the deposition rate over single wire without increasing heat input
- Less flux consumption
- Less distortion due to lower heat input
- Economy due to less number of welding passes

Submerged arc strip cladding has proven itself to be also a highly productive process for surfacing large areas.

Applications

The process has been made fully automatic for heavy depositions in various applications, such as, surfacing of continuous casting rollers, blast furnace bells, forging die block, inside of ball mill shell, etc.

Concast Roller:

In continuous casting of steel, the molten metal is poured through a tundish into a bottomless mould, where the skin formation occurs before being drawn through a series of caster rolls resulting in the formation of a slab or bloom, or billet or rod. Rolls at the top are exposed to very high temperatures because of the skin is in contact with molten metal at the interior. At the same time mechanical load is lower. Since the skin is quite thin, the material is quite prone to bulging and to prevent this, the top rolls are usually smaller in diameter and placed closer together in the caster. Down the line, the rolls are larger in diameter in order to support the increased mechanical load due to progressive solidification and cooling of the slab. The highest mechanical loads of the entire process are where the slab is converted from a curved to a straight section. The diameters of the steel rolls normally range from 6" (150 mm) to 18" (450 mm). To ensure that the slab does not bulge while solidifying, consistent roll pressure is to be maintained. Also it is necessary to ensure the rolls are not worn or bent. A castor roll can carry more than one-million tons of steel during its relatively short life, which averages only six months to a year. It is necessary to undertake preventive maintenance through weld surfacing of the rolls at regular interval in order to attain full life span. Rolls are subjected to thermal fatigue and stress corrosion cracking, due to

- cyclic loading due to passage of slab
- thermal stresses due to make and break of contacts by hot slab

- corrosion due to chemical reaction of ionized hydrogen and halogen from slag.

As a result of these factors pits and crevices are formed on the surface, which is known as 'fire-cracking or fine-checking'. Wear of as little as 0.050" (1.27 mm) can cause defects to appear on slab surface. Every four to six weeks most mills will replace a segment containing 6 to 10 resurfaced rolls from the caster, which can contain as many as 120 rolls (8). The rolls make contact with hot steels at temperature as high as 2400°F (1316°C) and then suddenly undergo extreme thermal shocks due to spray cooling process that controls the slab (bloom, billet or rod) formation process.

The continuous casting rolls are normally made from carbon or low alloy steels, such as DIN21 Cr MoV5.11 (0.22 C, 0.4 Si, 0.4 Mn 1.4 Cr, 1.1 Mo, 0.3 V) (16). The new rolls are weld surfaced by SAW process. The alloys used for surfacing and resurfacing of rolls are mainly from 400-series stainless steels, such as AISI 410, 420, and 414. The composite rolls provide resistance to abrasion, corrosion, and fire checking at the working temperatures. The consumable is in the form of strip (16) or more recently tubular metal cored wire (8). Both acidic and basic fluxes are used. A proper wire-flux combination is to be used for obtaining required deposit quality. In AISI 420 (0.2% C, 12% Cr) weld deposit, the chromium and carbon recovery vary significantly with acid flux, but not with basic flux, when the flux-to-wire ratio is varied (17).

Typically four or more layers of weld deposits are applied. The preheat and interpass temperature are maintained in between 300°C to 350°C (572°F-662°F), in order to avoid brittle fracture. The preheat and interpass temperatures are to be such as to produce high enough cooling rates for transformation of austenite to martensite. The post weld heat treatment (PWHT) is conducted to adjust the cladding hardness for machining and service. This metal cored tubular-flux combination has been proved successful in prolonging the life of castor rolls by 200% to 300%, replacing earlier strip cladding processes (8). One of the problems encountered in weld metal deposited by submerged arc welding is the initiation of cracks from the bead overlap areas (9). In order to minimize this problem, a wide bead (bead size = 3 to 4 times normal) technique has been adopted which would result in a substantial reduction in the number of bead overlap interfaces on each roll (8). PTA weld overlays on concast rollers are described in Chapter 2(18).

Strip Cladding in Nuclear Vessels (19,20,21)

Nuclear vessels are made from low alloy ferritic steels, such as, SA 508 CL2, 3 or SA 533 GR.B, CL1. The inner side of the vessel are normally weld clad with austenitic stainless steel to minimize the corrosive attack. The SAW process is used for cladding with AISI 309 L in the form of strip (Table 12.1.3).

Tab. 12.1.3 Compositions of selected alloys used for nuclear vessels

Alloy Grade	Weight % Elements							
	C	S	Mn	Ni	Cr	Mo	V	P
SA 5 C 8	0.18	0.3	1.41	0.95	0.22	0.58	0.003	0.005
309L	0.019	0.53	1.71	13	24.69	0.1	0.02	0.021

Few basic problems faced in this cladding process are:-

- *High residual stress* generated due to dissimilar metals joining may cause cracks (1). Due to the large difference in the coefficients of thermal expansion between ferritic base and the austenitic weld overlay high residual stresses are generated during the cooling process after welding. A potential problem with the cladded reactor vessel is the formation of underclad cracks. Residual stress of sufficient magnitude can cause brittle fracture, stress corrosion cracking and 'pop in' of shallow inside surface cracks. Maximum tensile stresses occurred at the bead overlapped regions and about 6mm below the fusion line in the base metal. The peak stress parallel to welding direction approached 331.2 MPa (19). The maximum stress level dropped down to 150 and 200 MPa after 42 hours PWHT.
- *Stress Intensity Factor and Defect Size* (19):- The maximum stress intensity factors, calculated theoretically from the residual stress distribution, were found to occur at crack sizes of 15mm for the surface(edge) and 7mm to 14 mm at the subsurface.
- *Carbon Migration during PWHT*:- The carbon migration reduces the strength of ferritic base, carbon-enrichment forms carbides in austenitic weld and less carbon at grain boundaries causes weld decay. The carbon concentrations in the weld during post weld heat treatment (PWHT) at $620 \pm 5^\circ\text{C}$, increases from 0.019% of 309 L to 0.02% after 20 hours, 0.03 after 40 hours, 0.0495 after 60 hours, 0.07 after 100 hours, and 0.125 after 200 hours (20). Normally PWHT is carried out 620°C for around 40 hours.
- *Dilution and Underbead Cracking* (21):- One of the factors responsible for underbead crack formation is the dilution. The lowest base metal dilution rate was found at heat input of 168 kJ/cm for 90 mm strip cladding (21).

12.1.5 Electroslag Welding

The process is initiated by a starting arc between the electrode and the base metal surface. The heat of the arc melts the added granulated welding flux. With the formation of sufficiently thick molten slag layer, all arc actions stop. The passage of welding current through the conductive slag leads to ohmic heating of consumable, base metal and the flux. The electromagnetic action leads to vigorous stirring of molten conductive slag. Heat diffuses rapidly throughout the entire cross section being welded. The electrodes used are of normally in the forms of wires (solid or metal cored) or strips. Since there is no continuous arc between the electrode and the workpiece as it is in SAW, ESW produces up to 50% less dilution compared to that of SAW (22). Travel speed and current are the parameters affecting dilution. With higher speed, the composition becomes leaner as a result of changed ratio of bead thickness to penetration. The increase in current has a similar effect on dilution. Although penetration increases, dilution decreases since there is a comparative increase in bead thickness. Since dilution is less with this process, specially formulated strip electrodes are being developed to obtain certain weld metal chemistry (22). The deposition rate in ESW using strip electrode can be as high as 30.0 kg/hr compared to maximum of 20.0 kg/hr. in SAW using powder and wire or 12 kg/hr. using strip (Table 12.1.4).

Tab.12.1.4.Typical deposition rates in SAW & ESW

SAW					ESAW
Consumables	Single wire	Two wires	Strip	Wire + Powder	Strip
Deposition(kg/hr)	8	14	12	20	30

Advantages claimed for this process include:-

1. Extremely high deposition rate of 15-30 kg/hr is obtained in a single pass.
2. No preheat is required
3. High quality weld deposit due to refining action of slag.
4. No weld spatter formation.

Applications

Surfacing of Metallurgical Rolls (23)

The main disadvantage in SAW process compared to ESW is the presence of nonmetallic oxide inclusions in the weld deposit. The high stress generated on the roll surface during rolling may lead to elongation of type II manganese sulphide inclusions and high strain areas around non-deformable oxide inclusions. The subsurface region containing these inclusions are the areas of decohesion and extension of the decohesion areas under load shall result in

early failure of the roll. The high quality deposit of ESW has led to the production of inclusion-free high quality deposits on the rolls for cold rolling. A cold rolling mill roll of 530 mm diameter and 1200mm barrel length was surfaced by ESW deposition of 960 kg in 150 minutes. The rolls after surfacing were heat treated and ground finished before putting in service.

12.2 Arc Light Assisted Processes:

The optical radiation from a high powered arc lamp has been used as heat source for surface modification. The short wavelength radiations ($>1 \mu\text{m}$) promote better absorption of the beams than $10.5 \mu\text{m}$ radiation from a typical 5 kW CW-CO₂ laser (24).

Arc Lamp Radiation Heating System

A 300 kW high pressure argon-filled DC-arc lamp radiates 40% of the power in the form of light in the spectral range of 0.2–1.4 μm . Arc is struck between two tungsten tipped electrodes placed inside the quartz lamp tube at a distance of ~110 mm apart. Arc lamps can run at a 1000 A current with a resulting power input of around 300kW. Visible white light radiates from the arc glow of similar length as that of the distance between the electrode tips. The electrodes are cooled by circulating water. The quartz lamp tube is cooled in spiraling recirculated water and argon streams. The water forms a thin layer on the inside surface of the tube and argon gas forms a vortex within the water wall. Light is reflected by water cooled reflector and focused onto the substrate surface. Of the three types of available reflector geometries, closely coupled elliptical reflector configuration provides a peak power density (Gaussian distribution) of more than 3.5 kW/cm^2 is preferred for surface treatment. The specimen is cooled by water circulating base plate attached to it (Fig. 12.2.1). The available commercial arc lamp heating systems include Vortek Water-Wall™ arc lamp (Vortek Industries, Vancouver, BC, Canada).

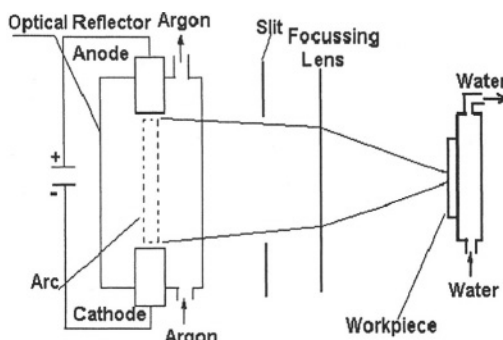


Fig.12.2.1.Schematic Diagram of Arc-Lamp Beam Heating System

Arc Light assisted surface hardening:-

For surface hardening, a beam of 40×100 mm is focused onto the workpiece with a traverse speed of 5-50 mm/sec in order to generate required heat of ~ 2 kW/cm². When a thin surface layer is heated above the critical temperature by a controlled light beam, the bulk of the material can serve as the quenching medium once the heat source is removed. A 40 kW beam can achieve 0.5 mm case depth in three times greater surface area compared to 20 kW CO₂ laser beam. An uniform case hardness of 900 HV was obtained in a tool steel surface. The process is faster than other surface hardening processes, and is an economical alternative and supplement to CO₂ laser for thermal surface treatment. Successful trial runs are conducted for surface hardening of A1S1 1040 rods, 1040-and 4140-flats, 1060-agricultural plow blades and sharp tool-steel die cutter blades.

Arc light assisted fusion of surface coatings (25) :-

Arc light has been used to fuse HVOF or arc spray coating of Fe-Cr-B alloy on mild steel surface. The coating thicknesses was maintained in between 0.5 to 0.635 mm .The coating was melted at a linear traverse rate of 8.38 mm/sec, with a peak power density of 2.1 kW/cm² at 1000 A. An irradiance up to 2.1 kW/cm² with wavelength from 200 to 1400 nm was achieved over a 2.2 cm \times 11.9 cm area. Under these conditions the thickness of the HAZ was optimized and was limited to 0.7 mm, i.e., the coating thickness. Remelted coating material showed finer, homogenous grains. The dense pore-free coating with strong metallurgical bonding to the substrate resulted by re-melting. The cooling rate (dT/dt) of the melted coating was determined from the secondary arm spacings (D) (26) using following equation:

$$D = 60 \times (dT/dt)^{-0.41}$$

The calculated cooling rates for D as 0.5 and 1.0 μm vary between 2.2×10^4 °C/s and 1.2×10^5 °C/s. When a thin layer of as-sprayed Fe-Cr-B was rapidly melted by arc light and allowed to cool at a rate faster than 10^5 °C/sec on highly conductive substrate, ultrafine crystalline or amorphous metal forms on the surface. An increase in scanning speed results in lower cooling rates and less refinement in the structure. The refinement across the thickness of HVOF coating has been observed at a scan rate not more than 4.32 mm/s (0.17"/s). The arc spray coating of the same material and thickness requires more power. At constant power density the microhardness increases with the decrease in scanning speed. The average microhardness of 1032 HV was noted for HVOF samples processed at 4.32 mm/s while average hardness of 696 HV was observed on surfaces scanned at 7.62 mm/s. The microhardness of arc sprayed

coating did not show any improvement by rapid solidification process and remained at 500 HV. The abrasive wear test conducted as per stipulations made in ASTM G-65 showed the wear of arc beam melted Fe-Cr-B surface almost as half of that observed for highly wear resistant D2 steel. High power arc-lamp has the following advantages over CO_2 laser for thermal treatment of the surfaces (24):-

- Visible shorter wavelength ($<1 \mu\text{m}$) of arc light compared to invisible longer wavelength CO_2 laser light ($10.6 \mu\text{m}$) results in increased absorption of beam at the surface.
- Beam power can exceed 50 KW compared to 25 KW for laser.
- Spot size is larger thus enabling heating larger area than laser.
- Due to 1, 2, & 3 it is possible to heat rapidly larger surface area by arc light compared to laser.
- High pressure arc light is comparatively cheap in both capital and running cost.

12.3 Advanced Arc Spraying Process:

In arc spraying, an arc is struck between the ends of the consumable wires, and the resulting molten metal is carried by high pressure jet onto the surface to be coated (Fig. 12.3.1). The use of compressed air jet for atomisation results in the formation of oxides and porosities in the deposit. Also high burn-off rates of oxidizable elements may lead to deposits with compositions different from that of the original wire. For example, burn-off rates of C, Si, Mn and Cr in an arc sprayed steel can be as high as 50%. In other words, only 50% of these elements in the original steel wire are likely to be present in the deposit. The use of inert gas resulted in slight reduction in burn-off and oxidation. However the turbulence of the atomising gas leads to mixing with the surrounding atmosphere.

For special coating compositions, arc can be struck between two wires of different metals or alloys and sprayed onto the substrate. The process can be used for only electrically conductive materials, hence composites containing tungsten carbide can be sprayed only when used in the form of carbide-cored tubular metallic wire. The use of cored wire, in general, has resulted in vast improvement in the quality of arc sprayed deposits.

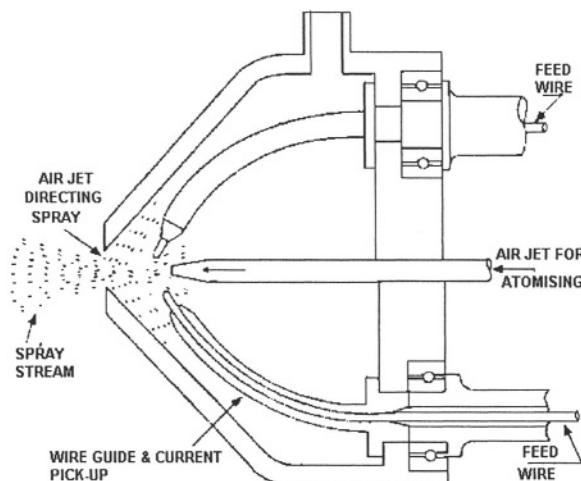


Fig.12.3.1 WIRE ARC SPRAY SYSTEM (SCHEMATIC)

Applications

Some major applications using arc spray process for deposition of wear resistant coatings, include Yankee dryer and black liquor recovery boilers.

Black Liquor Recovery Boilers (BLRB):-

It is a recovery boiler used in pulp industry for firing black liquor and inorganic compounds. The recovery boiler functions as a chemical reactor, the organic part of the fuel or the black liquor is burned and the inorganic part is reduced back to sodium sulfide. The boiler is divided in two parts, viz, one upper part with complete combustion and oxidising conditions, and the lower with oxygen deficient, reducing conditions. Water wall tubes, superheater tubes and other parts of the black liquor recovery boiler are subjected to corrosive attack of sulfur compound in the flue gas. The sulphidity of the fuel and operating pressure of the boiler affects corrosion rates. The sulfur from the flue reacts with iron forming iron sulfide. The corrosion rate increases when excess air is introduced in the boiler. The formation of sulfur dioxide increases the corrosion rate. The corrosion rate also increases rapidly at temperature above 300°C. Also the areas in contact with molten smelt is subjected to rapid corrosive attack.

The high aluminum containing Fe-22Cr-6Al coating material (27) resists corrosion due to sulfur and has thermal expansion coefficient in the temperature range of 20-600°C as $12 \times 10^{-6} \text{ }^{\circ}\text{C}^{-1}$, compared to that of steel tube material as $12.5 \times 10^{-6} \text{ }^{\circ}\text{C}^{-1}$. The almost identical thermal expansion characteristics prevents spalling or crack formation due to differential thermal

expansion. The high aluminum containing alloy is self bonding and thus no bond coat is required.

The bond strength of arc sprayed coating is 50 MPa (7100 psi) and the hardness of the coating is 230 VPN. Arc sprayed coating has superior bond strength than that of flame sprayed coating. However, the flame spray coating is less porous and contains less oxides. The porosity of flame sprayed coating is found to be around 5% by volume. A flame sprayed dense, low porosity top coat of Kanthal M on arc sprayed deposit of same material exhibits superior corrosion resistance. The coating thickness is limited to around 0.3-0.5 mm.

The corrosion rates of high nickel alloys (Ni-Cr-Mo-Al type) in sulfide atmosphere are found to be high due to penetration of corrosive fluids through the coating resulting in corrosive attack on tube and debonding of the coating (27). The field tests conducted with arc sprayed Ni-43Cr-4Ti alloy coating in the recovery boilers have shown encouraging results (28).

Yankee Dryer

Arc sprayed coating of AISI 420 stainless steel on the paper mill drying cylinders, in general, meets all the coating requirements, excepting poor heat conduction characteristics. The reduction in thermal characteristic is primarily due to thermal resistance of stainless steel. The presence of comparatively larger quantities of insulating materials like porosities and nonmetallic inclusions also reduces the heat transfer capacity of the coating. Because of lower heat transfer capacity compared to that of the original cast iron surface, the use of arc sprayed AISI 420 coating can result in lowering of cooling rate from 10% to 15%, particularly in the high speed tissue machines. However the coating is preferred in non tissue making lower speed machines. It is more economical to apply AISI 420 by arc spraying than producing plasma sprayed molybdenum coating. The coating provides a more uniform surface on the cast iron dryer and covers flaws on the cast surface. Also lower rate of heat transfer through the coating shall make the temperature across the face uniform. Uniform surface qualities and temperatures shall lead to uniform quality of the paper.

12.4 Electroconsolidation Cladding

In this process the green compact made from powder material is consolidated further by applying pressure through particulate conductive solid while the part is heated by current carried by granules. The spherical graphite granules are used as pressure and current transmitting medium. The electroconsolidation is also known as “soft tooling” or “pseudo-isostatic” process. Advantages claimed for the process over hot pressing and HIPing include elimination of encasing powder to be compacted, short cycle time, and very high temperature capability ($>2500^{\circ}\text{C}$). The process can be used for clad-

densification of green compacts making outer casing of the components. The hard casing materials for electro-consolidated clad layer include silicon carbide, oxide ceramics, and several metal powder systems including gamma prime phase (Ni_3Al) (29).

References

1. H. Yamamoto, S. Harada, and T. Ueyama, Inverters advance welding automation for joining metals, American Machinist, April, 1993, p29-32.
2. Dagobert Fleming, Stainless Steel Europe, Dec, 1990, vol2, issue7, p27
3. Mike Sammons, WJ, May 2000, p35-39
4. P J Alberry and J G Feldstein, W J, 66(12), 33-42, 1987
5. P R Vishnu, and K Easterling, A model based investigation into the promise of using pulsed GTAW for weld repairs, Proc. Int. Trends in Welding Science and Technology, 1-5 June, 1993, (Gatlinburg, TN), S.A. David, J.M. Vitek Ed., ASM International, p399-401
6. "High Temperature High Strength Nickel Base Alloy for Wear Resistant Weld Overlay on Horizontal Forging Tools", published literature from Thyssen Edelstahlwerke AG, Germany
7. Tim Heston, WJ, July, 2000, p45-47
8. Cored wire add life to caster rolls, article by The Lincoln Electric Co, Cleaveland, Ohio, in WJ, June 1996, p55-57
9. 'Process Compared for Roll Cladding', an article in the published literature of Welding Alloys Ltd, UK
10. Micheal H. Tusten and Philip A. Kestin, Proc. Int. Conf. on Structure-Property Relationships and Corrosion with the Environmental Degradation of Engineering Materials, Monterey, CA, 1992, IMS-ASM, published as Microstructural Science, vol. 19, p3-12
11. W.M.Matlock & others, Source Book of Wear Control Technology, ASM, 1978, p354-359
12. D.T. Spencer, A. Patel, J.H. Nixon, and S. Grainger, Comparison of GMAW, GTAW and PTAW for Wear Surfacing, Surface Engineering, June, 1987, p25-34
13. G.L. Swales & B. Todd, Proc. 28th Annual Conf. of Metallurgists of the Canadian Institute of Mining & Metallurgy, Meeting of Sea and Science, Halifax, Nova Scotia, 20-24 August, 1989
14. N Stephension, Versatility of highly alloyed Ni-Cr-Mo welding consumables – Part I, Welding and Metal Fabrication, August/September 1990, p376-386
15. Welding Handbook, AWS, vol 7, p1076-1077
16. Roger A. Swain, Strip Overlay Increases Caster Roll Service Life, Proc. ITSC'86, Sept.8-12, Montreal, Canada, 1986, p669-673
17. D.J. Kotecki, WJ, 1994, Jan, p16-s-23s

18. H. Hellen & Others, IITC'92, 28 May – 5 June, 1992, Orlando, Florida, USA, p. 893-897.
19. S-H. Nho, H-S. Ann, & C-W. Ong, Deviation of theoretical residual stress and stress intensity factors in dissimilar weld metal in nuclear vessel, Proc. Conf. Int. Trends in Welding Science & Technology, Ed:-S.A. David & J.M. Vitek, Gatlinburg, TN, June 1-5, 1992, ASM-Int, p117-123
20. B-C. Kin, K-S. Ann & J-T. Song, *ibid*, p307-313
21. S-W .Kin, & others, *ibid*, p825-830
22. S. Pak et.al., Svetsaren, vol 51, no 3, 1996, p28-33, Sweden
23. P. Blaskovic and J.W. Kiser, Proc. of ITSC'86, Montreal, Sept 8-12, 1986, p675-682, Pergamon Press
24. J.A. Vaccari, Arc Lamp Takes on Lasers, American Machining, Feb 1993, p45-47
25. Z.S. Wronaski & others, Rapid Solidification Processing of Thermal Spray Coatings using Powerful White Light Sources, Proc. ITSC'92, Florida, 28 May-5 June, 1992
26. W.E. Brower, R. Strachan, and M.C. Flemmings, Cast Metals J, 1970, 12, 176
27. S. Gustafsson, Thermal Coating As Corrosion Protection in Boilers, ITSC'86, p19-28.
28. M.L. Thorpe and R.H. Unger, ITSC'86 p3-17
29. Brain Merkle & Joshua Borton, PM2TEC 2000 Int. Conf. on Powder Metallurgy and Particulate Materials, 30 May-3 June, 2000, New York, MPIF.

This page intentionally left blank

Chapter 13

HOT ISOSTATIC PRESS (HIP)

13.0 Introduction

Hot isostatic press has been used in forming diffused coating of material deposited by processes like thermal spraying or pre-placed materials at the required locations on the surface of the component. An uniform pressure from all direction is applied on the pre-coated component through a fluid medium at high temperature leading to the formation of a dense diffused coating. The HIP process and its applications in forming wear resistant coatings are to be covered in this chapter.

13.1 HIP Process

The normal process of compaction of powder material involves uniaxial pressing in a die followed by sintering for densification. However better densification can be achieved by exerting pressure from all direction through a fluid medium on the powder material retained in container (die). The process for compaction by application of uniform pressure in all direction is known as isostatic compaction. If the operation is carried out at high temperature, the process is known as hot isostatic pressing or HIP. For cold process (CIP) the fluid medium used is water, while argon is used as fluid for hot process.

Process

In this process, the powder materials encapsulated in a sealed container is pressed from all sides with equal pressure (isostatic pressure) at elevated temperature for consolidation into a dense compact solid. Densification occurs mainly due to creep and sintering. Inert gas, normally argon is used as a medium for the application of isostatic pressure in a pressure vessel containing the sealed can with encapsulated powder materials (Fig. 13.1). The pressure used for compaction is in the range of 100-3300 MPa (15-45 ksi). Material used for canning is normally mild steel. Stainless steel and glass are also used for powder container. After inserting powder coated component the container is evacuated by vacuum suction and sealed hermetically. The temperature used normally is in the range of 1000 to 1200°C. However for ceramic and carbon base materials higher temperatures of around 1500°C have been used.

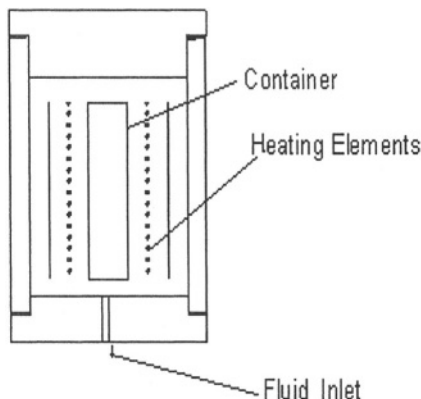


Fig13.1 Schematic Diagram of HIP

13.2 Diffusion bonding by HIP

Diffusion bonding of wear and corrosion resistant material onto the surface of base material by hot isostatic process has been utilised for a large number of applications. The diffusion bonding has been obtained between powder-solid, solid-solid or even powder-powder surfaces. The base or coating material, therefore can be either solid or powder form. The temperature at which diffusion bonding occurs during hot isostatic process is normally around 50-70% of the melting point of low melting point material. The pressure employed should be sufficient to close the pores. Both the treatment time and temperature should be kept at the minimum. This would not only decrease the cost but also prevent brittle intermetallic phase formation & excessive grain growth. Diffusion bonding involves no melting of either material, hence there is no segregation, no shrinkage crack formation at the interfacial mixed zone. In certain cases, diffusion barrier layer is used to prevent diffusion of undesirable elements from top layer to substrate. For example an 100 μm thick Ni-Cu-Ni interlayer has been used as carbon diffusing barrier between a tool steel & 17-4 stainless steel and also Stellite & 17-4 stainless steel (1). Examples of applications utilising diffusion bonding through HIPing include the followings (2)

- i. Nickel base superalloy, such as, Inconel 625(Ni-Cr-Cb) as corrosion resistant coating on a low alloy steel base (3)
- ii. Wear & corrosion resistant cobalt base superalloy, such as MPL-1 (Co-Ni-Cr-Mo plus minor additions of Ti, Nb or Al) alloy cladding on AISI 4140 steel (3)

- iii. Excellent adhesive wear resistant at high cutting speed in red hot condition, such as high speed steel, CPM9V (1.78C-5.25Cr-1.3Mo-9V), clad on exterior of AISI 4140 Cylinders (3).
- iv. Twin extrusion barrel internally clad with, high speed steel, such as CPM10V (2.45C-5.25Cr-1.3Mo-9.75V) against AISI 4140 steel (3)
- v. High speed steel, CPM10V clad to low carbon steel for segmented screws used in plastic extrusion barrel (4).

Industry-wise application list includes following:-

Automotive Industries (5):-

HIP process has been used to improve wear resistance of the automotive components, such as, turbocharger wheels and diesel engine valve lifters. A dual alloy wheel is made by diffusion bonding of an outer cast iron ring to the hub made from consolidated powder alloy by HIP. For diesel engine valve lifters, tungsten carbide is bonded to the working face of alloy steel lifters by HIP.

Aeroengine Components:

In order to reduce wear of turbine blades, abrasive tips are made from layered compacts of ceramic and metallic powders. Thermal spray coatings by plasma or HVOF process are used extensively for aeroengine components. Advanced spray systems with high flame velocities (>velocity of sound) are used to reduce the porosities in the coatings and improve bonding of coating to substrate. By hot isostatic pressing of the sprayed component it is possible to eliminate porosities in coating by further densification and improve bonding by diffusion to substrate.

Offshore, Chemical and Petrochemical Industries (5):-

HIP process is used for cladding with wear & corrosion resistant materials, such as stainless steel, Inconel, Monel, Hastelloy, Stellites etc of valve bodies, thick walled castings and producing compound tubes.

Tools and Dies (6):-

The process has been used for buildup of wear resistant materials on the working face, e.g., tungsten carbide on cutting edges of tool steel inserts, Stellite 21 on hot working tool steel backing for hot forging (gives 2-time life of welded overlay of St21), D2 steel cladding on stainless steel shaft (significantly more life than nitrided & weld-clad shafts used in a vegetable oil extraction plant).

Edge Forming Rolls (6):-

Bonding on hot-mill roll surfaces of a mixture of hard particle in a tough heat resistant matrix has provided a 10-fold increase in edger rolls.

Valve Lifters for Diesel Truck Engines (7):-

Bonding of WC to wear faces increased life by several folds.

Plastic Injection Mold and Extrusion Screw (7):-

Bonding a wear & corrosion resistant coating to the inside of the steel cylinder increased the life of the component substantially.

13.3 HIP Quenching of diffused layer (7):-

After HIPing, the diffused layer can be quenched by high-pressure argon gas at pressures of 200 MPa (29×10^3 psi) to obtain fast cooling rates of 500°C/min (900°F/min). High pressure argon gas with its very high and uniform heat-transfer coefficient results in improved metallurgical properties at a shorter HIP cycle.

References

1. Forecast Processes, AM&P, 2001, p59
2. J.J. Conway and F.J. Rizzo, Hot Isostatic Pressing of Metal Powders, Metals Handbook, vol 7, Powder Metal Technologies and Applications, ASM International, 1998, p605-620
3. J.J. Conway and J. H. Moll, Current Status of Powder Metallurgy, Near Net Shapes by Hot Isostatic Pressing, Int. 3rd Conf. on Near Net Shape Manufacturing, Pittsburgh, ASM Int., 27-29 Sept, 1993, p125-131
4. A. Guthrie and R.K. Wakerling, Vacuum Equipment and Technologies, 1949, p191
5. HIP makes great stride, Matls. World, 1999, November, p677
6. Brian Birch and David Wilkins, Advances in thermal processing techniques for tools and dies (part 2), Metallurgia, March 1993, p88-90.
7. Forecast Processes, Advanced Materials & Processes, January, 1991, p62-63.

Chapter 14

FLUID BED PROCESSES

14.0 Introduction

Fluids are used as media for fast transfer of heat from the source to the component during heat treatment and for fast dissipation of heat from the component during quenching. Both gases and liquids are used as heat transfer media. Also used are reactive fluid media, such as, fused salts (boride) or carbon monoxide (by dissociation of alcohol) or nitrogen (dissociation of ammonia) for diffusion of interstitials in surface layer.

14.1 Fluid Bed Processes for Thermal Treatments:

During heat treatment in hot fluids, such as gas or liquid, the heat transfer from the media to the components is extremely fast and uniform. The heat transfer coefficients (1) of liquid media are higher than gas (Table 14.1). The heat transfer coefficient of fluidised bed is in-between that of liquid and gas.

Table 14.1: Heat Transfer Coefficients of Selected Media

Quenching Media	Heat Transfer Coefficient (W m ⁻² K ⁻¹)
1. Gas Circulated (1000 mbar N ₂)	100-150
2. Gas (high pressure & velocity)	300-400
3. Salt bath (550°C)	350-450
4. Fluidised bed *	400-500
5. Salt bath *	600-800

*Depending on Temperatures

Molten salt baths have been used extensively to carry out a variety of thermal treatments including surface hardening, tempering, and cleaning. Heated liquids are extremely effective in encapsulating components without the formation of dead zones. The action of convection currents within the molten liquid ensures temperature uniformity and consistency of processing throughout the load. Surface cleaning can be carried out in oxidizing caustic molten salt. Alternatively salt bath as electrolyte can be used for surface oxidation or reduction by changing polarity. For example reduction cycle can be used to remove oxides and sands from special castings and oxidation cycle

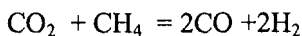
to remove graphite from cast iron surface in order to make the surface suitable for bonding or brazing (1).

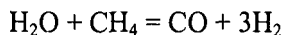
14.2 Fluidised Gas Bed (2)

In an enclosed chamber by controlling the pressure & volume of gas flow rates through a bed of particles, such as alumina, the particles are kept in suspension and form what is known as fluidised bed. In a fluidised bed system, a retort or chamber is filled with particulate material, such as, alumina, and through a diffuser plate at the bottom of the chamber, the gas is introduced in the chamber. Diffuser plate ensures even distribution of gas throughout the chamber. The pressure of the flowing gas inside the chamber causes the separated particles to levitate. The bed behaves like a liquid and provides a rapid heat transfer medium. The bed can be heated externally or the hot products of combustion are used to heat the bed. A fluidised bed can be either a dedicated one for a single process like carburizing, or meant for multiple processes. There are several feed lines for various gases and by simply using the control valves and adjusting flowmeters the gases can be led inside the furnace. In the late seventies, attention was focused on the use of internally heated fluidised bed. In this process a mixture of gas and air fed directly into the bed. The combustion of the fuel gas provided the necessary heat and the products of combustion was used as fluidising/carburising medium. More recently, an externally heated fluidised furnace was reintroduced. Here the total separation of heating and fluidising functions is claimed to allow greater control over processing, such as carburizing (Fig. 14.1). For carburising, a variety of fluidising media can be employed to provide the active atmosphere including hydrocarbon/air, hydrocarbon/nitrogen, and hydrocarbon/nitrogen/methanol.

14.2.1 Fluidised gas bed carburizing (3)

In fluidized bed carburizing, the specimen inside the chamber is heated to the carburizing temperature, before introducing the carburizing fluid, such as methanol. Since the temperature inside the chamber is maintained above the complete dissociation temperature of the methanol (870 to 925°C), liquid methanol dissociates as soon as it is introduced inside the furnace. The dissociation of methanol leads to formation of one part of carbon monoxide and two parts of hydrogen, which on blending with approximately 40% nitrogen form a simulated endothermic gas. An addition of 2 to 3% natural gas is made to reduce the decarburization by carbon dioxide and water vapor as follows:-





The fluidised bed carburising atmosphere leads to a carbon potential as high as 1.6% compared to 0.8 to 0.9% normally obtained during conventional gas carburising. The high surface carbon can lead to the formation of brittle carbide networks at grain boundaries. The surface carbon control is achieved by adjusting the ratios of methanol and nitrogen flow inside the chamber. The other alternative is the two stage boost-diffusion process, in which controlled carbon potential is maintained during the boost portion of the cycle, followed by replacing the carbon source fully by inert gas like nitrogen in the subsequent diffusion stage. In this process, the surface carbon is reduced as carbon diffuses inward during diffusion cycle. Quenching of carburized components can also be carried out in nitrogen or helium + nitrogen or nitrogen containing fluidised bed. Distortion can be minimised by combining a mixture of gases such as helium and nitrogen. Hardened parts are fluidised bed tempered (4). Carbonitriding can also be carried out in the fluidised bed. Advantages of fluidised bed carburising compared to that of conventional include low distortion and elimination of intergranular oxidation in carburised components.

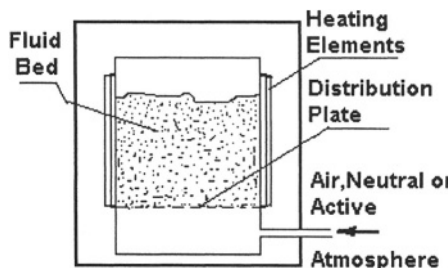


FIG.14.1. EXTERNALLY HEATED FLUIDIZED BED FURNACE

14.3 Thermal Processing in Molten Salt Bath

The heat transfer in the liquid bath of fused salt is higher than that of fluidised bed (Fig. 14.1). Salt bath has been used to carry out diffusion hardening processes like carburising, nitriding and surface hardening by electrolytic deposition such as, boriding. The action of convection currents within the bath ensures temperature uniformity and consistency of the surface hardening process. Heated liquids are extremely effective in encapsulating the components without the formation of dead zones. The environmental acceptability of some of the fused salt systems has improved considerably with the developments in equipment, control technology and non toxic polymer-based regenerators.

References

1. P.M. Astley, Metals & Materials, Nov, 1989, p650
2. Alan. J Hick, The Metals &Material Technology, 1983, July, p325-330
3. Marc Glasser, Adv. Mat. & Processes, June, 1998, p84 MM to 84OO
4. Ray W. Reynolds, *ibid*, p84GG to 84JJ

Chapter 15

POLYMERIC SURFACES

15.0 Introduction

The thermally assisted processes are used for both polymer surface modification as well as coatings of polymer on metals and ceramics. Polymeric surfaces provide excellent resistance to frictional wear and corrosion. The thermally assisted processes for producing wear and corrosion resistant polymeric surfaces are discussed in this chapter.

15.1 Thermally Assisted Surface Modification of Polymeric Materials

Polymer surface can be modified by various techniques including the followings:

- a. Metallisation by resistance heated metal
- b. Sputtering
- c. Physical vapour deposition
- d. Ion Implantation
- e. Plasma spraying
- f. H V O F
- g. Plasma Polymerisation

Some of the processes are listed in Table 15.1. Polymer with aluminum metal coating of 50-100 Å thick is used in food packing industry specially for packing milk and aerated water.

Implantation of B and N ions in polymeric materials result in significant improvement in sliding wear properties. Ion implantation with 200 KeV boron in three doses of 1.7, 5.0, and 17×10^{18} ions/m² on polyethylene, polypropylene, polystyrene & polyethersulfone led to improvement in sliding wear properties (1). The optimum doses of ions is required to produce best results. Ion implantation causes extensive cross linking at the surface leading to higher molecular weight and entanglement density. High molecular weight and entanglement density improve wear properties of polymer.

Using HVOF, a metallised acrylonitrile-butadiene-styrene (ABS) surface was coated with 30 micron (1-2 mils) of WC-Co (2). The metallized surface provided the bonding layer between the WC-Co and the polymer.

Table 15.1 Thermally Assisted Processes for Surface Modification of Polymeric Materials

Process	Coat		Applications
Plasma Polymerisation	Thin polymerized or co-polymerized coating		Wear and corrosion resistance
2. Sputtering	Thin metallic(aluminum),coating		Corrosion resistant coating for packaging industries
3. Vapour deposition (PVD)	Metal and nonmetallic materials		DLC as extremely hard coat for scratch resistant plastic surface
4. Plasma + HVOF	Bond coat a. Metallised using 1-3 processes as above. b. Al/Zn c. S.S. + LDP	Top coat Metallic or composite WC-Co Al-alloys or ZnAl alloys S.S. coating	For wear resistance For corrosion resistance ditto Corrosion & cavitation wear resistance

Plasma polymerization and co-polymerisation can be done on metallic or polymeric materials to form a thin wear and corrosion resistant coating. The process used is termed as plasma assisted CVD process (ref. section 2.9.1).

15.2 Polymer Coatings on Metallic Substrate

The thermoplastic and thermosetting resin powders can be applied to a clean metallic substrate by flame or plasma spraying or electrostatic spraying and heating in fluidised bed.

Thermoplastic based polymers flow under the action of heat to form continuous coating above fusion temperature through fusion coalescence process. On reheating, the coating shall remelt, since the thermoplastic material never reaches a cured or cross-linked state. Most of the thermoplastic materials need primer or bond coat.

Thermosettings are lower molecular weight resin systems, which on heating to fusion temperature undergo chemical reaction to form higher molecular weight polymer. The fully heat-cured fused polymer cannot be melted on reheating after cooling. However thermosetting resins have excellent adhesion to metal and do not need a primer or bond coat.

The temperature above which the polymer shows viscoelastic behaviour with essentially amorphous structure and below which the polymer behaves like rigid crystalline glass is known as glass transition temperature (T_g). The

glass transition temperature can be depressed with the use of “plasticizers”. The degree of crystallinity is the fraction of crystalline phase in volume percentage. The partly crystalline polymers such as PE, PTFE and PDM are mixtures of amorphous and crystalline materials. The crystalline form of plastic (below T_g) is expected to have similar frictional wear behaviour to that of other crystalline materials. The temperature at which a polymer burns is called the degradation temperature, T_d . Polymeric properties are retained in the temperature region from T_g to T_d .

15.3 Parylene Coating (3)

Parylene, a polymer applied from the vapor phase as coating has gained immense popularity to protect surface against environmental and electrical influences in electronic assemblies, sensors, medical devices, aerospace and avionics equipments. Four forms of parylene are commonly used for coatings. Para-xylene is the ‘mer’ of parylene-N polymer. Parylene N can penetrate in deep recesses and holes. Low dielectric constant irrespective of frequency and low dissipation factor make it ideal for high frequency applications. Parylene C is formed by adding chlorine to para-xylene monomer. The polymer can be deposited at a faster rate than the N grade. In comparison to N-grade, the polymer has similar deep penetration capabilities but the coating is more permeable to moisture and corrosive gases. In parylene D, two chlorine atoms are added to monomer and have superior physical & electrical properties and thermal stability in comparison to C and N grades. Parylene HT has fluorine atoms in the monomer and can withstand high temperature. This type is used mainly in the avionics and semiconductor industries.

Coating process

Surface of the material to be coated is cleaned thoroughly of contaminants. The clean surface is coated with an organo-silane bond coat to promote adhesive bonding of top coat to substrate. A dimeric powder of parylene (precursor) is vaporised at 150°C and 135 Nm^2 vacuum. The vapour is led to a second vacuum pyrolysis chamber maintained at $680^\circ\text{C} & 65 \text{ Nm}^2$, where dimeric para-xylenes get converted to highly active monomers. The monomer vapour is fed into a vacuum deposition chamber maintained at 35°C and 15 Nm^2 , where the condensation and subsequent polymerisation of monomer occurs on clean substrate’s surface (Fig. 15.1).

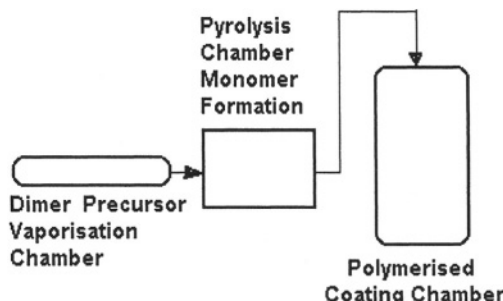


Fig 15.1.VAPOUR PHASE DEPOSITION OF PARYLENE

The vapor phase vacuum deposition process makes it possible to have defect (pinhole porosities, cracks & other holidays) free parylene film. The transparent bio-compatible parylene films are used for a large number of medical applications, such as, catheter mandrels (for lubricity), prosthetic components (lubricity/barrier), cardiac assist devices (barrier), needles, bone pins, brain probes etc. Parylene coating protects electronic circuits and solders from corrosion by effectively preventing ingress of water vapor and oxygen.

References

1. G.R. Rao, L.H. Lee and L.K. Mansur, Structure and Dose Effects on Improved Wear Properties of Ion-Implanted Polymers, *Proc. 9th Int. Conf. on Wear of Materials*, Part B, 13-16 April, 1993, (San Francisco, CA), Elsevier Sequoia, p 739-747.
2. B. Bouaife & others, Coatings for wear protection of polymeric substances deposited by high velocity oxy-fuel flame spraying, *Proc. Int. Thermal Spray Conf.*, (Kobe, Japan High Temperature Soc. of Japan, p 627-632.
3. Russ Wood, *Mat. World*, June, 2000, pp30-32

Chapter 16

CERAMIC SURFACES

16.0 Introduction

The stable ceramic materials with high fusion temperature need high energy beams, such as plasma, ion and laser for surface modification. High velocity flame spray process has also been used for deposition of ceramic materials. Ceramic surface can resist heat, wear and corrosion.

16.1 Ceramic Surface Modifications (1,2,3)

The processes used to modify ceramic surfaces are listed in Table 16.1. Plasma spraying and vapor deposition processes are used to deposit wear resistant ceramics materials on ceramics. For example, plasma spray yttrium oxide on furnace refractory surface acts as a protective barrier coating against the molten materials. Vapor phase deposition of titanium nitride, titanium carbide and aluminum oxide on tungsten carbide are made to reduce the flank wear of cutting tools. CVD coating of diamond like carbon (DLC) on carbide cutting tools reduces friction and improves cutting performance. PVD coating of MoS_2 on silicon nitride bearing reduces friction below 0.1. Laser glazing is used to seal the surface pores and cracks on ceramic surfaces and thus reduces friction. Pulsed laser ablation by nitrogen flux on graphite leads to the formation of super hard covalently bonded carbon nitride ($\beta\text{-C}_3\text{N}_4$) film (2). It has not been possible to measure the hardness of this coating. From binding energy considerations, the hardness of the carbon nitride is estimated to be comparable or greater than diamond.

Laser alloying has been used for producing Ti-rich layer on zirconia. Ti-rich alloy layer acts as solid lubricant and thus improves frictional wear resistance. Subsequent heating of Sol-Gel deposits of hydroxides has been used to form hard, scratch resistant film of titanium oxide or silica.

The different techniques for producing wear resistant ceramic coating on metallic substrate, along with some typical applications are listed in Table 16.2. The modified quaternary hardness diagram C-B-N-M shows some of the hard ceramic coating materials along with the hardness values (Fig. 16.2.1). Large number of high hardness ceramic compounds are formed in different binary systems, such as, Ti-N (e.g., TiN), Ti-C (e.g., TiC) Ti-B (e.g., Ti_2B), B-N (e.g. BN) and C-N ($\beta\text{-C}_3\text{N}_4$). Single layer or multilayer deposits of hard carbides and nitrides by vapor deposition processes are used to coat tool steels, high speed steels and carbide cutting & forming tools in order to

reduce frictional wear and improve performance. The element Ti can be replaced by W, Zr, Cr & Si. Carbides of W, Si, Cr are extensively used to improve the surface hardness and thus the wear resistance properties of the components. Chromium nitride and borides are the main constituents of hard surface layers of nitrided or boronized substrate alloys containing chromium. Carbon in the form of diamond has the highest hardness. Diamond or diamond-like-carbon (DLC) coatings can be formed on surfaces to improve the wear resistance properties of the materials.

Table 16.1: Surface Modification of Ceramics (1,2,3)

Process	Modification	Application
1. Plasma Spraying	Y ₂ O ₃ coating on Ceramic	High temperature protection against molten metal & fluxes
2. CVD	DLC on carbide cutting tools	Reduce friction & improve cutting properties esp., to cut advanced Al-alloys & MMC.
3. PVD	DLC on bearings MoS ₂ coating on Silicon nitride ball bearing Ti or Y on Alumina	Reduce friction to 0.15 Reduce friction below 0.1
4. Ion Implantation		Improve abrasive wear resistance at onset of amorphisation & improves friction after amorphisation
5. Laser Treatment		
5a. Laser Glazing	To seal the surface pores and cracks	Improve frictional wear resistance
5b. Pulsed Laser Ablation	High flux atomic nitrogen on graphite surface to form β C ₃ N ₄ film on Si or Ni surface	The hardness of β C ₃ N ₄ thin film is higher than diamond
5c. Laser Alloying	Ti alloyed to ZrO ₂ surface	Ti-rich layer works like solid lubricant & Improve frictional wear resistance

DLC (Diamond Like Carbon) coating exhibits low friction, high hardness and excellent chemical inertness. DLC is therefore, preferred to polycrystalline diamond in many friction and wear applications. The frictional coefficient of DLC in both high humid and dry sliding conditions is around 0.1. Application areas for DLC coatings include engine components, tools & dies, bearings and gears. An interesting development is the simultaneous vapor phase deposition of aluminum and oxygen to form sapphire on the surface (4). A beam of argon ions at 500-5000 eV strikes on aluminum target, dislodging and depositing aluminum atoms on the prepared substrate. Simultaneously monatomic oxygen at about 100eV is deposited on the same substrate. The hard, tenacious sapphire coating produces a very clear protective surface on polymeric windows, lenses and face shields. (4).

Tab.16.2 Selected Ceramic Coating Materials, Processes & Applications

Techniques	Coating	Typical Applications
Thermal Spray	Ceramic oxides (Al ₂ O ₃ , TiO ₂ , ZrO ₂ , Cr ₂ O ₃) Carbides(WC-Co) Nitrides	Mechanical seals Gas turbine Textile thread guide Automotive engine Marine engine
CVD	Carbides Nitrides Borides Diamond/DLC	Dies Tools Drills Slurry pump
PVD	Ditto	Ditto
Spark Deposition	WC-Co	Tools & Dies

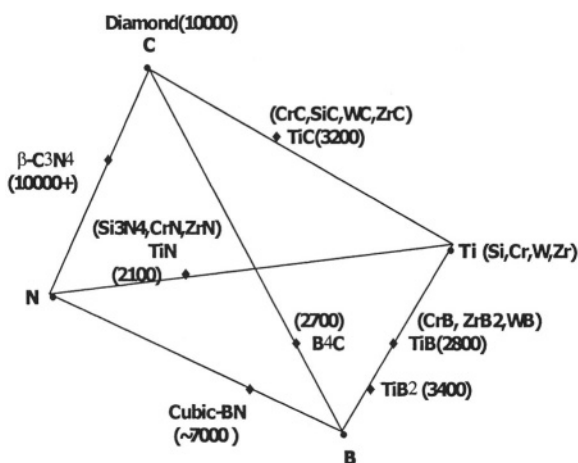


Fig 16.2.1: Modified Octetary Diagram of C-B-N-Tl

16.2 Ceramic Coating Materials/Processes

Ceramic oxides, carbides, nitrides and ceramic based composites are used as wear & corrosion resistance coatings by various thermally assisted processes.

16.2.1 Ceramic Oxides

The oxides, such as, alumina, titania, chromium oxide and zirconia are used extensively to produce wear resistant coating by thermal spraying. Different combinations of oxides are also used. Ceramic oxide materials are available in the form of sintered rods or powders for thermal spray applications.

16.2.2 Ceramic carbides, nitrides, and composites

Thin coatings of carbides and nitrides (e.g., TiC, TiN) are formed on metal and cermet (WC-Co) surface to extend the life of cutting tools.

The sintered tungsten carbide rod fitted in a copper coated steel tube, has been used as electrode for manual metal arc welding (MMAW). Also the tungsten carbide powder materials are encapsulated in steel tubes for use as MMAW or FCAW electrodes. The various processes for deposition of ceramic coatings are tabulated in Table 16.2.

Arc welding of tungsten carbide containing material produces deposit with lower toughness and abrasive wear resistance compared to that of the gas welding overlay. The dissolution of the angular carbide particles in arc welding results in lowering the toughness and wear resistance of the deposit. The relative abrasion resistance index can be half for arc welded carbide deposit compared to gas welded overlay (5).

The composite made from a mechanical mixture of fine tungsten particles (<75 micron) and a self fluxing nickel base powder alloy can produce thin coatings (0.25 to 3.0 mm) with excellent resistance to abrasive and erosive wear. The fused coating of the composite is made normally by spray and fusion process using an oxyacetylene torch. The composite is used extensively for building wear prone areas in rock drill bits and ID fan blades. The composite is also used as a matrix for making diamond tools.

The metal matrix composite consisting of titanium carbide in HSS (M6 type) has been found to produce coatings with excellent resistance to wear. The composite materials are available in the form of both powder and sintered rod. The powder is used for deposition by plasma transferred arc (PTA) process. The rod is used for coating with gas tungsten arc (GTA) welding. The composite alloy deposit is soft and machinable in annealed or with controlled cooling in as-welded condition. After machining the soft deposit to required dimensions, the matrix can be hardened by heat treatment to a hardness of around 62 HRC.

The GTA deposited M6 and M6+TiC materials on the flights of feed screws for extruding plastic containing 30% fiber glass, were allowed to make a production run for 200 hours. At the end of the trial run, the segments with M6 + TiC coatings did not show any measurable wear, while the adjacent segments with M6 deposits lost 17% of their volume (6).

The chromium carbide powder mixed with Ni-Cr matrix are used extensively as thermal spray coatings on boiler tubes for reducing wear due to corrosion and erosion.

Examples of the wear resistant nitride coatings include vapor phase deposition of TiN, TiAlN, AlN, plasma spray deposition of BN-Ni, laser deposition of β -C₃N₄ and glow discharge nitriding of Ti-alloys.

References

1. R. Chattopadhyay, *Surface Wear-Analysis, Treatment, and Prevention*, ASM International, 2001, ch 2, p128.
2. M. Leiber, *Adv. Mater. Process*, 1993, p16.
3. S Bull, *Mat World*, June 1993, 340-342.
4. B.A. Banks, *Adv. Mat. Process*, Vol 11, 1996, p12.
5. H.S. Avery, *Weld. J.*, Vol 30, (No 2), 1951, p144-190
6. T.R. Robisch, M.K. Mal, and S.E. Tarken, Proc. Int. Powder Met. Conf., 22-27 June, 1980, Washington, Metal Powder Industries Federation & American Powder Metallurgy Institute, p.467-484.

This page intentionally left blank

Chapter 17

DIFFUSED AND CVD COATINGS OF SINGLE AND MULTIPLE ELEMENTS

17.0 Introduction

Some important thermally assisted processes, such as carburizing, nitriding, aluminizing, chromising and siliconizing are based on high temperature diffusion of elements in the surface layer. The materials in elemental form can be deposited on the surface by various techniques, including CVD (C, N, Al, Cr), electrolysis in fused salt bath (B) or plating. Subsequent diffusion of deposited element from the surface to interior results in an enriched layer of the diffusing element with the required wear resistant properties. High temperature CVD processes normally involves diffusion.

17.1 Diffusion Process

Diffusion rate of element, as measured by the number of atoms passing through a plane of unit area in unit time, called unit flux, J , is proportional to the concentration gradient of the element from the surface to the interior of the substrate. The relationship can be expressed in terms of Fick's first law, which is as follows:-

$$J = - D \Delta c / \Delta x,$$

where, J is the flux in atoms/m^2 in unit time (s^{-1}), Δc is the concentration gradient over Δx distance, and D is the diffusivity or diffusion of an element per unit concentration gradient over unit distance. According to above equation there should not be any net diffusion of flux ($J = 0$), when there is no concentration gradient ($\Delta c = 0$). Normally diffusion occurs from higher concentration to lower concentration region. For example elements like C, N, Al, Cr etc deposited on the steel surface shall diffuse in the interior, with a rate depending on the differences in concentrations of the element in the surface & interior.

Temperature and Activation Energy of Diffusion:

The diffusion D , increases with temperature and is related to activation energy, Q , by the following equation:-

$$D = D_0 e^{-Q/RT},$$

where Q = activation energy in $\text{J}\cdot\text{mol}^{-1}$, R = Gas Constant = $8.314 \text{ J mol}^{-1} \text{ K}^{-1}$, T = Temperature in K, D_0 = Constant for a diffusion system. The above equation can be written in the following form:-

$$\log D = \log D_0 - Q/RT,$$

Plot of $\log D$ vs. $1/T$ results in a straight line, the slope of which is the activation energy (Q) required for the diffusion to occur. The heat for activation of diffusion is the minimum heat required to initiate the diffusion reaction. The ratio of activation energy for self-diffusion (Q) and melting point (T) in $^{\circ}\text{K}$ is roughly in the region 40 ± 5 for several elements with widely varying melting points, such as, W, Fe (α & γ), Co, Cu, Au, Ag, & Pb. Diffusion coefficient increases and the activation energy required for diffusion decreases with increase in temperature. The diffusion rate becomes appreciably high at a temperature above 0.4 times the melting point of the material. The substrate should be heated and held at such temperatures so as to allow the deposited element to diffuse for sufficient length of time at a reasonably fast rate to produce the required case depth. A gradual fall in the concentration of the diffused element from the surface towards the interior leads to a progressive change in properties across the section and improvement in the integrity of the hard surface layer. Activation energy & diffusion coefficient values of some elements are listed in Table 17.1.1.

Effect of Time on Diffusion

Fick's second law incorporates the effect of time on the flux as follows:-

$$\frac{dc}{dt} = D \cdot \frac{d}{dx} \left(\frac{dc}{dx} \right) = D \cdot \frac{d^2c}{dx^2}$$

In the case of diffusion of two pure metals with complete solubility in each other, a solution for this equation is as follows:-

$$C_\lambda = \frac{1}{2} [1 - \varphi(x/2Dt)]$$

where φ is the Gauss error factor and C_λ is the concentration at a distance λ from the interface.

An important practical relation involving Fick's second law is the time-distance relationship for a given concentration, c , expressed as follows:-

$$x^2 = D t$$

Table 17.1.1: Activation energy and diffusion coefficients of selected elements

Interstitial	Q (J.mol ⁻¹)	D ₀ (m ² s ⁻¹)
C in γ -iron	137,850	0.23 x10 ⁻⁴
C in α -iron	87,570	0.011 x10 ⁻⁴
N in γ -iron	144,970	0.0034 x10 ⁻⁴
N in α -iron	76,680	0.0047 x10 ⁻⁴
Substitutional		
Ni in Cu	242,600	2.3 x10 ⁻⁴
Cu in Ni	257,690	0.69 x10 ⁻⁴
Al in Cu	165,510	0.045 x10 ⁻⁴

It measures the distance (x) that an average atom will wander from its starting point by random migration and hence roughly gives the distance over which the concentration can change during a diffusional process like annealing. The equation can thus be used to estimate roughly the time of diffusion treatment to produce a given redistribution of solute atoms. For example, if x is the distance over which the concentration varies in a cored solid solution, the annealing time needed to remove coring substantially by diffusion is in the order of x^2/D .

To summarize : In order to produce a hard case with progressive changes in concentration across the section through diffusion, the main requirements are-

- There should be a concentration difference in the diffusing element at the surface and that in the interior.
- Temperature should be high enough to
 - a. provide the activation energy required for diffusion of the element in the substrate.
 - b. obtain optimum diffusion rate.
- Time required at the holding temperature is approximately equal to x^2/D .

Diffusion of interstitials like C, N & B in steel leads to the formation of hard carbides (martensitic matrix), nitrides and borides. The plasma carburizing and nitriding processes are already covered in earlier sections. Other case hardening processes such as vacuum carburizing, boronizing and

those due to diffusion of substitutional elements like Al, Cr and Si are to be discussed in this section.

17.2 Diffusion Coatings of Interstitials:-

Plasma carburizing, nitriding and boronizing processes are covered in chapter 2. Two innovative processes, such as, vacuum gas carburizing-cum-high pressure quenching and boronizing by electrolysis of fused salts are discussed in this section.

Vacuum Carburizing-cum-High Pressure gas Quenching:

Vacuum carburizing (1):- is carried out by heating the component to carburizing temperature in vacuum and subsequent introduction of hydrocarbon in the furnace, the thermal decomposition of which leads to surface deposition of carbon. Diffusion of deposited carbon leads to carbon enriched case, which is hardened by subsequent quenching. A typical cycle for vacuum carburizing and high pressure quenching is shown in Fig. 17.2.1.

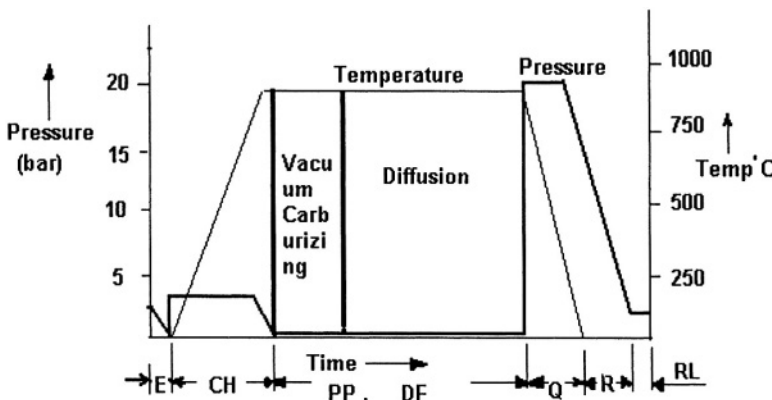


Fig.17.2.1 :Typical Cycle for Vacuum Carburizing & High Pressure Quench

E=Evacuation,CH=Convective heating (N),PP=Propane Pulsing,
DF=Diffusion,Q=Quenching,R=He/N Recovery,RL=Reloading furnace

High Pressure Gas Quenching:-

High pressure gas quenching or 'dry quenching' of carburized components (1) using inert gas as quenchant has gained popularity in recent years due to ecological and economic advantages over liquid quenching media. For example, quenching gases such as helium and nitrogen are inert and ecologically benign, and leave no residues on parts or equipments. Commercial gases available for gas quenching include, in order of increasing quenching capacity: argon, nitrogen, helium and hydrogen. The properties such as thermal conductivity, heat capacity and viscosity determine the quenching capacity of gas. The cooling action of gas can be increased by

raising gas velocity or pressure. Gas pressure of 40 to 10 bars with a gas velocity of 10 to 20 m/s respectively are used for quenching. The total operation of carburizing and quenching can be carried out in 2-, 3-, or multiple chambers for performing functions like carburizing the surface, diffusion of carbon from surface to required case depth and quenching. The three stages in liquid quenching include film boiling, nucleate boiling and convection. Each stage with different heat transfer coefficient, produces significant temperature gradients in parts. Deformation and distortion can result. In gas quenching heat transfer along the part's axis is more homogeneous, and there is less tendency for distortion during hardening.

Applications include automobile transmission gears and shafts which are vacuum carburized at 980°C and gas quenched with helium at 20 bar pressure.

Baronizing (or Boriding) (2).

The diffusion of interstitial boron into surface leads to the formation of hard borides in iron, nickel and cobalt alloys. Apart from glow discharge deposition process (3) used for plasma bonding, the other main technique is electrodeposition of boron from fused salt.

Process (4):-

The process is carried out by electrodeposition of boron from fused salt bath containing Li, Na or K - fluoride plus boron at a temperature of 800°C-900°C (Fig. 17.2.2). Parts can be borided at low temperature of 600°C. The component for bonding forms the cathode, and anode is made of pieces of boron in a copper basket. Current density at cathode is normally 0.5–2.5 amps per sq.dm. The deposition per amp per sq. dm is 1.34 mg boron per sq. cm per hour. The normal coating thickness range is from 0.0127 mm to 0.0508 mm containing 0.7 to 3.0 mg of boron per sq. cm of sample. The higher the current density smoother is the coating. Boriding at higher current densities results in more nuclei formation and the large number of small crystals form a smooth surface (Fig. 17.2.3). The boron diffuses faster in iron boride than iron causing porosity in the deposit. Boriding at low temperature leads to lower rates of diffusion of boron and thus reduced porosities. Post boriding treatments may lead to porosities in the deposit due to Fe_2B formation from FeB.

Ferrous Alloys: Diffusion of boron in the substrate leads to the formation of two types of iron borides viz, FeB and Fe_2B . The microhardness of boride coating is 2000 to 2100 Knoop/100 g (4). The corresponding macrohardness of 92.6 RA for boride coating is equivalent to the hardness of hardest tungsten carbide (WC). The extremely high hardness at the surface results in excellent resistance to galling and adhesive wear. Borided surface resists corrosion due to hydrochloric, hydrofluoric and sulphuric acids.

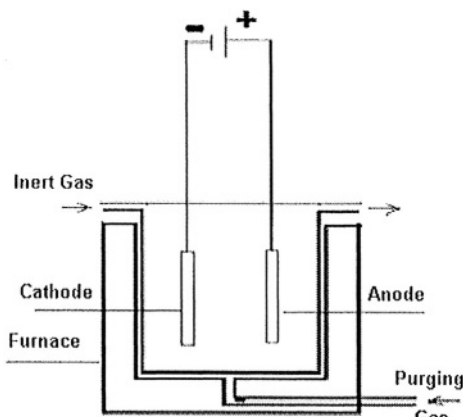


Fig.17.2.2.Schematic Diagram of Boriding in Fused Salt

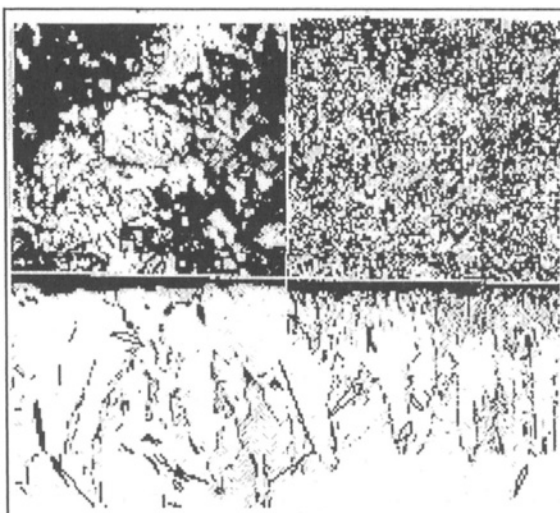


Fig.17.2.3 Microstructure of boronized surface layer; Use high current for smooth surface (top right) or low current for rough surface (top left); Finger type growth from surface to inside (lower left & right)

Ref. 4, Source Book of Wear Control Technology, ASM International, Ref.44073-0003, 1978, fig4, p364.

The boriding of mandrels, shaping dies, deep drawing dies, have shown improved wear life compared to hard Cr-plated and hardened tools. The bonding is used for plastic extrusion screws & dies, plastic injection equipment

Nickel Alloys:- Bonded surfaces in nickel alloys are extremely hard and comparable to that of tungsten carbide. For example, Inconel 718 borided at 760°C followed by second aging at 650°C exhibits a surface hardness of 1450 Knoop and resists wear due to galling and abrasion. Nickel base superalloys, such as, Inconel 718 and Nimonics possess good high temperature creep, hardness & wear resistance properties, due to the formation of nickel aluminide or gamma prime phase on aging. The surface hardness on ageing increases from 425 Knoop in uncoated Inconel 718 to 1450 Knoop in borided surface of same alloy. Most of this high hardness is retained at the elevated temperature. The thrust-vectoring nozzles-bearing components of a gas turbine engine (Pratt & Whitney F119-PW-100 engine powering US air Force F-22 Raptor) are borided to minimise wear, galling and corrosion of the nickel base superalloys (2).

Metal bonded Carbides:- The cobalt and nickel are used as binder for sintered carbides, such as tungsten and titanium carbides. The soft binder areas on the surface can be hardened by boriding so as to make the total working surface to similar hardness as that of tungsten carbide. The binder below the diffusion zone retains the softness and thus the toughness of the bulk material. The hard borided surface resists erosion by fine particles at 90° impingement angle at least 5-10 times more than corresponding carbides in applications, such as, paint spray nozzles or jet engine fuel pump cam blocks (2).

Cobalt based materials and other refractory materials are similarly borided to improve the wear resistance properties of the surface. Molybdenum forms a boride of ~3000 Knoop hardness.

Wear of Diffusion Treated Coatings

The abrasive wear resistance properties of carburized, carbonitrided, nitrided and boronized coatings on steel substrate are listed in Table 17.2.1 (ref. 3, 4, 5). Also included are the wear properties of diffused TiC and VC coatings. The rubber wheel abrasion wear tests were conducted as per stipulations made in ASTM G-65, Procedure A. The ranking of diffusion treated surfaces based on *abrasion test* results (WF values) is in the following order: VC → TiC → Boronized → Nitrided → Carbonitrided → Carburised.

The vanadium carbide (VC) and titanium carbide (TiC) coatings with high hardness in the range of 2500-3000 HV showed the lowest wear rates (0.11-0.12 cc) followed by boronized surface (0.3-0.4 cc) at a hardness level of 1500 HV. Both carburized and carbonitrided surfaces have same hardness (700 HV) and thus same wear factor of 0.429, but with slightly higher hardness of 800 HV, the wear factor of nitrided surface is 0.827 (Table 17.2.1).

Tab.17.2.1 Abrasive Wear Resistance of Diffused Coatings (ref.3,4,5)

Base Material	Diffusion Coating	Hardness HV	Wear Factor cc^{-1}	Abrasive Wear Resistance Ranking
4620 Steel	Carburizing	700	0.429	1.0
Nitriding Steel	Nitriding	800	0.847	1.98
AISI 4620	Carbonitriding	700	0.429	1.0
AISI 4620	Boronizing	1500	2.857	6.66
AISI 440C(SS)	TiC	3000	8.333	19.42
D2 Steel	VC	2500	9.09	21.2

17.3 Diffusion Coating of Substitutional Elements:-

The methods used are as follows:-

- Slurry Fusion
- Pack Cementation
- Chemical Vapor Diffusion

The most widely used process today is cementation. However chemical vapor deposition has been accepted for a number of applications due to certain advantages.

- Slurry Fusion/Sintering:- The slurry fusion or sintering was developed as a low cost alternative to other two processes for applying diffusion coating of materials, such as MCrAlY on turbine component. The MCrY part of the coating applied to the component by slurry spraying was followed by controlled reaction with aluminum and sintering in an aluminide pack of appropriate activity. The success of this process has been reported for NiCoCrAlY (6) and NiCrSi (7) coatings. At present, the slurry fusion process is not much used.
- Pack Cementation:- The pack metallizing process can be used for surface deposition and subsequent diffusion of substitutional elements forming a graded coating. In both CVD and pack metallizing processes, chemical vapor of the metal-halide decomposes on the substrate surface and due to high temperature the deposited element diffuses inward in order to reduce concentration gradient. However, in the case of pack metallization, the component to be coated and the metal to be deposited along with chemicals (normally halides) are

packed inside a basket and heated to required temperature. The chemical vapor of metal halide formed by reaction of the metal with the halogen decomposes on striking the substrate resulting in metal deposit on the surface. The deposited metal diffuses inside the substrate, which is maintained at high temperature.

- iii. CVD : As a matter of fact, the pack metallization process is also a chemical vapor deposition process where both the vapor formation and deposition on the surface occur in the same chamber.

17.3.1 Pack Alunising :

In the pack alunising process, the component is packed in a container containing a mixture of aluminum powder, a halide (e.g. ammonium chloride) serving as a chemical activator, and an inert filler such as alumina. At a container temperature of 820-980°C, aluminum chloride vapor is formed by reaction of aluminum and ammonium chloride. Aluminium is deposited on the component surface by decomposition of aluminum chloride. The coating process is probably more accurately described as a chemical vapor deposition (CVD) process. The interdiffusion between the deposited aluminium and the substrate alloy results in the formation of intermetallic aluminides. For a nickel-base alloy the intermetallic phases formed are Ni_3Al , NiAl , and Ni_2Al_3 . The deposition rate and morphology of the coating depends on pack activity, process time and temperature. The coatings are classified as either low activity, when outward diffusion of major substrate element (e.g., Ni in nickel base alloy) occurs, or high activity when inward diffusion of aluminum occurs. An inward coating is produced when the aluminium activity is high with respect to nickel. For example, the presence of high Al/and or activator and a reaction temperature of 760-982°C (1400-1800°F), lead to aluminum diffusion faster inward than the nickel outward through the initially formed Ni-Al intermetallic layer. With low aluminum activity in a low pack Al/activator contents and higher reaction temperatures of 982-1093°C (1800-2000°F), an outward coating is formed by outward diffusion of nickel and subsequent reaction with aluminum (Fig. 17.3.1) (ref 8).

In the case of most widely used nickel base alloys for turbines, the high activity coatings form a surface layer of Ni_2Al_3 and further heat treatment is required to convert this brittle layer into NiAl . The β - NiAl is stable for around 45-60 atomic%aluminum (9). However, by adding or 'stuffing' of extra aluminium atoms into the NiAl structure lead to the production of a more oxidation resistant hyperstoichiometric NiAl in the outer layer.

The solubility in NiAl of most of the other elements in superalloy substrate is very low. Therefore these elements are precipitated mostly in the intermediate inter-diffusion zone, between top layer and substrate. The precipitates are usually of carbides (M_{23}C_6 , M_6C , MC), metals (e.g., α -Cr), or

TCP (topologically closed packed) phases (e.g., σ , η). In the case of inward coatings precipitates are also present in the NiAl outer layer. The high aluminum containing NiAl top layer has a blue tint, unlike brown-colored normal NiAl, and results in the formation of a top “blue zone”(10, 8). This step is combined with the heat treatment to recover and improve substrate properties.

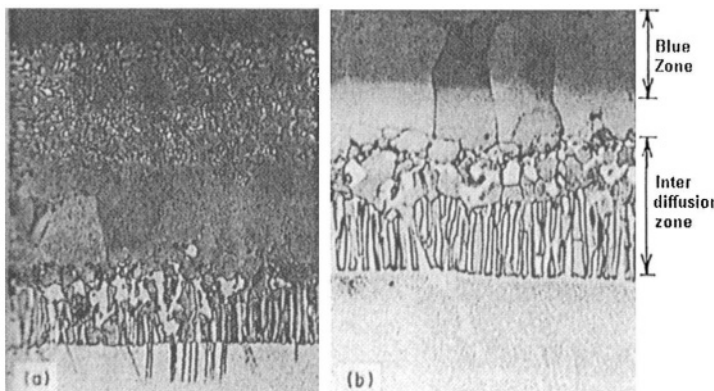


Fig.17.3.1 Microstructures of (a) high activity (inward) and (b) low activity (outward) diffusion aluminide coatings on a Ni-base superalloy,1000X
Ref.8, *Superalloys II*, Ed. Chester T.Sims & Others, p361. Permission to reproduce obtained from John Wiley & Sons, Inc, copyright, 1987.

A typical treatment cycle for a nickel base superalloy (IN738) consists of aluminising pack containing 2%aluminium at 900°C, followed by heat treatment for 2 hours at 1120°C, and then 24 hours at 845°C. For Co-base and Fe-base alloys, the intermetallics are CoAl and FeAl₂ respectively. The coatings produced in different superalloy substrates are different under the same processing conditions. For example, under the same conditions, the coating is thinner in cobalt base alloy than in nickel base alloy due to lower diffusivity of aluminum in cobalt. Even on nickel base superalloys of different compositions, the coating compositions and phases present shall depend on the interdiffusion and intermetallic phase formation by different diffusing elements. A typical aluminide coating contains more than 30% aluminium and are deposited to thickness between 30-70 μm . The layered microstructures (11) consist of a top Al-rich single phase of around 35 micron thick, followed by a mixed microstructural zone of about 50 micron thick (Fig. 17.3.2).

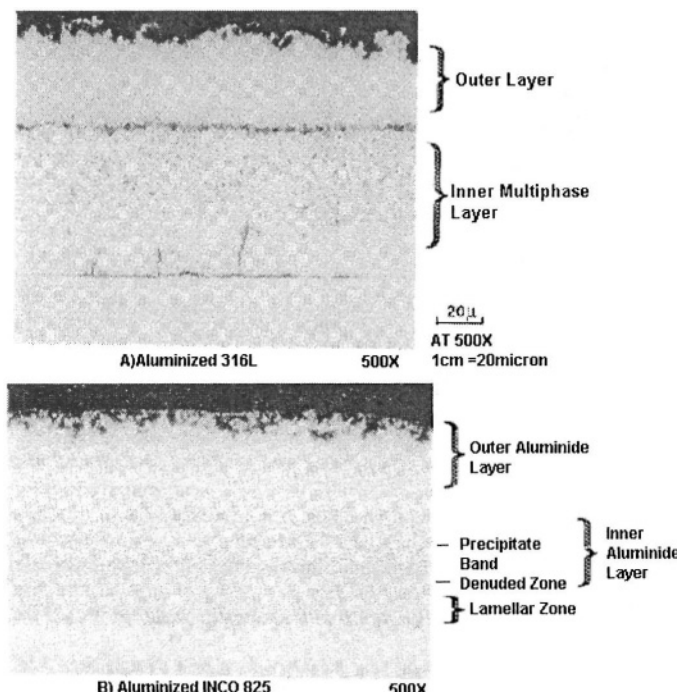


Fig.17.3.2.Effect of Base Metal on Diffusion Coating Morphology
 (Ref. 11. *Microstructural Science*, vol 19, ASM International, Materials Park, OH 44073-0002, 1992, fig 2, p587)

The nickel and cobalt aluminide coatings are still extensively used, probably satisfying 80-90% of the current world market, for protecting turbine blades under aero-, marine- and industrial turbine service (12). The aluminide coating is used to resist high temperature oxidation and 'hot corrosion'. Hot corrosion results mainly from sodium and sulfur in the fuel and gas stream at high temperatures. The protective aluminide coating has performed satisfactorily in many applications including aerospace, marine and utility turbines, where corrosion protection relies on the ability to form a protective alumina scale with reserve of aluminum should the coating become damaged (12). However under severe hot corrosion situations or at temperatures above 1100°C, aluminide coatings offer limited protection. Modified multi-element aluminized coatings have been developed for resisting hot corrosion at high temperatures (above 1100°C), which are as follows:-

- Co-deposition from pack cementation (Cr + Al) or from slurry (Ti/Si slurry or Al/Si slurry) followed by diffusion treatment
- Two step pack cementation processes, e.g., pack chromising followed by pack aluminizing

- Deposition of metallic layer using electroplating or PVD techniques prior to aluminising. For example, a platinum-aluminide layer formed by depositing platinum onto the substrate prior to aluminising. The other elements added include chromium, silicon, tantalum, the rare earths and precious metals. Most of these coating materials are available commercially. The development of platinum modified aluminide class of coating is considered as the most significant advance in this area. The first commercial coating was produced by electrodeposition of a thin layer of platinum, followed by pack aluminising at 1100°C (13).

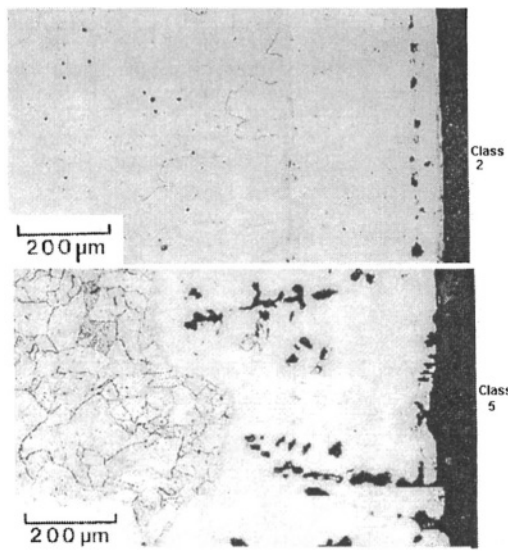


Fig.17.3.3 Chromized layer on steel tube with class 2 & 5 porosity rating

Ref. 14. *Microstructural Science*, vol 19, 1992, fig 3, p 802, ASM International, Materials Park, OH 44073-0003

17.3.2 Pack Chromising

The pack chromising process is carried out by one of the two following methods:-

- A basket packed with chromium metal and alumina powders surrounding the component is heated in a furnace above 1200°C for 3-4 hours. The chromium metal diffuses in the component to form chromium enriched layer at the surface.
- When a basket containing a mixture of chromium, alumina and ammoniacal chloride is heated at a temperature of 845°C, a gaseous Cr-compound is formed which dissociates on reaching the component surface resulting in the deposition of chromium. Due to lower diffusivity of chromium compared to carbon, the process temperature

or the time for chromising is quite high causing grain growth in the substrate material. Therefore normalising is carried out to refine the grain size of substrate material. In boiler applications, an additional tempering treatment is usually performed on chromised tube before being put in service. The diffusion of chromium towards interior depends on holding time. The chromised coating of thickness 75-300 micron can replace 30% chromium containing stainless steels in various corrosive and high temperature applications. The microstructure of chromised layer (14) consists of Cr-rich ferritic matrix interspersed with chromium carbides (Fig. 17.4.1). The extent of decarburisation and porosities depends on the process variables. According to an arbitrary porosity rating system (14) class 2 and class 5 conform to second lowest and the most heavy porosity containing microstructures (Fig. 17.4.1). The diffusion coating of chromium can also be obtained by chemical vapor diffusion process. The coating possesses excellent resistance to corrosion in alkalies, organic acids and fairly good resistance against saline water. The coated components find number of applications in chemical and marine environments. Chromized components exhibit superior resistance to aggressive corrosive environments, such as high temperature oxidation, sulfidation, and chloride related attack. The chromised tubes are therefore increasingly being used for hostile furnace environments in utility and chemical recovery boilers (14).

The chromised coating of thickness 15-20 micron on high carbon, tool and die steels improves the surface hardness to 75 HRC. The coating is carried out on wire drawing dies, taps, roller chain links, cams, pump gears, cold forming tools etc. in order to improve the wear life 10 to 15 times compared to uncoated component. In turbines, apart from hot corrosion and high temperature oxidation, another degradation process is low temperature corrosion. Most of the coatings developed for protection against hot corrosion and oxidation depend on alumina scales, which are generally proven ineffective in combating low-temperature corrosion (15). The chromide diffusion coating can form rapidly an adherent chromium oxide (Cr_2O_3) scale, which has proven effective in resisting low temperature corrosion in turbines. A thin coating produced by pack diffusion, 0.038-0.051 mm (1.5-2.0 mil) is more desirable from mechanical property standpoint, since high chromium compositions are less ductile and prone to cracking.

17.3.3 Siliconizing or Ihregizing:-

The thermal diffusion process of forming a high silicon surface layer is known as siliconising or ihregizing. Low carbon steel components are packed with silicon carbide or ferrosilicon mixed with mill scale (iron oxide) and

decomposable halide generating chlorine at 705°C and above. The chlorine reacts with carbon of SiC or iron of ferrosilicon and liberates silicon in nascent state at or above 705°C, which combines with iron at the surface and gets further diffused inside depending on the time of holding. After about 2 hours of holding time at 705°C, a siliconised layer of 0.13 mm thick is formed. By increasing the temperature or holding time, the coating thickness can be increased up to 2.54 mm. The siliconised layer is very hard and resists corrosion by non-oxidising acids, such as HCl and H₂SO₄, and oxidation at high temperature of up to 870°C.

In gas turbine, silicide diffusion coating is very effective in resisting low temperature corrosion due to SiO₂ scale formation but is not used due to deleterious effect of silicon interdiffusion in nickel base superalloy substrate. In order to minimise diffusion of silicon, the complex silicides, such as Ti-Si composition or Si-rich outer layers in duplex or graded coatings, are used (16).

iii Chemical Vapor Deposition

In CVD technique, a vapor of predetermined composition, produced in a separate chamber is introduced in the coating compartment where it reacts with the surface of the component. The advantage of this technique over the pack metallising is its ability to coat complicated parts such as serpentine internal cooling passages of film-coated airfoils. The substitutional element at the surface diffuses to the interior at a rate depending on the temperature and time of holding. In CVD processes, the catalytic decomposition of vapor at the reaction temperature results in the deposition of coating material on the substrate. The surface of the substrate acts as a catalyst for the decomposition reaction. The volatile chemical compounds of the coating materials are comprised of halides, hydrides or organometallics. The decomposition reactions occurring on the substrate surface are as follows :-

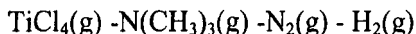
1. Pyrolytic Decomposition; e.g., $(C_8H_{10})Cr(g) \xrightarrow{400-600^{\circ}C} Cr(s) + 2 C_8H_{10}(g) \uparrow$
2. Hydrogen Reduction of Halides ; e.g., $TiCl_4(g) + 2 H_2(g) \xrightarrow{700 \text{ to } 1200^{\circ}C} Ti(s) + 4 HCl(g) \uparrow$
3. Displacement Reactions; e.g., $SiCl_4(g) + CH_4(g) \rightarrow SiC(s) + HCl(g) \uparrow$
4. Disproportion Process; e.g., $2 Ge_2(g) \rightarrow Ge(s) + Ge_4(g) \uparrow$

This is not a line of sight process like PVD or thermal spraying, hence uniform coating to all the exposed surfaces is possible. For CVD coating of

carbide or nitride, a mixture of gases is used. For example, the production of TiC coating requires a mixture of gases containing



For TiC-N coating, a mixture of gases containing



is used.

A high temperature in the range of 900-1000°C is employed for production of carbide and nitride coatings. If the coating material is soluble in the substrate, then the high mobility of atoms at coating temperatures shall result in gradual change in composition across the interface of coating and substrate. The interface regions with such gradual changes in compositions are known as “graded interfaces”. In case of limited mutual solubility, the intermediate phases are formed. The brittle intermediate phases affect the bonding strength of coating with the substrate. In order to avoid brittle intermediate phase formation and thus to improve the adhesive bond strength an intermediate buffer layer known as “barrier coating” is produced on the substrate. For example, chromium is used as barrier coat for hard TiC top coat on ball bearing steel (AISI 52100).

An advantage of CVD over the pack cementation is the compositional flexibility since the thermodynamics of vapor formation are separated from that of the thermodynamics of the metal-vapor reaction. High substrate temperatures employed in CVD coat of hard materials may cause distortion of the component. For CVD coating on plastics, glass, or low melting point metals, the maximum substrate temperature is to be maintained at 250°C.

17.3.4 Chemical Vapor Deposition of Multilayer Coating (17)

A multilayer coating with inner layer of columnar tungsten and outer layer of noncolumnar tungsten carbide (Fig. 17.3.4) was deposited by chemical vapor deposition at a temperature below 500°C, on Ti-6Al-4V alloy (17). Tungsten carbide, W_2C , can be produced from tungsten hexafluoride vapor by following reaction at 400-700°C:



Instead of benzene other organic compound like dimethyl ether can be used. An electroplated interlayer of nickel or platinum is used to protect the surface against corrosion by hot fluoride vapor.

The top layer in the multilayer coating is comprised of a mixture of tungsten and W_2C . It was deposited by adjusting partial pressure of dimethyl ether in a mixture containing hydrogen and diluent argon (18). The interfacing

bottom layer on the substrate was deposited by catalytic decomposition of WF6. The columnar tungsten inner layer is approximately 7 μm thick. The top noncolumnar, lamellar structure is a mixture of tungsten carbide (W_2C) and tungsten and approximately 12 μm thick. The hardness of the top layer of W_2C is 2400 kg/mm^2 , which is higher than the published hardness value of W, WC and W_2C (19).

PVD TiN coatings of approximately 10 micron thick (Fig. 17.3.5) are somewhat porous and exhibited columnar growth structures and lower hardness (about 2100 kg/mm^2) than CVD coating (17).

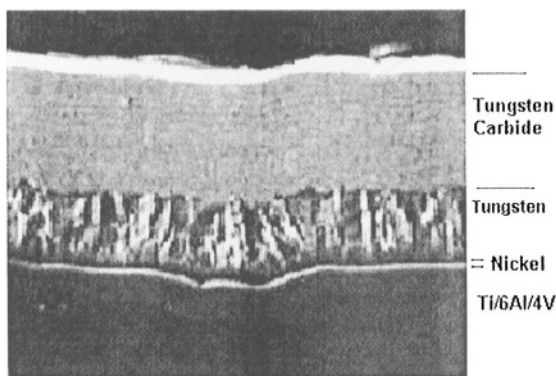


Fig.17.3.4 Microstructure of multilayer tungsten carbide deposit,X1000

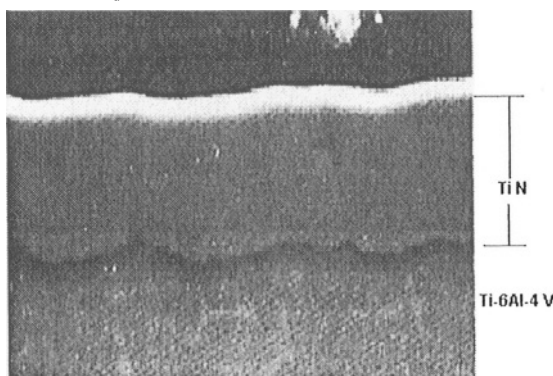


Fig.17.3.5.Cross sections of PVD titanium nitride coatings

(Permission to reproduce obtained from copyright holder D. R. Garg, Air Products & Chemicals, Inc., PA18195)

Use of Multilayer CVD Tungsten Carbide Coating To Resist Erosion in Turbines:

High pressure steam turbine blades are subjected to erosive wear by impingement of hard magnetite particles formed in the boiler and carried by steam (20). The magnetite particles impinge turbine blades at various angles,

damaging the leading and trailing edges as well as concave sides of blades. Similarly, compressor blades in gas turbines are damaged by ingestion of sand and dust (21, 22). In gas turbines, particles enter the engine at high angles, eroding leading edges of the blades and causing burring and rollover. After initial impingement the particles break up and hit the blades at low angles, eroding them above mid-chords and along trailing edges (22, 23). The surface flaws and reduced cross section of the blades due to erosion decrease their load bearing capability leading to failure.

In erosive wear, maximum wear occurs in ductile material at low angles (18° to 30°) of impingement. In either side of the peak, the wear in ductile material is low. In brittle materials there is an initial rapid increase of wear at lower angle followed by slow and almost steady rate till the maximum is reached at the striking angle of 90° . However in general the wear in brittle material is low when compared to the occurrence of a very high peak wear at lower angles in ductile material. In turbines erosive wear occurs at both low and high angles of impingement thus a very high hardness coating material like tungsten carbide is required to minimize wear.

Amongst the deposition techniques, the coatings made by thermal spraying techniques, such as flame and plasma spraying, as well as by PVD are found to minimise wear due to low impingement angle erosion environment. However, these techniques are not found to provide adequate protection in a harsh, high impingement angle environment (24, 25). Also they are line of sight process requiring complicated computer controlled manipulators to form uniform coatings in complex parts uniformly. In the columnar structure normally forms in CVD alloys, cracks propagate along the dendritic grain boundaries through the coating thickness resulting in high erosive wear. Also high temperature process of deposition leads to deterioration in mechanical properties and distortion of the parts.

Multilayer CVD coating of tungsten carbide carried out at low temperature results in fine grained non columnar top layer of W_2C with very high hardness. Erosion test results of this coating indicate excellent wear resistant properties in both low and high angles of impingement (17).

The multilayer coating is found ideal for extending erosive wear life of compressor and turbine blades and vanes used in the aircraft and industrial gas turbines and in complex parts that are difficult to coat using conventional line –of –sight processes.

Other Multicomponent Diffusional Coatings:-

The multiple diffusional coatings of interstitial plus substitutional or more than one substitutional elements can be produced by gas phase pack cementation or CVD.

Cyclone Separator

A low carbon steel component used in cyclone separator is subjected to heavy erosive wear by the dust particles in the flue gas. The component was initially carburised to a carbon content of 1%, followed by chromising to form high chromium, high carbon surface. The hard chromium carbide on the surface provides excellent resistance to erosion by hard abrasive, while the high chromium matrix resists corrosive attack from high temperature flue gas (26).

Stationary Gas Turbine Vanes & Blades

The vanes and blades of a stationary gas turbine in power plant are subjected to erosive attack of ash particles and sulphidation by flue gas at 700-800°C. The superalloy, such as, Udimet 500 (Nimonic type alloy) possesses excellent creep resistance at the operating temperature. A diffusion coating of chromium can reduce the erosive attack by particles in the flue gas due to improved hardness of the surface (600-700 DPN). High chromium resists corrosive attack of sulphur from flue gas. While chromised coating provides resistance to high temperature oxidation up to a temperature of 1000°C, aluminised layer can resist oxidation up to 1200°C. Aluminised layer also provides protection against sulphidation. The diffusion treatment has improved service life from 4400 hrs to 25,000 hrs thus reducing substantially maintenance and running cost (27).

Another example of duplex or multicomponent coating is the use of platinum-aluminide overlay in gas turbine components. The platinum-aluminide coatings have given satisfactory performance to 40,000 hours and beyond against hot corrosion for land-based turbines (28). A successful technique for the platinum aluminide duplex coating is to electroplate platinum on the substrate before aluminising. A multicomponent compound i.e., platinum-aluminide on the surface provides the protection against hot corrosion.

17.4 Diffusion Sinter Cladding:-

The sintering of the component with wear resistant green compact forming the outer casing results in diffusion bonding between the sintered case and the substrate. The key factors (29) affecting sinter bonding include the fit clearance (press fit, approaching interference fit) and the relative change in dimensions between the inner and outer components. The diffusion coefficients of the additive elements of the P/M component (s) in gamma-phase are also to be taken into consideration. Asaka (29) made studies on the factors controlling the development of bonding when the outer unalloyed iron green compact is diffusion bonded to an inner component of either a Fe-1%C green compact, a sintered compact of Fe-1%C, or a wrought plain carbon

steel. The highest bonding strength was observed in the case where both the components were green compacts. The second highest strength was found with wrought steel inner component and the lowest with sintered inner component. The sinter bonding has been tried in various applications, including composite automotive camshafts in which P/M cams of sinter-hardenable steel are diffusion bonded onto a low-alloy wrought steel shaft.

Summary

To summarise, diffusion processes are used to make the surface wear resistant through formation of required element or elements enriched layer. Once the element is deposited on the surface by pack cementation or by vapor phase deposition or through other methods, the subsequent diffusion process shall depend on the diffusivity of the element, temperature, concentration gradient and the time of holding at the temperature. Hard surfaces formed by diffusion of interstitials like C, B or compound like VC resist abrasive and adhesive wear. The substitutional elements like Al and Cr form corrosion and oxidation resistant surfaces. Multi-component CVD coating of WC plus W has been developed to resist erosive wear in gas turbine blades. Multi-component diffusion coating of chromium and carbon has been used in cyclone separator to minimize erosive and corrosive wear. Diffusion coatings of chromium and aluminium in nimonic blades are used to minimize wear due to high temperature oxidation and corrosion in stationary gas turbine blades and vanes.

References

1. Friedrich Preisser, Richard Seemann and Wilfred Rzenker, AM&P, June, 1998, p84II-84LL
2. John Cataldo, Frank Galligani, and Dave Harrandan, AM&P, April, 2000, p35-38,
3. P. Jewsberry, Materials Forum, 9(3), p179-181
4. Howard C. Fielder & Richard J. Sierski, Source Book of Wear Control Technology, ASM, 1978, p364-367
5. K.G. Budinski, Wear resistance of diffusion treated surfaces, Proc. Int. Conf. on WOM, San Fransico, CA, Pt B, April 13-16, 1993, Elsevier, p757-762
6. L. Hsu and A.R. Stevens, Proc. Conf. on Met. Coatings 1980, San Diego, CA, Vol. II, J.N. Zemel (ed), Elsevier Sequoia, Lausanne, April, 1980, p4419
7. E. Fitzer et.al., Proc. Conf. on Materials and coatings to resist high temperature corrosion, D.R. Holmes and A Rahmel (Eds), Applied Science, 1977, p313

8. SUPERALLOYS II, Edt. Chester T. Sims & others, Copyright © 1987, John Wiley & Sons, Inc., Chapter 13 on Protective Coatings, by John H. Wood and Edward H. Goldman p361
9. M. Hansen, Constitution of Binary Alloys, McGraw-Hill, New York, 1958
10. G.W. Goward and D.H. Boone, *Oxid. Met.*, 3, p475, 1971
11. T.E. Swarr, Aluminized Steel for Molten Carbonate Fuel Cells, *Microstructural Science*, vol 19, ASM International, 1992, p583-596
12. J.R. Nicholls and D.J. Stephenson, *Metals & Materials*, March 1991, p157-163
13. G. Lehnert and H. Meinhardt, *Surface Treatment*, 1972, 1, 72
14. V. Ellis, *Microstructural Science*, Volume 19, ASM International, 1992, p597
15. J.H. Wood et.al., ASME Paper no.85-GT-9, March, 1985
16. John H. Wood and Edward H. Goldman, Chapter on 'Protective Coatings', in Superalloys II, (Ed.Chester T. Sims & others, John Wiley & Sons, NY, 1987, p378
17. D. Garg & P.N. Dyer, "Erosive wear behavior of chemical vapor deposited multilayer tungsten carbide coating", Proc. Conf. On 'Wear of Materials', Part A, (Ed, K.C Ludema & others), p 552-557, San Francisco, CA, April 13-16, 1993, Elsevier Sequoia, SA, Laussane
18. D. Garg & others, Low temperature CVD tungsten carbide coatings for wear/erosion, *J. Amer. Cer. Soc.*, 1992, 75(4), 1008-1011
19. W.A. Gibeaut and E.S. Bartlett, in "Coatings of High-Temperature Materials", Pt2, H. Hansner (Ed.), Plenum, NY, 1966, p101
20. J. Qureshi, Characterization of coating process for steam turbine blades, *J. Vac. Sci. Technol.*, 1986, A4(6), 2638-2647
21. J.E. Newhart, Evaluating and controlling erosion in aircraft turbine engine, Naval Air Propulsion Test Centre, Trenton. 1983.
22. J.D. Schell and K.P. Taylor, Sputter coating processes for compressor airfoils, Technical report no NADC-86144-60, General Electric Company, September, 1986
23. D.W. Richerson, *Modern Ceramic Engineering*, Marcel Dekker, NY, 1982
24. J.M. Rashid, M. Freling and L.A. Friedrich, Materials for advanced turbine engines (MATE), project 4- Erosion resistant compressor airfoil coating. Report prepared by NASA Lewis Center under contract NAS3-20072, by United Technologies Corp, Pratt & Whitney, East Hertford, CT, May, 1987.
25. M.T. Groves, Environmental Protection to 922 K (1200 F) for Titanium Alloys, Report prepared for NASA Lewis research Center under contract NAS3-14339, by TRW Inc., Nov, 1973

26. A Kempster, Handbook on Choosing the Right Engineering Surface. The Welding Institute, Abington Hall, Cambridge, 1989
27. Y. Harda, J. Met. Finishing Soc. Japan, 1972, 23, G, 509
- 28 J.H. Wood, Protective Claddings and Coatings for Utility Gas Turbines, Final Report, Project 1460-1, Palo Alto, CA, Nov, 1983
29. Kazuo Asaka, PMTEC 2000, Powder Metallurgy and Particulate Materials, New York, 30 May-3 June, MPIF

This page intentionally left blank

Chapter 18

MISCELLANEOUS PROCESSES

18.0 Introduction

The use of fused wear paste, wear plates, or hard top casting are the few new concepts in thermally assisted surface engineering. A brief discussion of these items are included in this chapter.

18.1 Fused Paste Coating (1):

The wear paste is a mixture of wear resistant materials in fine powder form along with a suitable binder (liquid polymer or solid polymer powder plus water) made into a semi-solid paste form. The powder mixture may contain metals, alloys and carbides. The paste is applied to the workpiece by spatula and dried subsequently or by attaching pressed-and-dried strips on the surface before fusing with carbon or plasma arc welding. The alloys or composites based on self fluxing alloys, such as NiCrBSiC alloys or NiCrBSiC plus WC composites can be fused by oxyacetylene torches. SMAW or FCAW processes for deposition require multilayered deposits to take care of dilution and thus wear resistant properties of the top surface layer. Gas welding results in almost negligible loss in alloying elements. However, in arc fusing of high alloyed paste mixture results in the development in wear resistant properties in the first or in second layer, despite burn-out during arcing and heavy dilution with the mild steel base plate. The layer thickness of the paste is normally of 6mm. Because of the high operator fatigue, the fusion welding process is normally made automatic. In the carbon arc process for fusing 6mm thick dried paste the current used is in the range of 450 to 900 amps at a matching welding speed of 0.24 to 0.35 m/min depending on current. The melting rate at 600 amps using a copper coated carbon electrode of 16 mm is 7 to 8 kg/hour. A 600 amps plasma arc torch with an electrode diameter of 12 to 15 mm and 35 to 45 volt results in the same melting rate while using weaving of the full paste width at a rate of 50 to 60 weaves per minute. In plasma welding a blanket of subarc neutral welding flux can be used instead of protective gas shielding. The hardness of the fused layer varies from 450 to 850 HV 30, depending on the composition. Normally used compositions conform to that of high chromium white iron with or without boron addition.

The nominal composition, deposit hardness, and the wear properties of various alloys are indicated in Table 18.1.1. Fusion of the applied wear pastes were carried out by carbon arc, plasma transferred arc and oxyacetylene gas

welding torch. The second layer of carbon arc fused chromium white iron deposit (35% dilution*), first layer of PTA fused high alloy white iron deposit (10% dilution**) and the first layer of oxy-acetylene fused self fluxing nickel base alloy deposit (no dilution***) formed the surfaces for wear tests (Table 18.1.1). Dry sand rubber wheel tests were conducted on carbon arc and PTA fused samples as per ZIS 116 specification, using a sliding distance of 2000m, load 100N/cm² and sliding velocity of 1.2m/s. A case-hardened 0.15 carbon steel of 800 VPN surface hardness was used as reference material. The abrasive wear of reference material was found as 0.9. The oxyacetylene fused self-fluxing Ni-base alloy was tested for erosive wear as per ASTM G76. The abrasive wear resistance of arc fused high carbon, high chromium alloy (Fe-5.7C-49Cr-0.8B) is found to be best (Table 18.1.1). The oxyacetylene fused tungsten carbide containing nickel-base alloy has been found to possess excellent erosive wear resistance properties.

Tab.18.1.1.Compositions & properties of fused paste

Materials	Fusion Process	Deposit (HV)	Dry Wear	Applications
Fe-3C-35Cr-8B	Carbon Arc	750-850	0.15 (A)	Rotary bucket excavator
Fe-5C 49Cr-8B	Carbon Arc	750-850	0.06 (A)	Briquetting dies
Fe-6C 22V-20Cr 9Ni-1.3Mo -1Si	PTA	450-550	0.2 (A)	Sacrifier teeth & bucket blades
50%NiCr BSiC + 50%WC	Gas	700	0,1 (E)	ID Fan blades

A=Abrasion test results;E=Erosion test results

The major applications include bucket excavators, briquetting press, mixer and scrapper blades, spiked roll crushers and screw conveyors.

18.2 Wear Plates

Surface engineered plates with thick welded overlay of wear resistant materials with appropriate profiles are available for placement in wear prone areas. The wear plates are basically mild steel plates with thick weld overlay of wear resistant alloy. The wear facing alloys, mostly of high chromium white irons are deposited on the mild steel base by flux cored wire,

submerged arc or plasma transferred arc welding process. The duplex wear faced plates inspite of high surface hardness can be pressed into curved and conical shapes typically down to 200 mm radius with inside cladding and 2000 mm radius with outer surface cladding. Plasma cutting is used for profiling. The alloy face can be ground to required finish. Thick alloy deposits of high hardness Cr-C type material exhibits stress relief cracks, which normally do not penetrate into the base plate, but does reduce the wear life of the component. The selection of appropriate wear facing material for a particular application combined with proper fitting & installation of wear plates can result in improved life of the component. Based on the type and severity of wear at different locations of the same component appropriate types of wear plates are normally recommended. For example, tungsten carbide in severe wear area, complex chromium carbides in the surrounding section with less severe wear, and simple chromium carbide in the secondary wear sites can be a techno-economically viable proposition for uniform low wear over the total component surface. For high impact areas high manganese steels or stainless steels can be used.

18.3 Hard Top Casting

The extremely wear prone components, such as, coal crushing hammer can be made from a composite casting in which wear resistant capping or surfacing material is integrally cast onto the tough base material. The beater plates in a coal pulverizer hammer are made by cast bonding of a white cast iron layer on steel substrate. There are several examples where hard top castings are found to have produced satisfactory results (3). Hard top casting is the extension of similar foundry practice followed in the case of chilled cast iron. The hard chilled surface of white cast iron possess excellent wear resistant properties. Hard top casting of cast iron on steel plate has been carried out after coating the substrate steel surface with a self fluxing nickel base alloy (4). The self fluxing alloy used was an alloy of nominal composition as Ni-0.8C, 4.5 Si, 4.5 Fe, 3.3 B, 15 Cr, 2 Cu, 4 Mo. The thickness of the thermally sprayed coating was 150 μm . Self fluxing nickel base alloy provides good bonding of cast iron to steel while reducing dilution. Molten cast iron (3.49 C, 1.58 Si, 0.5 Mn, 0.4 P, 0.1 S) was poured onto mold containing sprayed steel plate. The hardness of the composite alloy formed at the surface was 700 VPN compared to the hardness of carbon steel as 300 VPN and that of cast iron at 400-500 VPN.

The steel surfaced light weight high strength aluminum alloy components leads to vast improvement in wear and heat resistance in applications such as piston head. In this process, a specially prepared thin sheet of steel is inserted into a sand or metal mold, and the molten aluminum is poured in the mold.

The steel forms a strong bond with aluminium as it solidifies, thus producing a light weight casting with hard wear resistant top (5).

18.4 High Density Infrared Processing of Surface Layer

Plasma arc lamp (10 to 35 cm) producing infrared radiations of high power densities in the region of 1.2 to 3.5 kW/cm^2 has been used (6) to modify surface properties of different materials and coatings without affecting the bulk properties. The potential applications of the process include, fusing of predeposited or preplaced coatings, surface hardening and closing the surface pores of thermal sprayed ceramic materials. The process can be used for hardening or fusing inner diameter surface.

References

1. E. Kretzschmer, Protection against wear with welding pastes, Proc, ITSC'86, Montreal, Canada, Sept. 8-12, p661-667.
2. R. Chattopadhyay, "Report on Wear Resistance Paste Development", Reports no CA/PA/2-95, Conick Alloys Ltd, Mumbai, India
3. B.K. Arnold, T. Heijkoop, P. G. Lloyd, G. Rubenis, I.R Sare, Wear of Cast-Bonded Components in a Coal Pulveriser Mill, *Wear*, Volume 203-204 (No. 1,2), 1997, p663-679
4. H. Yara, K. Miyagi and A. Ikuta, Proc. Int. Thermal Spray Conf., Kobe, May, 1995, p163-170
5. Scott Huang, Steel-surfaced aluminum resists heat and wear, *Ad. Mat. & Processing*, May, 2002, p17-18
6. James K. Wessel and William G. Lang, Industrial Materials Future, *Adv. Matl. & Processing*, June 2003, p.55-57.

Chapter 19

QUALITY OF THE ENGINEERED SURFACES

19.0 Introduction

Quality of engineered surface should conform to the stipulations made in quality control and assurance manuals. The stipulations in the form of specifications are made in the manual with the sole objective of satisfactory & reliable performance of the engineered surfaces in the intended wear applications. In addition to evaluation of wear-related properties, such as microstructure, composition and hardness, some form of application oriented standard wear tests are required to be carried out on the modified surface. Laboratory tests provide extremely useful information about the expected behavior of the engineered surface and thus in fact provide data required for the design and operation. However, it is the wear simulation or field tests that would give a true picture of the performance in field wear environment.

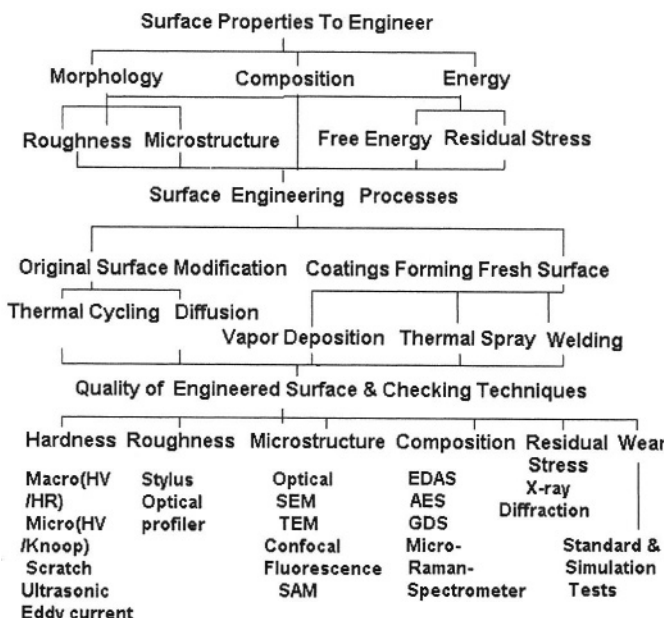
19.1 Quality Checks of Engineered Surface

Quality assurance has been gaining more and more importance in order to comply with stricter laws concerning product liability (1). Another perspective involves tougher competition among the manufacturers using different processes, procedures, and/or techniques etc.. Also good quality control system results in overall improvement in manufacturing and the quality of the product. The routine quality control exercise consists of checking the product qualities against the stipulations made in the product specification.

The routine quality checks of engineered surface include modified surface thickness, microstructure, composition & hardness plus any other specified property or properties.

Table 19.1 lists the surface properties to be modified, the surface engineering processes employed for modification, and the normally used quality control methods.

The exact nature and extent of the modification in surface properties depend on the processing route. Therefore the quality requirements for different properties shall vary in accordance with the process. Also wear being environment specific, the properties should be tuned to meet the specific application requirement. Each one of the main processes, such as, thermal spraying, welding, vapor phase deposition and diffusion requires additional tests to check the special attributes of the process.



Tab.19.1 Surface Engineering & Quality Control

19.1.1 Microstructure

The microstructure of engineered surface provides information on size, shape and distribution of different phases, matrix grain size, grain boundaries, defects and flaws which are related to strength, toughness and wear.

The list of different hard phases responsible for producing wear resistant surfaces include, martensitic matrix (induction or case hardening), nickel-carbides, -borides, -silicides (spray fused self fluxing nickel based alloys), TiC, TiN, TiAlN (vapour phase deposition), iron nitrides, borides, nickel-aluminide (diffusion control process), tungsten-, chromium-, vanadium-columbium-carbides in metal matrix (weld overlays) and hard oxides, carbides and nitrides (thermal spraying).

It is possible to do a complete surface analysis by quantitative micro-analytical technique in optical and SEM modes (2). Energy dispersive X-ray analysis (EDAX) is used to find phase composition. Transmission electron microscope (TEM) is also used for finding crystal structure of the phases by selected area diffraction.

Modified surface thickness

The surface engineering processes produce a wide range of modified surface thickness to suit different application requirements. The thickness of the modified layer or coatings can be determined from metallography,

hardness or compositional changes across the section. Also nondestructive techniques like ultrasonics can be used to measure the coating thickness or case depth.

Porosity & inclusions

Porosities are the structural discontinuities and there are acceptable limits as to the size and distribution for different surface modification processes. Metallographic techniques are used to find out the type, size and distribution of porosities in the modified surface.

Adherence of coating to substrate

Destructive optical microscopy is used to study the interface between the coating and substrate. In processes, such as thermal spraying & PVD, the demarcation line between the coating and substrate is sharp without any diffused layer in either side indicating the mechanical nature of bonding.

Microscopes

Optical microscope can be used to observe microstructures up to a useful magnification (i.e., magnification accompanied by resolution) of up to X2000.

In an electron microscope, the electron beam is focused on an electrically conductive surface of the specimen, by using magnetic lens system. The resulting signals, which include secondary, backscattered, Auger electrons, characteristic x-rays, photons and cathodoluminescence provide information regarding spatial and compositional characteristics of the material. The electron microscopy using secondary and backscattered beams is known as *scanning electron microscopy*. The shorter wavelength of an electron beam enables greater resolution and depth of focus in SEM, when compared to light optical microscope. The surface for SEM studies does not need any special preparation. Even the worn and fractured surface can be directly observed under SEM. Back-scattered technique allows to find the elemental distribution in the scanned area.

The transmitted electron beam through the specimen is used in transmission electron microscopy (TEM) for which specially prepared thin foil or plastic (or carbon) replica is used. TEM is used to find the presence of fine precipitates, dislocations etc. Selected area diffraction technique is used to find out the crystal structure of the phases and thus to identify the type of phases present in the selected area of the matrix.

Other advanced microscopic techniques include the followings:-

Confocal laser microscope is used to scan the surface morphology with laser optics. The imaging system can differentiate the differences down to 50 nm in heights and provides lateral optical resolution between 0.3 to 0.2 micron. The technique (3) is used to evaluate the surface texture of PVD/APS

thermal barrier coating (TBC) and imaging of thermal stress cracking. Fracture surface topography (FRASTA) combines confocal SLM with appropriate software to reconstruct 3-dimensional images of fractured surfaces. This method can provide data on fracture toughness, crack nucleation times, and grain growth (4).

Fluorescence microscopy uses the absorption of light and optical properties of fluorescence to characterize thermally sprayed coatings with respect to porosity, cracking and debonding (5).

Scanning acoustic microscope (SAM) (6) uses an acoustic lens which transmits an ultrasonic pulse burst, focused into the material. The back reflected acoustic energy from coating surface in the focused zone is recaptured by the lens and sent to a receiver for signal processing. Low frequencies (15-100 MHz), are used for characterization of deep layers such as diffusion bonds, cracks, delaminations, etc. High frequency (100 MHz-5 GHz) is used for examination of grain structures, film adhesion, porosity, microfractures, etc. SAM has been used to characterize several engineered materials including, polymer, ceramic and metal matrix composites, vapor deposited thin films (diamond coating) and adhesive bonding.

19.1.2 Composition

Chemical compositions of the modified layer or coating including depth compositional profile should conform to specified compositional limits of wear or corrosion resistant surface material. SEM-EDAS, AES and GDS are commonly used to find the compositional variation across the coating or diffused case.

In the electron optics used for SEM, the reflected beams emitting characteristic X-rays are used in energy dispersive analytical system (EDAS) for chemical analysis. Auger Electron Spectroscopy (AES) uses Auger electron emission in electron-optical system to detect atoms at or near surface regions. An Auger electron has the characteristic energy of the atom from which it originates. The AES detects and identifies contaminants and diffusion at grain boundaries and surfaces in metals, insulators and semiconductors. Micro Raman Spectrometer where SEM-EDAS is outfitted with Raman photoluminescence & cathode luminescence spectrometer can provide molecular and structural analysis of polymeric and other non-metallic material coatings (7).

Glow discharge spectroscopy (GDS) is an atomic emission technique used for depth profile & bulk analysis. A glow discharge lamp is used to generate a high-velocity plasma, which on striking the sample surface, emits characteristic radiations of the atomic species. The wavelength is used to

identify the element and the intensity for determining the concentration. The wide range of surfaces that can be analyzed by GDS includes conductive and non-conductive surfaces, such as decarburized, carburized, carbonitrided, PVD coated, ceramic TBC coated, and polymer coated surfaces.

19.1.3 Hardness

One of the most important and easily measurable properties having considerable effect on the wear of materials is the surface hardness. It is essential to check the hardness of the modified surface as a routine quality control measure while producing wear resistant components.

Vickers hardness testing uses a diamond pyramid indentor with the load in the range of 1 kg to 120 kg (2.2 to 265 lbs). *Rockwell hardness* is indicated by the inverse of the depth of penetration of a standard ball or diamond indentor under a specified load in the range of 15 to 150 kg (33 to 330 lb). The low load range (15-45 kg) is used for superficial hardness testing and expressed in N, T, W, X, or Y scale, while hardness at higher loads are expressed in B, C & A scales. *Micro hardness* is measured at low load (1 g to 500 g) in Vickers or Knoop scale for thin coating and for microconstituents. *Scratch hardness* (8), is measured by sliding a pin indentor under load over the specimen and similar to Vickers, the hardness calculated from the load divided by projected area. The scratch hardness has been found to be a better index of abrasive (8) wear than indentation hardness. High temperature scratch hardness values are used to study wear at elevated temperatures.

Non-destructive hardness methods, such as Ultrasonic or Scleroscope hardness testers are used to measure hardness of finished surface. In Scleroscope a hard ball indentor is dropped on the surface and the rebound taken as an index of hardness. Scleroscope is used to find the hardness of the surface of induction hardened or hardfaced rolling mill rolls.

Ultrasonic and eddy current are also used for hardness evaluation. Hardness of different materials are shown in Fig. 19.1 (8). Some typical hardness values of modified surfaces, using different processes and consumables are listed in the Fig. 19.1. In weld-overlay of hardfacing alloys, the deposit hardness can vary from 340 VPN (Stellite 21) to 700 VPN (Alloyed White CI). In interstitial diffusion controlled processes, the hardness can vary from 700 VPN (carburized) through 800 (nitrided) and to a maximum of 1300 VPN (boronizing). The thermally sprayed ceramic oxides and refractory carbide can produce surface hardness values in the range of 1330 VPN (Al_2O_3) & 2100 VPN (WC + Co). In vapor phase deposition processes, the deposit hardness values for nitrides, carbides and borides of titanium are in the range of 2100 (TiN) to 3500 (TiB₂). Ion implantation of B and N in HSS steels can result in surface hardness of 3500 VPN. The maximum hardness of 7000 and above are obtained by diamond-like (DLC)

and diamond coatings. Pulsed ablation by nitrogen results in the formation hardest coating of $\beta\text{-C}_3\text{N}_4$, which has an estimated hardness of higher than diamond.

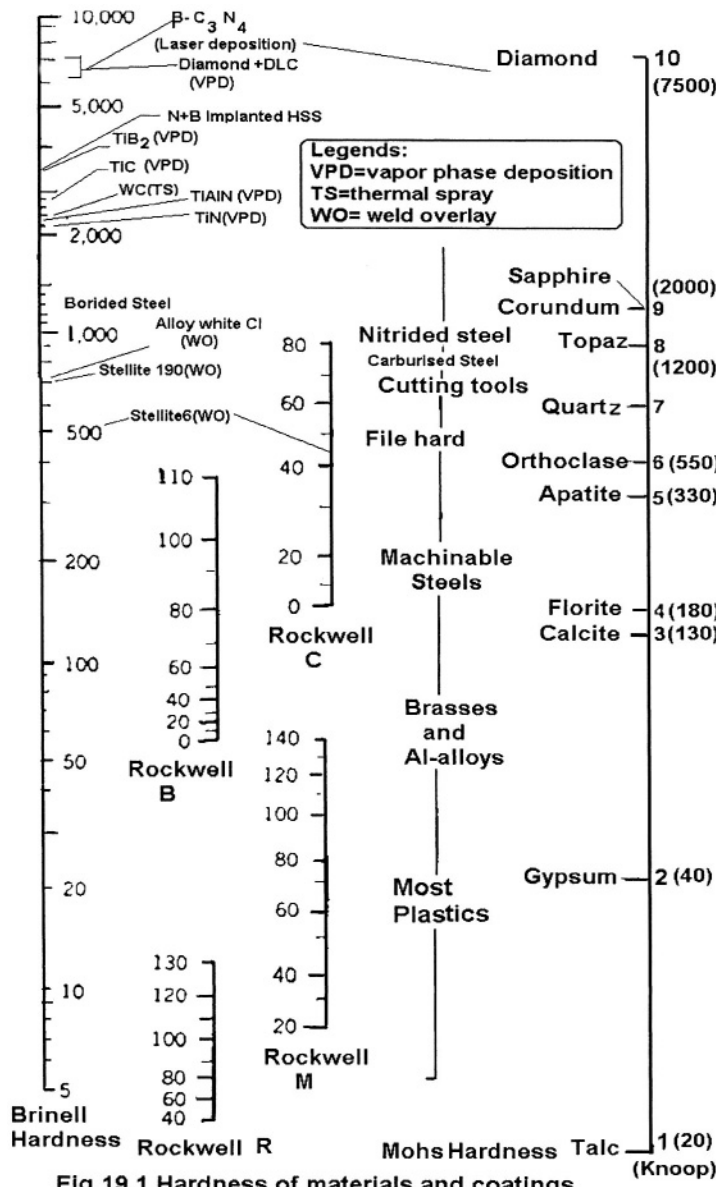


Fig.19.1 Hardness of materials and coatings

Hot hardness measurement

The hot hardness has been used as an index for high temperature wear, specially for hard coatings. Microhardness values are determined in Vickers or Knoop scale. The whole operation is carried out in vacuum chamber, after heating the specimen and the indentor to the same temperature. The commercial equipment available is Nikon High-Temperature Microhardness Tester QM-2 (Nikon Corporation, Tokyo, Japan) with capabilities of measuring hardness up to 1600°C (8).

The hot hardness values are determined up to the application temperatures. The hardness values at the application temperature are used to rank the materials with respect to wear resistance.

19.1.4 Surface Roughness

The surfaces of engineered components bear the specific marks or texture of formative processes, viz. rolling, casting, extrusion, milling etc. The thermally assisted engineered surfaces can be rough (laser peened), porous (thermal spraying), dense (weld overlay or fused deposit), smooth (RST surface) etc. Finishing may or may not be required depending on applications. The finishing processes can be of single interaction type e.g. turning, or can have multiple interactions with the surface e.g. polishing or blasting. The roughness or shape of the surface is described by the deviation from its nominal or reference standard surface. Of the commonly used roughness parameters, such as, Ra (average roughness), Rq (root mean square roughness), Rz (average of the maximum peaks and minimum valleys), the most popular one is Ra. The average variation from the reference standard is the Ra value. Some surface roughness (Ra) values due to formative processes and the respective applications are listed in Table 19.2. The two dimensional average roughness (Ra) parameters are normally specified for controlling surface quality of engineered surface. The surface roughness (9) exists both at right angles to the surface plane and parallel to the surface plane. The former is characterized by height while the latter is known as 'texture' and thus characterised by some kind of wavelengths. Normal industrial practice is to use stylus type of equipment to measure roughness. In this type of equipment a stylus is connected to a transducer, which gages the depth of surface roughness.

Tab.19.2 Roughness Values of Engineered Surfaces

Roughness in micron	Surface Formative Process	Applications
15.0	Thermal spray/oxyfuel & arc	Boiler tubes
7.5	Plasma spray	Thread Guide/Osepa separator
6.5	Plasma spray/EDM/milling rough grinding	Clearance surface/ rough machined
3.2	Broaching/EDM/Laser/rough grinding	Mating surfaces/soft gaskets
1.6	-----ditto-----	Rolling surfaces/work roll in CR mill/ piston pin bores/brake drums/gears shafts/piston crown/turbine blades dovetails
0.80	Electrolytic grinding/ roller burnishing	Sealing surfaces e.g., hydraulic tube fitting/grinding/honing/ antifriction bearing seats/gear teeth/press-fit parts
0.40	--ditto-- plus Electropolish/ lapping/super finish	Antifriction bearing faces & bores /motor shafts/ air-foil/ compressor blades/gear teeth for heavy loading
0.32	-----ditto-----	Cylinder bore/piston OD/ Crankshaft bearing
0.20	-----ditto----	Tappet valves & camfaces /hydraulic cylinder bores
0.10	-----ditto-----	Ball bearing racee/hydraulic piston rods /piston pins
0.5	-----ditto-----	Measurement gauges/anvil
0.2	-----ditto----	Ditto + Bearing ball

However, the three dimensional roughness map of the surface by optical profiler is reported to represent true picture of surface roughness (10). Unlike 2-D Ra tracing, the optical 3-D profiler provides a fast large area measurement system covering three dimensional irregularities such as deep pits, sharp spikes, lay and scratches. The skewness and valley depths were found responsible for corrosion of a steel strip with Ra values within the specified limits (10). Similarly skewness and kurtosis in a clutch plate surface are correlated well with wear and friction processes (10).

19.1.5 Performance Tests

Standard

The ASTM standard practices for wear tests are formulated by ASTM committee G-2. The tests include G-65 (dry sand abrasion), G-99 (Pin-on-Disk for adhesive wear), G-76 (solid particle impingement using gas jet for dry erosion), G73 (liquid impact erosion), G59 (Conducting potentiodynamic polarization resistance measurements).

The results of wear tests are reported in terms of volume loss in cubic centimeter for the particular practice followed. The wear coefficient (K) value is calculated from the volume loss, applied load, sliding distance and the hardness of the coating material. Minimum 'K' value for adhesive (metal-metal pair) and fretting wear is 10^{-7} . For 2-body abrasion the minimum 'K' value is equal to the average of the maximum 'K' values for adhesive wear (metal-metal-pair), i.e., $10^{-2.5}$. The loss of material in abrasive wear can be 10^5 -folds than that of adhesive wear (8).

In practice a combination of wear processes occur on the component surface during usage. In such a situation, normal practice is to conduct a wear simulation test.

Corrosion Tests of Coated Surface

Corrosion tests are conducted by exposing the component surface to specific chemical environment and measuring the weight loss or by electrochemical methods. In standard chemical methods the specimen weight loss is reported in terms of corrosion rates, such as mils per year (mpy). In the electrochemical methods, such as, potentiostatic or potentiodynamic technique, the corrosion rate can be directly calculated in mpy units from corrosion current.

19.2 Surface Modification Processes and Surface Qualities

Depending on the modification process and application, several other properties of the modified surfaces are to be determined. Some of these are to be discussed along with different processes.

19.2.1 Diffusion Control Processes

In this process controlled diffusion of interstitials (C, N and B) makes the surface hard and that of substitutional (Cr, Al) elements results in the formation of corrosion and oxidation resistance surface. The diffusion of multi-elements like Cr and C results in hard carbide formation in a corrosion resistance surface. Diffusion of Al in nickel base alloy may lead to gamma prime phase formation.

Modified surface thickness

The thickness is normally determined by metallography or hardness for hardened surface. The thickness of interstitial diffusion layer varies from 10-20 μm (boronizing) & $<25\ \mu\text{m}$ (ferritic nitrocarburising), to higher values of $<500\ \mu\text{m}$ (carbonitriding) and $<750\ \mu\text{m}$ (carburizing). The chromised layer thickness is in the range of 75 to 300 μm .

Surface hardness

The depth hardness profile across the section in diffusion hardened sample shows gradual transition from high hardness case to softer core. The surface hardness after boronising is the highest at 1500 HV, followed by nitriding at 800 HV and then the carburizing at 700 HV.

Microstructure

The hardened zones contain martensite in carburized case, iron nitrides spikes ($\gamma'' + \epsilon$) in nitrided portion and iron borides (FeB and Fe_2B) in the borided surface. In aluminized coatings on nickel base alloys, the top layer consists of aluminum rich single phase followed by a mixed microstructural zone interfaced with the substrate. The chromised layer consists of Cr-rich ferritic matrix interspersed with varying amount of chromium carbides. Grain growth, decarburisation and porosities for high temperature processes are to be checked. Quality checks are done against a set of standard photomicrographs.

Compositions

There is no need to do a routine check on composition so long the process parameters are not altered from optimum settings and the other properties, such as microstructure and hardness conform to set standards. A composition scan across the modified surface shall reveal the concentration gradient of the diffused elements. Also selected area diffraction shall indicate the presence of a second phase, e.g., nickel aluminide, which acts as a barrier to further diffusion.

19.2.2 Vapor Phase Deposition

Coating Thickness

This is largely done for thin coatings by destructive metallography. However, considerable effort is currently being expended to identify nondestructive techniques such as radiography, ultrasonic and thermoelectric probes for coating thickness measurement.

Apart from the measurement of coating thickness of the finished product, the measurements of layer thickness during the process are required in certain applications as prerequisites for successful layer development. Total interference contrast (TIC) microscopy is used to measure coatings down to nanometer range, while the extended depth of focus system is used for viewing parts in real-time (11). The coating thickness in vapor phase deposition processes for both PVD (ion plating, magnetron sputtering, arc evaporation) and CVD of common coatings, such as, TiN, TiAlN, ZrN, HfN on tool materials is within the micron range.

Microhardness

Due to micron range coating thickness, only microhardness technique is used to determine the hardness of the vapor phase coatings. The load used for microhardness testing should not allow indentor to penetrate to substrate. For example, with a coating thickness of 2.8 micron, the use of 15 g load showed a typical microhardness of 2000 VPN for TiN, but at 25 g load hardness observed was 1000 VPN and at 50 g load the observed hardness was 500 VPN (12). For high temperature microhardness evaluation the coating thickness should be at least 8 micron at 50 g load, to prevent indentor penetration to substrate (13).

Vickers microhardness values at room temperature under 50 g load of PVD coated (by high rate magnetron sputtering) TiN, ZrN & HfN are 2300, 2600 and 3000 kg/mm² respectively. However with increasing temperatures, both the hardness and the hardness differences tend to decrease until the hardness values become equal at 1000°C, to approximately 500 kg/mm² (13). PVD coated TiAlN (25-50% Al) with higher hardness (~2400 kg/mm²) than TiN, maintains some difference in hardness up to 800°C beyond which the hardness difference becomes negligible. The microhardness of PVD coatings depends on the processing technique. The PVD coatings deposited by ion plating (IP) and high rate magnetron sputtering (MS) possess higher microhardness than the PVD coatings produced by vacuum arc evaporation (AE).

The microhardness of CVD coating is less than PVD coating of same material, such as, TiN, HfN etc. The hardness of TiN CVD coating is 1800 kg/mm². The microhardness of PVD HfN coating exceeds that of CVD HfN deposit by a factor of 2.5 at room temperature (13). The hardness difference with CVD coating is significantly higher for deposits using processes, such as IP and MS-than those produced by AE, where the difference is marginal. However the difference again decreases with the increasing temperature and the hardness values merge to an almost identical one at 1000°C.

Coating Composition

Both AES and EDS are used to determine the coating compositions. AES and EDS compositional analysis indicate that the PVD TiN coating has slightly higher N:Ti ratios compared to that of CVD TiN coating (13). The finding supports the view that the PVD processes allow nitrogen atom incorporation within interstitial sites (14), which expands the TiN matrix.

Coating Microstructure

Both SEM & TEM are used for microstructural studies. Tung & Cheng (15) have reported to have produced thin foil of the EBPVD coating by using a single crystal of NaCl as substrate on which thin films of Ag/Mo are co-deposited under similar parameters as normal production coating. After

dissolving the substrate, the thin foil was used for observing the microstructure under TEM and also to find the crystallinity by selected area diffraction.

TEM studies showed the PVD coating of nearly stoichiometric TiN is free from unusual features such as Ti_2N second phase formation or voids at the grain boundaries (14).

The main microstructural differences between CVD and corresponding PVD coating are in grain size and lattice defects. CVD produces relatively larger, defect free grains which are thermally equilibrated due to high processing temperature. PVD process leads to coatings with finer, defect-containing grains, and unequilibrated microstructures that are promoted by energetic bombardment, low deposition temperatures and high deposition rate.

The CVD coating has columnar grains. Depending on the temperature and time of holding, post coating heat treatment is a necessary step for refining the microstructure.

Residual Stress

PVD coatings may retain high compressive residual stress of the order of 0.1-1% of the Young's modulus (13). The high lattice strain and the resulting residual stress has a profound effect on the microhardness of the PVD coating. For example, using magnetron sputtering, the increase in microhardness PVD coatings over bulk or corresponding CVD coatings is highest in HfN, followed by ZrN and TiN. The increase in elastic moduli of these coatings follows the same order. Due to substrate thermal expansion mismatch the CVD coatings contain low residual stresses.

Bond test for PVD coating

Kunz and others (12) have used scratch test (commercial Revetest Scratch Tester) for evaluating the PVD coating adherence to substrate. In the scratch test, a Rockwell C diamond indentor (tip radius 0.2 mm, cone angle 120°) is to be drawn over the surface until the coating materials get detached or cracked. The lower critical load (L_{c1}) is the load at which first cracking of the coating appears and thus indicating cohesive bond strength. The upper critical load (L_{c2}) is the load at which delamination occurs and thus represents the strength of adhesive bonding.

Wear & performance tests

Normal wear tests can be carried out on the vapor phase deposited coating at lower loads. Results from standard tests on the coatings are discussed in Chapter 20.

19.2.3 Ion implanted Surfaces

Ion implanted layer being a part of the bulk material the adherence to the substrate is excellent. Surface topography is not dramatically different after implantation, hence can normally be implanted on the finished component.

Microstructure

TEM has been used for observation of microstructural changes in implanted layer. Nitrogen ion implanted surface forms hard nitride at high doses and nitrogen diffused layer with low doses. TEM observations on nitrogen implanted surface layer show the presence of highly oriented mixed nitrides (Chapter 3/Fig. 3.3.1).

Composition

Miyamoto & others (16) have used secondary ion mass spectroscopy to analyse C+ concentration depth profile in a C+-implanted silicon. The nitrogen ion implanted surface in steel can contain up to 50 atomic percent of nitrogen which is nearly five times the nitrogen than that obtained in ion nitriding.

Hardness

High surface nitrogen content can produce an equivalent hardness of 85 HRC. The hardness of implanted (B+N) surface of high speed steels (M-series) is found to be in the range of 3000 to 4000 VPN, almost similar to the hardness in DLC. The near surface hardness of ion implanted polymers were evaluated by using an ultralow-load nanoindentation technique (17).

Wear tests

The implantation of both nitrogen and boron improves vastly surface hardness and lubricity and thus wear resistance. With a fraction of the costs required for diamond or diamond like coatings, ion implantation can result in a coating surface with wear resistance similar to that of diamond. Chromium, nickel & other metals are implanted to produce corrosion resistant surface in steel. Ion implantation of Ti or Y on alumina improves wear resistance due to abrasion at the onset of amorphisation and that due to friction after amorphisation. The near surface wear properties of ion-implanted polymers were evaluated by a reciprocating tribometer with a nylon ball as the counterpart (17).

Tab.19.3.Process parameters &coating properties in thermal spraying.

Parameters	Thermal Spraying Systems						
	LVOF	HVOF	D-Gun	HVF	Arc	Plasma Arc	V. Plasma
Jet							
Temp. ($\times 10^3$ °K)	3.5	5.5	5.5	4.0	15	15	12
Velocity ($\text{ft/s} \times 10^3$)	2.7	2.5-4	>3.7	4-6	8-1.1	.8-1.8	.53-1.6
Mach	< 1	>2 to 5	>4.5	5-7.5	1-2	1-2.5	.42-2.0
Spray distance(in)	4-10	6-18	—	6-18	2.5-6	2.5-6	2-6
Power Input(KW)	20	150-300	—	—	2-5	40-200	40-200
Particle Feed							
Particle Temp. ($\times 10^3$ ° C)	2.5	3.3	---	---	3.8min.	3.8min	3.8min
Particle Velocity ($\times 10^2 \text{m/s}$)	.5-2	8	---	>10	1-2	3-5	4-6
Material Feed ($\times 10^2 \text{g/min}$)	3-5	15-5	---	---	1.5-2.0	5-1.5	.25-1.5
Coating Properties							
Density (%)	85-90	>85	>95	96-99	90	90-95	90-99
Bond Strength (Mpa)	5-15	>70	>70	>70	15-30	35-70	>70
Oxides	H	M-D	L	VL	M-H	M-C	N
Porosity(%)	5-15	0.5-2	0.5-2	0-0.5	5-10	1-5	0-0.5

D-Gun = Detonation Gun, HVIF=High Velocity Impact Forging, Arc=Arc Spray, V =Vacuum, LVOF=Low Velocity Oxy-Fuel Torches, HVOF=High Velocity Oxy-Fuel System. H=High, M=Medium, D=Dispersed, L=Low, VL=Very Low, C=Coarse, N=N1

19.2.4 Thermal Spraying

A wide range of consumables, such as, metals, ceramics, plastics and composites are used on similar and dissimilar substrate surfaces. The quality checks on the thermally sprayed surface are carried out on the similar line as PVD coatings.

Thickness

In process thickness of the layered deposit is measured from the dimensional difference from the original surface by using a caliper. Thinner coatings may require microscopic methods for thickness determination.

Hardness

The hardness determination with ball indentor is more appropriate for porous sprayed low hardness coatings. For higher hardness coatings Vickers and Rockwell C or A-scales are used. The hardness varies from 90 HRB for soft metallic coating to 2500 HV for ceramic deposits.

Microstructure

The polished cross section reveals wavy outlines of the lamellar structure of the sprayed deposits. In SEM at a magnification of 4500X, microcracks are observed in high hardness deposits due to thermal contractions during the cooling. Some rapidly cooled WC-Co HVOF deposits are found to possess amorphous structure. The post-coating heat treatment resulted into recrystallisation of the amorphous product into eta-carbides ($\text{Co}_2\text{W}_4\text{C}$ & $\text{Co}_6\text{W}_6\text{C}$) with vastly improved wear properties (Chapter 8, ref.14). The adoption of combustion under high pressure (HVIF) leads to the formation of extremely high velocity jet which enables the particles to be forged onto the substrate surface on impacting. The coating becomes more dense with the high velocity processes.

Composition

Compositional changes occur mostly in the atmospheric spraying processes. For example, in HVOF and plasma spraying, some of the tungsten carbide particles dissociate into tungsten and carbon, and thus decarburized by oxidation of the freed carbon. The compositional check consists of finding out the conformity of the deposit chemistry with the specification.

Residual stress

The surface residual stress increases with the thickness of the coating. Initial compressive residual stress on the shot blasted surface becomes tensile in nature with higher coating thickness (>3 mm) leading to crack formation and failure of the coating.

Bond Test

The standard test method for adhesion and cohesive bond strength of the thermal spray coating is to follow the practice as stipulated in ANSI/ASTM C633-69-74. The test consists of coating one face of a substrate fixture, bonding this coating to the face of a loading fixture by a specified adhesive (normally epoxy type), and subjecting this assembly of coating and fixtures to a tensile load normal to the plane of the coating. The adhesive bond strength is expressed as the stress at which the coating is detached from the substrate. The bond strength of sprayed coating is normally below 10,000 psi, the maximum adhesive bond strength of the specified epoxy used for the test.

Spray & Fused Coatings

A number of applications require post spray fusion operation for closing the pores and also to obtain better bonding to substrate. The fused deposit should be free from cracks, blowholes and good metallurgical bonding with the substrate. Low fusion temperature nickel self-fluxing and cobalt base

alloys on fusion form a brazed joint with the steel substrate. In thermal spray ceramic, only the surface layer of coating is fused.

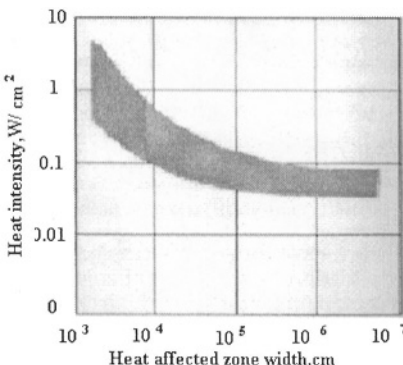


Fig.19.2 HAZ width vs. heat intensity in welding
(ref.19, Adv. Matls & Processes, May,2001, fig4,p 40,
©ASM International, Materials Park, OH44073-0002)

19.2.5 Welding

The overlay process should result in welds that are characterized by: superior strength plus bend and impact toughness, narrow heat affected zone (HAZ), narrow fusion zone, low dilution, reduced weld shrinkage and distortion, low residual stress and improved microstructure. Quality checks include these parameters and few others, such as, nondestructive testing (NDT) of flaws.

The weld quality is mainly dependent on the intensity of heat source in welding. In advanced processes using concentrated heat beams and rays, more energy transfer is directed to the weld deposit and less to the base metal, producing the narrowest possible heat affected zone & other desirable features (19).

HAZ

Heat affected zone in the substrate forms the interface with weld and is therefore subjected to heating close to melting point. Rapid heating in the high intensity beams not only produces a narrow HAZ but also reduces coarsening of the microstructural constituents. HAZ width (Fig. 19.2) (ref.19) decreases steeply by more than 10^2 times from arc welding (10^3 W/m^2) to plasma welding (10^5 W/m^2). However within the region of high intensity sources, such as, plasma (10^5 W/m^2) and electron beams (10^6 W/m^2), the HAZ width remains almost constant.

Penetration or depth (d) to width (w) ratio (d/w)

Higher intensity source increases rapidly the heat penetration as measured by the ratio of depth to width (d/w) of the weld cross section, thereby allowing higher welding speeds for same penetration.

Fusion zone:-

The cross sections of welds done by high heat intensity electron beam and lower heat intensity gas tungsten electrode show a large difference in the fusion zone width (Fig. 19.3a & Fig. 19.3b) (ref.19). High intensity beams with less dwell time leads to the formation of lower fusion and heat affected zones in the welding process.

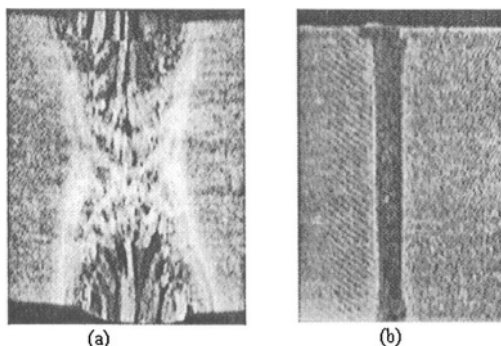


Fig19.3a & b are fusion zones of GТАW and EBW respectively
(ref.19..Adv.Matls. & Processes,May,2001, fig5,p 41,
©ASM International ,Materials Park ,OH44073-0002)

The high intensity heat sources are used for welding high strength alloys without any significant loss in strength properties (19).

Angular Distortion

Lower heat input in welding from a more concentrated heat source like that of electron beam compared to that of gas tungsten arc results in less distortion (ref. 19). In GТА welding, the angular distortion (α) increases steeply with increase in the section thickness (t) of material to be welded. On the other hand, there is slight decrease in angular distortion (α) with weld thickness (t) in electron beam welding.

Dilution

For dissimilar metal welding high dilution results in different composition of the weld from that of either of the alloys. Excessive dilution can alter the wear resistance properties of weld overlay. With high intensity sources such as, electron, plasma and laser it is possible to control the dilution in the very

first layer within the acceptable compositional limits of the wear resistant material.

Capital Cost

The capital cost of the equipment is roughly proportional to the intensity of the heat source (Fig. 19.4) (ref.19). The productivity in terms of weld length per second increases with the intensity of heat source. The ratio of capital cost/ productivity for high intensity source like laser is around $10^{4.5}$ compared to that of lower intensity arc source as 10^3 . However the higher capital cost of high intensity power source can be justified by improved quality of the weld.

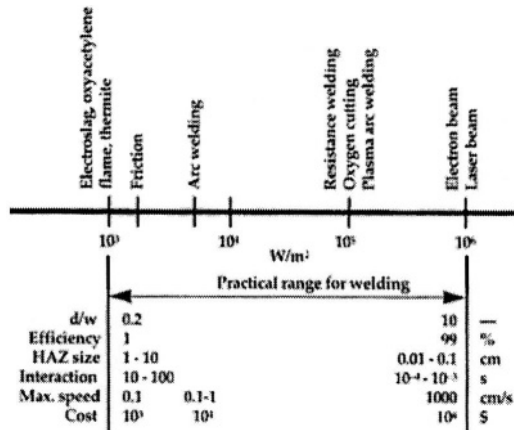


Fig.19.4.Characterisation of welding processes according to heat sources
(ref.19, Ad. Matls. & Processes, May,2001, fig 1,p 40, ©ASM International Materials Park, OH44073-0002)

References

1. R. Chattopadhyay, Quality Control, Assurance & Product Liability-An Overview, Intensive course on metallurgical quality control and assurance in engineering industry, IIM Bombay chapter, 1985, April 19-21, Bombay, India
2. R. Chattopadhyay, Wear resistant plasma transferred arc coating on engine valves, Proc. 14th Int. Thermal Spray Conf., 22-26 May, 1995, Kobe, Japan, High Temperature Society of Japan.p31-34
3. Hans G. Kapadia, Microstructural 3D analysis of materials surfaces using confocal scanning microscope LSM, Microstructural Sciences, vol. 19, p61-68 ASM-International, 1992
4. T. Kobayashi and D.A. Shockley, Ad. Matls. & Processes, vol 11, 1991, p28-34

- 5 Kenneth W. Street & Todd A. Leonhardt, Fluorescence metallography for the characterization of structural integrity, Microstructural Science, vol 19, p68-84, ASM International.
6. B.R. Tittmann & others, Scanning acoustic microscopy of engineered materials, *ibid*, p85-95
7. Charles Nelson, Micro-Raman spectrometer identifies polymer materials, JEOL, USA Inc., *Adv. Matl. & Processes*, June, 2003, p.20.
8. R. Chattopadhyay, Surface Wear : Analysis, Treatment, and Prevention, ASM International, 2001
9. J.B.P. Williamson & others, Rough Surfaces, T.R. Thomas, Ed., Longman Group Ltd, UK, 1982.
- 10 Micheal Zecchino, Why average roughness is not enough, *Adv. Matrls. & Processing*, March, 2003, p25-28
- 11 Light microscopy-probing into the nanoworld, an article from Carl Zeiss, UK, *Materials World*, March, 2003, p16 18
12. A. Kunz, B. Matthes, E. Broszeit and K.H. Kloss, Int. conf. on Wear Of Materials, ptB, p966-970, held at San Francisco, 13-16 April, 1993, Elsevier Sequoia, Lausanne, Switzerland.
- 13 D.T. Quinto, G.J. Wolfe, P.C. Jindal, *Thin Solid Films*, 1987,(153)p19-36
14. J.E. Sundgren, *Thin Solid Films*, 1985, 128, p21
- 15 S.C. Tung & Y.T. Cheng, Int. conf. on Wear Of Materials, ptB, p763-771, held at San Francisco, 13-16 April, 1993, Elsevier, Lausanne, Switzerland
16. T. Miyamoto, S. Miyake & R. Kaneko, Int. conf. on Wear Of Materials, ptB, held at San Francisco, 13-16 April, 1993, Elsevier Sequoia, Lausanne, Switzerland *ibid*, p733-738.
17. G.R. Rao et.al., *ibid*, p739-747
18. Patricio F. Mendez and Thomas W. Eagar, Welding processes for aeronautics, *Advanced Materials & Processes*, May, 2001, p39-43

This page intentionally left blank

Chapter 20

PROGNOSTIC AND LIFE CYCLE EXTENSION

20.0 Introduction

The useful life or the life cycle of the modified surface in the working environment is a key factor for the selection of surface engineered component. The choice of the surface engineering process and material are therefore based primarily on the life span of the engineered surfaces. Some of the material properties affecting the working life include, fracture toughness, esp., for high hardness (e.g., ceramics) or high strength materials (e.g., maraging steels), fatigue and creep. The wear of high hardness material is related to fracture toughness and that of thermal wear and thermal fatigue to creep, whereas wear life on repeated application of stress or impact to fatigue. The life cycles in different wear processes, such as, abrasion, adhesion, erosion, thermal and corrosion can be estimated from standard wear tests. Wear life for a particular application involving a number of wear processes, is however, to be determined by carrying out wear simulation experiments followed by field tests.

20.1 Prognostic

‘Prognosis’, ‘prognostic’, ‘diagnostic’, ‘health monitoring’ are the buzzwords today in critical advanced industrial segments, such as aerospace, defense and nuclear, where assured performance within a predictable life cycle is required to avoid any disastrous consequences due to premature failure. Prognosis has become key tool for prolonging the life cycle of aging fleets of modern jet aircrafts (prohibitively costly), nuclear reactors & facilities (hazardous /disposal problem), & defence equipments like missiles (to maintain start-ready condition for 24 hours without being in operation). The determination of remaining life is required to decide on future performance capabilities. In many critical components, the remaining life can be extended beyond the designed life by refurbishing the components through surface engineering processes. The life cycle of equipment and machinery is similar to that of human being. The methodology for prolonging the life cycle is akin to that followed in medical science. In medical science, ‘diagnostic’ or ‘**diagnosis**’ (*gignosko* in Greek ‘*to know*’) is the method of “*identification of disease by means of patient’s symptoms*” & ‘**prescription**’ is the process of “*laying down rules for cure*” of identified disease. The combined action is known as **prognostic** (or prognosis or prognose) i.e., *diagnose the cause +*

prescribe cure. Diagnostic involves prediction of usable life for OEM and assessment of remaining life for the component in use. The prescription involves recommendation of appropriate technology to prolong the life of the component. RUL or remaining useful life allows refurbishing actions to schedule in an optimum fashion. Surface engineering processes form the major part of the *prescription*, and thus play key role in prolonging the life cycles of the components in OEM and M&R stages.

Life of Engineered Components

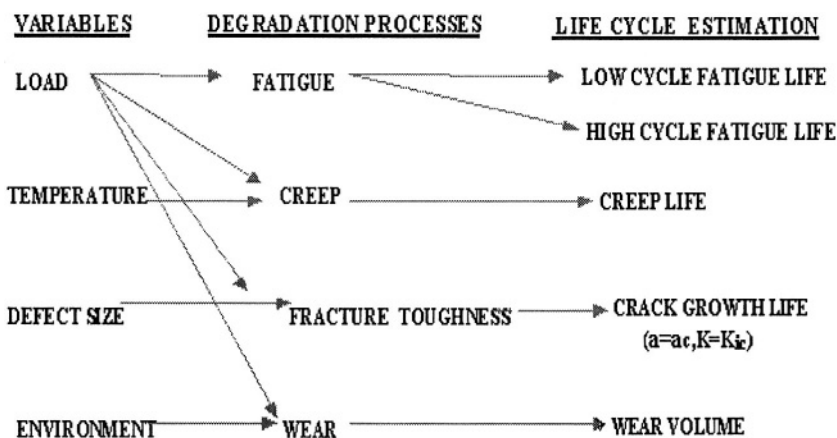
Wear, like fatigue, fracture toughness and creep is a part of the aging processes leading to ultimate failure of the component. Wear of components results in dimensional losses, thus causing poor performance and ultimate failure below design load due to reduced cross section. The volume or dimensional loss of modified material with the progress of time shall normally decide the wear life of surface engineered components. The equipments and machineries are subjected to fluctuating stresses (fatigue), load & temperature (creep) and exposed to attack by hostile surrounding environment and thus undergo degradation (wear) with increasing age.

It is possible to make an estimate of the probable life span of a component, where failure occurs due to aging process. In the aging process there is a progressive and measurable deterioration and degradation in fatigue, creep, fracture toughness and wear properties with time allowing the estimation of probable life cycle (Table 20.1) (ref 1).

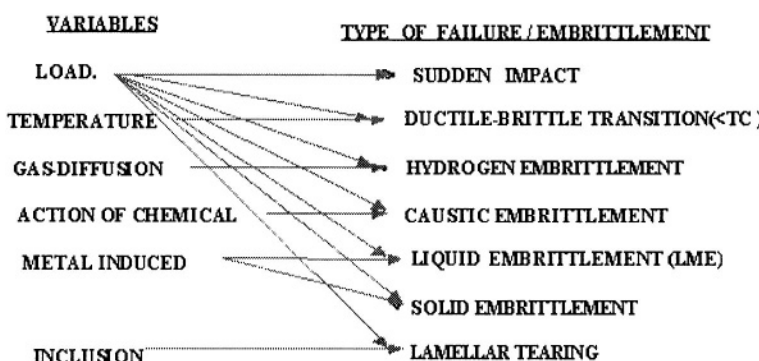
However the unpredictable or sudden failure of component can occur due to various factors, such as, hydrogen cracking (delayed fatigue) due to hydrogen pickup in fusion welding overlay process, embrittlement, ductile to -brittle transition at low temperature of welded ferritic materials, etc. Hydrogen embrittlement or cracking, also known as delayed fatigue, which is caused by the presence of high diffusible hydrogen (>5 ppm), in weld deposited structure can occur suddenly without any prior indication after a short or long service .The various processes leading to unpredictable life of a component are listed in Table 20.2 (ref 1).

Methodologies

Apart from the changes in morphology, chemistry and stress level, the formative processes lead to introduction of flaws in the materials. Life cycle estimation & remaining life assessment is made by following the changes occurring in these parameters during the aging processes by various modes, such as fatigue, creep, corrosion and wear.



Tab.20.1.Variables, degradation processes & life cycle estimation



Tab.20.2 Variables & unpredictable life cycle (sudden failure/embrittlement)

In the high temperature processes like creep and thermal wear there are significant changes in the microstructures with the aging. In creep & thermal wear progressive changes in microstructure are used to ascertain the age of the component. In high cycle fatigue (HCF), fracture occurs or material fails when N (number of cycles) is greater than 10^4 cycles. In low cycle fatigue (LCF) failure occurs at N less than 10^4 cycles. In repeated impact wear, which is similar to fatigue, measurable wear occurs only when the number of cycle, N exceeds a threshold value. The linear elastic fracture mechanics (LEFM) are used to find the fatigue and creep life from the time (or number of cycles in fatigue) taken for a preexisting crack to grow to a critical size. However life of a component in various wear modes, such as, abrasion erosion, adhesion and corrosion is normally estimated from the volume loss of material during the aging process.

Under normal operating parameters, the property changes during usage normally occur in three different stages as follows:-

- Primary or early stage or run-in period, where rate of changes can be high. Apart from creep and fatigue processes, the initial high rates are also observed in the early stages in some wear processes, such as, run-in wear in between two mating surfaces, adhesive-impact wear of materials with high work-hardening rates (stainless steels, high manganese Hadfield steels) etc.
- Secondary or mid-age process where a steady rate of aging process is maintained. The useful or working life is comprised mostly of the life span at this stage.
- Tertiary or old-age stage, where rapid rate of aging leads to early failure.

In extreme conditions, such as, higher temperatures, strain rates, stress and sliding velocities etc., the secondary stage is shortened and the primary stage tends to merge with the tertiary stage. In other words, working life is considerably shortened in extreme conditions.

Fracture Toughness & Life Cycle

The toughness of the high strength and high hardness deposited overlay materials like, maraging steels, Stellites, or ceramic coating materials are far too low to be expressed in terms of CVN (Charpy V- Notch) values. The toughness and thus the fracture mode is governed by the temperature at fracture, the rate at which loads are applied, and the magnitude of constraints that prevent plastic deformation. The toughness of materials are determined by the energy required for the extension of a pre-existing crack.

The failure of material can occur below the designed load due to presence of discontinuities beyond the permissible size.

The basic equation for crack extension in plane strain condition in mode 1 is:-

$$K_I C = E \cdot G_c / (1 - \nu^2) , \quad \text{eq.20.1.1}$$

where ν = Poisson's ratio, E = Young's modulus, G_c = stress energy release rate. According to linear elastic fracture mechanism (LEFM) concept, failure occurs when local stress intensity factor, K_I exceeds a critical value, K_{Ic} . The critical defect size, a_c , for failure to occur in plain stress and strain conditions are as follows

$$\text{PLANE STRESS CONDITION} : a_c = 1/\pi \cdot (K_{Ic}/\sigma)^2 \quad \text{eq.20.1.1a}$$

$$\text{PLANE STRAIN CONDITION} : a_c = 1/\pi \cdot (K_{Ic}/\sigma) \cdot (1 - \nu^2) \quad \text{eq.20.1.1b}$$

The critical stress intensity factor is the stress at which the crack propagation becomes rapid. For low toughness thicker materials, the crack propagation is governed by plane stress condition, where strain is zero in through thickness or z- direction. At this stage when the defect size is a_c , the stress intensity factor is expressed as K_{1C} , i.e., critical plane strain intensity factor or plane strain fracture toughness index. K_{1C} is an indicator of toughness of high strength materials and their deposits. The high value of K_{1C} indicates difficulty in rapid crack propagation. In general, the fracture toughness increases with increasing temperature, decreasing load rate, and decreasing constraint.

a. Fracture toughness & critical defect size of weld overlay

A fracture toughness test for weld overlay consists of applying a slowly increasing load to a fatigue-cracked test-piece and monitoring both the load and associated crack opening. The toughness of the material is then analyzed in terms of either stress intensity factor (K) or crack opening displacement (COD) of crack.

Critical or tolerable defect size calculation from experimental COD (δ_c) values (2, 3)

In a welded 100 mm mild steel structure with yield strength of 360 N.mm^{-2} , the toughness values are found from laboratory experiments in terms of critical crack tip opening displacement, δ_c , as 0.074 and 0.091 mm for as-welded and stress relieved conditions respectively. The critical defect sizes of the welded structure at applied stresses in the range of 45 to 75 Nmm^{-2} are calculated at two levels of δ_c values, i.e., 0.074 and 0.091. The total stress at crack tip (σ) for maximum applied stress ($\sigma_a = 75 \text{ Nmm}^{-2}$), in the as-welded condition, where σ_R is assumed equal to σ_y , is $75 + 360 = 435 \text{ Nmm}^{-2}$, and for stress-relieved condition is 75 Nmm^{-2} . The Young's modulus (E) value is assumed as $2.075 \times 10^5 \text{ Nmm}^{-2}$. The total strain (e) is obtained by dividing σ (total stress) by E (Young's modulus) & elastic strain (ϵ_y) is calculated by dividing σ_y with E. The critical defect size (a_c) is calculated from the following relation:-

$$a_c = C \cdot \sigma / \epsilon_y, \quad \text{where, } C = 1/2\pi (e/\epsilon_y - 0.25)$$

The calculated values of critical defect sizes at two δ_c values (0.074 and 0.091 mm) at different applied loads are tabulated in tab.20.3a. At $\delta_c = 0.074$, the calculated values of all the parameters along with a_c are included while for $\delta_c = 0.091$, final values are indicated in Table 20.3a.

The life of an engineered component is equivalent to the time required for an existing defect to grow to critical size under the total stress consisting of

applied plus residual stress. Lower applied stress and residual stress lead to larger critical defect size (Table 20.3a). Larger critical defect size leads to higher fracture toughness and longer life of the component.

Tab 20.3a. Estimated critical defect size from COD in a welded structure

Total stress (Nmm ⁻²)	Total strain(e) $\sigma /E \times 10^{-3}$	e/ey	C	ac (mm)	
				$\delta_c = 0.074$	$\delta_c = 0.091$
435	2.09	1.204	0.1667	7.23	8.76
325	2.518	0.875	0.254	10.86	13.36
225	1.084	0.625	0.424	18.136	22.30

Residual stress can reduce drastically the fracture toughness of overlay materials. The residual stress generated by weld deposition process leads to relief crack formation on the surface of wear resistant high hardness alloyed white cast iron deposits. The residual stress is reduced by post weld heat treatment, thus improving fracture toughness of the material.

The stress concentration occurs due to presence of discontinuities such as notches, holes or due to ductile brittle transition. A multiplying factor, called, stress concentration factor (SCF), for applied stress (σ_a) is used to take into account the presence of such stress raisers. The total stress (σ) is calculated as: $\sigma = \sigma_a \times \text{SCF} + \sigma_R$.

The 9%Ni ferritic steel is used for cryogenic applications due to its unique toughness properties even at subzero temperatures (3).

However, in a welded structure, the residual stress and the SCF can reduce the toughness considerably (Table 20.3b). In a 23" thick 9% NI-steel plate, joined by matching consumable, where $K_{1c} = 5000 \text{ Nmm}^{-3/2}$ at 77°K (-196°C), & design stress, $\sigma_a = 294 \text{ N/mm}^2$, $\sigma_R = 365 \text{ N/mm}^2$, & 0.2% PS = 72.8 N/mm², the calculated 'ac' values in as-welded is 5.12 & in partly stress-relieved state as 8.40 (Table 20.3b). The ductile to brittle transition in this steel occurs at 77°K, hence SCF value in this condition is assumed as 3. With stress concentration factor at 3 and $\sigma_R = 365 \text{ N/mm}^2$ the ac is at 5.12. At room temperature (RT) the material is in ductile region, the SCF equals to 1. Under same applied and residual stress conditions, ac or tolerable defect size increases from 5.12 at 77°K to 11.5 at room temperature. By reducing residual stress to 25% of yield strength level, the tolerable defect size at 77°K becomes 8.40 (Table 20.3b). To improve the life of the surface engineered materials, such as those containing weld overlays, SCF and residual stress are to be reduced. The stress relief treatment reduces the residual stress level in the weld. However the compressive residual stress improves fatigue life of the carburized or nitrided surfaces.

Tab.20.3b.Tolerable defect sizes in 9%Ni-steel weld

Material Condition	σ_a N/mm ²	SCF	σ_R N/mm ²	σ Total	ac mm
At RT	294	1	365	659	11.5
At 77°K	294	3	365	1247	5.12
Stress Relieved					
At 77°K	294	3	0.25 σ_a	973.25	8.40

Stress Concentration Factor (SCF) at 77°K is assumed as equal to 3.

b. *Fracture toughness & wear of ceramic materials:*

The wear in crystalline ceramics is due to crack formation during deformation and subsequent growth of the cracks. The failure of brittle ceramic materials depends on the fracture toughness. The fracture toughness of ceramic material is related to hardness by the following equation (4)

$$K_{Ic} = 0.016(E/H)^{1/2} (P/C)^{3/2} \quad (\text{eq 20.1.2})$$

where K_{Ic} = Fracture toughness (MPa \sqrt{m}), P = Indent or load, (kgf), C = Crack length (mm), E = Young's Modulus, (Gpa), H = Hardness, (Gpa)

The equation for wear of ceramic materials based on fracture mechanics as proposed by Evans and Marshall (5) is as follows:-

$$V = Pn^{1.125} \bullet K_c^{-0.5} \bullet H^{-0.625} (E/H)^{0.8} \bullet S \quad (\text{eq 20.1.3}),$$

Where V = wear volume, m^3 ; S = sliding distance, m; Pn = applied load, Mpa, K_c fracture toughness (MPa \sqrt{m}); H = hardness, Gpa; and E = elastic modulus, GPA.

Equation 20.1.3 can be expressed roughly as follows (5):-

$$\frac{V}{S} = K \cdot \frac{F_n}{\sqrt{K_c \cdot H}} \quad \text{Eq. 20.1.4}$$

where $F_n = Pn = \text{Applied load} \equiv Pn^{1.125}$, $1/\sqrt{H} \equiv H^{-0.625}$ and $K = \text{Wear constant} = (E/H)^{0.8}$

The above equation (20.1.4) is in line with the general wear equation for the metallic material. The hardness and fracture toughness are the key elements controlling the wear of ceramic materials. The normal practice is to use the value of H^4 , K_{Ic}^4 as an index for abrasive wear resistance of the ceramic

material (6). The hardness, fracture toughness, calculated wear resistance and the experimental wear resistance values of selected ceramic and composite materials are indicated in Table 20.4.

Tab.20.4. Calculated & experimental wear parameters of selected ceramics

Material	Fracture toughness, K_{1c} , MPa.m $^{1/2}$	Hardness, H, GPa	Abrasion wear resistance parameter $(H^{1/2} \cdot K_{1c}^{1/2}) \times 10^{-1}$	Abrasion W. F $\text{mm}^{-3} \times 10$	Adhesion W.F mm^{-3}
Al ₂ O ₃	2.3	15.6	0.738	0.24	6.25
Al ₂ O ₃ -TiC	3.2	17.2	0.992	2.08	6.99
Sialon	4.0	12.2	1.192	1.02	0.41
SiC	3.3	18.57	1.055	1.36	1.477
WC-Co	5.2 13.0	14.4	1.307 2.598	1.22 0.7	250 12.5

WF=Wear Factor

Dry sand abrasion tests were carried out as per ASTM G65, procedure A (7). The ring-on-block adhesive wear tests were carried out for 10,000 revolutions using a cemented carbide wheel under 27.2 kg load (7). The volume loss obtained in abrasion and adhesion tests are converted into wear factors in order to compare the same with the calculated wear resistance parameters. The test results show the differences in the wear rates of the same material under two different wear modes. In abrasive wear situation, the best wear life is obtained from Al₂O₃-TiC and the least from Al₂O₃. The cemented carbide shows a wide variation in wear life depending on the composition, such as, WC & W₂C and the amount of binder. Cemented carbide containing the least amount of binder shall result in very low wear rate compared to the one containing high proportion of WC. Both W₂C & WC have low adhesive wear. The calculated wear resistance parameters differ widely from that based on experimental WF values (Table 20.4).

The hardness and fracture toughness of the ceramic materials, however, depend on chemical composition, crystal structure, grain size and porosity.

The two different *stoichiometric compositions* of tungsten carbides, WC and W_2C , widely differ in hardness and wear resistance properties.

The increase in wear is exponentially related to porosity. The pore may function as initiation points for slip bands or twins thus increasing wear. Large pore size can cause heavy wear.

The friction coefficient for ceramic pair can be high e.g, $\mu > 0.5$, in a range of operating environments. The ceramic to ceramic contacts of two brittle materials with low fracture toughness and high coefficient of friction can lead to early fracture and high wear.

Prescription to improve fracture toughness & life in surface engineered ceramics

Nonequilibrium, high energy processes using laser, plasma and ion beams are used for surface modification of ceramics. Ion bombardment can introduce biaxial compressive residual stress in the surface of ceramic material thus improving the fatigue life. The damage caused by the ions results in an expansion of the layer and the resulting compression stress leads to closure of surface flaws (8). The closure of surface flaws improves the toughness of the ceramics. Ion implantation with nickel in the outermost layer (<1 micron) improve the fracture toughness of alumina (8).

By laser glazing the surface melts and ceramic fills the surface pores and flaws and thus improves fracture toughness of ceramics. Ceramic surfaces can be coated with molybdenum sulphide (PVD) or DLC (plasma CVD or Ion beam) in order to reduce friction coefficient and thus increase life cycle in adhesive wear.

Fracture toughness concept is used to improve the properties of thermally sprayed ceramic coatings on metallic substrate. It has been reported (8) that the toughness of plasma sprayed magnesia stabilised zirconia coating can be improved by controlled precipitation of monoclinic ZrO_2 needles. For example, the measured K_{1c} value for 0.4 mm coating of $ZrO_2 + MgO$ has been found to be as high as $2.7 \pm 0.5 \text{ Nm}^{3/2}$, whereas the more common range of K_{1c} is between 1.3 to $2.0 \text{ Nm}^{3/2}$, depending on structure. An increase in K_{1c} should increase the coating adherence particularly in comparatively thicker coating where failure occurs within the coating thickness.

Fatigue life

The life of a component during applications involving dynamic (or fluctuating) work load (fatigue), depends on the number of cycles under stress and the associated growth of preexisting flaw (LEFM). Fatigue damage occurs in areas where the total strains exceed the elastic limit. Therefore the common sites for fatigue damage includes the regions of stress concentration such as notches, nicks, gouges, toes or terminations of weld and other abrupt change in surface geometry. Also because the plastic deformation is

accommodated at free surfaces, fatigue damage occurs at external surfaces, or at internal voids or free surfaces of weak interfaces between particles or coating and substrate. The higher stress level is normally reached at the sub-surface region during contact fatigue wear and the growth of sub-surface defects in the modified surface can lead to fatigue failure. The **high cycle fatigue** (HCF) is basically stress-controlled and therefore S-N curves are widely used for HCF design. In stress-life or S-N curve, the stress is plotted against life or number of cycles (N). In HCF, fracture occurs or the material fails when N (number of cycles) $> 10^4$ cycles. The **low cycle fatigue** (LCF) design is based on ϵ -N curves (ϵ = strain) and failure occurs at $N < 10^4$ cycles. The variation of fatigue crack propagation rate (da/dN) with alternating stress intensity (ΔK) follows a sigmoidal curve (Fig. 20.1) (ref.9). The three regimes for crack growth are as follows:-

Regime A

The behavior in this regime exhibits a **fatigue threshold stress intensity**, ΔK_{th} above which the fatigue cracks grow under cyclic loading (Table 20.1). The fatigue-crack initiation for steels improves with increased yield strength. The magnitude of the threshold value can be predicted from the following relationship:-

$$\frac{\Delta K_{th}}{\sqrt{\rho}} = 10\sqrt{\sigma_y}, \quad \text{Eq.20.1.5}$$

where, σ_y is the yield strength and ρ is the notch tip radius. The **effective toughness** of material resisting growth of cracks can be rightly represented by stress intensity value ΔK_{th} (Regime A, Fig. 20.1), rather than fracture toughness K_c , where failure occurs (Regime C, Fig. 20.1)

Regime B

The behavior in this regime corresponds to a region of crack propagation that can be represented by a power law equation, such as, eq.20.1.6. The crack growth rate in this regime is related to stress intensity factor (K) by the following relationship:-

$$\frac{da}{dN} = c (\Delta K)^n \quad \text{Eq.20.1.6}$$

where a = crack length, N = number of fatigue cycles, c & n are constants; ΔK = stress intensity factor in $\text{MPa}\sqrt{\text{m}}$ units = $\Delta Q \sigma \sqrt{(\pi a)}$, where σ is the applied stress and Q represents a geometrical factor.

Most of the finite life is governed by the behavior in this region. The damage tolerant design based on **linear elastic fracture mechanics** (LEFM) concept has been used to study the crack growth in both LCF and HCF. The

life cycle prediction technique relies on the integration of equation 20.1.6 for the growth of crack size from 'ao' to 'a crit' as follows (10):-

$$N_t = \frac{2}{(n-2) \cdot C Q^n \pi^{n/2} \Delta \sigma^n \left[\frac{1}{a_0^{n-2/2}} - \frac{1}{a_{crit}^{n-2/2}} \right]} \quad \text{Eq. 20.1.7}$$

The above equation (20.1.7) shows large power (n) dependence of crack growth rate on stress intensity, i.e., the estimated life (N_t) is propagating to the reciprocal of σ^n , where σ is directly proportional to ΔK . With n = 2-4 for metallic materials, the predicted life can get reduced by an order or two in proportional to K and that for ceramics, with n > 20, a small increase by a factor of two in applied stress reduces the projected life by 6 to 30 orders of magnitudes. The crack growth approach can therefore, lead to a large variation in the predicted life for a small change of applied load for brittle ceramic materials. A significant portion of life time may be involved in crack initiation (Regime A) during fatigue loading, which is not included in the crack growth approach of predicting life. Inspite of limitations, the fracture mechanics approach has found acceptance (10). In this region each stress cycle corresponds to a distinct increment of crack extension that usually leaves a striation on the fracture surface.

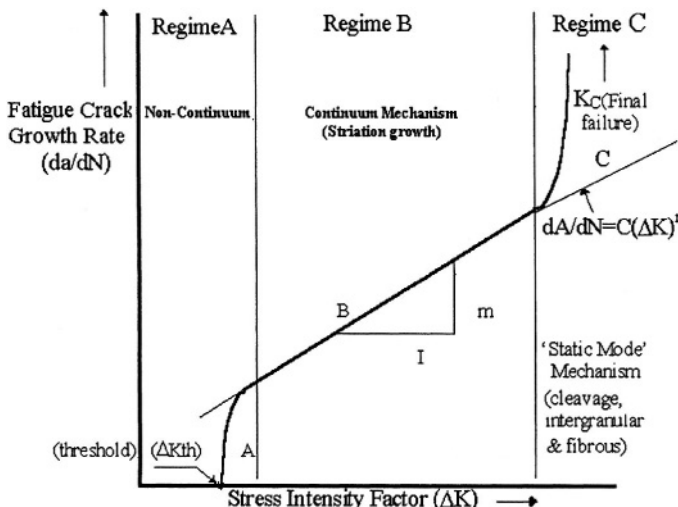


Fig.20.1. Fatigue crack propagation with alternating stress intensity

Regime C

The start of accelerated crack propagation rate marks the transition from B to C regime. The mechanism involves the superimposition of a brittle or

ductile tearing mechanism that leaves fatigue striations on the fracture surface (11). The mechanisms occur when the stresses or strains in the vicinity of the crack tip reach critical values.

Prescription to improve fatigue life

The rolling-contact-fatigue is a major cause of failure in rolling-element bearings and in rail-wheel contacts. The time-to-failure for the bearing materials has been increased by the enhancement of near surface properties using such techniques as ion implantation (12), Cu and TiN coating (13), DLHC (diamond like hydrocarbon) coatings (14). In rail-frog contact wear, weld overlays of high manganese steel and ferritic stainless steel are used to improve the wear life (1). Laser peening (ref. Chapter 6), carburising, nitriding (Chapter 2) increases compressive residual stress on the surface and thus improve fatigue resistance.

Creep Life

The creep life is defined as the time taken by a component for failure to occur due to progressive increase in strain under stress at elevated temperatures. The creep life can be determined from the growth of the existing crack to critical size and also from the microstructural changes occurring at different stages of creep process.

Creep & LEFM

In addition to creep tests, creep crack growth can be used to assess creep life. Creep crack growth rate is expressed by an equation similar to that of fatigue crack growth (eq.20.1.8) as follows:-

$$\frac{da}{dN} = A (C^*)^m \quad \text{Eq.20.1.8}$$

$$t = \int_a^{ac} \frac{da}{A(C^*)^m} \quad \text{Eq.20.1.9}$$

where C^* is a function of geometry, A and m values can be obtained by carrying out appropriate tests or from literature (21). Similar to fatigue the creep life is governed by the time, t, required for a defect of size, a, to grow to the critical size, ac , and can be assessed by integrating equation 20.1.8 as shown in equation 20.1.9 (ref.15). In a low alloy steel, the early stage changes include, precipitation and solid solution strengthening, inter-particle spacings of carbide, hardness, spheroidisation of carbides, and carbide chemical composition. The cavitation sets in at a later stage leading to final failure.

Creep & microstructural changes

At a given temperature and stress-strain condition, the extent of microstructural change is related to the time elapsed. The microstructural changes during creep process (16) can be indicative of different stages in creep life (Fig. 20.2). The initial fine grained matrix with fine dispersion of precipitates undergo coarsening from a temperature A, upto recrystallisation temperature B. At B, the recrystallisation process sets in and a new set of grains is formed. With further increase in temperature the grains grow and the precipitates become coarser until temperature C is reached. Further increase in stress or temperature leads to the formation of voids or cavities at grain boundaries and the subsequent growth of which can result in failure by fracture at D. Life estimation is carried out by comparing the microstructure of the component with that of the standard micrographs of the same material at different stages of creep life (Fig. 20.2). RUL (remaining useful life) is ascertained from observations in microstructural changes occur during use and accordingly action plan is recommended to prolong the life of the component. The repair is not normally recommended during secondary creep stage (B or A-B). From B, more frequent inspections at shorter intervals are required to locate C, where repair is recommended. At D, the component is to be repaired immediately to prevent failure.

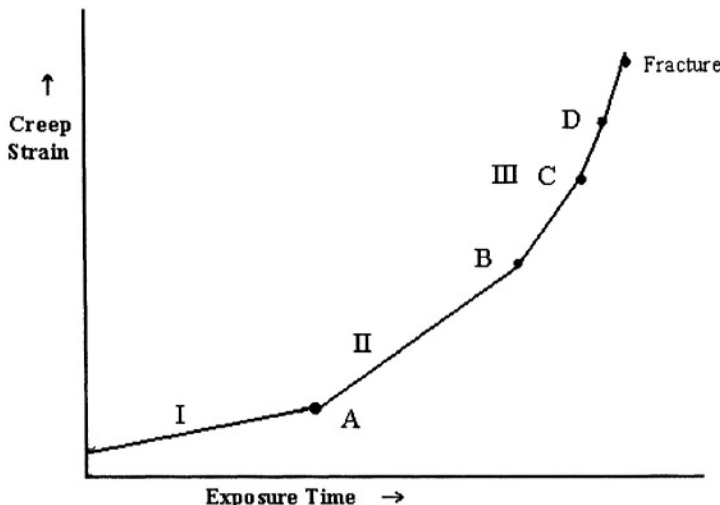


Fig 20.2 Diagram showing different stages of creep damage and residual life estimation from microstructural changes(schematic)

Legends:-I,II &III are primary,secondary and tertiary creep ranges; and A&B mark end-points of primary & secondary,while C & D mark the begining and mid-point of tertiary creep.

For high temperature applications like boilers, the remaining life assessment during scheduled maintenance shall provide the information for

the need to repair. The aeroengine components undergo scheduled resurfacing of worn coating. Before resurfacing, it is necessary to check for the remaining or residual life of the creep damaged component from microstructural observations.

Prescription to improve creep life : Thermally assisted processes used to improve creep and wear life of the components include, depositing PTAW or GTAW weld overlay of creep resistant alloys such as Nimonic (in bar forging hammer), maraging steel (forging anvil), satellites (engine valves), thermal spraying (Plasma or HVOF) of thermal barrier coating (TBC), such as stabilized zirconia (in piston crown of automotive engine, aeroengine components), EBPVD or thermal spraying of MCRAIY to resist high temperature oxidation and hot corrosion in aeroengine components.

Wear life in different wear processes :-

The useful wear life can be defined, as the period of operation after which the component loses its dimensional tolerance beyond that specified for the application. The dimensional tolerances for engineering components can be a fraction of a millimeter (e.g., bearings, bushings) to several centimeters (coal crushing hammers). The wear life standards for specialised applications are set by the relevant authorities in compliance with safety regulations. For example, the wear life of railway crossings is assessed in terms of the number of GMT (Gross Million Tonnes) of load carried till the nose of the crossing goes down by 6 mm due to wear. The crossing life of 18 GMT for an average annual load of 12 GMT means that the wear life of crossing is 18 months (17).

Methodologies:- Wear life can be estimated from wear equation, standard test data , wear map, zero wear equation and wear simulation studies. The wear simulation test on wear resistant surface with low wear rate is normally performed over an extended period of 50 to 100 hours in order to make the prediction of a more accurate wear life. The dimensional or material loss occurring during the wear process is estimated by techniques such as, thin layer activation technique, ferrography of wear debris, surface profilometry etc. Hardness and metallography of the surface are also used to indicate the loss of coating material from the surface. Some of the important methods are described.

Wear equation, map, and test: The wear volume (V) is directly proportional to sliding distance (d) and applied normal force (FN) and inversely proportional to hardness or yield stress (H) of the softer surface as follows :

$$V = K \frac{FN}{H} \cdot d$$

$K = \text{constant} = \text{wear coefficient}$. Also $V/d = \text{Wear area} = K$, if $FN/H = 1$. i.e., hardness (H) or shear yield stress of the material is equal to applied force (FN), the wear volume is equal to wear coefficient per unit sliding distance ($d = 1$). The wear coefficient thus represents the wear rate of materials per unit sliding distance. The data on wear coefficients (K) for various types of wear in different materials are available in the literatures or can be determined by conducting standard wear tests. The wear coefficients for adhesive wear between similar material pairs are in the range of 10^{-2} to 10^{-7} . Thus the adhesive wear rate between two similar material surfaces can vary over a wide range of 10^{-5} . For 3-bodies abrasive wear, K_{ab} values vary from $10^{2.5} - 10^{-5}$ i.e., over a comparatively narrow range of $10^{2.5}$. The wear mechanism maps under various loads and sliding velocities of different materials are available. The wear map is useful for finding frictional or adhesive wear rates over a wide range of normalised velocities and pressures (Fig. 9.2 in chapter 9). In standard wear tests, the wear volume loss over a specified test period is obtained. The volume loss can be converted into wear rate in terms of unit time or unit gram weight of impacting particles in the case of erosive wear. The values obtained from standard tests are used to rank the engineered surfaces with respect to wear life.

Adhesive Wear Life

In addition to short time standard wear tests for ranking the modified surfaces, it is possible to find out the useful life by conducting long time wear tests. This is particularly true for adhesive wear, where wear behavior follows a normal 3-stage pattern of high run-in wear, followed by steady state wear and final high wear leading to failure. The extent of steady state behavior vary with sliding velocity or applied load. The constant wear rate, $\Delta W/\Delta t$ in second stage (steady state) can be used to find the working or useful life (Fig. 20.3).

In unlubricated sliding wear test as per ASTM D-3702-78, of plasma sprayed and CVD coatings against ceramic oxide impregnated hard disc of proprietary composition (18) it was found that the coatings reached a steady state wear rate after approximately 1 hour of testing and that remained constant until incipient failure of one or both of the surfaces occurred. The wear rates of CVD coatings are much less than that of plasma sprayed coatings (Table 20.5a) and the rounded grains TiB_2 coating showed lowest wear rate. The adhesive wear life of CVD coatings can be 5 to 20 times than that of plasma sprayed coatings (Table 20.5a).

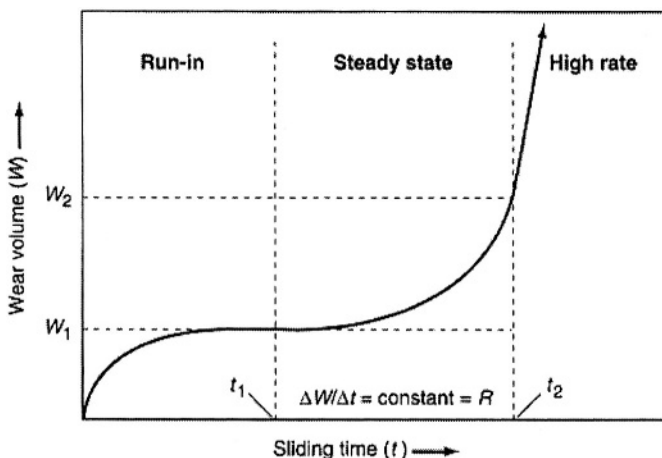


Fig.20.3.Wear volume vs.sliding time In adhesive wear(schematic)

Tab.20.5a Comparative Adhesive Wear Life of Selected Ceramic Coatings

Coatings	Process	Wear rate at RT cc/cm ² 25x10 ⁻⁸	Comparative wear rates
Cr ₃ C ₂	plasma spray	15.625	17.85
WC-Mo	plasma spray	10.145	11.46
Al ₂ O ₃ -TiO ₂	plasma spray	18.60	21.02
TiB ₂ -nodular grains	CVD	2.221	2.5
TiB ₂ -rounded grains	CVD	0.885	1

To obtain similar wear life for coatings with different wear rates, the coating thickness can be reduced in a similar ratios as the corresponding comparative wear rates (Table 20.5a) (ref.6, 18). The adhesive wear factors (WF) and the comparative life of diffused coatings are indicated in Table 20.5b. The data are based on tests conducted as per ASTM G-77 (19,1). Nitriding results in lowest wear rate amongst the diffused coatings.

Abrasive wear life

The abrasive wear factors and the comparative wear life of weld overlays (white cast iron and alloyed white cast iron) and diffused coatings (C, N, B, TiC and VC) were evaluated as per stipulations in ASTM-G65-85 (ref. 1, 19, 20). The results are indicated in Table 20.6.

Tab20.5b Comparative wear resistance of diffusion treated surfaces

Diffusion	ASTM G-77 (WF=1/mm ³)		Comaparative Wear	
Treatment	Self-mated	Against AISI4620	SM	AISI4620
Carburizing	4	5	3	5
Nitriding	1.33	1.0	1	1
Carbonitriding	5	0.71	3.76	0.71
Boronizing	12.5	10	9.4	10.0
Nitrocarburising	0.71	10	0.53	10.0

Examples of highly abrasive wear applications include agricultural & mining equipments & tools. The hardness of the common silica abrasive is 2600 HV and that of hard martensitic matrix is 700 HV. Hence the hard coating matrix of iron base materials, such as carburised steel surface or that of white cast iron weld deposit has very little effect on abrasive wear. The presence of hard chromium-carbide (1700 HV) in white iron weld overlay and other hard carbides, borides in the coating shall considerably reduce wear due to abrasion (Table 20.6). The best results are obtained with diffused coatings of TiC and VC.

Mostly high hardness to brittle materials are used as coatings to resist wear due to abrasion. Predominant modes for removal of coating materials by abrasives are cutting for hard ductile materials and fragmentation for brittle materials. The degree and extent of cracks depend on hardness and fracture toughness.

Erosive wear life

The wear volume loss, V , due to erosion can be expressed in terms of mass of impacting particles, m , striking at an angle, α , with velocity, v , as follows:-

$$V = k \left[\frac{\frac{1}{2}mv^2}{3H} \right] f(\alpha)$$

where H is the hardness of the material. The wear volume is thus directly proportional to m , v and α . For ductile materials, wear is a cosine function of α , with maximum wear at 20° and minimum at 90° . For brittle materials, wear

follows a $\sin \alpha$ pattern, with minimum at low angle and maximum at 90°. The shape, size and hardness of the particles affect erosion wear rates.

Tab20.6. Wear life of engineered surfaces according to ASTM G65-85 tests

Surface treatment /composition	Wear factor cc^{-1}	Comparative wear life
White CI weld overlay		
1. NiCr2 (2.6C,4Ni,2.5Cr)	0.77	1
2. Cr27 (2.8C,28Cr,1.3Si)	0.806	1.05
3.15-2-1 (2.8C,15Cr,2Mo)	0.83	1.08
4.17-3 (3.3C,17Cr,2.5Mo)	0.84	1.09
Allloyed white CI weld		
Alloy1 (5C,28Cr,5Cb)	2.3	2.99
Alloy 2 (5.5C,25Cr,6.5Cb, 6Mo,0.8V,2.5W)	4.1	5.3
Diffusion treatment		
Carburizing	0.448	0.58
Nitriding	0.847	1.1
Carbonitriding	0.429	0.557
Boriding	2.857	3.71
Titanium carbide	8.34	10.83
Vanadium carbide	9.09	11.8

Dry erosion

Dry erosion tests are conducted by impingement of solid particles carried in gas jets for a specified period. In ASTM G76, a gas stream containing 50 μm angular alumina particles are impacted on the specimen at a particle velocity of $30 \pm 2 \text{ m/s}$ ($100 \pm 6.5 \text{ ft/s}$) for a normal test time of 10 minutes. The dry erosive wear properties of different materials including engineered surfaces are evaluated by a large number of investigators using different test parameters (21, 22, 23, 1). Some of these results converted into wear factor and life along with important application areas are indicated in Table 20.7. The erodent was 25 gm of 74 micron of mixed oxides. The velocity of the air stream carrying erodent was 150 m/s. The test temperature used was 538°C (22) and the testing time was 26 minutes so as to obtain the wear volume at

the steady state condition. The coating systems were evaluated primarily to improve the erosive wear at elevated temperature service of ferritic stainless steels components, such as nozzle and blades of steam turbines (22). Other applications for the coatings are also listed in Table 20.7.

Tab.20.7 Erosion wear life of selected modified surfaces

Material	Process	WF(30°) $\text{cm}^{-3} \cdot 10^5$	Wear life rating(30°)	WF(90°) $\text{cm}^{-3} \cdot 10^5$	Wear life rating(90°)	Application
1. Cr_3C_2	D-Gun	15.87	13.8	7.69	4.7	Boiler tubes
2. WC- NiCrB	Clad	6.14	5.34	4.0	2.44	ID fan
3. FeB, Fe_2B	Diffused	8.13	7.07	2.78	1.70	Dies
4. CrB	Diffused	5.26	4.58	11.12	6.78	Bearings
5. WC-Co	Plasma spray	4.76	4.15	1.786	1.09	Abradable gas turbine coating
6. NiCrB	Plasma spray	1.149	1	1.64	1.0	Osepa separator
7. TiN	PVD	7.69	6.69	1.96	1.19	
8. Cr_3C_2 +T.800	Sputtered	—	Wore through	—	—	—

WF=wear factor=1/wear volume; T800= Tribaloy 800

The small grains, low porosity and the absence of cracks in the microstructures led to increased wear resistance. The hardness, composition and distribution of second phase hard particles had less influence on coating life. The microstructural features of some of the coatings are as follows:-

D-Gun coating of Cr_3C_2 showed highest life cycle rating at $\alpha = 30^\circ$ and the second best at $\alpha = 90^\circ$. Microstructure consists of fine grain particles in the matrix with very little porosity.

Plasma sprayed WC-Co coating has higher wear rate than chromium carbides due to the presence of fine network of pores evenly distributed in the matrix. Abradable gas turbine clearance coating of WC-Co should be readily abradable (sacrificial) and yet resist particle impact erosion from engine ingested abrasive dust moving at high velocity.

Plasma spray NiCrBC: structure has large and small pores and crack network. The wear life of the coating is low.

Electro-spark deposited sputtered Cr₃C₂ + Tribaloy 800 coating contains severe crack network in the as-formed condition resulting in the removal of large pieces of coating during erosion tests.

Liquid Erosion: A study of the erosion behavior in turbine blades and erosion shield by impact erosion by controlled water drops over a range of impact velocities up to 315m/s (1040 ft/s) indicates that the erosion curve follows the pattern of a initial incubation period and then a steady state and finally a decreasing rate of wear (25). A second steady state wear tends to occur in the final stage. The rate of mass loss during initial steady state period has been used to measure relative erosion resistance. The three stages of wear in two pure metals (Cu & Cr) and a stainless steel are shown in Fig. 20.4 (ref.1).

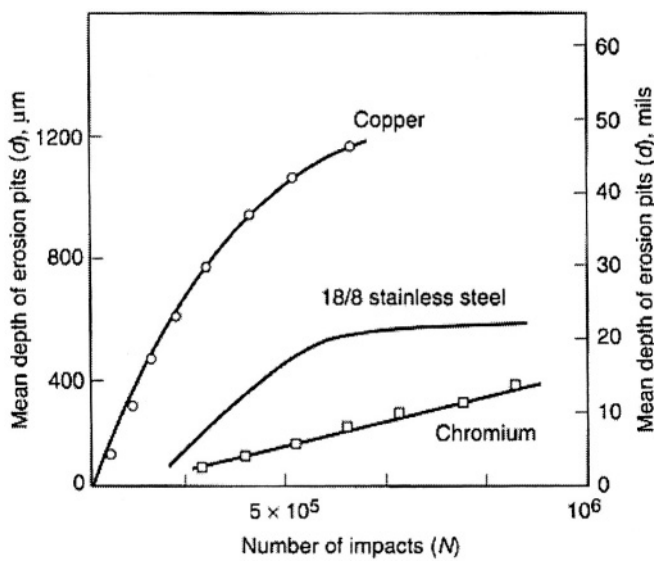


Fig.20.4 Liquid impact erosion.curves

Thermal wear

Wear volume (V) for unit sliding distance and unit load is given by

$$VH = K$$

where K is the wear coefficient and H is the hardness of the material.

From the hardness values of the material at different temperatures, the wear volumes at respective temperatures can be calculated, assuming room temperature K for respective materials. The inverse of the wear volume is the wear factor for thermal wear. The thermal wear properties of weld overlays (PTA) of some selected alloys were determined from hot measurements in a Nikon hot hardness tester over a range of temperatures. The selected list of alloys include Hastelloy C276 (Alloy 1), Nimonic 80A (Alloy 2), Stellite 6 (Alloy3) and Stellite21 (Alloy 4). The wear coefficients of the alloys at room temperatures determined from the results of ASTM G65-85. The wear factors at different temperatures are indicated in Table 20.8 (ref. 26).

Tab.20.8 Wear factor(WF) values at different temperatures (°K)

Alloy	WF values at Temperatures in °K							Wear Coeff(K) at RT x 10 ⁻³
	303	689	773	923	973	1033	1143	
1	1.4	-	1.22	1.18	0.95	0.66	-	1.86
2	1.9	-	1.6	-	1.58	-	1.29	1.99
3	3.28	2.37	-	2.0	-	1.35	-	1.5
4	2.84	-	2.32	1.57	-	1.15	-	1.17

Zero wear or IBM equation (24):

The zero wear equation relating number of cycle (N_t) for initiation of wear with the maximum applied shear stress (γ_{max}) and shear yield stress of the material (γ_y) is as follows:

$$N_t = \left(\frac{\beta \gamma_y}{\gamma_{max}} \right)^2 2000 \quad \text{Eq.20.1.10}$$

The equation 20.1.10 can be used to find out the *threshold numbers of stress cycles*. *No* (Fig. 20.5) below which no visible wear occurs. The wear constant, β for unlubricated wear is equal to 0.2, and for boundary lubrication condition is 0.5.

The wear life of components undergoing repetitive impacts, such as forging hammer has been estimated using the zero wear equation. The service life span of the forging hammer with superalloy weld overlay as reported by original equipment manufacturer and that found by using zero wear equation (26) were of the same order of magnitude.

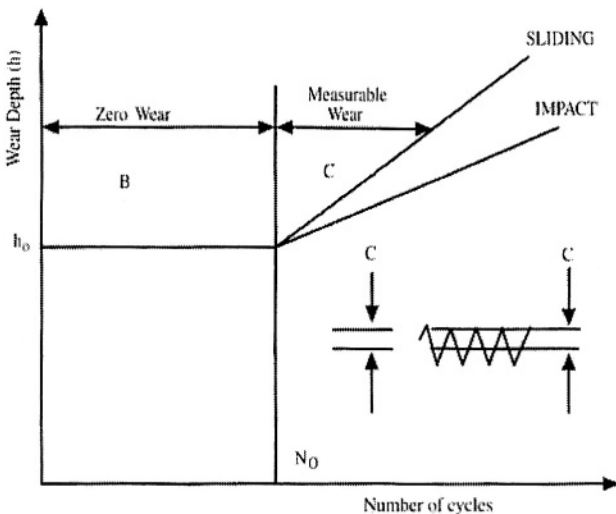


Fig.20.5 Plot of wear depth(h) vs. number of cycles(N) (schematic)
 B=zero wear,C= measurable wear, N_0 =No. of cycles below which wear is zero.

Corrosive wear life

The rate of metal loss by corrosion is related to the corrosion current (I_c) by Faraday's law:-

$$\text{Corrosion rate (mpy)} = \frac{0.131 \cdot I_c \cdot E_w}{\rho}$$

where mpy represents mils per year (0.001 in./yr), E_w is the equivalent weight of the alloy, and ρ is the density of the alloy. The corrosion rates of weld overlays (PTA) of a cobalt and a nickel base alloys in different media are tabulated in Table 20.9 (ref.1). The I_c values were determined experimentally by using a potentiostat. The corrosion rates were calculated from the corresponding I_c values. Corrosion like any other wear process is environment specific and reported in terms of dimensional loss rather than weight loss. The same weld overlay (Co-base alloy) with a slow corrosion rate of 1.29 mpy in saline solution (3.5% NaCl), can corrode at a very fast rate of 349 mpy in HNO_3 solution.

Corrosion life using fracture mechanics (28,29)

Fracture mechanics (LEFM) and fundamental engineering principles, are integrated into a new damage tolerance approach to assess the life of aged components under the combined action of corrosion and fatigue. The

integrated approach accounts for material initial quality states, multi-site damage, corroded surface morphologies and corrosion mechanical effects.

Tab.20.9.Experimental values of corrosion rates of selected alloys in different media

Environment(a)	Corrosion, mils/yr	
	Cobalt-base alloy overlay	Nickel-base alloy overlay
HCl	13.6	12.21
H ₂ SO ₄	81	59
HNO ₃	349	340
10% NaOH	4.41	3.37
3.5% NaCl	1.29	20.73

a = Room temperature

At OEM stage, the combined effect of corrosion and fatigue leads to 3-stage growth of the crack till critical crack length is reached (Fig. 20.5). The steady state crack growth rate portion represents the useful life of the component of new (OEM) component. The number of cycles required to reach the critical crack length is calculated from an equation of the type eq. 20.1.6.

However for the age-degraded components the formation of multi-site defects and reduction in critical defect size leads to low RUL (Fig. 20.6). With an initial flaw size of .0033 inch including all age based effects, reaches the critical crack lengths for age-degradable scenarios of approximately 0.6"-0.7" within 10,000 cycles. The OEM single crack growth follows the traditional fatigue process, with number of cycles decreasing by half to reach the critical size with an increase in 10% stress (28, 29).

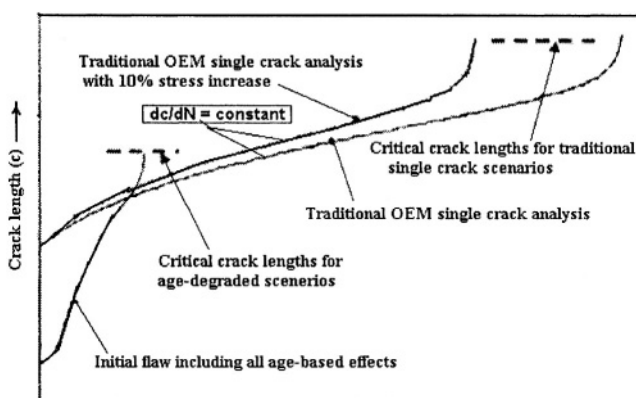


Fig.20.6 Corrosion-fatigue combined model (schematic)

Wear life from long time wear simulation tests

Normal working environment consists of a combination of different wear processes. The viable solution of the critical wear problem can only be obtained by carrying out wear simulation tests. The validity of the results of wear simulation tests can be ascertained by carrying out field tests. The laboratory test parameters are suitably altered till the field results tally with the laboratory test data.

Two examples of wear of simulation studies, viz., high silt erosion-cavitation wear of hydroturbine runners and the repetitive impact-adhesion wear under high load on high GMT railroad frog are to be briefly discussed.

High silt erosion-cavitation wear of hydroturbine runners (30):-

The presence of large quantities of silts (mostly sand particles) in the river water in northern part of India, some parts of China and Russia lead to heavy wear in the turbine components, like runners and guide vanes. In some cases half of the blade has been reported to have disappeared in six months time.

Laboratory wear simulation tests were carried out on the weld overlays (PTA) of prospective alloys covering the base metal (CA6NM) along with the base metal sample. The results are shown in Fig. 20.7. CA6NM is the cast form of AISI 410 type of stainless steel. The lowest wear rate is observed in Stellite 6 overlays followed by 15Cr-15Mn weld overlay. The wear rate of Stellite 6 drops considerably at the steady state and remains almost constant compared to other alloys, where the wear rates continue to increase in the steady state and beyond.

Repetitive impact-adhesion wear under high load on high GMT railroad frog

To improve the wear life of the medium carbon rail steel crossings used in Indian railroads, the normal practice is to use high manganese steel (Hadfield type) weld overlays during refurbishing the worn crossings. In addition to high initial wear in high GMT areas the battered manganese steel overlays layer normally get detached from the substrate at the nose portion and beyond (17). The difference in thermal coefficient of expansion and rate of work-hardening between austenitic coating material and ferritic substrate results in the peeling of the coating during service particularly in high GMT regions. The wear simulation studies conducted in the laboratory resulted in the development of a ferritic stainless steel coating with improved life with no coating detachment (Fig. 20.8). The excellent correlation was found between laboratory wear data with results of field test carried out on 100 crossings in high GMT areas (17).

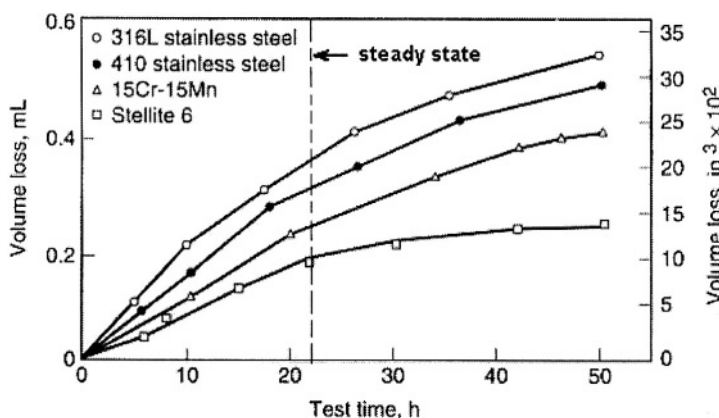


Fig.20.7 Wear of materials with time during wear simulation tests

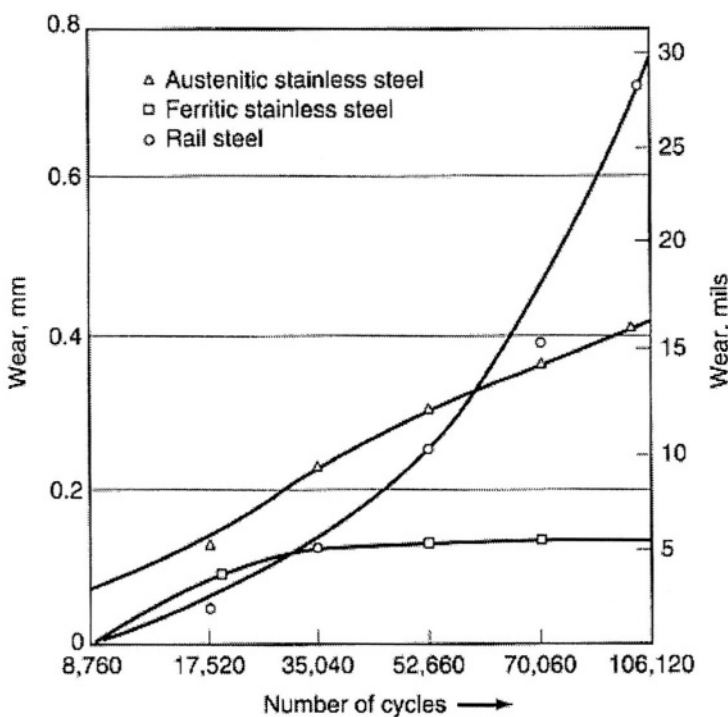


Fig.20.8 Wear of materials in rail-frog wear simulation test

On-line Wear Health Monitoring:-

On-line sensing techniques for monitoring wear, deterioration and failure from the engineered surfaces provide important information on the dynamics of wear processes. In comparison to conventional post-mortem analysis, the

on-line health monitoring system has the advantage of knowing exact time when the worn component is to be sent for restoring the original health by reconditioning or recoating before being damaged beyond repair. The information on the dynamics of wear process shall lead to proper prognosis of the aging components.

Thin layer activation (TLC) (ref.1):

A thin layer of the surface, around 100micron thickness, is activated by ion bombardment. With the progress of wear the loss of material from the activated surface shall result in decrease in the activity. The decrease in activity in the activated layer is proportional to wear. It is possible to measure very small surface loss. The sensitivity of the technique is 0.2 to 0.025 micron. The technique is applicable to all types of materials, such as metal, plastic, ceramics, and can be used during operating condition.

Acoustic Emission

On-line estimation of the wear rate of materials subjected to wear has been carried out by using acoustic emission (AE) sensing (31). Acoustic emission in wear studies refers to elastic waves produced by microscopic deformations occurring in materials as they are stressed and which comprise part of the elastic energy released during deformation. Acoustic emissions also known, as stress wave emissions are associated with dislocation movements under plastic flow, with crack growth, void crashing and similar processes occurring during wear. Detectable emission has been observed in frequencies above 10 MHz and in ultrasonic range for a wide variety of materials (32). The energy in the AE signal is indicative of mass loss by wear from the surface (31). The wear coefficient can be estimated and monitored indirectly on-line using AE (r.m.s) signal without direct measurement of wear volume (31).

References:-

1. R. Chattopadhyay, Surface Wear- Analysis, Treatment, and Prevention, a book published by ASM International, 2001.
2. R. Chattopadhyay, The origin, significance and prevention of defects in welding, Invited talk at Nat. Seminar on Productivity Improvement through Repair and Reconditioning welding, National Productivity Council, New Dehli, 1987.
3. R. Chattopadhyay, Defects in Welding, Int. Conf. on Welding Technology, September, 1988, Roorkee University, India
4. G.K. Beshish, C.W. Florey, F.J. Worzula and W.J. Lenling, J. Therm Spray Technol. Vol 2 (No. 1), March, 1993, p35-38

5. A.G. Evans, D.B. Marshall, Fundamentals of Friction and Wear of Materials, D.A. Rigney, Ed., American Society for Metals, 1981, p439
6. ASM Engineered Materials Reference Handbook, p.114-159, ASM-International, 1989
7. P.K. Mehrotra, WOM, 1987, vol 1, ed. K.C. Ludema, ASME, p301-312
8. Steve Bull, Surface Engineering of Ceramics, Materials World, June' 1993, p340-345
9. P. Chauhan and B.W. Roberts, Fatigue Crack Growth Behavior of Short Crack in a Steam Turbine Rotor Steel-An Investigation, The Metallurgists and Material Technologists, March, 1979, p131-136
10. R.H. Dauskadt, R.O. Ritchie, and B.N. Cox, Fatigue of Advanced Materials, Adv. Mater. Process, vol 8, 1993, p30-35
11. J.M. Barson and S.T. Rolfe, Fracture and fatigue control in structures, Prentice-Hall, Inc., Englewood Cliffs (1987)
12. R.G. Vardiman and J.E. Cox, A study of the mechanism of fatigue life improvement in an ion implanted nickel-chromium alloys, Acta. Metall., 33(11), 1985, 2033-2039
13. R.F. Hochman and others, Rolling contact fatigue behavior of Cu and TiN coatings in bearing substrates, J. Vac. Sci. Technol., A3(6), 1985, 2348-2352
14. Ronghua Wei & others, Rolling- contact- fatigue wear characteristics of diamond-like hydrocarbon coatings on steels, WOM, 1993, ptA, p558-568
15. H. Riedel, Creep crack growth, Ed. R. Raj, ASM, Philadelphia, October, 1983
16. B. Neubauer and U. Wedel, Rest Life Estimation of Creeping Components by Means of Replicas, Int. Conf. In Life Prediction Methods, 1983, (NY), American Society of Mechanical Engineers, p307-313
17. R. Chattopadhyay, Rail Wheel Contact Wear, International Symp. on Tribology, 18-23 Feb. 1993 (Beijing, China), Nat. Science Found of China, Chinese Mech. Eng. Soc. and Tsinghua University
18. A. Levy and N. Jee, Unlubricated wear of ceramic materials, WOM, vol 2, p459-475
19. K.G. Budinski, The wear resistance of diffusion treated surfaces, WOM, 1993, p757-762.
20. I.R. Sare, Impact abrasion testing of alloy white CI, WOM'93, p790-801;
21. A.J. Ningham, and A.V. Levy, The erosion of metal composites, WOM, 1987, vol 2, p825-831,
22. A.V. Levy and B. Wang, Erosion of hard material coating systems, WOM, 1987, vol2, p477-495,
23. A. Nenham, The effect of mechanical properties on erosion, WOM, 1987, vol2, p813-823,

24. Peter A. Engel, Impact Wear of Materials, Elsevier Scientific Publishing Co., NY, 1987, p206.
25. A.A. Fyall, Phil. trans. Royal Soc. (London) A, vol 260, 1966, p290-291
26. R. Chatopadhyay, Microstructural Science, vol 19, ASM-International, 1992, p477-504
27. R.G. Bayer, A.T. Shacky and A.R. Wayson, Machine Design, vol 41 (No.1), 1969, p142-151.
28. D. Simpson and C. Brook : Integrating real time age degradation procedures into the structural integrity process”, Proc. of the NATORTO’s workshop 2 on fatigue in the presence of corrosion, October, 1998, Corfa, Greece.
29. Craig L. Brooks, Scott Prost-Domasky, and Kyle Honeycuu, Corrosion is a structural and economic problem; transforming metrics in a life prediction method, Analytical Processes, Engineered Solutions, 3542 Oxford, Av., St. Louis, Missouri, USA 63143
30. R. Chatopadhyay, High Silt Wear of Hydroturbine Runners, Int. Conf. on Wear of Materials, 13-16 April, 1993, San Francisco, CA, Part B, Elsevier Sequoia, Laussane Switzerland.
31. Kaoru Matsuoka, David Forrest and Ming-Kai Tse, On line wear monitoring using acoustic emission, WOM, 1993, PtA, p605-610
32. S. Lingard, C.W. Yu and C.F. Yau, Sliding wear studies using acoustic emission, WOM, 93, p597-604

SUBJECT INDEX

A

Abrasion1,2,4,,5

hardness vs. wear,4,5
standard test methods 319
wear coefficient range 345

Abradable coatings in gas turbine 73,
74(T), 76,77

Abrasive wear life 346,348(T)

Adhesion 1,2

standard test methods 319,220(F)
wear coefficient range 345
Adhesive wear life of coatings 346, 347(F)(T)
Adhesion or friction welding 219-227

Aerospace

Ion beam aluminum coating on titanium
fasteners in aircraft and spacecraft 120
Ion beam TiN coating as dry lubricant in high
vacuum application in space-crafts 123
Parylene coatings in aerospace,
avionics,277,278
Plasma spray MCrAlY on Ti-alloy airframe
(F-22jet) 77
Refurbishing aircraft engine component
184, 185
Special oxidative ion implantation of
polymers and composites to minimize erosive
wear in FAO (fast atomic oxygen) fluxes of
spacecraft in low earth orbit 130

Aero-engine *see under Gas turbine,*

Al &Al-alloys

Al-alloy 5083 plus hard carbides for PTA
deposit 86
Diffusion coating of aluminium 293-296
Hard top cast steel on Al-alloy 310
IBV deposition of Al on Ti-fasteners 120
Inter-metallic laser coat on Al-alloy 175
Nitrogen ion implantation in aluminum 127
TBC on Al-alloy piston crown 68,69
Aluminum oxide glue 142

Amorphous phase

Plasma assisted coat 105-106
Laser assisted coat 171-175
EBPVD process coat 145,146

Anodizing 120

Arc assisted surface modification processes 243-264

**Arc assisted Electro-consolidation (soft
tooling or pseudo-HIP)** carbides, oxides &
aluminides clad layer 263,264

Arc Light assisted Processes 259-261

Arc light radiation heating system 259,260(F)
Arc light assisted surface hardening
259(F),260
agricultural plow blades & die cutter
blades 260
Arc light fusion of surface coatings 260,261
finer structure of fused deposit 261
comparison with CO₂ laser 261

Arc phenomena in welding & developments 243-245

Advanced power supply devices 244
Thyristor control 244
Solid state or transistor control of
wave form by chopper, analog or
inverter 244
Benefits of waveform control 244,245,
improved arc strike 244
short circuit current control 244
pulse current control 245
Inverter control 244,245

Arc welding by EW 258,259

Process 258,
Advantages 258(T),
Surfacing CR rolls 258,259
Arc welding by GMAW 245(F) 247- 250
Applications 249,250
superheater tubes by combining with
GTA 249-250
concast Rollers 250
nuclear reactor ,250.251

Flux cored electrode 249
 Metal cored electrode 249
 Short circuit, globular and spray transfer 247,248,249(T)
 Synergic 249

Arc welding by GTAW
 245(F),246,247
 Advantages 246,247
 Applications 247
 Engine valves 247
 Bar forging hammer 247
 Process 246
 wire or rod consumable 246
 shielding gas 246
 Repair weld by half bead, butter bead, temper bead 246

Arc welding by PAW with wire or rods 251-254
 Applications 251,251
 engine valve 251,252(F)
 Bore surfacing, ID torch 253,254(F)
 Comparison with GMA & GTA 252, 253(T),254
 Process 251

Arc welding by SAW process 254-258
 Applications
 concast roller 255,256
 nuclear vessels 257(T)
 Process 254(F),255
 Wire, strip & powder consumables 254,255

Arc Spraying Process 261-263
 Applications
 black liquor recovery boilers 262,263
 Yankee dryer 263
 Process 261,262(F)

Auger electron spectroscopy 312,314

Austenitic stainless steel
 PTA coating for corrosion cavitation 309Cb,316L,87(T),91
 valve materials,21-2N 87,21-4N 87,88

Average roughness, Ra 317,318

B

Beta-carbonitride (β -C₃B₄) coating by laser ablation 177, 279,281(F),
Boiler
 Arc spray of black liquor recovery boilers 262,263

Cladding waste heat boiler superheater tubes by combining GMA with GTA 249-250
 Plasma spray of boiler tubes 72,73

Bond coat materials
 Diffused Al₂O₃ as glue to MCrAlY & ZrO₂ top coat 142
 Reactive ion sputtered bond coat of amorphous silicon-hydrocarbon for DLHC 131
 Thermal Spray 58,59(T),

Boronizing or Boring
 Fused salt boronizing
see under Diffused coating
 290(F),291

Plasma boronizing, 96

C

Capacitance discharge welding,
See under 'Spark deposition processes',p239-242

Carbon-arc fusing 307,308

Carburizing 14,95-96(F)-98,288-289,
see under 'Diffused coating' p-288-289
 and also under 'Plasma carburizing 95-96'

Cast Iron
 Fe-C phase diagram 29(F)
 Graphitization 32
 ledeburite eutectic,28,30(F)
 white alloyed,91

Ceramic coating materials
 Carbides 280,282,283
 Composites 282,283
 DLC 280,
 Nitrides & borides 281,283
 Oxides 282
 Processes for ceramic coatings 281(T)
 Quaternary C-B-N-M diagram 281(F)
 Simultaneous vapor phase deposit of Al & O to form sapphire coating 280

Ceramic & composite coating by thermal spray (TS)
 Al₂O₃, 65(F)
 Al₂O₃+TiO₂ 66(F)
 Cr₂O₃ TS 60, 65(F),
 MCrAlY, TS 66(F),
 TiO₂, 6(F),69
 ZrO 66, 61
 Carbide coatings, thermal spray (TS)
 WC-Co TS 62
 NiCr+Cr₂C₃ 74

Ceramic materials

hardness vs. wear 5
 thermal conductivity, thermal expansion coefficient, microhardness & Young's modulus of oxides at RT & high temperature 65(T)

Ceramic Surfaces 279-283

Ceramic surface modifications 279,280(T)

Laser alloyed Ti-rich layer on zirconia 279
 Plasma spray yttria on furnace refractory 279
 Pulsed laser ablation to form superhard carbon nitride 279
 PVD deposited MoS_2 on silicon nitride bearing 279
 Vapor phase TN, Al_2O_3 & DLC on WC cutting tools 279

Coating 22,33-37,40-44

Diffusion 33,45(T)
 Post spray processes 42-43,42(T)
 Thermal spray 34,37,40(T) 40-43,
 Vapor phase deposition 33,43,44(T)
 Welding 34,37-39,38(T)

Combustion 4,35,201-217

Combustion intensity (specific flame output) 202
 D-gun 207,208(F),
 Flame assisted vapor deposition process 215
 flame velocity 202
 flame temperature 202(T)
 heat & flame of oxy-fuel combustion 201,202(T)
 High velocity flame spraying 207-213,
 D-Gun 207,208(F)
 HVOF/HVAF 207-212
 Applications 211, 212
 burners 208(F),209
 CAPL & CGL hearth rolls (CoCrAlY- $\text{Y}_2\text{O}_3/\text{CrB}_2$) 211
 fuel ratio 209,
 microstructure 210,211(F)
 particle feeding, standoff distance, particle size 209, 210
 velocity 210
 sink rolls(WC-Co coating) 211

High Velocity Impact Forging or Cold Gas Dynamic Spray Method(CGSM)213
 Hot chemical gas flame for diamond film deposition 213-215
 process 214(F),215
 microstructure 214 215(F)
 properties and applications 215

Hyper Velocity Impact Fusion 212(F),213
 316L powder 100% dense coating 213
 Burner212(F)
 Combustion at high O_2 pressure 212
 Enthalpy from kinetic energy 213
 Fusion by hyper-velocity impact energy 212
 Rocket type burner 212
 WC-Co dense coating 213
 Moderate capacity flame spray/fusion system 204-207
 Spray system 204
 Spray Fuse System 204-207
 composite 205,206(T)
 compressor plunger 207
 LMM rolls 207
 microstructure of Ni-alloy+WC
 roll cavity forming 207
 self-fluxing alloys and spray fusion 204,205(T),206,207
 WC+Cu-alloy brazing rod 207
 Pulse combustion 202-203
 Surface modification by furnace atmosphere control 203,204
 addition of carbon 203-204,
 addition of nitrogen 204
 bright annealing of steel strips 203
 removal of carbon 203

Composites,

Al+SiC on Al-alloy by spark deposition 242
 Ceramic-composites for thermal spraying 60,61,62(T)
 HVOF spray CoCrAlY- $\text{Y}_2\text{O}_3/\text{CrB}_2$ on CAPL & CGL hearth rolls 212
 Polymer composites as abradable coating for gas turbine 64

Ni-Cr+Cr₂C₃ 73,74

WC-Co, thermal spray deposit (F)

Con-cast rollers

GMAW cladding 250
 PTA cladding 91
 SAW cladding 255,256,

Co-polymerisation 109

Corrosion 1,6-16,45

Anodic & cathodic protection 13
 composition 8
 crevice 11
 current & voltage 8
 galvanic corrosion 9,10
 general corrosion 9,10(F)
 hot corrosion 13-15
 inter-granular 10,12(F)

microstructure 8,9
life 352,353(T,F)
parting 10,11(F)
pitting 11
polarization curves 7(F)
polarization curve of stainless steel,8(F)
polarization curve, effect of alloying elements 9(F)
prevention 12-13
principles 6-7
rate 7
salts,alkalis,acids 9
stress 8,11,12
Tefel's equation 6
Tests 319

Corrosion, hot 13-14,15(T),16
Oxidation, carburizing, nitridation halogen erosion, sulphidation 14
Molten salt corrosion 15
Types & resisting alloys 15(T),16
Creep 333,342-344

D

Decarburization 203

Degradation temperature of polymers 277

D-Gun spray 208,209(F)

Diamond Coating Techniques 103
Hydrogenated amorphous (α -C:H), metal doped hydrogenated amorphous (Me: α -C:H).diamond like carbon(DLC) 103
Plasma activated CVD (PA-CVD) 103
Thermally activated CVD (TA-CVD) 103,214-216
TA-CVD & PA-CVD 103

Diamond coating formation mechanism & types 103,104
black diamond for tools 104
polycrystalline diamond formation 103,104
white transparent diamond 104

Diamond coating properties & applications 104,105
Corrosion resistance 104
Cutting tools for nonferrous metals & ceramics 104
Hardness, molar density, thermal conductivity, sound velocity, friction coefficient 104
Low lubricity diesel fuel injection system with diamond coating 104

Low wear diamond coated carburized transmission gear 104,105

Diffused Coatings 13,31,32,141, 285-306
Corrosion prevention 13
Carbon diffusion, vacuum carburizing & high pressure quenching 288(F),289
Carburized auto-transmission gears & shafts 289
Boronizing by electrodeposition in fused salt at 850°C 289, 290(F)
Borided Nimonic alloy for thrust vectoring nozzle bearing components of gas turbine engine 291
Borided Co-binder in WC-Co surface of jet engine fuel pump 291
Borided steel for mandrels, dies, plastic extrusion screws 290
Borided steel microstructure 290
Borided molybdenum 291
Diffusion coated surface wear 291,292(T)
Diffusion coatings of substitutionals 292,293
chemical vapor diffusion 292,293
pack cementation 292,293
slurry fusion 292,293

Diffusion coating of aluminium 293-296
blue zone formation in Ni-base superalloy 294 (F),295,141
high activity(inward) and low activity(outward) diffusion aluminide coatings 294(F),295
high Al 'stuffing' in NiAl outer layer
microstructure of alunised INCO 825 & 316L 294(F),295(F)
multielement aluminide coatings of Cr/Al, Ti/Si,Pt/Al 296,141
NiAl & CoAl coatings in turbine blade in aero-marine & industrial applications 296
Pack alunising 293,294,295,296

Diffusion coating of Chromium 296,(F),297 processes 296,297
hot corrosion resistant chromised layer for utility & chemical recovery boilers297
chromized layer for dies, tools 297
chromized layer for low temperature for gas turbine 297

Diffusion coating of silicon 297,298

Diffusion
Diffusion barrier oxide layer formation in TiAlN 32

Diffusion of elements in Cu-Ni system with complete solubility 31(F)
 Diffusion of elements in Cu-Ag system with limited solubility 31(F)
 Fick's first law 285
 Fick's second law & effect of time 286,287,288
 Temperature and activation energy of diffusion 285, 286,287(T)

Diffusion processes 44
 Classification 44 (T)
 Interstitials & substitutionals 44
 Combustion, plasma, fused salt electrolysis & CVD processes, 45

Diffused CVD coating 298-302
 Barrier coating 300
 Graded interfaces 299,300
 Multicomponent diffused coatings 302
 Cyclone separator 302
 Stationary gas turbine vanes & blades 302
 Process 299-300
 Reactions for producing coating
 pyrolytic decomposition 298
 hydrogen reduction of halides 298
 displacement, disproportion & deposition processes 298
 Tungsten plus tungsten carbide multilayer coatings 299, 300
 WC top & W inner columnar layers on Ti-6Al-4V gas turbine blade 300(F),301

Diffusion Sinter Cladding 302,303

E

Electroconsolidation Process for Cladding 263-264
Electroslag welding 258,259
Electron beam processes 135-147
Electron beam assisted physical vapor deposition (EBPVD) 136-147
 Advantages of EBPVD 139-140
 Amorphous corrosion resistant deposits of Ag-Co,Cu-Ag, Cu-Sn 145
 Applications 140-146
 Al-coated steel strip 140,
 Aluminide diffusion barrier plus MCRAIY first layer 141-142,143(F)
 Diffusion barrier plus stabilized zirconia top layer 141,142,143(F)

Al₂O₃ glue formation by oxidation of diffused Al or LPPS deposition at the interface of MCRAIY and top ZrO₂ coating 142
 Process 136,137(F)
 Columnar grains & leaders defect 137,138(F), 139(F)
 Deposition rate 137,138
 Diffusion, glass bead peening & laser glazing to remove leaders defect 138,139(F)
 Electron gun
 operating voltage, acceleration, spot diameter 135,136(F)
 power density,35,135
 Frictional wear resistant Ag/Mo nano-crystalline binary coatings 144
 Graded coating resistant to thermal spalling 144
 Low friction DLC-WC coatings for automobiles 143,144
 Multilayer coatings on high TET gas turbine blades 140-143
 Plasma assisted EBPVD 145-146
 Post coating diffusion treatment 138,139(F),
 Segmented fine crack network in TBC 138,139,
 TiC, TiN, TiAlN, TiCN, Cr N wear resistant coatings on tools 142,143

Electron beam welding 145,146
Electron diffraction in TEM 313,314
Electro-discharge machining 239
Electron volt & plasma density 50,51(F),52
Electroslag welding *see under Arc assisted processes* in 258,259

Energy dispersive analysis by X-rays (EDAX)312,314
Energy, generated by different heat sources 35(T)
Engine valves 85, 86(T),88(F),90(F)
Erosion
 Dry erosion equation 347,348,349(T)
 ductile materials 301, 347
 brittle materials 301,347,348
 Erosive wear life 347,348(T),349,350(T)
 Hardness vs. wear 5
 Liquid erosion 350
 Simulation test for hydroturbine runners 354,355(F)
 Tests for dry erosion 319
 Tests for liquid impact 319

Evans and Marshall's Equation 327,5

F**Fatigue life** 339-342**Fluid Bed Processes** 271-274

Externally heated fluidized bed 272,273(F)

Fluidised gas bed 272,273(F)

Fluidised bed carburizing 272

Heat transfer coefficients of gas, high pressure gas, fused salt and fluidized bed 271 (T),272

Molten salt bath 274

Faraday's law rate of metal loss related to corrosion current 7**Fracture Toughness**

Calculation of wear volume from fracture toughness & experimental values 338(T) 339

Fracture toughness & life cycle 334 -336

fracture toughness & critical defect size in weld overlay 334-335

tolerable defect size calculation from COD of weld 335-336(T),337(T)

fracture toughness & wear of ceramics 337,338(T)

Prescription for improved fracture toughness 339

Friction Weld, Friction Stir Weld 219-227

Advantages 225

Ceramic cladding for high temperature corrosion with Al_2O_3 , ZrO_2 , SiC , SiN 226, Composite cladding with Al-SiC particulate for airframe, front disc brake rotors, turbocharger impeller, missile bodies, aircraft wing skins 226

Friction or adhesion wear characteristic 220, 221, 222

deformation or delamination wear 220,221(F)

deformation wear rate equation 221

melt dominated wear 220, 221

normalized velocity & pressure 220

oxidation dominated wear 220,221

seizure 220,221

sliding velocity 220

Friction wear map with normalized pressure and velocity as axes 221(F)

Friction & frictional heat 219,220(F),221,222

Friction welding process 222,223(F),224

heating time 224,

pressure 223,224

speed-223

surface preparation 224

Limitations 225,226

Metal cladding with HSS SS, Inconel & Stellites for industrial knife, valve, pump compressor & plastic extrusion screw 226

Structure & properties of friction weld overlays 224,225

HAZ, HDAZ, TMAZ 224-225

Microstructure 224,225(F)

Fused paste coating 307-308

Applications 308

Hardness & dilution 308

Paste mix & fusion by gas, carbon arc and plasma arc 307,308(T)

G**Gas metal arc welding**, *see under Arc assisted processes* 245(F), 247 250**Gas tungsten arc welding (GTAW)** *see under Arc assisted processes in* 245(F),246,247**Glow discharge spectrometry** 312,315**Grains size & wear** 18,20**Graphitization kinetics**32**H****Hardness** 4,5,22-23,315-325**Hard top casting** 309,310

CI on steel with Ni-base alloy bonding 309

Steel on al-alloy 309,319

Heat 23

Heat sources & surface engineering 36(F),37

Clapeyron – Claussius equation 26

Free energy & latent heat 24, 26

Enthalpy &entropy 25(T), 26

Energy & power density,23. 35(T),

Equilibrium & kinetics 32, 33

Eutectoid, eutectic &peritectic,28,30(F)

Heat for diffusion 43, 44(T)

Heat for thermal spray 39,40(T),41,42(T)

Heat for vapor phase deposition 42,43(T)

Heat for welding 37,38(T),39(F)

Heat for melting, vaporization & condensation 26,27,

Langmuir equation 27

Phase rule & transformations 27-29(F),30(F)

Phase stability 32

Phase diagram, Fe-C, 29(F)

Phases diffusing 31(F)

Surface engineering processes based on heat sources 33,34(T),

Sources 34,35(T),36

Specific heat & heat capacity 23,24(T);

Health monitoring 355-356

High speed steel

- Ion beam TiN coat on HSS 429,121
- Laser coat of HSS on C-steel 176
- PTA coat of HSS+TiC 86
- Hot Isostatic Press (HIP) 267-270**
 - Diffusion bonding applications
 - abrasive tips of gas turbine blades 269
 - edge rolling rolls clad with hard composite 270
 - tools & dies clad with WC,D2 269
 - turbocharger wheel and valve lifter in automotive 269
 - valve bodies ,compound tubes clad with Inconel &, Monel in chemicals, petrochemicals & Off-shore 269
 - Diffusion bonded materials 268
 - Inconel 625 to low alloy steel base 268
 - Co-base MPL-I to AISI4140 269
 - CPM9V clad on exterior of 4140 steel cylinder 269
 - CPM10V internal clad of twin extrusion barrel (4140 steel) 269
 - CPM10V clad on segmented screw of plastic extrusion barrel (C-Steel) 269
 - HIP quenching 270
 - Process 267,268(F)

I

Induction surface modification processes 229-242

Induction coupled RF plasma 236, 237

Induction heating of surface by eddy current & hysteresis loss 229

- frequency & case depth 229-230
- infra-red fiber optics for temperature measurement 236
- magnetic flux concentrator 230
- proximity effect 230
- reluctance 230
- uniform magnetic heating (UMH) 236

Induction Fusing 233-236

- comparison with other processes 235,236(T)
- microstructures 234,235(F)
- process 234(F)
- properties 234,235(F),236(T)

Induction hardening 230-233

- Transformation hardening in steel 230-233
- Applications 233
 - long shaft 233

rocker arm 233

torque transmission component 233

valve seat 233

Case hardness, depth 231,232 (F)

CCT-diagram 231(F)

Critical cooling rate 231

Ms-Mf temperature 230,231(F)

Quenching severity of different media 232

Sub-zero cooling 232

TTT-diagram 230,231(F)

Induction hardening of cast iron surface 233

Infrared radiations (high density) for surface modifications 310

Ion beam processes for surface modification

Ion beam, power density 35

Ion source 117(F)

Comparison of PVD with thermal spraying 118(T)

Ion source & ion extraction-cum acceleration system 117(F)

RF discharge plasma, DC discharge plasma & surface ionization by application of heat 117

Ion beam vapor deposition processes 118-125

Glow discharge argon plasma process 118

Ion sputtering 118-119

Ion plating, Ion vapor plating (IVP) or Ion vapor deposition (IVD) 119

Ion beam coatings 120-124

Advantages 123

Designing of coating 124

Aluminum coating on titanium fasteners in aircraft and spacecraft 120

Anodising replacing conventional anodizing processes 120,121

Diffusion barrier coating of Ni-13Al in aeroengine components 121

Hard chromium coating for impeller,piston & shafts 120

TiN coating on HSS, D2, H13, AISI 429,304,316, WC 121,122

TiN coatings

- on twist drill, gear cutting tool, metal forming tools, plastic molding & extrusion 121,122

- on automotive titanium alloy gear boxes, wheel hubs, differentials and steering racks in Formula One racing car, valve stem 122,123

as dry lubricant in high vacuum application in space-crafts & stainless steel screw threads, nuts, studs in nuclear 123

Ion beam (dual) assisted deposition process (Dual IBAD) 119,124-125

Coatings 124,125(T)

DLC, ceramic oxides, carbides and nitrides, lubricating metals (Ag, Pb, MoS₂ & WS₂), 124,125(T)

Diffusion barrier (Pt, Pd, Rh TiN), corrosion resistant passive film (Cr, Ta, Mo), oxidation resistant

(MCrAlY, Pt, SiC) 124,125(T)

Electron beam evaporation with simultaneous ion-stitching 124

Low temperature, non-columnar

microstructure 124

Ion implantation 125-130,323

Advantages 127

Applications

bearings 129

ceramic materials like WC blanking cutting & forming tools 128,129

DLC like high hardness B+N ion implanted HSS surface 127

Examples of ions implanted, N (in Al or stainless steel), B(stainless & tool steel), Cr (steel), Ti or Y (alumina) 127

Limitations 128

Mechanism of increased wear resistance 127

Microstructure and wear of nitrogen implanted austenitic stainless steel 126(F) mold cavities 128

Process 125

prosthesis 129

punches & dies 129

Special oxidative ion implantation of polymers and composites to minimize erosive wear in FAO (fast atomic oxygen) fluxes of spacecraft in low earth orbit 130

Plasma source ion implantation 130

Reactive ion sputtered coating 130-132

bond coat of amorphous silicon

hydrocarbon(α -SiHC) to produce adherent

hard DLHC top layer on bearing steel 131

highly adherent graded coating of ZrO₂ on metal substrate 131

Raman spectra indicates amorphous carbon & no diamond in DLHC 131

sputtered coating for surface etching, texturing and simultaneous deposition & etching 131,132

Ion beam assisted EBPVD 132

High performance, dense, adherent coatings of ZrO₂ (TBC), TiC, TiN, TiAlN 132

Ihregizing 298, see under Siliconizing

J

Jet flames & properties 324(T)

Plasma 54,55,324

HVOF, HVIF 202,208,324

Arc 324

LVOF 324

Arc 324

K

Kinetics

Equilibrium and kinetics 32

Reaction kinetics of graphitization 32

Rapid solidification 33

Kinetic energy of plasma 50

Kinetic energy & velocity in thermal spraying 41

L

Laser beam 35,157

Carbon di-oxide laser 160(F),161

convective cooling 160(F),161

diffused cooled extended electrode CO₂

transverse electromagnetic mode (TEM_{pl} mode) 161, 162

Current traversing at p-n junction (semiconductor laser) 159

Comparison of different lasers 166(T)

CW or pulse mode 167

Excimer laser XeF 158,164

Flash tube (solid & liquid laser) 158

Focusing of laser beam 164,165(F)

optical focusing by polariser, grating, lens, mirror, prism, beam splitter 164

fibre optics for low power short wavelength lasers 164

relation of beam power with focal length & divergence 164

transmissive optics (ZnSe & KCl crystals 164

Formation & properties 157(T),

Formation techniques 159(F)160(F)

Gas discharge (gas laser) 158

Gases (CO₂ + He + N) 158
 Inert gas halide for excimer 158
 Liquids (Nd-oxide containing solution) 158
 Heat of fusion & evaporation 168
 High powered diode laser (HPDDL)
 162,163(F)
 Copper channel cooling system 163
 Fast axis 62,163(F)
 High purity n-doped GaAs single crystal
 wafer lasing element 162
 Lasing elements 158
 Laser absorption & materials characteristics
 heat absorption 167
 reflectance & absorptivity 167
 thermal diffusivity 167
 Nd-YAG 159(F),160
 Multielement 'laser bar' 162
 Power density 35
 Material characteristics 167
 Processes 168,169(F)
 Pumping systems 158,159
 Radiation characteristics 165
 wavelength 165,
 absorptivity 165,
 divergence 165,
 beam diameter 166,
 focal length 166
 interaction time 166,167
 Semi-conductors (n-doped GeAs) 158,
 Solid elements (ruby) erbium garnet,Nd-doped-Al₂O₃ Na 158,
 Stripe 162
Laser ablation 176-177
Laser assisted vapor deposition 178, 179,
 CVD diamond coating 178(F),179
Laser boronizing 177
Laser for direct metal deposition 188, 189
Laser fusion of thermal sprayed deposit 178
Laser hardening by solid state transformation 169
 Austenite, martensite, critical cooling rate &
 Ms-Mf range 169,170
 Hardening of roll surface 169
Laser melting 170 171,
 Alloy systems forming metallic glass 173,
 Applications 173
 Amorphous phase 171,172(F)
 Commercial processes for surface glazing &
 simultaneous deposition and fusion
 173,174(F)

Glass transition temperature (T_g), glass forming tendency (GFT) and reduced glass transition temperature (T_{gr}) 171
 Heat flow model in rapid solidification 171,172(F),173,174(F)
 Non-equilibrium crystalline phase 171
 Properties of amorphous metals 173
 Rapid solidification process 171
 Supersaturated solid solutions 171
Laser nitriding 176
Lasershot peening 168,169
 Compressive residual stress 169
 Compressors and turbine blades 169
 Nd-doped phosphate glass slab laser 168
Laser spraying 186, 187(F),188
 Process 186,187(F)
 Ti-TiN gradient TBC 187,188
Laser surface alloying 175(T)
 Intermetallics on Al-alloy 175
 Composite (SiC) on Al-alloys 175-176
 Corrosion resistant surface on mild steel 176
 HSS surface on C-steel 176
Laser welding 179(F)
 Applications 181-185
 boiler tubes 184,185
 engine & process control valves 181 182,183
 gas turbine blades 183
 hydroturbine components 182,183
 naval applications 181
 refurbishing aircraft engine components
 183,184
 steam turbine blades 183
 Comparison with GTAW and PTA parameters
 180(T)
 ID weld overlay 184
 Induction assisted laser welding 185
 Laser tempering of laser weld 185
 Process comparison with GTA & PTA 180(T)
 Plasma arc augmented laser welding 185
 Properties 180(T)
 Fused ceramic surfacing by laser welding 186
Life cycle extension *see under Prognostic & Life cycle extension 331-357*

M

Matrix structure 20

Microwave 35,149-156

Power density 35
 Carburizing 154
 Ceramic surfacing 155

Diffusion of substitutional elements 154
 Electromagnetic spectrum 149,150(F)
 Electron-cyclotron microwave plasma 154
 Formation & properties 149
 Generation and transmission 152
 Hot electrons' & cool ions & neutrals' in microwave 153
 Loss factor 151(F)
 Microwave energy absorption vs. effective conductivity 151(F)
 Mechanism of heating 151-152
 Microwave frequency band 150(F)
 Microwave plasma CVD diamond applications 154
 mechanism 153
 process 152, 153,154(F)
 Power density 35
 Poynting vector 150
 Sintering 155
 Surface fusion by 'thermal run-away' effect 155

N

Nickel alloys
 Inconel 800,PTA coating 87
 Inconel 625,PTA coating 87,91
 Hastelloy 276,PTA coating 87,91
 Ni-Cr-B-Si-Fe-C(Ni=11)self-fluxing alloys,87,88
 Ni-Cr, Ni-Al, NiCrAlY as bond coat for thermal spraying 55,59(T)
 Udimet520, PTA coating 87,91

O

Oxidation 14,15(T)
 Oxidation resistant coatings,15(T),293,297
 Oxides 66,61,142,282,

P

Parylene coating 277,278(F)
 Applications in aerospace, avionics and medical devices 277,278
 catheter mandrel(for lubricity) 278
 prosthetic components(lubricity/barrier) 278
 cardiac arrest devices, brain probe, bone pins, needles 278
 Bond coat of organo-silane 277
 Coating processes 277,278(F)
 vacuum pyrolysis of dimmer to active monomer 277

vacuum deposition & polymerization of monomer 277

Parylene N,C,D & HT grades,277
 Precursor of dimeric parylene 277

Phase rule 27-28

Phase transformations

Eutectic 28, 30(F)
 eutectoid 28, 30(F)
 melting & solidification 28
 peritectic 28
 transformation temperatures 29(F),30

Phase or equilibrium diagram

Fe-C phase diagram 29(F)
 stable phase formation & diffusion barrier 31(F)

Equilibrium & kinetics 32,33

Point & plane defects 21

Plasma beam

Formation & properties 49,50(F),51(F)
 Ionization of plasmagenic gas 50
 Power density 35

Potential & kinetic energy of plasma beam 50

Plasma density vs electron volt 51(F)
 Plasma flame, glow discharge and arc energies 51(F),52

Post spray thermal processes 42(T),43
 Plasma assisted vapor deposition 99
 Saha's equation on ionization 49

Plasma assisted amorphous metal deposition 105,106

Amorphous alloys with nil equilibrium solubility (Ag-Ni), difficult alloys (Cu-Ag) & novel compositionally modulated alloys 106
 Applications, tape recorder heads, razor blades 106

Magnetron plasma sputtering 105

Plasma gun technique 105

Sputtering 105

Vacuum evaporation 105,106

Plasma boriding 52,96

Borax paste boronizing 96
 Hardness & hard borides in boronized surface 96

Plasma carburising 52,95-96

Advantages over conventional carburizing 96
 Applications, aircraft & automobile industries 96

Dry quenching or high pressure gas quenching 96

Process 95(F)

Plasma CVD 41,42,52,97(T),101

- Process 102
- Variables 102
- Plasma enhanced chemical vapor deposition process (PECVD) 102
- Thermal plasma CVD 102
- Microwave plasma CVD 102
- High energy intensified plasma assisted processing (HEIPP) 102
- Aluminum nitride coating 102,103
- Plasma nitriding 52,90-95(T)**
 - Abnormal glow discharge 91(F)
 - Applications
 - dies & tools 93
 - automotive components 95
 - Current-voltage characteristic in electric discharge 91(F)
 - Gas mix 92
 - Glow discharge 90-92
 - Mechanism of plasma nitriding 93
 - Microstructure 93,94(F)
 - Microhardness profile 93,94(F)
 - Nitriding steels 93
 - Nitriding of titanium 93
 - Process 91(F),92
- Plasma non-transferred arc spraying processes 52**
 - Classification 53(T)
- Plasma spray process based on DC arc 52,54(F),52-79**
 - Applications 67
 - Automotive, 9,70(T)
 - cylinder bore 72,
 - piston ring grooves 72,
 - piston rings 70,71(T),
 - TBC on piston crown 68,69(T),70(T)
 - Paper &pulp (MG cylinder using Mo + NiCr) 67,68(T)
 - Power, boiler tubes 72,73
 - Gas turbine 73,74(T),75-77
 - abradable coating 73,76,77
 - antifretting coating 73,75,76
 - diffusion barrier 76
 - graded coating 76
 - oxidation &corrosion resistance coating 73,74,75
 - thermal barrier coatings 73,75
 - Coating on Ti-alloy (F22 jet) 77
 - Textile 68
 - Plasma spray atmosphere
 - Open air 56
 - High pressure plasma 57-58,
 - Reduced or low pressure plasma 56-57,
 - Vacuum plasma 57
 - Water stabilized plasma 58
- Plasma spray gun or torches 54,55(F)**
 - Normal torch 54(F)
 - Twin anodes 54-55
 - Grator Guard 55
- Plasma spray system 53,54(F),55,56**
 - Plasmagenic gas 56
 - Carrier gas 56
 - Power supply and cooling system 56
- Coating technique**
 - Surface preparation, cleaning & roughening 58
 - Bond coat 58,59(T)
 - Top coat materials, metals 59,60(T), ceramics 60,composites 61,62(T),63 & polymer compsites,61, 62(T)
 - Coating properties 63,65(T)
 - bond strength,63
 - porosity & hardness 64
 - microstructure of Cr_2O_3 , ZrO_2 , Al_2O_3 , TiO_2 , $\text{Al}_2\text{O}_3+\text{TiO}_2$, MCrAlY deposit 65(F),66(F),67
 - Plasma spray polymeric coating materials 62(T)
- Polymer & polymer composites for thermal spray 61,62(T),63**
 - Thermosetting resins
 - Epoxy 61,62(T)
 - Polyester 61,62(T)
 - Thermoplastics
 - Polypropylene 61,62(T)
 - Polyvinyl chloride (PVC) 61,62(T)
 - HDPE TS 61
 - LDPE TS 61
 - Polymer+ MCrAlY+ RA, abradable coating on gas turbine 76,77
- Plasma non-transferred arc scan hardening 77,78**
 - Surface hardening of 5% Cr die steel SAW overlay 78
 - Tools, dies & machine components used for hot deformation processes 78
- Plasma assisted vapor phase deposition 97(T)**
 - Plasma PVD 97**
 - Advantages of sputtering 97,98
 - Applications, TiC & Ti N coating on cutting tools, plastic extrusion dies, moulds 101

Chromium nitride coating on cobalt base alloys, Hynes 25 & Stellite3 & for nuclear applications 101

ISO/Euronorm carburising steels with high tempering temperature for CVD coating on finished tools 101

Line of sight process 103

Magnetron plasma sputtering 99, 100

Plasma evaporation process 99(F)

Plasma sputtering process 98,99

Reactive DC or RF sputtering for nonconductive materials 98

Segmented structures to improve thermal cycling life 100,101

Substrate temperature vs. microstructure of vacuum evaporated deposit 98(F)

Plasma assisted polymer surface modification 106,107(F),108(F),109

Applications, automotive components 107

Copolymerization 109

DC or AC plasma using a bell jar 108(F)

Fluorinated compound coatings resist mechanical & contact wear 109

Formation of thin coating of new types of polymeric materials 107

Induction coupling process using a tubular reactor 107, 108(F)

Low temperature vacuum plasma process using RF source 106, 107(F)

Organic precursor to control plasma copolymer (PCP) composition 109

RF plasma generated UV radiation treatment 106,107(F)

wood grain effect on ABS 107(F)

improved wettability and bonding for PTFE 107(F)

RF or Corona discharge plasma polymerization 107(F),108(F),109

Thin, clean, flawless & uniform PCP coating 109

Twin coating of methyl-methacrylate corrosion protective coating 109

Plasma source ion implantation 101

Plasma transferred arc processes 78-90,251-254

Plasma transferred arc welding with powder consumable 52,78-90

Applications 85,86(T)-90

Con-cast rollers 89,90

Engine valves 85

valve materials 85

coating materials 86,87,

microstructures 88(F), 89

coating hot hardness 87(F)

Hydroturbine components 90

Process control valves 89

Rock bit 89

WC in Ni-alloy matrix 85

Coating powder materials 84, 85

Process control 81,82,83

bead area 83

current 82

feed rate /travel speed 82

arc voltage control 81

gas 79

pilot arc 81

Properties

dilution 82,83

HAZ 84

productivity 84

savings 84

System 79(F)

powder feeder 81

power supply 79,80

torch 79,80(F)

torch for internal diameter welding 81

torch oscillation 81

Plasma arc welding with wire or rods, see under Arc assisted processes in 251-254

Plasma transferred arc scan hardening 90

Post-plasma spray processes 79

Polymer surface modification 109-11,275-278

Processes, applications 275,276(T)

metallisation by resistance heated metal 275

sputtering 275,276

ion implantation,275,276

HVOF 275,276

plasma polymerization,276

polymer coatings and properties 276,277

glass transition (Tg) temperature 276,277

degradation temperature(Td) 277

Parylene coating 277-278(F)

parylene C,N, D and HT 277

process and applications 277,278

Prognostic & Life cycle extension 331-358

Creep life 342-344

Creep & LEFM 342

Creep & microstructure 343(F),344

Prescription to improve creep life 344

Definition of prognostic 331-332

Definition of life of engineered components 332, 333(T),333,334

Fatigue life 339,340,341(F)-342

- high cycle fatigue 340
- low cycle fatigue 340
- fatigue threshold value340
- effective toughness 340
- steady state growth rate equation & LEFM 340 341(F)
 - Static mode & failure 341,342
 - Prescription for improved fatigue life 342

Fracture toughness & life cycle 334 -339

Fracture toughness and wear of ceramic coatings 338(T) 339

- Evans and Marshall equation 337
- Index for abrasive wear 337
 - Fracture toughness & wear of ceramics 337,338(T)
 - Prescription for improved fracture toughness 339

Fracture toughness & critical defect size in weld overlay 335-337

- COD of weld 335,-336(T),337(T)
 - tolerable defect size calculation of a weld 336,337(T)

Predictable life 333(T),334

- Aging processes & life prediction from steady state property changes 333(7), 334

Unpredictable life 333(T)

Wear life in wear processes 344-

- Methodologies 344
- Wear equation, map and test 344,345
- Adhesive wear life of coatings 345
- 346(F)(T),347(T)
 - Abrasive wear life 346, 348(T)
 - Erosive wear life, dry 347,348,349(T),
 - Liquid erosion life 350(F)
 - Thermal wear life 350,351(T)
 - Zero wear (IBM) equation 351,
 - Wear life using zero wear eq. 352(F)
 - Corrosive wear life 352, 353(T,F)
 - From corrosion rate 352,353(T)
 - Using fracture mechanics 352,353(F)
 - Wear life from long time wear simulation tests 354,355(F),
 - High silt erosion wear of hydroturbine 354,355(F)
 - Repetitive impact adhesion in railroad frog 345,355(T)
 - On-line health monitoring 355-356
 - Thin film activation 356

Acoustic emission 356

Q

Quality of the engineered surfaces 311-329

Quality checks for engineered surfaces 311,312(T)

Adherence or bonding of coating 313

- PVD 323
- Thermal spraying, 326

Coating properties

- diffusion processes 319-320
- thermal spraying processes 324(T),325,326
- vapor phase deposition 320,321,322
- welding 326, 327(F),-328(F)

Composition 314-315,320,323,325

- checking by EDAS,AES,GDS and, Micro Raman Spectrometer 315

Diffusion 320

- ion-implanted 323
- vapor phase 322
- thermal spraying 325

Hardness 315,316(T)

- Vickers, Rockwell-315
- Microhardness by Knoop, Vickers and Scratch 315
 - Ultrasonic & Eddy current tests for hardness 315

Hardness range 315,316(T),317,320,323,325

- Diffusion 320
 - boronized 317,320
 - carburized 320
 - nitrided 320
 - DLC 316,317,323
- Ion implanted 323
 - Thermal spraying 325
 - Vapor phase deposits 321,322
- Hot hardness measurement 317
 - Hot hardness of PVD and CVD coated TiN, Zr N, HfN 321,322
- Microstructure 312,314,320,323,325,327(F)
 - Microscopes 313-314
 - Confocal laser microscope 314
 - Fluorescence microscopy 314
 - Scanning acoustic microscope 314
 - SEM 313
 - TEM 313,314
 - Diffusion 320
 - Ion implantation 323
 - Thermal spraying 325
 - Vapor phase 322

- Weld 327
 - Performance tests 318,319,324
 - standard wear tests 318, 319
 - corrosion tests 319
 - Ion implanted 324
 - Porosity & inclusion 313
 - Residual stress 322
 - Vapor phase 322
 - Thermal spraying 324
 - Spray & fused coatings 326
 - Welding 326-328
 - Angular distortion 327,328
 - Capital cost 327,328(F)
 - Dilution 328
 - Fusion zone 327(F)
 - HAZ 326(F)
 - Penetration 327
 - Characteristics of welding processes 328(T)
 - Roughness of the surface, 317,318(T)
 - Ra,Rq,Rz 317
 - Stylus 2-D Ra profiling 317,318
 - Optical 3-D profiling 317-318
 - 3-D roughness & wear and corrosion 318
 - Roughness range of modified surfaces 318(T)
 - Thickness of modified surface 313,
 - diffusion 320
 - Vapor phase 320,321
 - Thermal spray 325
 - Quenching**
 - Dry 96
 - High pressure 288,289
 - Quenching severity of different media 232
 - Heat transfer coefficients of gas, high pressure gas, fused salt and fluidized bed 271(T),272
 - Quality control of surface engineered products 311=329
 - R**
 - Rapid Solidification Process (RSP) 33,171-174**
 - Laser melting & RSP 171,172(F), 173,174(F)
 - Plasma assisted vapor phase amorphous metal deposition 105,106
 - Rocket combustion, power density 35**
 - S**
 - Saha's equation on ionization,49**
 - Sapphire coating**
 - by simultaneous vapor phase deposit of Al & O to form sapphire coating 280
 - Self-fluxing alloys 30,198**
 - Siliconizing or Ihregizing 298-299**
 - Pack siliconizing process 298
 - Non oxidising acid corrosion resistance 298
 - Coating for low temperature corrosion resistance in gas turbine 298,299
 - Solar energy for surface modifications 193-199**
 - Heating rates of ceramics & metals in solar furnace 195(T),196(T),197
 - Heating system 193,194(F),195
 - attenuator 194,
 - heliostat 194,
 - primary concentrator 194
 - sample chamber 194
 - secondary concentrator 194,
 - shutter 194
 - Microstructures of sunbeam fused NiCrB alloy, SS & WC-Co spray deposits 198(F)
 - Power density 35,195
 - Solar furnace 93,194
 - Solar hardening 197
 - Solar heating 193
 - Solar radiation 193
 - Sunbeam fusing 197-199
 - layered PVD deposits 199
 - thermal spray coatings 198(F)
 - thin layered deposits 198,
 - Time ratios for fusion of different materials 196(T)
 - Spark deposition process 239-242**
 - Al+SiC composite joining to Al-alloy base 242
 - Power vs deposition characteristics 241(T)
 - Principle 239
 - capacitance 240
 - volt 240
 - capacitor discharge 239
 - equation for energy stored in a capacitor 240
 - Farad & microfarad 240
 - reversing polarities of EDM,239
 - Process 240(F),241
 - Thickness & surface roughness 241
 - Ultrafine diamond particles and carbides deposit on punches, flutes of taps & drills, cutter, end mills dies 242
 - Stellites, cobalt based alloys 85-90**
 - Stellite 1,86(T),89,St6 ,86(T),89,90,

St12,86(T),St 21,86(T),St32 or F 85,86
St306,86(T)

Submerged arc welding (SAW) process
See under Arc assisted processes in 254-258

Surface
Phase 1
Properties & wear 16
Engineering 1
Surface energy & wear equations 16-17(T),18
Alison 16
Griffith 17
Hall Petch 18
Robinowicz 18
Smith16
Surface roughness & wear 18,19(F)20(T)
Surface microstructure & wear 20,21(T)
Surface composition & wear 22
Surface hardness & wear 22,23
Surface property modification & thermal processes 33,34(T)

T
Textile components, thermal spray coatings 68
Thermal Spraying
Arc spray 261-263
D-Gun 208-209(F)
Heat sources, flame & particle temperature, velocity, & coating properties 324(T),201,202
HVOF/HVAF 208,209,212(F)
High velocity impact forging 214
Plasma spray 52-77
Processes classification 40(T),
Flame temperature,40-41
Comparison of PVD with thermal spraying 118(T)
Plasma spraying 52-79
Titanium
CVD diffused inner columnar tungsten & outer tungsten carbide layer on Ti-6Al-4V 300(F)
Ion beam TiN on automotive Ti-alloy components in Formula 1 car 122,123
Plasma spray MCrAlY onTi-6Al-4V & Ti-6Al-2Sn-4Zn-2Mo in F-22 aircraft 78
Plasma nitriding of titanium 95
Turbine
Gas turbine
Abrasive tips of gas turbine blades by of thermal spray deposit 77
Antifretting coating by thermal spray 77
Chromized for low temperature corrosion resistance 298
Borided Nimonic alloy for thrust vectoring nozzle bearing components of gas turbine engine 291
Borided Co-binder in WC-Co surface of jet engine fuel pump 291
Diffusion barrier coating 76,131,141, 142,143 (F), 294,295
Gas turbine blades by laser welding 184,
Graded coating by thermal spray 77
Hipping 269
Mid-span damper/blades contact surfaces-antifretting castings 73,75-77
Plasma spray coatings 73-77,74(T)
Primary zones of combustors, nozzle & guide vanes -TBC 76-77;
Shrouds, lybrinth seals – 77-78
Thermal barrier coatings by thermal spray 76,77
Turbine blades- corrosion & oxidation resistance coatings 76
Hydroturbine
Slurry erosion resistant coating on hydroturbine components 91

U
UV radiation generated by RF plasma for polymer surface treatment in vacuum 106,107(F)
Improved wettability and bonding for PTFE 107(F)
Wood grain effect on ABS 107(F)
Unpredictable life due sudden failure 333(T)
Hydrogen cracking 333
Ductile brittle transition at subzero333
Ultrasonic & Eddy current tests for hardness 315
Ultrafine diamond particles and carbides deposit on punches, flutes of taps & drills, cutter, end mills dies 242

V
Vapor phase deposition 43
Advanced heat sources 43, 44(T)
Vapor phase deposition of amorphous materials 107
Plasma gun technique 107
Sputtering 107

Magnetron plasma sputtering 108
Vacuum evaporation
Amorphous alloys with
nil equilibrium solubility (Ag-Ni) 108
difficult alloys(Cu- Ag) 108
novel compositionally modulated alloys 108
Applications, tape recorder heads, razor
blades 108

thermal spray 75(T),76,77
ion sputtering 131
Zirconia, stabilized by
Yttria,Ceria,Magnesia,75,76,77
Zirconia stabilized, used as TBC
in automotive engine 77,
in aeroengine 132
Zero wear, IBM equation & graph
351,352(F)

W

Wear

base material 2
classification 3(T)
counter material 2
definition 2
DIN50320 2(F)
Equation 4
wear coefficient 4
wear mating,2
wear system or envelope 2,3

Wear Plate 311

Weld, overlay to prevent corrosion 13

Welding arc

Energy requirements for different process
39(F)
Power density 35
Weld overlay processes 37,38(T) comparison
based on heat 38
White cast Iron
PTA coating material on concast roller 87(T)

X

X-ray diffraction for residual stress
determination 322,312
Xylene monomer plasma polymerization to
parylene 277,278(F)
Xenon fluoride Excimer laser 158,164

Y

Yttria-stabilized zirconia 212
Yttria coating on CoCrAlY on CAPL &
CGL hearth rolls by HVOF 212
Young's modulus of ceramic oxides at high
temperature 65(T)
Yankee dryer, thermal spray coatings
67,68,263

Z

Zirconia, thermal barrier coatings by
ion beam plus EBPVD 132,

Author

Ram N. Chattopadhyay completed his B.Sc (Hons). and Ph.D in engineering at the University of London. He is a fellow of the Institute of Materials (UK), chartered engineer of Engineering Council (UK), member of Convocation (University of London) member of American Society of Materials–International, American Welding Society. He is a life-member of several Indian professional societies relating to metal, welding, powder metallurgy and tribology.

He has been a member of prestigious Metal Handbook Committee of ASM-International. His basic training in research was in Sweden and shop floor experience at a fabricating shop in Germany. In his first assignment in India, he initiated the research project and did extensive work on the development of microalloyed HSLA steels at National Metallurgical Laboratory of India. He played a leading role in making the first successful commercial heats of microalloyed HSLA steels in India. .

His failure investigation work during his tenure at Tube Investment of India(a subsidiary of TI,UK) was instrumental in winning the first product liability case in India. His next assignment was a green field project to build and run an advanced research center on wear & corrosion control through surface engineering by an unit of Larsen & Tourbo Ltd, in association with Eutectic + Castolin, Switzerland.. A premier research center on wear control technology was established in record time. He has solved a large number of critical wear & corrosion problems faced by industries, such as, cement, mining, steel, automotive, railway, power, aerospace, petrochemical & chemical.

Dr. Chattopadhyay has participated and presented research papers in national and international conferences, on wear, corrosion, thermal spray, welding, surface engineering etc, held in India and abroad. He has conducted courses on various subjects including surface engineering areas organized by professional bodies(ASM-International, India Chapter, UNDP), academic institutions(IIT) & industries(Steel, Petrochemical).He has been a visiting faculty member at the IIT (Mumbai) and a member of expert panels for various committees constituted by different agencies of the Government of India.

His first book covering the entire field of wear and its control, entitled as *Surface Wear: Analysis, Treatment, and Prevention* has been published by ASM-International, Materials Park, OH, in 2001. In addition, he has more than 100 research and technical publications to his credit. In 1999, he was awarded the Jindal Gold medal by the Indian Institute of Metals for his outstanding contribution in his area of work.

His current activities are listed in his website: www.wearprognosis.com